DOCTOR OF PHILOSOPHY

Alginate from brown seaweeds: extraction, characterisation, modification and the studies on its applications for hydrogels

Alshareef, Sohad Abdulkaleg

Award date:
2019

Awarding institution:
Bangor University

ALGINATE FROM BROWN SEAWEEDS: EXTRACTION, CHARACTERISATION, MODIFICATION AND THE STUDIES ON ITS APPLICATIONS FOR HYDROGELS

Thesis submitted to The School of Natural Sciences, Bangor University in partial fulfilment of the requirements for a Doctor of Philosophy (PhD) Degree

By

Sohad Alshareef MSc

School of Natural Sciences, Bangor University, Bangor, LL57 2UW, UK.

PhD Supervisor: Dr **Hongyun Tai**

May 2019

Declaration and Consent

Details of the Work

I hereby agree to deposit the following item in the digital repository maintained by Bangor University and/or in any other repository authorized for use by Bangor University.

Author Name: .....

Title: .....

Supervisor/Department: .....

Funding body (if any): .....

Qualification/Degree obtained: .....

This item is a product of my own research endeavours and is covered by the agreement below in which the item is referred to as "the Work". It is identical in content to that deposited in the Library, subject to point 4 below.

Non-exclusive Rights

Rights granted to the digital repository through this agreement are entirely non-exclusive. I am free to publish the Work in its present version or future versions elsewhere.

I agree that Bangor University may electronically store, copy or translate the Work to any approved medium or format for the purpose of future preservation and accessibility. Bangor University is not under any obligation to reproduce or display the Work in the same formats or resolutions in which it was originally deposited.

Bangor University Digital Repository

I understand that work deposited in the digital repository will be accessible to a wide variety of people and institutions, including automated agents and search engines via the World Wide Web.

I understand that once the Work is deposited, the item and its metadata may be incorporated into public access catalogues or services, national databases of electronic theses and dissertations such as the British Library's EThOS or any service provided by the National Library of Wales.

I understand that the Work may be made available via the National Library of Wales Online Electronic Theses Service under the declared terms and conditions of use (http://www.llgc.org.uk/index.php?id=4676). I agree that as part of this service the National Library of Wales may electronically store, copy or convert the Work to any approved medium or format for the purpose of future preservation and accessibility. The National Library of Wales is not under any obligation to reproduce or display the Work in the same formats or resolutions in which it was originally deposited.

Statement 1:

This work has not previously been accepted in substance for any degree and is not being concurrently submitted in candidature for any degree unless as agreed by the University for approved dual awards.

Signed …….. (candidate)

Date ……..

Statement 2:

This thesis is the result of my own investigations, except where otherwise stated. Where correction services have been used, the extent and nature of the correction is clearly marked in a footnote(s).

All other sources are acknowledged by footnotes and/or a bibliography.

Signed ……. (candidate)

Date ……..

Statement 3:

I hereby give consent for my thesis, if accepted, to be available for photocopying, for inter-library loan and for electronic storage (subject to any constraints as defined in statement 4), and for the title and summary to be made available to outside organisations.

Signed ……. (candidate)

Date ……..

NB: Candidates on whose behalf a bar on access has been approved by the Academic Registry should use the following version of Statement 3:

Statement 3 (bar):

I hereby give consent for my thesis, if accepted, to be available for photocopying, for inter-library loans and for electronic storage (subject to any constraints as defined in statement 4), after expiry of a bar on access.

Signed …… (candidate)

Date ……

Statement 4:

Choose one of the following options

a) I agree to deposit an electronic copy of my thesis (the Work) in the Bangor University (BU) Institutional Digital Repository, the British Library ETHOS system, and/or in any other repository authorized for use by Bangor University and where necessary have gained the required permissions for the use of third party material.	
b) I agree to deposit an electronic copy of my thesis (the Work) in the Bangor University (BU) Institutional Digital Repository, the British Library ETHOS system, and/or in any other repository authorized for use by Bangor University when the approved bar on access has been lifted.	
c) I agree to submit my thesis (the Work) electronically via Bangor University's e-submission system, however I opt-out of the electronic deposit to the Bangor University (BU) Institutional Digital Repository, the British Library ETHOS system, and/or in any other repository authorized for use by Bangor University, due to lack of permissions for use of third party material.	

Options B should only be used if a bar on access has been approved by the University.

In addition to the above I also agree to the following:

1. That I am the author or have the authority of the author(s) to make this agreement and do hereby give Bangor University the right to make available the Work in the way described above.

2. That the electronic copy of the Work deposited in the digital repository and covered by this agreement, is identical in content to the paper copy of the Work deposited in the Bangor University Library, subject to point 4 below.

3. That I have exercised reasonable care to ensure that the Work is original and, to the best of my knowledge, does not breach any laws – including those relating to defamation, libel and copyright.

4. That I have, in instances where the intellectual property of other authors or copyright holders is included in the Work, and where appropriate, gained explicit permission for the inclusion of that material in the Work, and in the electronic form of the Work as accessed through the open access digital repository, *or* that I have identified and removed that material for which adequate and appropriate permission has not been obtained and which will be inaccessible via the digital repository.

5. That Bangor University does not hold any obligation to take legal action on behalf of the Depositor, or other rights holders, in the event of a breach of intellectual property rights, or any other right, in the material deposited.

6. That I will indemnify and keep indemnified Bangor University and the National Library of Wales from and against any loss, liability, claim or damage, including without limitation any related legal fees and court costs (on a full indemnity bases), related to any breach by myself of any term of this agreement.

Signature: …… Date: ……

Acknowledgments

I would first like to thank my supervisor Dr. Hongyun Tai for her help and her support throughout my entire studies here at Bangor University. She has always given me helpful advice and comments and has been a massive support for me here in Bangor.

I would secondly like to thank the entire research groups situated on the 5th floor of the Alun Roberts building. Everyone has been so friendly, helpful and I consider them some of my best friends that I have met since I have moved to the United Kingdom and they are my Bangor Family.

Finally, I would like to thank my family as they have supported me throughout my studies and my children have been so understanding as they have been the primary cause of me wanting to further my studies so I can give them a better life in the future.

Table of Contents

Abstract

The aims of the present work are to study alginate extracted from little studied species of brown seaweeds sourced in the local area with the aim of determining the chemical structure, particularly the M/G ratio, and physical properties including gelling, as they relate to commercial and biomedical applications. The M/G ratio is known to be an important indicator of the strength of gels. The obtained alginate was further modified with Poly-lactic-co-glycolic acid (PLGA) and Poly-caprolactone (PCL) to introduce hydrophobic character in an effort to further widen applicability in biomedical uses.

Gels prepared from alginate and its derivatives and their properties were studied with respect to swelling and drug release.

As the local area (the North wales coast) has an abundance of certain species of brown seaweed these were used to investigate how differences in geographic location affect the alginate content and structure. This study was performed over two years to ascertain the effects of both environment and seasons.

As an introduction **Chapter 1** details the chemical structure and sources of alginates and their main methods of extraction. The characteristic chemical and physical properties were outlined. Methods of chemical modification to synthesise derivatives, which enhance physical and chemical properties such as gelation were reported. Gelation methods were also detailed.

Chapter 2 outlines the main techniques used to characterise the alginates and their derivatives.

Chapter 3 details the extraction of alginate from Irish and Welsh seaweeds. The effects of geographic location and other environmental factors such as season of harvesting were studied. as to how they determine yield and chemical structure. The different methods of extraction and their effects on the properties of the extracted alginate were reported. Extraction was performed using the traditional method employing sodium carbonate but also enzymic assisted methods were compared with the finding that extraction temperature is an overriding factor for higher yields. Enzyme extraction of alginate gave the highest yield with the least protein impurity. Hydrolysis using different methods, acidic and enzymatic, was undertaken to compare effect on the M/G ratio.

Chapter 4 concerns how alginate was modified by grafting with PCL to introduce increased hydrophobicity and to enhance biodegradation. For the PCL grafts, linear polymers of various molecular weights were used. Hydrogels were then prepared by ionic crosslinking using Ca^{2+}

at different concentrations and subsequently the bulk gels were used in swelling studies in de-ionised water and in saline solution.

In **Chapter 5,** description was given for the preparation of spherical beads of both alginate and its more hydrophobic grafted PCL derivatives, which were used as matrix carriers for two model drugs, hydrophilic carmoisine and, hydrophobic β-carotene. The traditional method of external ionotropic gelation was compared to a novel two-step procedure, which uses both internal and external gelation to increase the cross-linking density leading to an improvement in encapsulation efficiency and control of swelling which in turn affect the release profile of the cargo drug.

Chapter 6 details the preparation of PLGA/alginate composite microspheres intended for use for delivery of the hydrophilic protein BSA. The microspheres were prepared by a double-emulsion using commercial alginate and Welsh alginate for comparison. The micro-particles were characterised by SEM. The encapsulation efficiency and release of the protein drug from each type of microsphere was compared and release profiles in various media were studied.

In conclusion, it was found that the extracted alginates in this study were relatively high in M content. High M content confers higher elasticity in the material that may be of particular value for use as a food additive. It was further found that derivatives synthesised by grafting improved its mechanical properties making for a more rigid gel and this may of particular value in medical applications in, for example, as wound dressings. In addition, properties of swelling and drug release can be modified as required and by altering the hydrophilic/hydrophobic nature of such gels can facilitate loading with a wide range of drugs.

List of Tables

List of Figures

Fig (5-7): SEM surface micrographs of model drug-loaded freeze-dried beads: **(A)** (Ca-ALG -1step), from alginate 0.5% (w/v), **(B)** (Ca-ALG-2step) from sample 11 in Table (5-1). Magnification is 300, (scale bar: 100 μm). **(C)** and (D) are, respectively, wet and freeze-dried beads of (Ca-AlG-2step) from sample 11 in Table (5-1).

Fig (5-8): The effect of M/G ratio on formed spherical beads: **(A)** commercial alginate, **(B)** commercial alginate –graft **(C)** Welsh alginate and **(D)** Irish.

Fig (5-9): β-carotene loaded alginate beads formed by: **(A)** two step ionotropic gelation method according to the procedure 5.2.3.1, **(B)** water/oil emulsion method and **(C)** oil/water emulsion method.

Fig (5-10): Swelling profile of freeze-dried beads showing the effect of cross-linking density on swelling, **(A)** in NaCl 1 %(w/v), **(B)** in distilled water. Data points represent the average within an error range of ± 2%.

Fig (5-11): Swelling profile of freeze-dried beads showing comparison swelling of pure and grafted alginate. Data points represent the average within an error range of ± 1.5 %.

Fig (5-12): Swelling profile of freeze-dried beads in **(A)** Saline 1 % (w/v), **(B)** distilled water. Data points represent the average within an error range of ± 2%.

Fig (5-13): Swelling profiles of freeze-dried beads of Welsh alginate (W) and its grafted derivative loaded with carmoisine. Data points represent the average within an error range of ± 1%.

Fig (5-14): Dye loading during preparation into commercial alginate beads: (**A**) (Ca-ALG-2step) beads loaded with β-carotene and prepared by ionotropic gelation method, (**B**) (Ca-ALG-2step) beads loaded with β-carotene and prepared by hexane/ water emulsion method and (**C**) (Ca-ALG-2step) beads loaded with carmoisine in aqueous preparation.

Fig (5-15): Calibration curve for carmoisine dye in $CaCl_2$ solution.

Fig (5-16): The calibration curve of carmoisine: **(A**) in NaCl 1% (w/v) and **(B)** in distilled water respectively.

Fig (5-17): Release profile of carmoisine dye (model drug) from freeze-dried Ca-(ALG) beads in swelling media: (**A**) water and (**B**) NaCl 1 % (w/v). Data points represent the average within an error range of ± 1.5 %.

Fig (6-11): Scanning electron micrographs of BSA-loaded MS1 (PLGA/ ALG-A) composite microsphere prepared with commercial alginate: **(A)** MS1 before incubation in aqueous media, **(A-H_2O)** after 10 days incubation in H_2O, **(A-NaCl)** after 10 days incubation 1% NaCl and **(A-PBS)** after 10 days incubation in BPS.

List of Schemes

Abbreviations

AAS	Atomic absorption spectroscopy
AlgE4	mannuronan C-5 epimerase
AU	Absorbance units
CMPI	2-chloro-1-methylpyridinium iodide
CSAD-3	Sodium alginate derivative grafted with 3 cholesteryl groups per 100 hexuronic acid residues
DMF	Dimethyl formamide
DMSO	Dimethyl sulfoxide
DSC	Differential Scanning Calorimetry
ε-CL	Caprolactone
EDC-HCl	1-ethyl-3-(3-dimethylaminopropyl) carbodiimide hydrochloride
F. vesiculosus	*Fucus vesiculosus*
FT-IR	Fourier Transform Infra-red Spectroscopy
G	α-L-guluronic acid
GPC	Gel Permeation Chromatography
HOMO	Highest occupied molecular orbital
LHRH	Luteinizing hormone-releasing Hormone
LUMO	Lowest unoccupied molecular orbital
M	β-D-mannuronic acid
Mn	Number average molecular mass
Mn-MRI	Manganese-enhanced magnetic resonance imaging
Mw	Weight average molecular mass
NMR	Nuclear Magnetic Resonance Spectroscopy

PBS	Phosphate buffer solution
PCL	Poly-Caprolactone
PDI	Polydispersity Index
PEG	Poly (ethylene glycol)
PGA	Propene glycol esters of alginate
PLGA	Poly (lactic glycolic acid)
ROMP	Ring Opening Metathesis polymerisation
ROP	Ring opening polymerisation
S. fluitans	*Sargassum fluitans*
S.vulgare	*Sargassum vulgare*
SEC	Size Exclusion Chromatography
SEM	Scanning electron microscopy
TBA	Tetrabutylammonium
TBAF	Tetrabutylammonium fluoride
TGA	Thermo Gravimetric Analysis
TMS	Tetramethylsilane, $(CH_3)_4Si$
UV/vis	Ultraviolet-Visible Absorption Spectroscopy

Chapter 1: Introduction

1.1 **Seaweeds and polysaccharides.**

More than 70% of the world`s surface is covered by water, hosting a wide diversity of marine organisms including algae, and in particular, edible seaweeds, have long been regarded as a good source of fibre and also nutrients e.g. proteins, vitamins and carbohydrates in particular polysaccharides.[1]

Seaweeds are in evolutionary terms amongst the oldest studied living organisms with the blue-green algae (*Cyanophyta*) appearing first. Later red algae (*Rhodophyta*) appeared, followed by green algae (*Chlorophyta*) and finally the brown algae (*Phaeophyta*). Thus, the three major divisions of marine algae are:

-*Chlorophyceae* (green algae)

-*Rhodophyceae* (red algae)

-*Phaeophyceae* (brown algae)**.**

Most algal cells are enclosed by a polysaccharide-rich cell wall, constituting a major deposit of photosynthetically fixed carbon.[2] These polysaccharides, which confer flexibility, enable algae to adapt to the tidal environments in which they grow.

The chemical composition of the algae, including variations in the structure of their polysaccharides will depend on environmental conditions and season in addition to phase of life cycle and particular species.[3]

Polysaccharides are generally long chain biopolymers made up of carbohydrate residues, usually hexoses, linked by glycosidic bonds. Polysaccharides can exist as short oligosaccharide chains and may also be linked to other biopolymers, as in glycoproteins, glycolipids, etc. Those polysaccharides composed of only one kind of repeating monosaccharide are called homopolysaccharides or homoglycans. Molecules can also be formed of two or more different monomeric units and these are known as heteropolysaccharides or heteroglycans.[4]

Polysaccharides from natural sources have gained increased attention with the potential applications ranging from food, personal care products and medical devices, by virtue of their

unique characteristics of biodegradability and biocompatibility. They also possess desirable physical properties, for example some are able to gel and therefore act as thickening and film-forming agents in addition to their capacity to be processed into forms such as fibres, capsules and beads.[3]

The total polysaccharide content in seaweed ranges from 4% to 76% of dry weight.[5] These polysaccharides offer a wide range of important biological useful chemicals of use in, for instance, immunomodulation, and other applications such as antiviral, anticancer, antioxidant, anticoagulant, antiallergy, and anti-inflammation agents.[1] Polysaccharides extracted from seaweeds include Ulvan which is isolated from green algae, Carrageenan and agar from red algae and Laminarans, fucoidan and alginate from brown algae.[6]

Ulvan offers various physiochemical and biological properties of potential interest in food, agricultural, medical, and chemical applications. Ulvan is composed of D-glucose, L-rhamnose, uronic acids, xylose, and sulphate [7] and is used to regulate immune functions and also can act as antioxidant and has antibacterial properties.[8] **Fig (1-1) (a)** shows the disaccharide unit in the structure of Ulvan.

Carrageenans are highly sulphated galactans consisting of a linear backbone of alternating 3-linked-D-galactopyranose and 4-linked-D-galactopyranose and are widely used as food additives, performing functions such as stabilizers, emulsifiers, or thickeners. [9 ,10] **Fig (1-1) (b)** is the structure of Carrageenans showing the disaccharide λ-Carrageenan.

Agar, like carrageenans, are hydrophilic galactans consisting of galactopyranose units with alternating α-1,3 and β-1,4 linkages, but, whereas the α-linked galactopyranose is in the D-configuration in carrageenans, Agar is made up of L-galactopyranose units. Some agars contain traces of its precursor porphyran: D-galactose and L-galactopyranose 6-sulfate agar is used in the food industry as a gelling agent in, e.g., ice-cream and jam, in cosmetics as, e.g., a thickener in creams, and in pharmaceuticals as, e.g., an excipient in pills.[11] See **Fig (1-1) (c)**.

Fucoidan are a family of sulphated homo and heteropolysaccharides that are mainly composed of (1→3)-linked-D-fucopyranose residues. In addition, Fucoidan can have a backbone of alternating (1→3) and (1→4)-linked-L-fucopyranose residues, and sulfate groups are located

mainly at C2, sometimes C4, or disubstituted at both C2 and C4. Additionally, acetyl groups and D-galactose, D-xylose, D-mannose, L-rhamnose, and D-glucuronic acid residues were found to be constituents of fucoidan, see **Fig (1-1) (d)**. Fucoidan have potential use as therapeutics exhibiting anti-inflammatory, anti-tumour, anti-thrombosis and anti-coagulant properties preventing the proliferation of cancer cells.[12,13,14]

Laminarans are a class of low molecular-weight β-glucans consisting of (1→3) -D-glucopyranose residues in which some 6-O-branching in the main chain and some (1→6)-intra-chain links are present and has been shown to possess anti-apoptotic and anti-tumour activities. [13, 15] See **Fig(1-1) (e)**.

The alginates are the major polysaccharide found in brown seaweeds and will be described in this chapter.

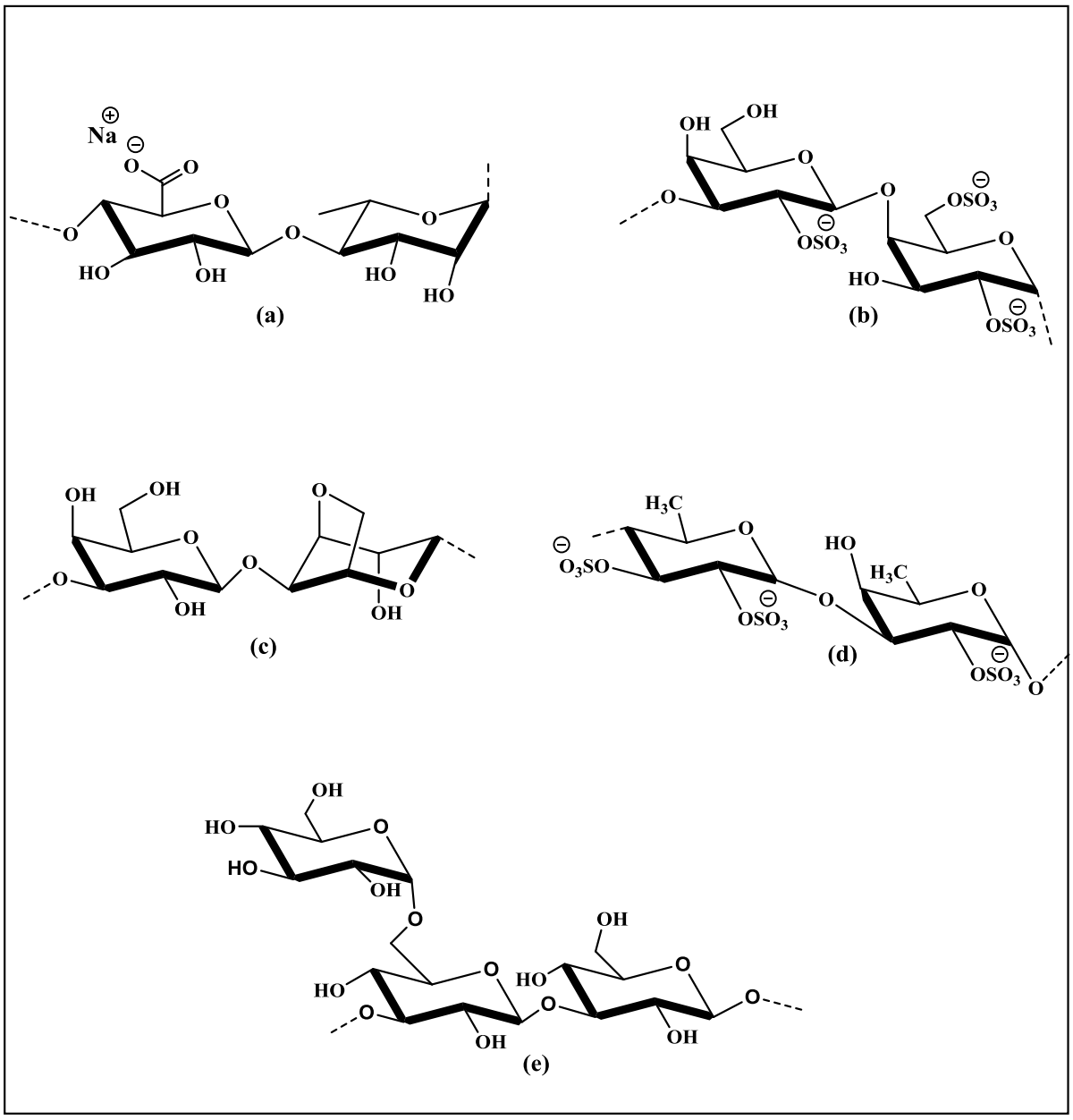

Fig (1-1): Structure of polysaccharides from seaweeds: **(a)** Ulvan from green seaweed,[1] **(b)** λ-Carrageenan from red seaweed,[1] **(c)** Agar from red seaweed,[16] **(d)** Fucoidan from brown seaweed [1] and **(e)** Laminarans from brown seaweed.[17]

1.2 Alginate.

Alginates are a family of poly-anionic copolymers isolated mainly from brown seaweeds. Since they were discovered in 1880s by a British pharmacist Stanford, they have since received great attention. Their many interesting chemical and physical properties resulted in many commercial applications with the industrial production of alginate beginning in California in 1929. [18]

1.2.1 Sources and extraction method.

Alginates are mainly produced from two sources, algae and bacteria. Commercially available alginates are derived primarily from brown algae. Alginate constitutes a key component of the seaweed cell walls and also appears to be present in the intercellular space matrix. Alginate content in seaweeds vary, based on dry weight: *Ascophylum nodosum* contains 22–30%; *Laminaria digitata* fronds, 25–44%; *L. digitata* stipes, 35–47%; *L. hyperborea* fronds, 17–33% and *L. hyperborea* stipes, 25–38%. Alginate contents of between 17 and 45% have been reported in *Sargassum* spp. The common algae species that are commercially important include *Luminaria hyperborea, Ascophyllum nodosum and Macrocystis pyrifera.* In the native state alginate is found as a mixed salt, in both soluble and insoluble forms, of sodium and of calcium and magnesium respectively. These forms are in rapid ion-exchange with sea-water.[6, 19]

The extraction of alginate can be considered as a process in two steps: the transformation of the insoluble alginate into a soluble form, sodium alginate, this is followed by diffusion of the soluble alginate into solution.[20,19,6] The commercial production of alginates is performed mainly by the alkaline extraction processes, as follows.

Brown algae is harvested and dried and subjected to various chemical treatments to remove impurities (e.g. endotoxin, proteins, heavy metals, other carbohydrates and polyphenols) that are normally present. The counter ions are removed through proton exchange using mineral acid. Sodium alginate is then produced by solubilising the insoluble alginic acid with the alkali sodium hydroxide or with sodium carbonate by a process of neutralisation. The material is subjected to a thorough filtration to separate out particulate matter. The sodium alginate obtained is then precipitated directly with alcohol, calcium chloride or a mineral acid, and then is dried see **Fig (1- 2)**.[21]

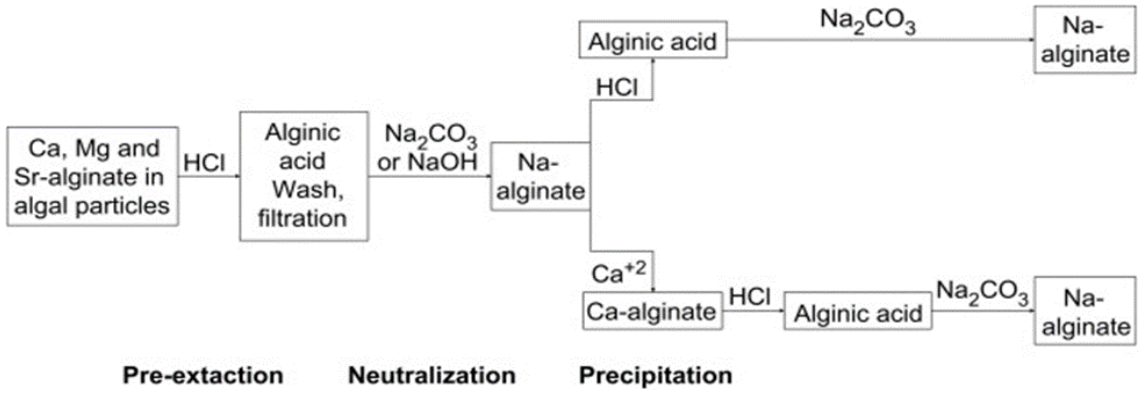

Fig (1-2): Schematic showing alginate extraction procedure from algae.[21]

The alginates isolated from bacterial species such as *Azotobacter* and *Pseudomonas* are not economically viable for commercial use, and are generally used in small-scale research studies.[20]

1.2.2 Chemical composition and confirmation.

Alginate is a linear polymeric acid composed of 1,4-linked *β*-D-mannuronic acid (M) and *α*-L-guluronic acid (G) residues. Mannuronic and guluronic acids are classed as uronic acids. The uronic acids are monosaccharides in which the primary hydroxyl group at C6 has been oxidized to the corresponding carboxylic acid. Their names retain the root of the parent monosaccharides, but the -ose sugar suffix is changed to -uronic acid.

Since its polymeric structure contains two types of monomer acids, alginate can be regarded as a block copolymer of *β*-D-mannuronic acid and *α*-L-guluronic acid. It has been shown that the polymer chain is made up of three kinds of blocks. The GG blocks contain only units derived from L-guluronic acid, the MM blocks are based entirely on D-mannuronic acid and the MG blocks consist of alternating units from D-mannuronic acid and L-guluronic acid.[6,3]

The monomer units of alginate, G and M, are C5 epimers of each other, and occur in pyranosic forms. The orientation of the carboxyl group at the C5 carbon of the six –membered ring is above the plane of the ring in the M epimer and below the plane in the G epimer.[22, 23] Due to the different configuration in the carboxyl group they attain to different chair conformers, i.e. α-L-guluronate favours the $^{1}C_{4}$ conformation while the β-D-mannurate adopts the $^{4}C_{1}$ conformation. As a result, the β (1- 4) glycosidic bond is equatorial in the mannuronate residues but

axial in guluronate residues. Alginates, therefore, exhibit all the types of glycosidic linkages: equatorial-axial (M-G), axial-equatorial (G-M), di-equatorial (M-M) and di-axial (G-G).

As a result, the M-blocks show linear and flexible conformation resulting in the mannuronate chain having a ribbon-like structure. The guluronic acid, with its α (1–4) linkages, introduces steric hindrance around the carboxyl groups, giving rise to a folded and rigid structural conformation in the G-blocks and is responsible for a pronounced stiffness of the molecular chains of the bulk structure. Alternating G and M blocks are considered to produce the most flexible chains.[3, 24]

Alginates extracted from different species of seaweeds differ in M and G content and their M/G ratio. The M/G ratio and their distribution along the chain has an impact on physical properties of the alginates.[3, 24]

The composition and the structure of alginates was found to be affected by season and location, as cited in the literature and is discussed further in **Chapter 3.1**.
The most widely used method for molecular structure determination and characterisation is that of NMR. The basic principle of this method is given in **Chapter 2.1**.

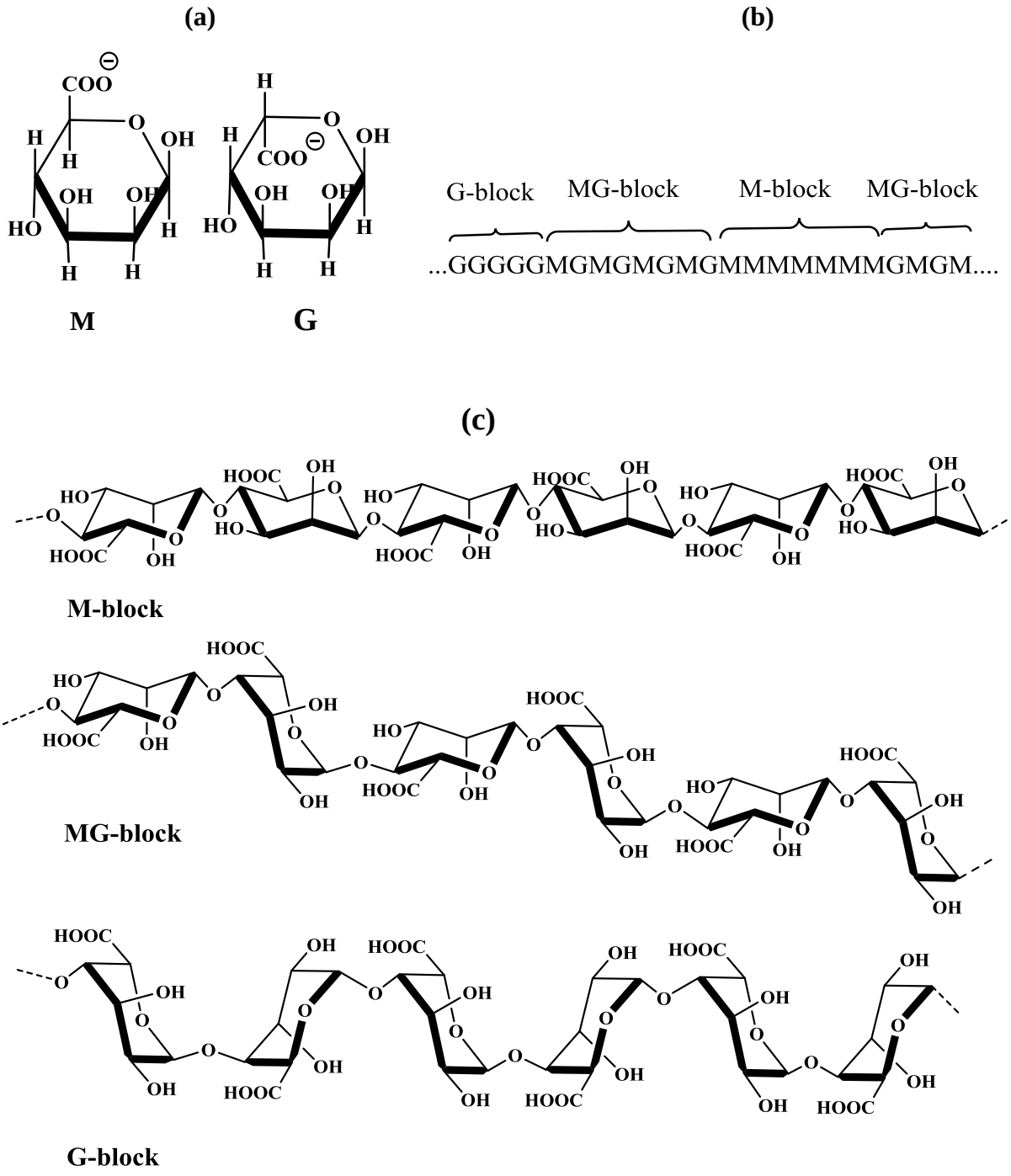

Fig (1-3): Alginate chemical structures: **(a)** Haworth formulas of *β*-D-mannuronic acid (M) and *α*-L-guluronic acid (G) residues, **(b)** block composition in alginate and **(c),** conformation of alginate blocks with M and G in chair conformation $^{1}C_{4}$ and $^{4}C_{1}$ respectively.[25]

The general ^{1}H NMR spectra of alginates normally shows proton's resonance between 3.5 - 5.5 ppm. The anomeric protons which are the characteristic signals of alginate appear at 4.4 –

5.3 ppm as shown in **Fig (1-4)**. G-1(A) refers to the anomeric proton of G residues excluding the G unit at the "reducing end", while M-1M (B4) and M-1G (B3) represent the anomeric protons of M residues adjacent to another M unit or a G unit, respectively. The H5 of G units (C) are more shielded than the other protons in the sugar ring therefore, it resonates upfield. However, the shielding varies with the neighbouring sugar units, such that the chemical shift of H5 of G-units in the GG sequence differs from H5 of G-units in the GM sequence.

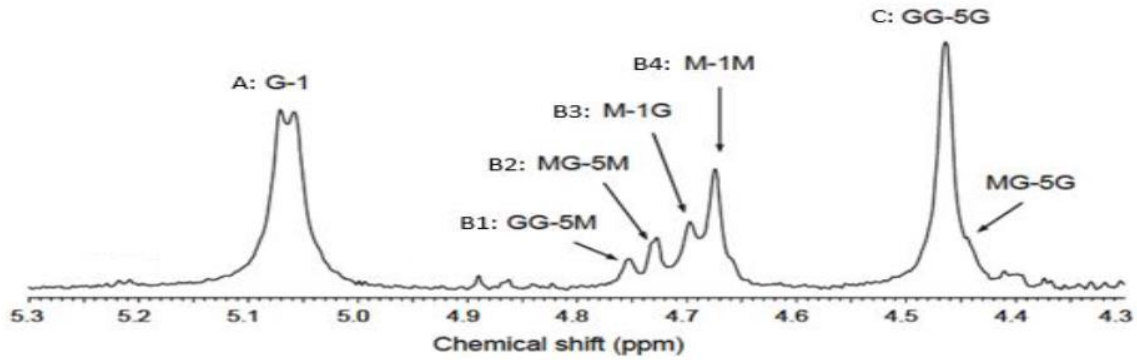

Fig (1-4): ^{1}H NMR spectrum of the anomeric region of an alginate isolated from *Laminaria hyperborean*.[26]

Grasdalen (1983) [26] described a relationship to identify the block length of G and M residues in alginate by calculating the relative integrations of each resonance peaks in which:

G = 0.5(A + C + 0.5(B1+B2+B3))

M = B4 + 0.5(B1+B2+B3)

GG = 0.5(A + C - 0.5(B1+B2+B3))

MG, GM = 0.5(B1+B2+B3)

MM = B4

The boundaries for the integrations of peaks were taken as the midpoint of the curve joining the peak vertical line and the horizontal base line of the peak.

And compositional and diad fractions are calculated as

F_G = G/ (M+G)

F_M = M/ (M+G)

F_{GG} = GG/ (M+G)

F_{MG}, F_{GM} = MG, GM/ (M+G)

While integration of triad's peaks is as following:

GGM, MGG = ((B1)0.5(B1+B2+B3))/ (M+G)

MGM = ((B2)0.5(B1+B2+B3))/ (M+G)

GGG = GG- GGM

1.2.3. Molecular weight.

Alginate is commercial available with molecular weight average between 10^5 and 10^6 g/mol, however, lower molecular weight alginates and alginate monomers can be easily prepared by partial or complete depolymerisation of the polysaccharide chain. Interestingly, the molecular weight of alginate in seaweed has not yet been determined because chain cleavage always takes place during the extraction process. [27]

Both algal and bacterial alginate were found to be polydisperse in their molecular weight.[28] The averages most commonly used are number-average molecular weight (M_n) and weight-average molecular weight (M_w).The ratio of M_w/ M_n represents the polydispersity index (PDI).[29] The polydispersity index is a useful parameter, which allows estimation of the distribution of molecular mass within a given polymer, sample and measures the heterogeneity with respect to molecular weight. Monodisperse polymers have by definition a PDI equal to 1. Typically, non-treated alginate is found to have PDI in the range of 1.5 – 3.[30]

The basic principles and methodology used to determine M_w, M_n and PDI will be discussed in detail in **Chapter 2.3**.

1.2.4 Physical properties.

Physical properties of alginate such as solubility, viscosity and interaction with metal ions are strongly correlated with the chemical structure which differs according to the species, seasons of harvest, geographical locations and age of population.[3]

1.2.4.1 Solubility and viscosity of alginate solutions.

Monovalent salts of alginate are hydrophilic, however the presence of divalent ions which bind strongly to the polymer, reduces the solubility. Alginate solubility is to some extent controlled

by the pH of the solution. The pKa constant of guluronic acid and mannuronic acid are 3.65 and 3.38 respectively, but when the solution pH drops rapidly to below 3 and the carboxylic groups become fully protonated, alginic acid precipitates because it is not fully soluble in water.[28, 31] Indeed, alginic acid is not soluble in most solvent systems. Apart from the pH, the solubility of alginates in water is influenced by several factors including; polymer concentration, molecular weight and sequence. The solubility of the MG block is found to be higher than the M block which is higher than the G block. This is mainly attributed to flexibility and low intermolecular hydrogen bonds in the MG blocks.[30]

To dissolve alginates in organic media requires the synthesis of the tetrabutylammonium (TBA) salt. This allows complete dissolution in polar aprotic solvents containing tetrabutylammonium fluoride (TBAF). TBA-alginate is completely soluble in ethylene glycol, polar aprotic solvents and water provided TBAF is added.[32]

The viscosity of an alginate solution is related to the concentration of alginate and to the length or number of monomer units in polymer chains. At similar concentrations, alginates with longer chains were found to have higher viscosities, this also implies that viscosity of alginate solution can be affected by the molecular weight of the constituent alginate polymers. The intrinsic viscosity is related to molecular weight through the Mark-Houwink-Sakurada (MHS) equation:

$[\eta] = k.M_w{}^a$

Where k and a are constants related to the conformation of a given polymer under specified conditions. There has been some controversy regarding the values of k and a for alginates of different composition, as the literature is not clear-cut. This may be due to the lack of well-defined samples and in particular the presence of aggregates, differences in instrumental setups and data processing. The relative viscosity of the three types of blocks (in 0.1M NaCl) has been found to increase in the order MG < MM <GG based on light scattering data, viscometry and theoretical considerations.[33, 34]

1.2.4.2 Stability.

The glycosidic linkages in alginates are susceptible to degradation by acid hydrolysis, enzymatic or alkaline catalysed β- elimination and oxidative reductive depolymerisation.[35]

Therefore, alginates have to be preserved in certain conditions such as neutral pH with limited heating and be contamination free. The acid hydrolysis of the glycosidic linkage is kinetically a first order reaction. The generally accepted mechanism involves three steps. Firstly, protonation of the glycosidic oxygen produces a conjugate acid in a rapid step. The second step involves the unimolecular heterolysis of the conjugate acid to produce a non-reducing end-group and a carbonium–oxonium ion, this is a slower rate limiting step and is followed by the third step with the addition of water to the carbonium–oxonium ion, forming a reducing end-group and a proton.[35] See **Scheme (1-1)** below.

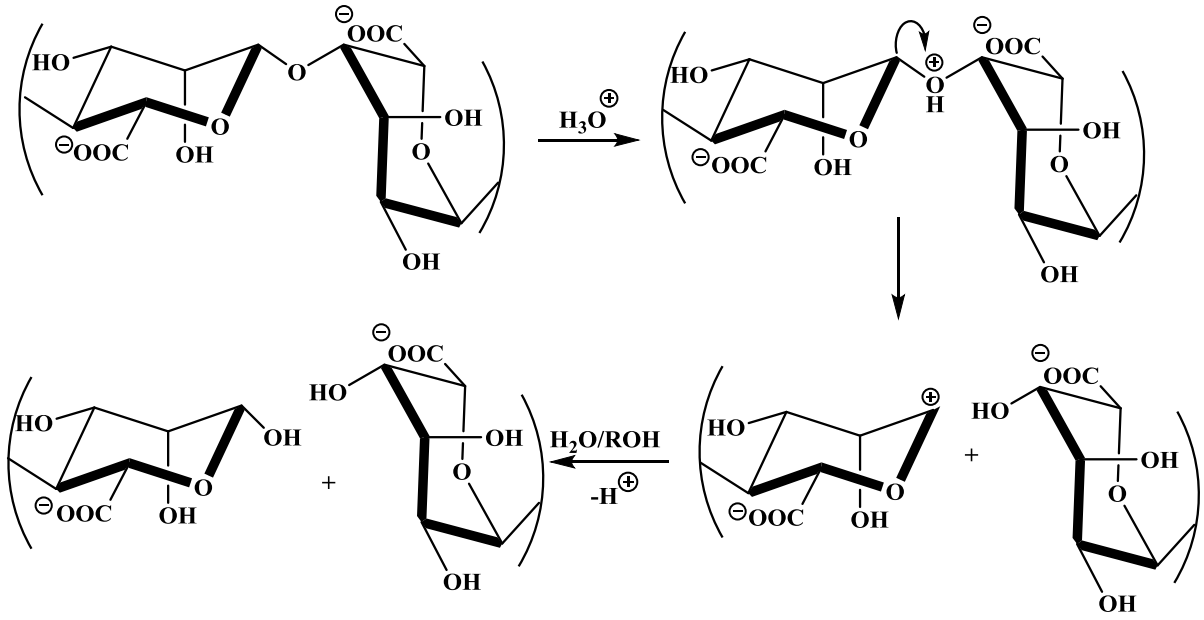

Scheme (1-1): Acid catalysed degradation of the glycosidic linkage of alginate.[21]

The degradation rate under acidic conditions is dependent on hydrogen ion activity and below pH 2, the degradation rate of glycosidic bonds in alginate proceeds at a lower rate than in the correspondent neutral sugars. This is attributed to the inductive effect of carboxyl groups which become fully protonated at low pH, resulting in a lower protonation rate of the glycosidic bond as well as in the electron transfer step.[35] However, above pH 2, the carboxylic group is partially ionized, with the result that the degradation rate is higher than that of neutral sugars under the same conditions. The higher hydrolysis rate results from the contribution of the protonated carboxyl groups ionising to yield protons which then catalyse the glycoside cleavage.[36]

The hydrolysis rates for the various types of glycosidic bonds in alginate was found to vary. The di-equatorial M-M bond undergoes hydrolysis is faster than the di-axial G-G bond between pH 2-4.5. While the hydrolysis rate for the G-M glycosidic bond was found to be greater than the M-G glycoside bond, as mannuronate has a markedly greater tendency than the guluronic acid residues to be at the non-reducing end. Thus, the hydrolysis rate constant found to decrease in the following order: $k_{G\text{-}M} > k_{M\text{-}M} > k_{MG} > k_{G\text{-}G}$.[36]

In strongly alkaline conditions, alginate degrades by means of a β- elimination mechanism, see **Scheme (1-2)**. Initially, nucleophilic abstraction of the proton at C5 is followed by cleavage of the C4-*O*- glycoside forming a new reducing end and simultaneously a 4-5 unsaturated (4-deoxy-Lerythro-hex-4-enepyranosyluronate) non-reducing end.[37] The rate of depolymerisation is also highly dependent on the nature of the C6 group, i.e. whether it is an electron withdrawing or a donating group. Alginate thus shows more stability toward β- elimination than the neutral sugar due to the presence of carboxylic group.[38]

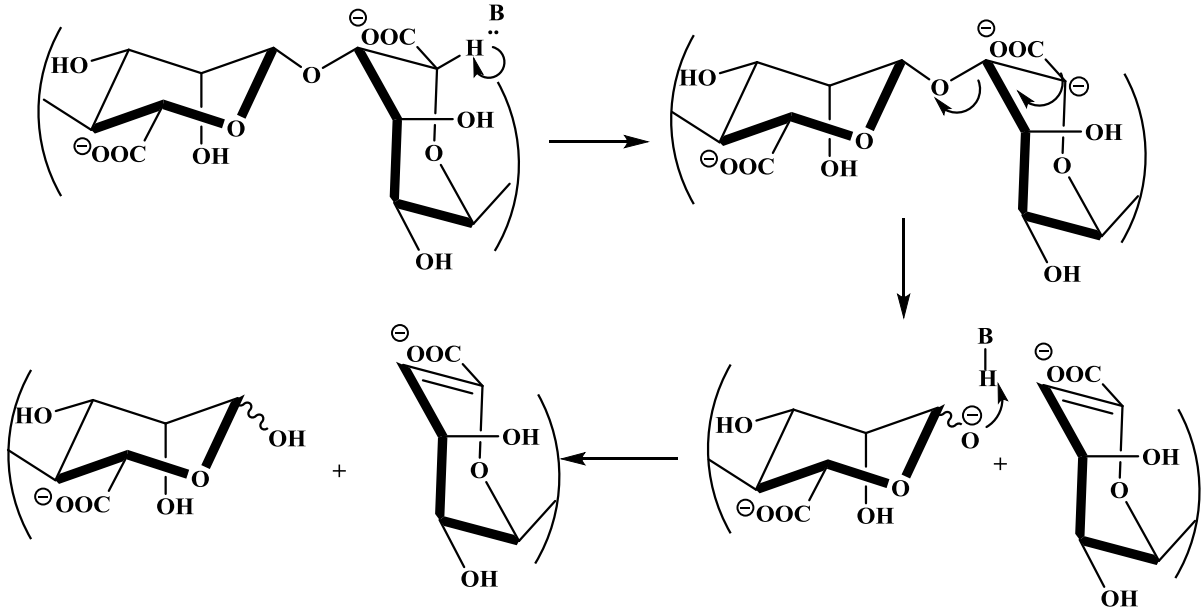

Scheme (1-2): Base catalysed degradation of the glycosidic linkage of alginate (β-elimination).[21]

Alginates chains degradation occurs not just at high or low pH, but also at neutral pH when catalysed by reducing agents. Reducing agents including phenolics, sulphide and sulphate salts and ascorbic acid, often present in algae species can cause degradation of the alginate. These

compounds start a series of reduction reactions resulting in a peroxide that eventually breaks down the alginate through a free radical chain reaction.[21]

1.2.4.3 Ion binding.

The ion binding properties of alginate are important since they determine to a large extent the behaviour of the polymer in solution. Above critical concentrations the binding by different cations leads to the formation of ionically cross-linked gels whose physical properties are dependent on the type and concentration of the ions inducing the gelation. From studies of various pairs of divalent cations, it is found that the binding by divalent ions is a selective process and increases with increased guluronic acid content. The selectivity coefficient, kCa/Mg, is approx. 20 times higher for G blocks compared to M-blocks, indicating that the interaction is not purely electrostatic but may indicate a more favourable co-ordination..[39] The affinity of the alkaline earth metals for G-blocks increases in the order: $Mg^{2+}<Ca^{2+}<Sr^{2+}<Ba^{2+}$ [40] ,whereas, M- and MG-blocks shows little or no preference to these ions. Calcium ions bind to G-blocks in a cooperative process giving rise to the formation of a polymer network,[41] which in terms of molecular structure is described as the "egg-box" model depicted in **Fig (1-5)**.[42]

The minimum number of consecutive G units required to form stable junctions has been investigated by Ca^{2+} activity measurements in solutions of oligo-and poly-guluronates[43] and by studying the size and composition of alginate leaching from alginate gels. [44]

The availability of an alginate with a strictly poly-alternating sequence has made it possible to study the role of MG sequences in calcium alginate gels. Weak secondary MG/MG junctions are also known to exist and were directly demonstrated by Donati *et al.*[45] who made a weak hydrogel from this material. The existence of mixed MG/GG junctions was also confirmed in this study.

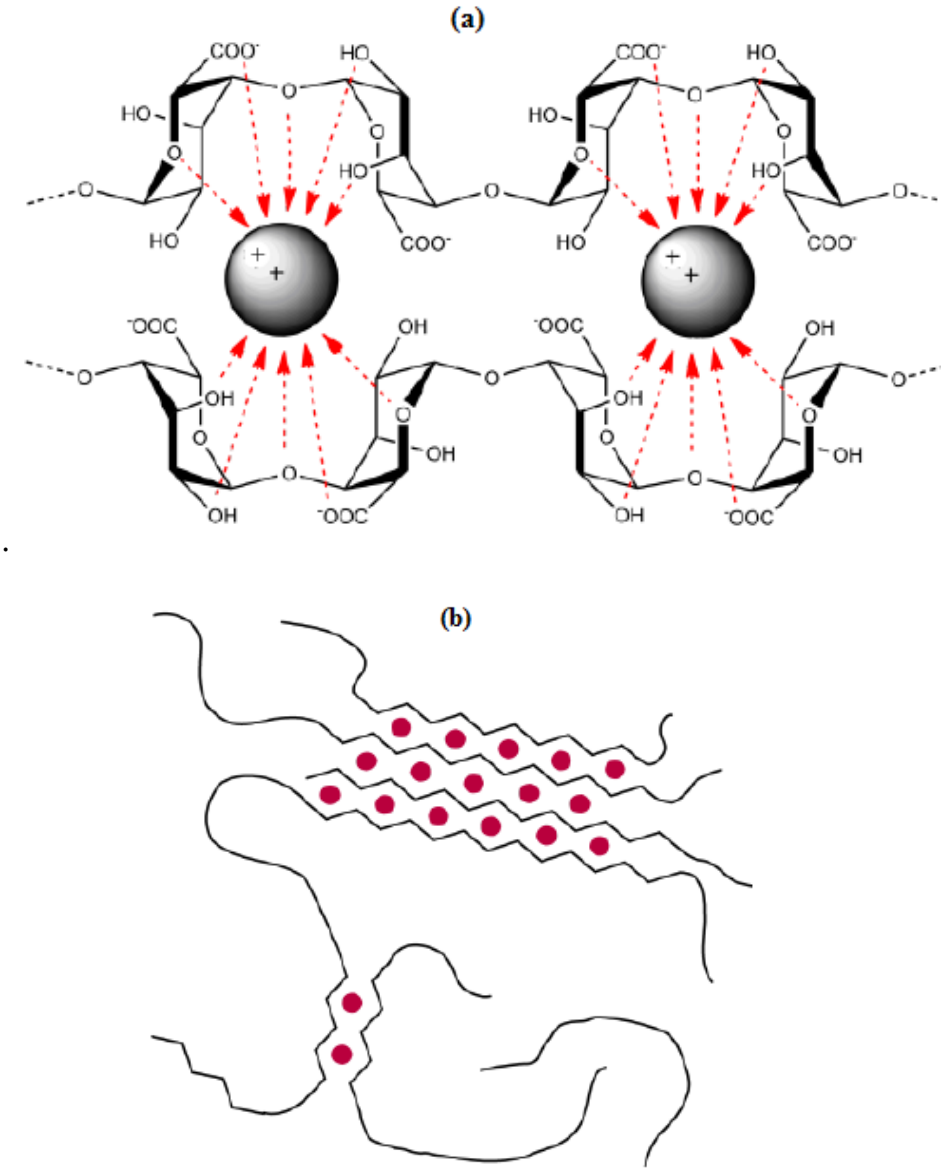

Fig (1-5): The egg-box model: **(a)** formation of junction zone in alginate caused by co-ordination of Ca^{2+} ions between adjacent dimers[25] and **(b)** lateral association of alginate chains.

1.2.5 Chemical modification of alginate.

Alginate has free hydroxyl and carboxyl groups distributed along the backbone. Therefore it is an ideal candidate for chemical functionalization. By forming alginate derivatives through functionalizing available hydroxyl and carboxyl groups, the properties such as solubility, hydrophobicity, physicochemical and biological characteristics may be modified.

1.2.5.1 Chemical modification of the hydroxyl groups.

Typical reactions with the hydroxyl group involve methods such as oxidation, sulphation and phosphorylation, and extends the range of properties, which may be of practical use.

Oxidation

Through oxidization, alginate hydroxyl groups can be converted to aldehydes with significantly higher reactivity.

Sodium alginate was activated using sodium metaperiodate, which oxidises the two secondary hydroxyl groups at C-2 and C-3 positions under rupture of the carbon–carbon bonds giving rise to two aldehyde groups, **Scheme (1-3)**.[46]

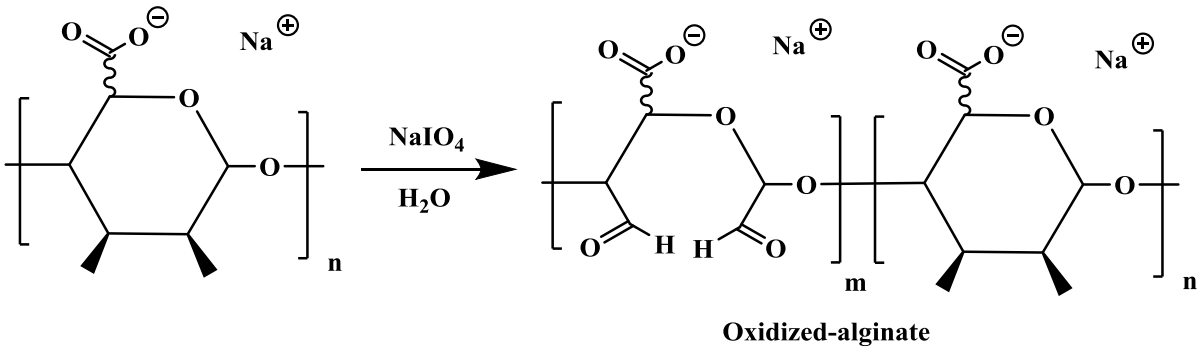

Scheme (1- 3): Oxidation of sodium alginate.

Gomez *et al.*[47] were able to synthesize oxidized alginates at ambient temperature within 24 hours using sodium periodate in the dark, in an aqueous sodium alginate solution. Oxidation of alginate chains produced a decrease in the stiffness of the polymer by breaking the C2–C3 bond by chain scission. For over 10 % mol oxidation, it was observed that gels were not formed in excess of calcium.

To improve the biodegradability of alginate an oxidation reaction was performed with sodium periodate using commercial high molecular weight alginate.[48] The oxidized alginate fully degraded when tested under physiological conditions (37 ˚C, at pH 7.4 in PBS) and incubated for 100 hours. It was found that the molecular weight reduced from 11.2×10^4 g/mol to 3.6×10^4 g/mol.

Partial oxidation of alginates may be of use for biomedical applications because they degrade in aqueous media, while unmodified alginates do not.[49]

Sulphation.

Sulphated alginate acquires blood compatibility because the structure has similarity to heparin, which has been used in anticoagulant therapy for the past 60 years.[50] Yumin *et al.* performed the first sulphation of sodium alginate by reaction with chlorosulfonic acid in formamide,[51] see **Scheme (1-4)**. The *in vitro* anti-coagulation demonstration of human plasma containing the sulphates showed that alginate sulphates possessed high anticoagulant activity, especially, with regards to the intrinsic coagulation pathway.

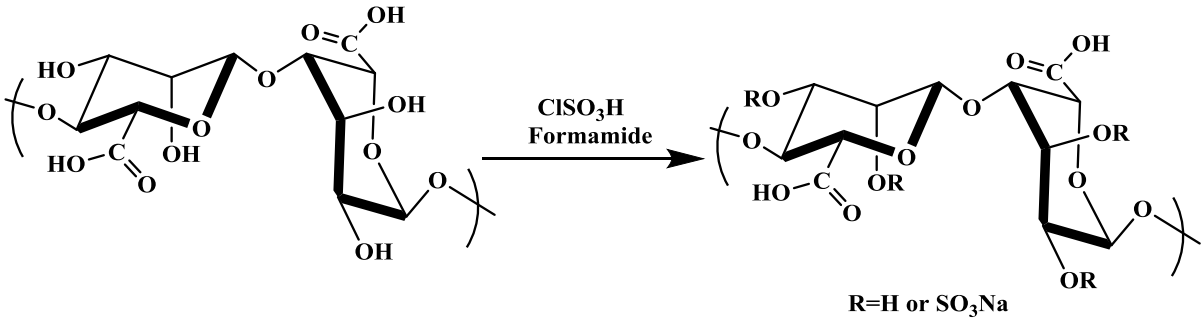

Scheme (1-4): Sulphation of sodium alginate.[21]

Fan *et al.*[52] used an uncommon reagent and performed the sulphation of alginates using sodium bisulphite and sodium nitrite in an aqueous solvent. Standard methods of sulphation use reagents such as sulphuric acid and chlorosulfonic acid, which cause hydrolysis of alginates. The method by Fan *et al*. overcomes this limitation.

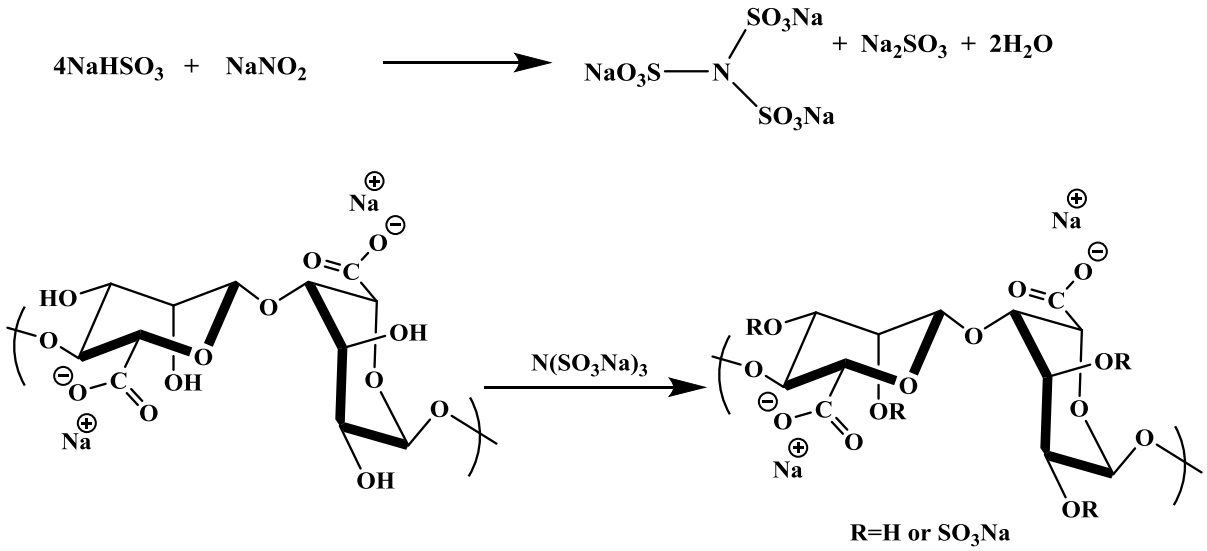

Scheme (1- 5): Sulphation of alginate using sodium bisulphite-sodium nitrite reagents.[52]

Phosphorylation.

Phosphorylated alginate derivatives have been synthesised to evaluate their capacity to induce hydroxyapatite nucleation and its growth.[53] Phosphorylation was performed employing urea/phosphoric acid as a reagent requiring the creation of a suspension of alginate in DMF, see **Scheme (1-6)**. However, as a strong acid, phosphoric acid may give rise to alginate degradation.

The regio-selectivity of the phosphorylation at four possible substitution sites (2-OH and 3-OH positions of each G and M residue) has been studied. The analysis found phosphate substitution on M residues with greater phosphorylation occurring at the 3-OH site when compared to the 2-OH site. This regio-selectivity resulted from the higher reactivity of the equatorial 3-OH site. Equatorial sites are thought more accessible compared to axial during phosphorylation. The regio-selectivity between 3-OH and 2-OH sites was much weaker for G residues compared to those for M residues. Reduction in molecular weight during reaction as well as conformational changes as a result of phosphorylation are possibly the reason why these alginate-phosphate derivatives fail to form gels. Ca^{2+} cross-linked gels can, however, be formed by mixing unreacted alginate with phosphorylated alginate. Gels made from alginate blends were more resistant to calcium extraction than gels formed from unmodified alginates. It is thought that phosphate groups were likely to have participated in the chelation, thus conferring more stability to the gels.

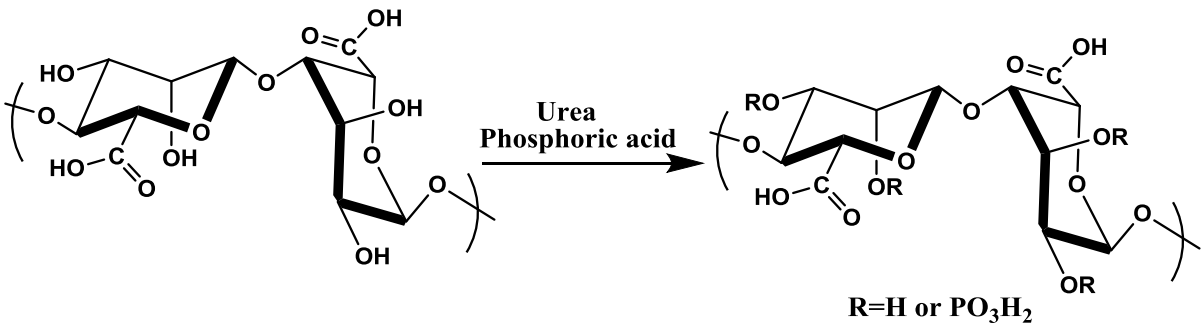

Scheme (1-6): Phosphorylation of alginate.[53]

1.2.5.2 Chemical modification of the carboxyl group.

Esterification and amidation are two examples of modification of alginate using the -COOH site. A coupling agent, such as 1-ethyl-3-(3-dimethylaminopropyl) carbodiimide hydrochloride (EDC-HCl), is usually required for this reaction to take place.

Amidation.

The hydrophobically modified alginate (Alg-CONH-C8) was synthesised by coupling n- octylamine to the backbone carboxylic acid groups using EDC-HCl to form amide linkages between the amine-containing molecule and the carboxylate moieties of the alginate polymer backbone, see **Scheme (1-7)**.[54]

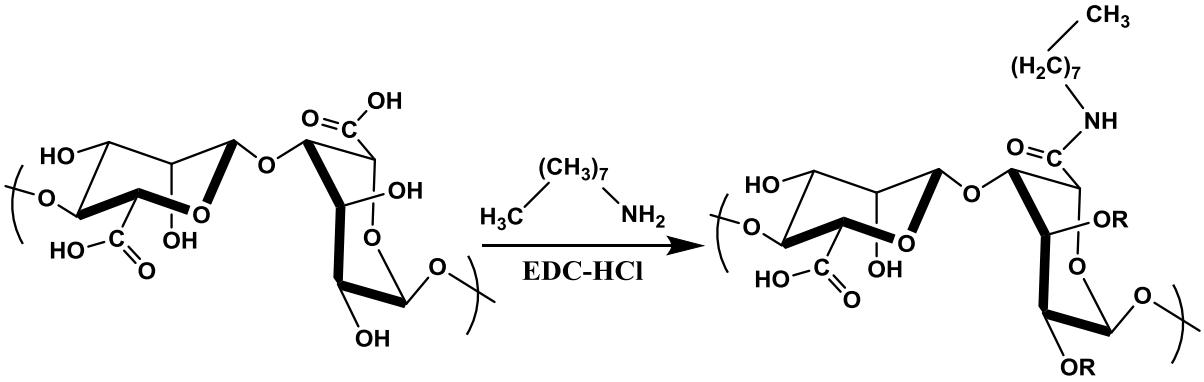

Scheme (1-7): Reaction scheme for the synthesis of (Alg-CONH-C8).[21]

The mechanism of carbodiimide mediated coupling of carboxylic acids to amines is depicted in **Scheme (1-8).**

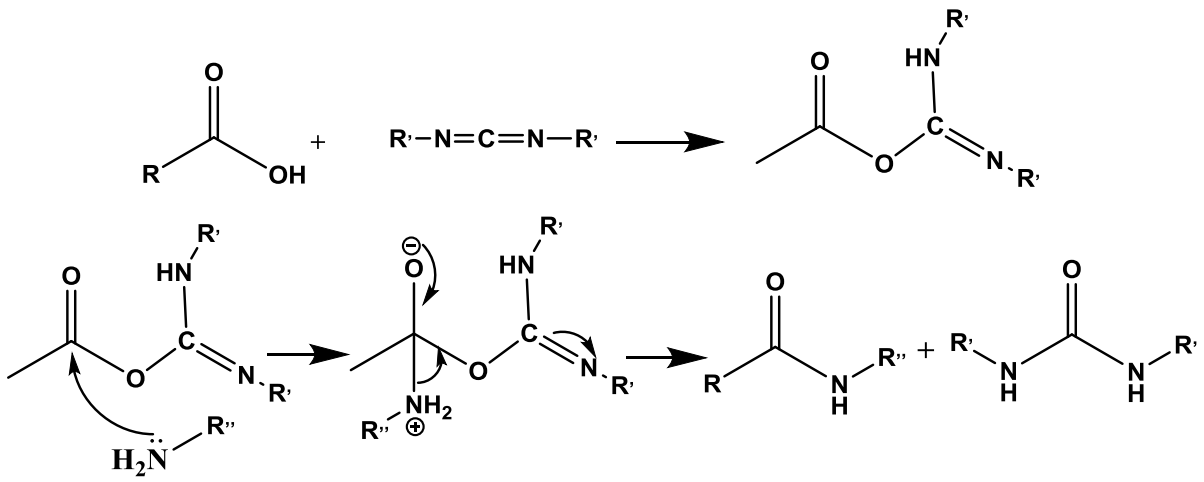

Scheme (1-8): Mechanism of carbodiimide mediated coupling of carboxylic acids to amines.[21]

Abu-Rabeah, *et al.* [55] demonstrated the coupling of N-(3-aminopropyl) pyrrole to alginate via an amide linkage by means of a two phase (hydrophilic/hydrophobic) reaction using a carbodiimide-mediated activation to produce a pyrrole−alginate conjugate. The pyrrole–alginate conjugate prepared to 30% molar modification can be efficiently electro-polymerized, to provide a biocompatible matrix capable of retaining enzyme molecules by the mechanism of gellification and by electrochemical cross-linking.

Amphiphilic derivatives of sodium alginate can be prepared by covalent attachment of dodecylamine to the polysaccharide via amide bonds with different substitution ratios, using 2-chloro-1-methylpyridinium iodide (CMPI) as the coupling reagent, **Scheme (1-9)**. This reaction requires alginate to be converted to its acidic form, and then neutralized to pH 7 with TBA hydroxide. The resulting TBA-alginate salt was dissolved in DMF, then CMPI and an excess of dodecylamine was added. Triethylamine was added to the solution at a concentration of the same order to that of dodecylamine. Aqueous NaCl was then added in order to facilitate exchange of the TBA^+ by Na^+ ions. Finally, the polymers were purified by means of a precipitation in 7:1 EtOH–water, then washed and dried under low pressure.[56]

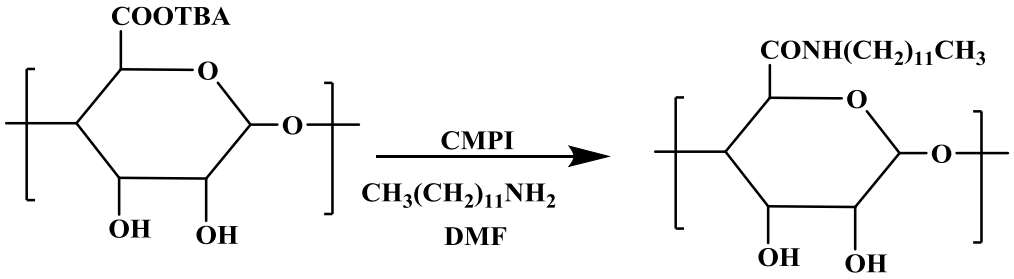

Scheme (1-9): Amidation of alginate using CMPI as coupling agent.[57]

Esterification.

Native alginate can undergo direct esterification with many alcohols in the presence of a catalyst. The alcohol should be present in excess to ensure that the equilibrium is in favour of product. These reactions enable an alkyl group to be added to the backbone-structure of the alginate and enhance its hydrophobic properties. Of the esterified derivatives of alginate, the only derivative of commercial value is the propylene glycol esters of alginate (PGA) made by esterification of alginate with propyleneoxide.[58]

Broderick *et al.*[59] reports the synthesis of the butyl ester of alginate by means of the esterification of sodium alginate with butanol in the presence of the catalyst concentrated sulphuric acid. The ester is capable of encapsulating both hydrophobic and hydrophilic molecules. Importantly, the gelling and non-toxic properties of the native alginate were retained.

Esters of alginates, **Scheme (1-10),** can also be prepared from alkyl halides and the alginate TBA salts in a homogeneous medium. Dodecyl chains are covalently linked to the carboxylate groups of the backbone by this method. The TBA-alginate for the procedure was synthesized by converting Na-alginate to alginic acid and subsequently neutralised with TBA^+ OH^-. This reaction was carried out using a dodecyl bromide reagent making use of a nucleophilic displacement.[60 , 61]

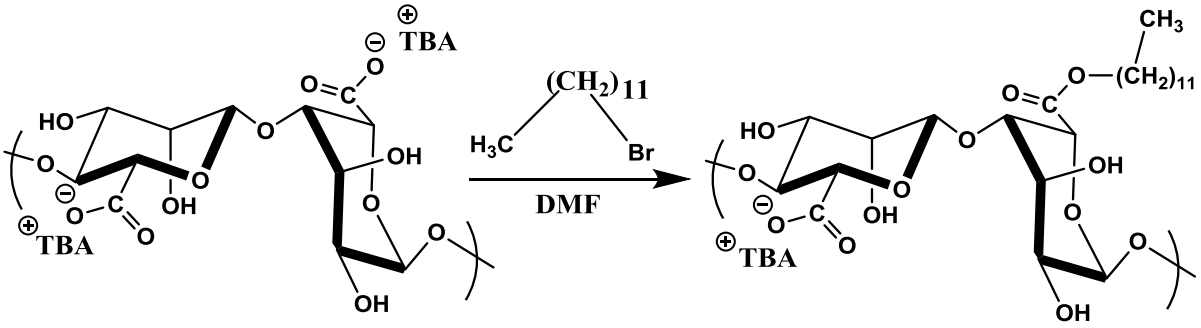

Scheme (1-10): Esterification of alginate.[21]

1.2.5.3 Graft copolymerization of alginate.

Graft copolymerization is accepted as a powerful method for derivation and the modification of the physical and chemical properties of alginates. Grafting synthetic polymer chains to the alginate backbone via hydroxyl and or carboxyl groups affords a means of introducing steric bulkiness and hydrophobicity, which prevents the polysaccharide backbone from undergoing rapid dissolution and erosion.[21] The grafted polymers can be synthesized by conventional redox grafting methods, by microwave irradiation, gamma-ray irradiation and using an electron beam.[62] In **Chapter 4.1** more details about the grafting technique will be discussed.

Liu and Cao [63] produced a superabsorbent, resistant to saline solution and prepared from a copolymer of sodium acrylate with sodium alginate, **Scheme (1-11)**. They showed that the superabsorbent when allowed to swell in either distilled water or in a 0.9% aqueous solution of NaCl, at room temperature for 30 min, the water absorbency was approximately 1000 and 85 times its own mass in each medium, respectively. Meanwhile, the superabsorbent also had excellent hydrogel modulus. In addition, grafting reaction can also take place at the hydroxyl group site.

Sen *et al.* [62] report the synthesis of graft copolymers of acrylamide and alginate using microwave irradiation to generate free-radical sites within the polysaccharide backbone, grafting occurs at hydroxyl sites. This copolymer was trialled as a commercial flocculent for kaolin suspensions and it was also found that the copolymer, containing a higher percentage grafting with high molecular weight was a good flocculent for coal suspensions.

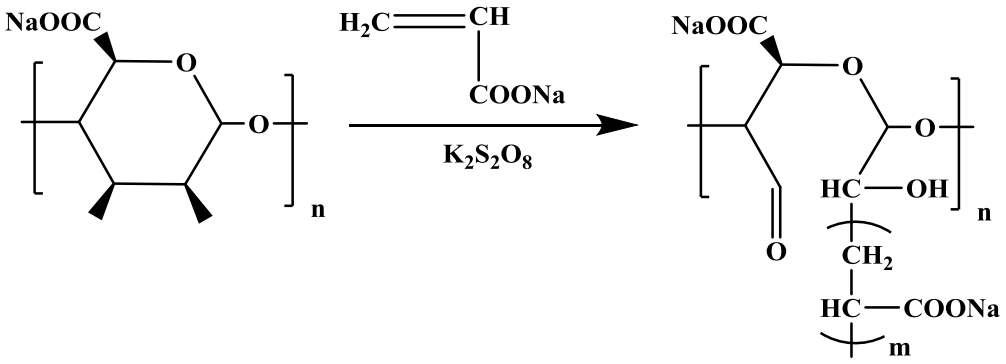

Scheme (1-11): Copolymerization of sodium acrylate with sodium alginate.[57]

Sand *et al.* [64] reported an alginate-g-vinyl sulfonic acid prepared by a potassium peroxydiphosphate/thiourea redox system. The graft copolymer showed improved performance for metal ion uptake, swelling, flocculation and resistance to biodegradability in comparison to alginate.

A novel amphiphilic cholesteryl ester of alginate has been synthesized as a graft with cholesterol chains attached to the alginate backbone. This sodium alginate derivative was grafted with 3 cholesteryl groups per 100 hexuronic acid residues (CSAD-3).
N, *N*′-dicyclohexylcarbodiimide was employed as a coupling agent and 4-(*N*, *N*′-dimethylamino) pyridine was used as a catalyst, the reaction was performed at room temperature. The reaction occurs between the carboxylic groups of the protonated sodium alginate with the hydroxyl group of the cholesterol, over 24 hours, and is illustrated in **Scheme (1- 12)** which is adapted from the reaction scheme given by Yang *et. al.*[65] . CSAD-3 forms more stable and compact nano-scale self-aggregates in aqueous NaCl solution compared to the parent sodium alginate. The stability of these nano-self-aggregates arises from intra- and intermolecular hydrophobic interactions between the cholesteryl grafts. CSAD, therefore, has potential as novel material able to self-aggregate and able to encapsulate hydrophobic compounds such as pyrene.[65]

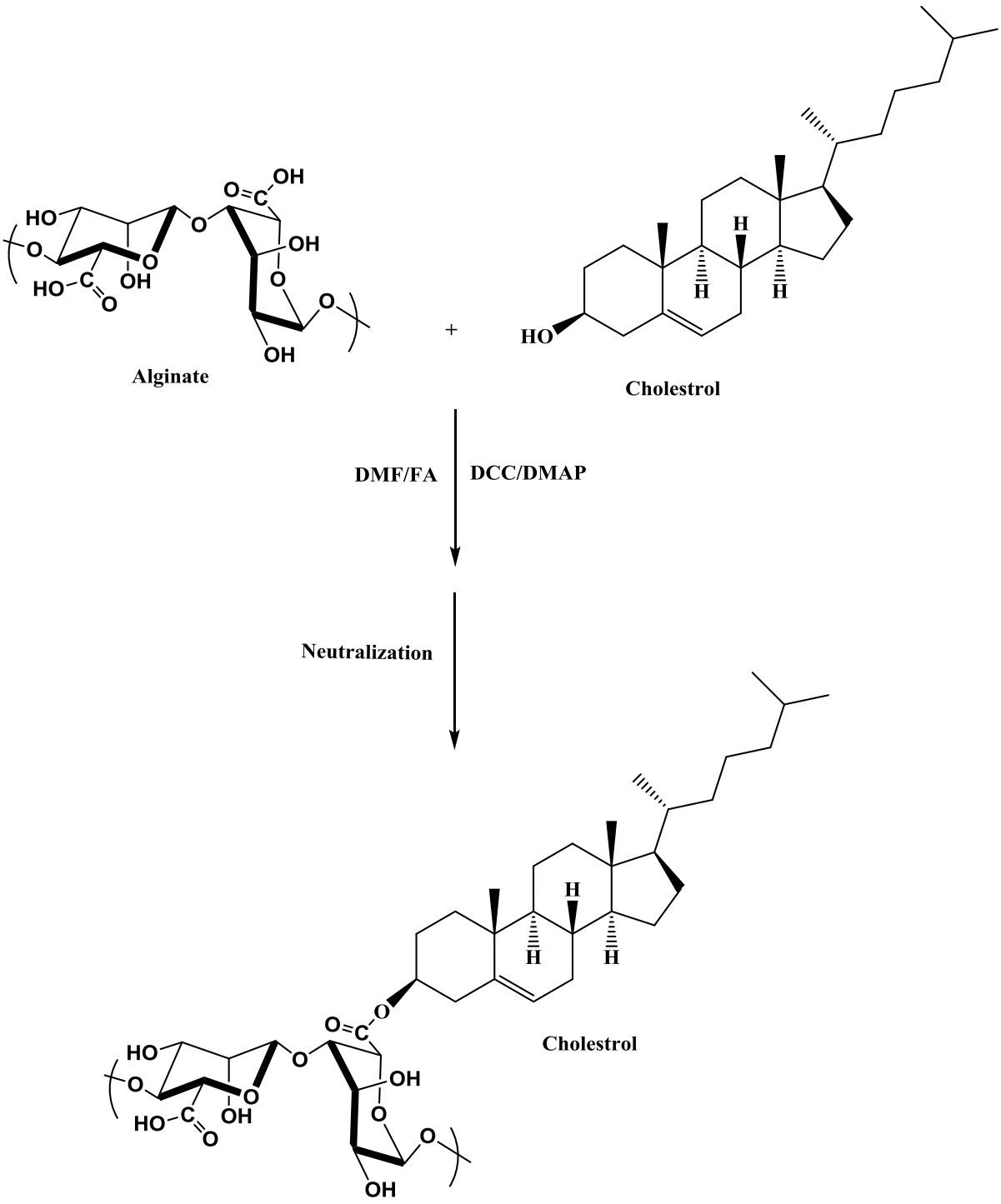

Scheme (1-12): Cholesterol-g-alginate.[65]

1.2.6 Alginate hydrogel.

Gel formation is a very important characteristic for alginates. Alginate is typically used in the form of a hydrogel in regenerative medicine, including wound healing, drug delivery and tissue

engineering applications. Hydrogels are three-dimensionally cross-linked networks composed of hydrophilic polymers with high water content. Hydrogels are often biocompatible, as they are structurally similar to the macromolecular-based components in the body, and can often be delivered into the body via minimally invasive administration.[66]

1.2.6.1. Method of gelling.

Chemical and/or physical cross-linking of hydrophilic polymers are typical approaches to form hydrogels. Hydrogels can be classified into two groups based on type of cross-linking.

In physical gels, the nature of the crosslinking process is normally achieved via utilizing physical processes such as association, aggregation, crystallization, complexation, and hydrogen bonding. On the contrary, chemical covalent crosslinking is utilized to prepare a chemical hydrogel with permanent junctions, while physical networks have transient junctions that arise from either polymer chain entanglements or physical interactions such as ionic interactions, hydrogen bonds, or hydrophobic interactions.[67, 68]

Ionic gels are prepared by ionic cross-linking with multivalent cations. This is the most common method for the formation of alginate gels. This method can take place under gentle conditions, making it ideal for the entrapment of sensitive materials. The gelation of alginate occurs by an exchange of sodium ions from the guluronic acid (G) blocks with multivalent cations, and the stacking of these G blocks to form a characteristic "egg-box" structure.[69 , 70]

Each chain can be linked with many other chains, resulting in the formation of a three dimensional gel network. These gels can have water contents greater than 95%.[71] Gels prepared from alginates with a high G content tend to form stronger, stiffer, more brittle and more porous gels. It has also been reported that the higher the G content, the greater the restriction to solute transport. Conversely, high M content results in gels which are more elastic and weaker. Various cations show different affinity for alginate, whereof calcium is most frequently used for alginate gelation, but calcium does not form the strongest bonds with alginate. Monovalent cations and Mg^{2+} ions do not result in the formation of a three-dimensional gel network.[69]

The gelation of alginate solutions with cations can occur through external gelation, internal gelation and gelation upon cooling.[33] More discussion on external and internal gelation of alginate are covered in **Chapter 5.1**.

The gelation via the cooling method uses an alginate solution with a calcium salt at elevated temperatures (90 °C), which is then allowed to set through cooling.[72] The elevated temperature in this method makes it less gentle and is unsuitable for thermally labile material.

Acidic gel. Alginate solutions treated at a pH below the pK_a of the uronic acid can, under certain conditions, lead to the formation of acid gels. The latter, in contrast to ionic gels, are equilibrium gels, which have been shown in swelling studies, to be stabilized by hydrogen bonding. It has been shown that the gel strength of acid gels becomes independent of pH below 2.5. However, acid hydrogels resemble ionic ones in the sense that the gel strength seems to be correlated with the content of G-blocks in the alginate chain, pointing to a possible cooperativity in the gel formation process. With the exception of some pharmaceutical uses, the number of applications for alginic gels is so far limited.[30]

Chemical gel. Chemical cross-linking is an attractive strategy for overcoming drawbacks in ionic –crosslinking which are, unfortunately, subject to limited stability *in vivo*. In ionic cross-linked gels in physiological media, ion exchange with monovalent ions causes destabilization and rupture of the gel. Covalent cross-linking can create a more stable and robust network.[21] However, covalent cross-linking reagents may be toxic and the unreacted chemical needs to be removed thoroughly from the gel.

Covalent cross-linking of alginate with poly (ethylene glycol)-diamines of various molecular weights was first investigated in order to prepare gels with a wide range of the mechanical properties. The elastic modulus initially increased gradually with an increase in the crosslinking density or weight fraction of poly(ethylene glycol) (PEG) in the gel.[73] The introduction of hydrophilic cross-linking molecules as a co-polymer (e.g. PEG) can compensate for the loss of hydrophilic character of the hydrogel resulting from the cross-linking reaction.[74]

Another example of covalent cross-linking of alginate has been investigated using glutaraldehyde, see **Scheme (1-13)**.[21]

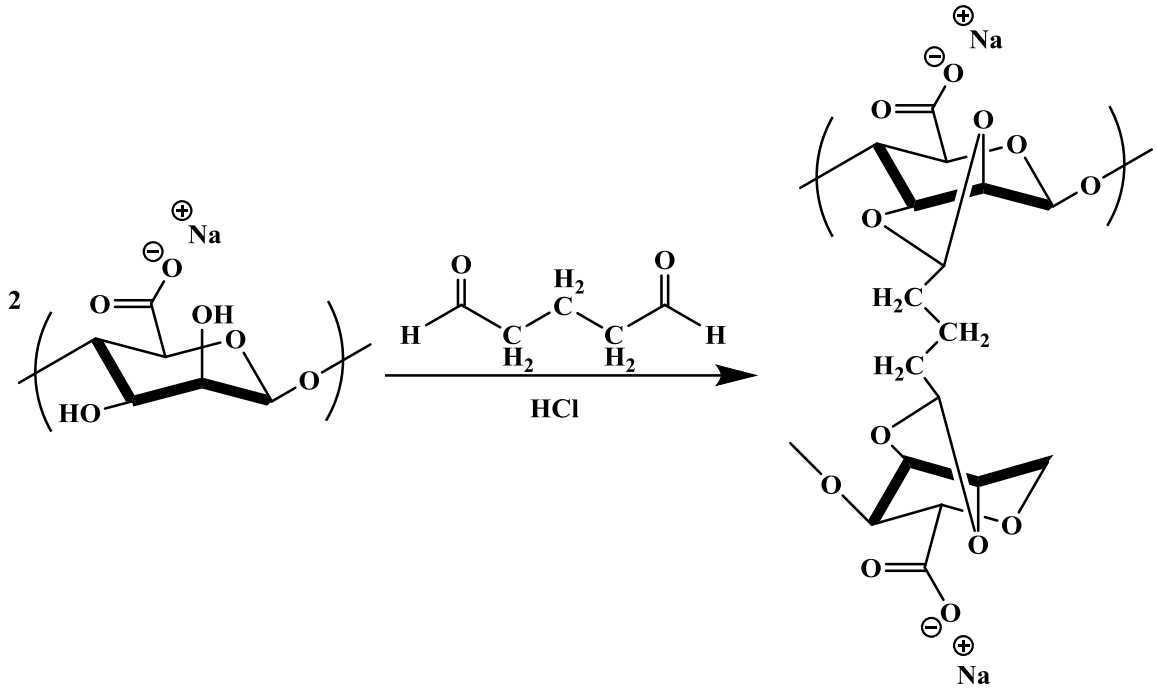

Scheme (1-13): Reaction scheme for covalent crosslinking of Na-alginate using glutaraldehyde.[21]

Neufeld *et al*.[75] studied the reaction kinetics of alginate crosslinking by glutaraldehyde. The reaction rate was found to be independent of the alginate M/G composition and sequences. Thus, both M and G were equally reactive towards glutaraldehyde. However, the reaction rate increased with an increase in the alginate molecular weight. Higher molecular weights caused lower mobility of chains, thus improving the probability of collision with glutaraldehyde.

.

1.2.6.2 Hydrogel properties.

Hydrogels are generally characterized by their ultimate capacity to absorb liquids (swelling thermodynamics), the rate at which the liquid is absorbed into hydrogel structure (swelling kinetics), as well as their mechanical properties.[68]

Hydrogels and their physicochemical properties are highly dependent on the kind of cross-linking and the cross-linking density, in addition to the molecular weight and chemical composition of the polymers.[76, 77]

"**Syneresis"** is the term used to describe the slow shrinking of alginate upon increasing the divalent cross-linking ion concentration.
Macroscopically, syneresis is detected as a release of water from the gel with a consequent decrease in its dimensions and increase in polymer concentration and defined as:

$S = ((W_0-W)/ W_0) \times 100$
where W_0 and W is the initial and final weight.[78]

The alginate gel shrinkage has been reported to depend on the composition of the alginate sample. In fact, alginates containing long G-blocks will shrink less than alginates with shorter G-blocks owing to the formation of strong irreversible junctions, thus hindering reorganization of the network structure.[79] A high degree of syneresis has been attributed to the amount of alternating sequences (MG-blocks) through a "zipping" mechanism between secondary MG/MG junctions, leading to a partial network collapse under calcium-saturated conditions.[80] In addition, syneresis increases with increasing calcium concentration, gelling time,[79] and alginate molecular weight.[78]

The mechanical properties.
The mechanical strength of a gel is often characterised using Young's modulus (E), which is defined as:

$E = (F/A) / (\Delta L/L)$
Where F is the force required to compress a material with contact surface A to a fraction ΔL of the total length. It is a function of the number, the stability and length of cross links in addition to the length and flexibility of elastic domains between junction zones.[81]

Since G-blocks form the primary junction zones in calcium cross-linked alginate gels, the rigidity is observed to increase with the content of guluronic acid and with the average G-block length[82,83] as might be expected. The presence of divalent ions possessing a greater affinity for the G-blocks result in a stronger gel as a consequence of the strength and number of stable crosslinks increases.[84]

Furthermore, a higher average number of junction zones in each chain, indicates that the molecular weight is important and thus the modulus is found to increase with increasing molecular weight up to about $2.4x10^5$ Da, independent of alginate concentration. Syneresis should be considered when rigidity is compared between different alginate gels since

$E = k \cdot C_{Alg}^2$

where C is the concentration of alginate.[79]

Rubber elasticity theory when applied to synthetic polymer networks can be used to calculate the deformation properties. The theory models networks as point-like cross links between flexible coils in which energy is stored in the form of reduced entropy when under deformation.[85]

Although some predictions hold for alginate gels, Modulus-Mw dependency for instance, and a low ratio of the loss and storage moduli compared to the low frequency dependency (in the range 0.01 to $50s^{-1}$), a complete description of the stress-strain curves for alginate gels has not been achieved.[86]

Since an alginate networks consist of junction zones and not points and the lengths of elastic chains between the junctions are too short and cannot be considered as flexible coils, the main assumptions in rubber elasticity theory do not apply. The temperature dependence of modulus in alginate gels is found to be negative and, therefore, the elasticity is enthalpy driven.[86, 87]

Rupture strength and deformation at rupture is relevant for many of the applications where large deformations often result such as when alginate hydrogel is used as a scaffold e.g. in bone-tissue engineering. Alginate gels, in common with many other biopolymers, show strain-hardening behaviour, which is thought to result from deformation of junction zones.[88]

Fracture in alginate gels may be described as a cascade process, the junction bearing the highest stress gives way first and the energy released contributes to the breakage of neighbouring junctions. Rupture strength is dependent on the number and length of crosslinks, but is also on how stresses are distributed through the gel. High modulus gels, a consequence of high G content, are, in general, more brittle than the low-modulus gels with their high M content, and which also possess a higher number of network chains. If alternating sequences of low G content alginates are enriched by epimerization with the enzyme mannuronan C-5 epimerase (AlgE4), this will lead to an increase in both rupture strength and deformation at rupture.[89] MG/MG junctions act as weak reels when embedded in the network acting to dissipate applied stress by sliding over one another.

1.2.7 Applications of alginate.

Most of the present applications of alginate are based on either its rheological properties i.e. water binding, viscosity and shear thinning, or the unique gelling characteristics allowing temperature independent gelling under physiological conditions. Commercially available alginates are extracted from algae with an annual production estimated to about 38,000 tonnes.[90]

Industrial applications of alginates include its use as a thickener in water soluble textile printing paste, glazing of paper, creaming of latex and as a water binding agent in the production of ceramics.[91] Alginates are also widely used in the food industry and biomedical applications.

1.2.7.1 Food industry.

Alginates have been classified as safe for additive-level use both in the EU and in the USA and have high bioactivity at low concentration.[30] Alginates are available at a wide range of viscosities, offer stability to foodstuffs under both high and low temperatures, and therefore have a wide range of uses as **gelling agents**. As alginates form gels at low temperatures, this is particularly useful in the restructuring of foodstuffs that may become damaged or oxidised under high temperatures (e.g. meat products, fruits and vegetables). The most common restructured foods produced using alginates are reconstituted onion rings and pimento sections for use in olives.[92] For both of these products, alginates allow the production of products of uniform size and consistency. In these two cases, restructuring also greatly facilitates mass production of these products. Alginates also have a number of similar applications in meat,[93,94] seafood,[95] fruit,[96] vegetable[97] and some extruded food products e.g. pastas and noodles.[92]

Alginates are commonly used as **thickening** agents in jams, marmalades and fruit sauces, as alginate–pectin interactions are heat-reversible and give a higher viscosity than does either individual component.[92] Alginates are also used to thicken desserts and savoury sauces, including mayonnaise [98] they can be used for a number of stability applications in food processing.[99] Routine use of alginates in bakery creams endows the cream with freeze/thaw stability and reduces separation of the solid and liquid components (syneresis) [92] it also increases heat-shock resistance, reduces shrinkage and ice crystal formation, and endows the ice cream with the desired melting characteristics.[100]

Alginates is one of many polysaccharides which in addition to proteins have been used as edible coatings for a number of foodstuffs. Food coatings made from sodium alginate have excellent tensile strength, resistance to tearing and mechanical flexibility, and are impermeable to food oils. However, because of the porous nature of alginate gels, these coatings have a high permeability to oxygen and water.[101]

1.2.7.2 Biomedical and pharmaceutical applications.

Alginate has been used as a gelling agent in moulds to obtain dental impressions,[102] as a stabilisation factor for emulsions used in cosmetic preparations and as a binder in lozenges and tablets. Alginate fibres/film are used in haemostatic bandages and gastro-enteric coatings for tablets, in particular, the sodium or calcium salt of alginate have been used as a haemostatic for many years.[103 ,104] Alginate is used as a pharmaceutical in the treatment of oesophageal reflux. An alginate solution also containing dissolved sodium bicarbonate gives rise to a buoyant acid gel with entrapped CO_2 in the presence of gastric juice and can therefore, serve as a mechanical barrier to prevent reflux of the stomach contents into the oesophagus.[91,105]

Alginate can also be woven into gauze dressings when used in the form of calcium alginate fibers, and these can form an adherent biofilm absorbing exudate, providing a moist environment for wound healing.

The high M-content of alginates is known to have an immune stimulating effect which may also be utilized in this context in the treatment of chronic wounds. A well-known absorbent and haemostatic wound dressings is Kaltostat® with the ability to absorb blood up to 20 times its own original volume. The principal component of the wound dressing consists of alginate fibres (the non-woven salt of sodium calcium alginate) formed into flat sheets. Its attractiveness lies in its high efficiency and the low cost. It was originally developed to dress the exposed wounds in skin and used effectively for deep hand bums and as a dressing for skin grafts.[106 ,107] Kaltostat® has also been shown as a satisfactory healing environment for tooth extraction sockets.[108]

Since alginate is non-toxic, and biodegradable with readily adjustable rheological properties, many studies have been undertaken with a view to assessment as a matrix in drug delivery

systems.[109 , 110] Gel beads of alginate can be used as an oral controlled release system for polypeptide drugs and vaccines.[111] Acid labile, gastric irritant or insoluble drugs can be loaded into alginate beads, tablets or microcapsules to produce a delayed and diffusion controlled release. Therapeutic proteins may be administered locally and released in a controlled manner by injecting alginate microcapsules incorporating the relevant protein. Alginate capsules have also been used as a means of controlling release of Mn^{2+} ions in the technique of manganese-enhanced magnetic resonance imaging (Mn-MRI).[112]

Alginates are one of the most important agents for immobilisation and entrapment of cells.[113] This is performed under the mild conditions required with the majority of living cells. Some uses of alginates are:

1. Entrapment of animal cells for implantation as artificial organs.
2. Immobilisation medium for dead or living cells under bioreactor environments.
3. Immobilisation medium for hybridoma cells in the production of monoclonal antibodies.
4. Containment of artificial seeds used in plant propagation by virtue of its low toxicity and its ease of capsule formation.[114]

Novel medical applications have also resulted from the finding that low molecular weight guluronic acid oligomers are can disrupt intermolecular interactions in mucosal tissues.[115] Cell-matrix interactions can also be seen in the binding of galactose-modified alginate with asialoglyco protein receptors on hepatocytes.[116]

1.3 Aim of my PhD project.

This thesis focus on the investigation of alginate extracted from brown seaweeds grown in the cross border of the Irish sea mainly North Wales and Dublin areas, it explores how their chemical structures, particularly the M/G ratio, and consequent physical properties including viscosity and gelling behaviours vary. These are the important factors with regard to their potential wide commercial and biomedical applications.

The specific objectives of this thesis include:

(1) Study the effects of geographic locations and seasons on the yields and the properties of isolated alginate.

- Source alginate from brown seaweed and compare how the geographic location, i.e. from specific sites in Wales & Ireland, affects the yield and chemical structure of extracted alginate.
- A comparison of how the harvesting season (for the period winter 2015-summer 2017) affects the yield and M/G ratio of extracted alginate.

(2) Optimisation of extraction methods

- Compare the extraction methods, traditional & enzymatic, to determine how these affects the yield and nature of the alginate.
- A systematic study of the extraction conditions e.g. time, temperature to optimise yield of a given alginate product.

(3) Undertake a comprehensive characterisation of alginates used including ^{1}H NMR, FT-IR, GPC and DSC/TGA.

(4) Modifications of alginate

- Acidic and enzymatic hydrolysis of alginate to generate fractions with differing M/G ratios thus affording a method to tailor its properties.
- Grafted with the bio-degradable hydrophobic polyesters PCL.
- Preparation of alginate and PLGA physically linked composite microspheres.

(5) Gelation, swelling and release evaluations of hydrogels from alginates and modified alginates.

- Perform swelling studies in the bulk state for alginate and the alginate –PCL graft co-polymer. Spherical particles of alginate and the graft co-polymer to be made and subject to swelling studies and a drug release study using model drugs.
- Alginate and PLGA composite microsphere will be used as a carrier for the protein drug BSA and subject to a 10-day release study.

Chapter 2: Instrumentation and Methodologies.

This chapter describes the basic principles for the main techniques used for the analysis and characterisation of alginates and their derivatives. These include Nuclear Magnetic Resonance Spectroscopy (NMR), Fourier Transform Infra-red Spectroscopy (FT-IR), Gel Permeation Chromatography (GPC), Differential Scanning Calorimetry (DSC) and Thermo Gravimetric Analysis (TGA), Ultraviolet-visible Absorption Spectroscopy (UV-vis), Atomic Absorption Spectroscopy (AAS), Scanning Electron Microscopy (SEM) and Dialysis.

.

2.1 Nuclear Magnetic Resonance Spectroscopy (NMR).

NMR is the most widely used technique for the determination of chemical structures. Many isotopes possess nuclear spin, for ^{1}H and ^{13}C this is equal to 1/2. Interaction with an applied external magnetic field (B_0) will give rise to two spin states, +1/2 and -1/2. The lower energy +1/2 spin state is aligned with the field, but the high energy -1/2 spin state is aligned against the external field, the energy difference between the two states being very small and depends on the strength of the applied external field.[117] Strong magnetic fields are, therefore, necessary for the NMR experiment. This small energy difference is commonly quoted as a frequency, in units of MHz (10^6 Hz), and ranges from 20 to 900 MHz or higher. Irradiation of the sample with radio waves of a particular frequency delivers energy matching exactly the energy separation of the two spin states and will flip nuclei in the +1/2 state to the higher -1/2 spin state. On relaxation of the higher energy state to the lower state energy is emitted, as electromagnetic radiation, and it is this which is detected and analysed.

Since all ^{1}H nuclei and all ^{13}C nuclei have the same magnetic moment they will give resonance signals at the same frequency values and, therefore, might be thought limited as an analytical method. However, in covalent compounds and ions, as the electron density surrounding these isotopes is charged, in the external magnetic field a secondary field is generated in opposition to the applied field and this shields the nucleus. The external field, therefore, must be increased accordingly in order to achieve resonance.

The NMR resonance signal is dependent on the strength of the applied magnetic field and also the frequency of the radio wave irradiation. In any spectrum, the location of an NMR signal must be referenced relative to a signal from a standard compound. Tetramethylsilane, $(CH_3)_4Si$, (TMS), is usually used as such a standard as it is unreactive and can be readily removed from the sample.

Since the resolution of NMR signals depends on the strength of the applied magnetic field, to correct for their field dependent frequency differences, the difference obtained between the sample resonance signal and that of the reference is divided by the spectrometer frequency. This number is then multiplied by a million to give the Chemical Shift (δ) in parts per million (ppm.).[117]

2.2 Fourier Transform Infra-red Spectroscopy *(*FT-IR).

The Infra-Red (IR) region of the electromagnetic spectrum ranges from 700 nm to 1 mm. Wavelength is measured in wavenumbers units (cm^{-1}) where the wavenumber is the reciprocal of the wavelength in centimetres. IR radiation, unlike higher energy UV, cannot cause electronic transitions, on absorption IR can only induce transitions in molecules where there are small energy differences between the various possible vibrational and rotational states. For a molecule to be IR active absorption of radiation must lead to vibration or rotation accompanied by a change in the dipole moment of the molecule. In fact, the oscillating electrical and magnetic field of the radiation resonates with the fluctuating dipole moment of the molecule resulting in a change in the amplitude of molecular vibration.[118]

In energy terms the rotational transitions are quantized and give rise to line spectra upon IR absorption in gases. However, these lines broaden in liquids and solids giving the appearance of a continuum due to molecular collisions and are therefore not very useful.[119]

The positions of atoms in a molecule are not fixed rigidly and undergo a number of different kinds of vibrations particularly stretching and bending. In stretching the inter-atomic distance along the bond axis is changed. In bending the angle between two bonds is altered. There are four kinds of bending modes i.e. rocking, wagging, scissoring and twisting.[118]

At a first approximation, for a two-atom system, Hooke's law may be applied in which the frequency of vibration is seen to be proportional to the strength of the atom to atom bond and the frequency is inversely proportional to the masses of the two atoms. Different bonds of the different groups within a molecule will, therefore, vibrate at different frequencies and provides a means of identifying many function groups.

Fourier Transform Infra-Red (FTIR) is a modern computational form of dispersive infrared spectroscopy. In infrared spectroscopy, infra-red radiation is shone through a sample which absorbs a fraction of it whilst the remainder is transmitted. The detector records the spectrum of the absorption and transmission, revealing a unique molecular fingerprint of the sample.

Infrared spectroscopy is useful analytically as it can identify unknown materials and it can also determine quality or consistency in a sample and the semi-quantitative amount of components in a mixture.[119]

2.3 Gel Permeation Chromatography (GPC).

The characterisation of a pure polymer requires a determination of the molecular weight and distribution of the various molecular size components within the material as these factors affect the properties of a given polymer [120, 121] Thus, the molecular weight of a polymer cannot be given as one single numerical value but it frequently is given an average value e.g. M_w and will have a distribution and range which will depend on the method of synthesis/biosynthesis.

The numerical value is usually reported as the average molecular weight and this can be defined in a number of ways but typically as Number Average Molecular Weight (Mn). For any synthesis, the individual polymer molecules come in different sizes, e.g. as different chain lengths for linear polymers, the average molecular weight, therefore, depends on the statistical measure used for averaging. The Number Average Molecular Weight (Mn) is defined as the ordinary arithmetic average or mean of the molecular weights for all the individual molecules. It is calculated by totalling the molecular weight of *n* polymer molecules, and dividing by *n*. Mn is a useful parameter, particularly, when considering a property which is sensitive to the number (concentration) of molecules present rather than by the size of any particle. Thus, Mn is relevant to the colligative properties of a solution e.g. boiling point elevation, freezing point depression,

and the osmotic pressure. Mn is not a continuous function, M_n being a multiple of the monomer molecular weight. However, in condensation reactions, in which the by-product consists of small molecules such as water, which are lost during the reaction, the monomer molecular weight is the residue weight after loss of the by-product of condensation.

Each individual value of the molecular weight is labelled Mi. If Ni is the number each with molecular weight Mi. then the total weight (mass) of all polymers is

$$Total\ Weight = \sum_{i=1}^{\infty} NiMi \qquad (1)$$

Therefore, the total number of polymer molecules is

$$Total\ Number = \sum_{i=1}^{\infty} Ni \qquad (2)$$

Mn- number average molecular weight is

$$Mn = \frac{\sum_{i=1}^{\infty} NiMi}{\sum_{i=1}^{\infty} Ni} \qquad (3)$$

For certain properties such as light scattering the size or weight of each polymer molecule is important rather than the number of polymer molecules, thus a more relevant measure is weight- average molecular weight. The weight average molecular weight is given by

$$Mw = \frac{\sum_{i=1}^{\infty} NiM_i^2}{\sum_{i=1}^{\infty} NiMi} \qquad (4)$$

Polydispersity Index (PDI) is the ratio of weight-average molecular weight and number-average molecular weight and gives a measure of the distribution of molecular weights in the sample.

$$PDI = \frac{Mw}{Mn} \qquad (5)$$

As the molecular weight distribution becomes narrower the PDI tends to unity. Thus, a PDI of unity indicates that all the polymer molecule chains are essentially the same length. PDI in the range of 1~1.5 indicates a controlled/living polymerisation.[122] PDI greater than 1.5 indicate less controlled polymerisations such as free radical polymerisation.

The most common method for molecular weight determination of polymers is Gel Permeation Chromatography (GPC) / Size Exclusion Chromatography (SEC) and a schematic is given to illustrate the component parts, see **Fig (2-1).**

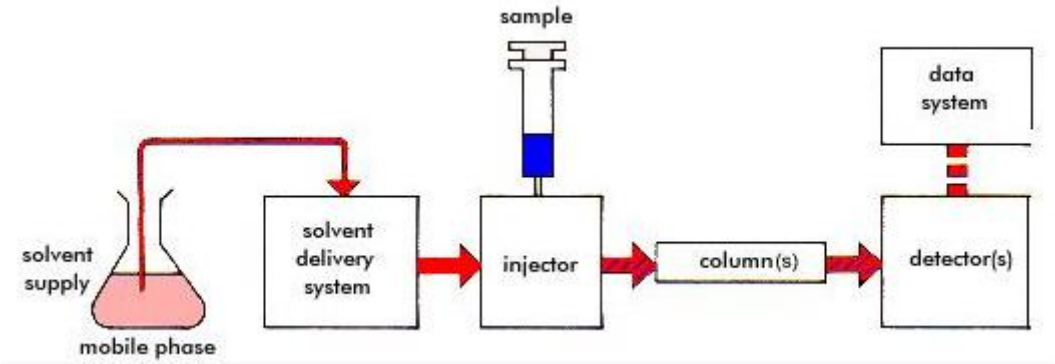

Fig (2-1): Schematic diagram of GPC components.

Fig (2-2): GPC-50 instrument showing separation columns within the oven.

The GPC method is based on separation in columns filled with porous beads in which there is no interaction between the sample material and the column packing. This method contrasts with conventional HPLC in which separation is achieved by interactions such as adsorption, partition, etc.

Preferably, the polymer sample is dissolved in the same solvent used as eluent. The mode of separation depends on the hydrodynamic volume of the molecular species in the sample material when in solution. Separation is based on using porous, mechanically stable and highly cross

linked gels as beads packed into a column which through their sieving action separate the sample into fractions based on their molecular volume. The pores in the packing material hinder movement of the smaller molecules of the sample which will enter into most of the pores and are retained relatively longer than the larger particles which will not fit into the smaller pores and pass straight through, see **Fig (2-2)**.[120,121]

As the eluent fractions leave the column they can be detected by various types of detector including UV and viscometry but for this study a differential refraction detector was used which detects differences in the refractive index between the analyte and the eluent. It is therefore important to choose calibrants which are very similar to the analyte and which while soluble in the eluent offer the greatest possible difference in refractive index between the sample and the eluent.[120]

The chromatogram of the analyte plots the detector response verses the retention time, and this is then compared to a calibration curve obtained from the standards. The calibration curve is obtained by measuring the retention times of a series of monodisperse polymer standards of known molecular weights. Please see **Table (2-1)** for calibration data and **Fig (2-3)** for calibration curve. For our study of alginates it was found that Pullulan was the most suitable standard.

Table (2-1): Calibration data for GPC measurement.

Calibration Points			
Pts	**Peak Max. RT (mins)**	**M_W (g/mol)**	**Log M_W**
1	11.72	642000	5.808
2	12.30	337000	5.528
3	12.85	194000	5.288
4	13.73	107000	5.029
5	14.67	47100	4.673
6	15.52	21100	4.324
7	16.87	6100	3.785
8	18.90	667	2.824
9	19.80	180	2.255

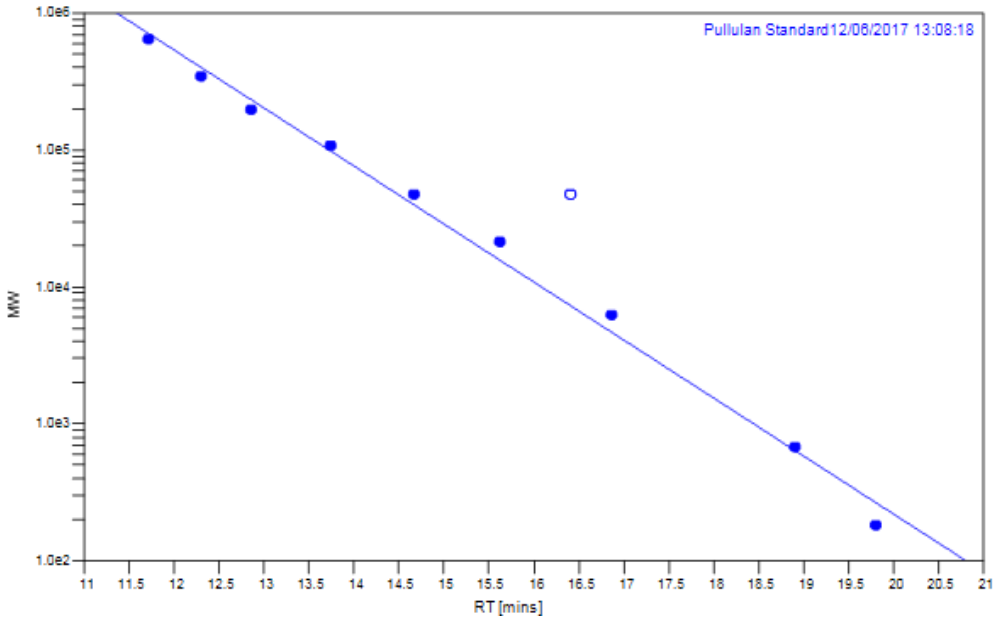

Fig (2-3): The calibration curve for GP measurement**.**

A typical chromatogram is given in **Fig (2-4)** below. This was obtained for commercial alginate (ALG-A) and shows the calibration curve as a straight line overlaid on the curve. Thus, the bulk of the sample is indicated by peak 1, which corresponds to a molecular weight of 237.2 kg/mol with PDI of 9.2.The area of the peak is 90.1% of the sample.

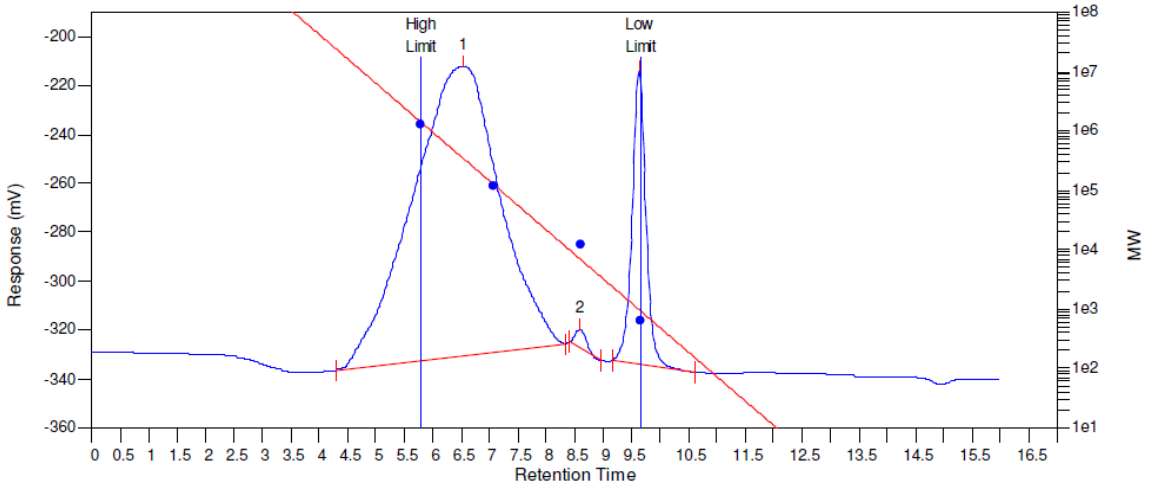

Fig (2-4): GPC chromatogram for commercial alginate (ALG-A).

2.4 Differential Scanning Calorimetry (DSC) and Thermo Gravimetric Analysis (TGA).

DSC is a technique in which the difference in heat input required to raise the temperature of a sample and a reference is measured and expressed in terms of temperature. The sample and reference are maintained at more or less the same temperature throughout. Generally, the sample holder temperature increases linearly with time.[123]

When the sample undergoes a physical transformation such as a phase transition more or less heat will be required so that it and the reference are maintained at the same temperature. The amount of heat that must flow to the sample depends if the process is endothermic or exothermic. Thus, if a solid sample melts to form a liquid, more heat is required to the sample to increase its temperature to match that of the reference due to the absorption of heat by the sample to change phase from solid to liquid. As the sample undergoes an exothermic transition (such as a crystallization less heat is needed to raise the sample temperature. Therefore the difference in heat flow between the sample and reference is a measure of the amount of heat absorbed or released during the transition. DSC can also detect more subtle physical changes such as glass transitions.

The result of a DSC scan is a plot of heat flux versus temperature. Two different conventions apply to presentation of the plot: exothermic reactions in the sample are shown with a negative or a positive peak depending on the instrument.

Differential scanning calorimetry is able to identify certain characteristic transitions of a sample. It is possible to identify crystallization and glass transitions temperatures T_g. DSC can also identify oxidation and other chemical reactions.[123, 124, 125]

A glass transition can occur as the temperature of an amorphous solid is increased and is seen as a step in the baseline of the DSC signal. This is due to a change in heat capacity although no formal phase change occurs.[123, 126]

As temperature increases, the amorphous solid will become less viscous as the molecules obtain enough freedom of motion to arrange themselves into a crystalline lattice. This is the crystallization temperature (T_c). This transition from the amorphous solid state to crystalline solid state is an exothermic process resulting in a peak in the DSC signal. As the temperature increases the sample will eventually attain its melting temperature (T_m). Melting results in an

endothermic peak in the DSC curve. Determine of transition temperatures and enthalpies is of use in making DSC a valuable tool in producing phase diagrams for chemical systems.[123]

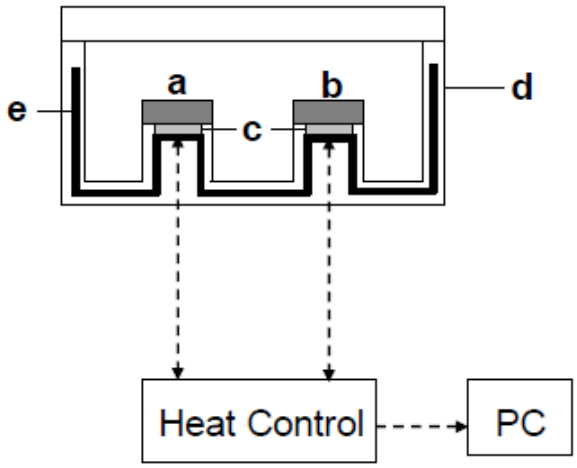

Fig (2-5): Schematic of The Differential Scanning Calorimetry technique: **(a)** the sample pan; **(b)** the reference pan; **(c)** thermo-couples; **(d)** balance cell head and **(e)** heating element.

A typical DSC heating curve is given in **Fig (2-6).**

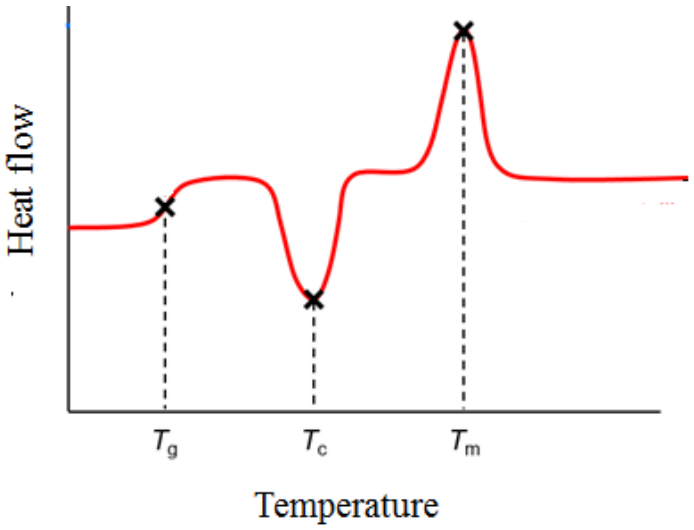

Fig (2-6): A typical heating curve obtained by use of the the Differential Scanning Calorim try Technique (reproduced courtesy of Wikimedia Commons AliceChem)

TGA is a method in which the change in mass of a sample is determined with time as the temperature changes thus providing information about physical events such as phase transitions as well as chemical changes including thermal decomposition.[127] TGA is performed on an instrument referred to as a thermo-gravimetric analyzer or carried out simultaneously when DSC is performed. A typical TGA instrument consists of a precision balance with its sample pan contained within a furnace. The temperature is increased at constant rate to incur a thermal reaction. The thermal reaction may be conducted under a variety of atmospheres including ambient atmosphere, inert gas and vacuum and under defined variety of pressures. The TGA data is collected and compiled into a plot of mass or percentage of initial mass on the vertical axis v either temperature or time on the horizontal axis. A TGA can be used for characterisation of characteristic decomposition patterns. It is especially useful for the study of polymer materials.

TGA can be used to indicate the thermal stability of a material. For a given temperature range, for a species to be thermally stable, there will be no observed mass change therefore little or no slope in the TGA trace. TGA can also give the upper limit of temperature for a material`s use. Above this temperature the material will begin to degrade.

TGA is used in the analysis of thermally stable polymers. Most polymers melt or degrade below 200°C. However, some polymers can withstand temperatures of at least 300°C in ambient air and 500°C in inert gases without changes in structure or strength.[128, 129]

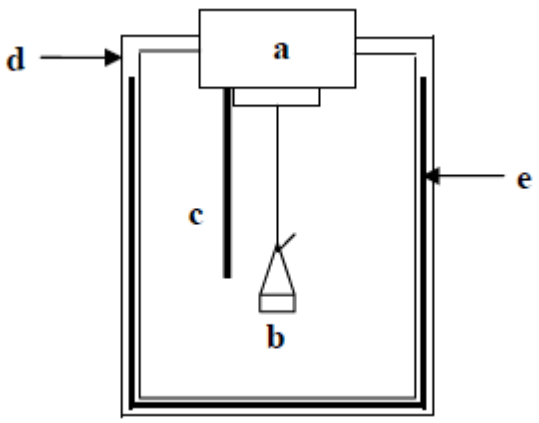

Fig (2-7): Schematic drawing of TGA: **(a)** balance, **(b)** sample pan and pan holder,**(c)** thermo-couple, **(d)** furnace and **(e)** heating element.

A typical heating curve obtained by TGA is given in **Fig (2-8)**. The significant transitions are shown and include moisture loss at 100°C, loss of volatile material at 300°C and decomposition at 600°C.

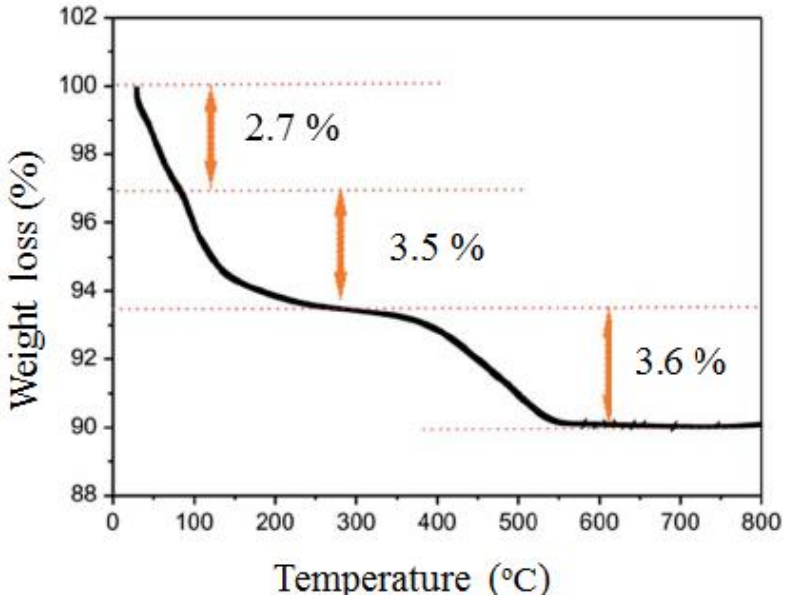

Fig (2-8): Typical TGA heating curve.

2.5 Atomic Absorption Spectroscopy (AAS).

AAS is a quantitative analytical procedure for the determination of chemical elements by means of the absorption of radiation (light) by free atoms in a gas particularly the absorption of light by free metallic ions.

AAS can be used to determine the concentration of a particular element in solution (the analyte) in a sample out of more than 70 different elements, and also directly measure the content in solid samples by a procedure involving electro-thermal vaporization.

The technique makes use of the atomic absorption spectrum of a sample to assess the concentration of particular analytes within it. Standards with a known analyte content are used to establish the relation between measured absorbance against the analyte concentration by application of the Beer- Lambert Law.[130]

In principle, the electrons of atoms in the atomizer are promoted to higher orbitals (excited state) for a short period of time, a matter of nanoseconds, by absorption of a defined quantity of energy (i.e. radiation of a given wavelength). The particular electron transition in a particular element can only occur if light of a particular wavelength is absorbed. Therefore, each wavelength corresponds to only one element, the width of an absorption line is only a few picometers (pm), giving the technique its high selectivity for detecting the unknown element. The light intensity with sample and with no sample in the atomizer is measured and the ratio between the two values (giving the absorbance) is converted to analyte concentration using the Beer-Lambert Law.

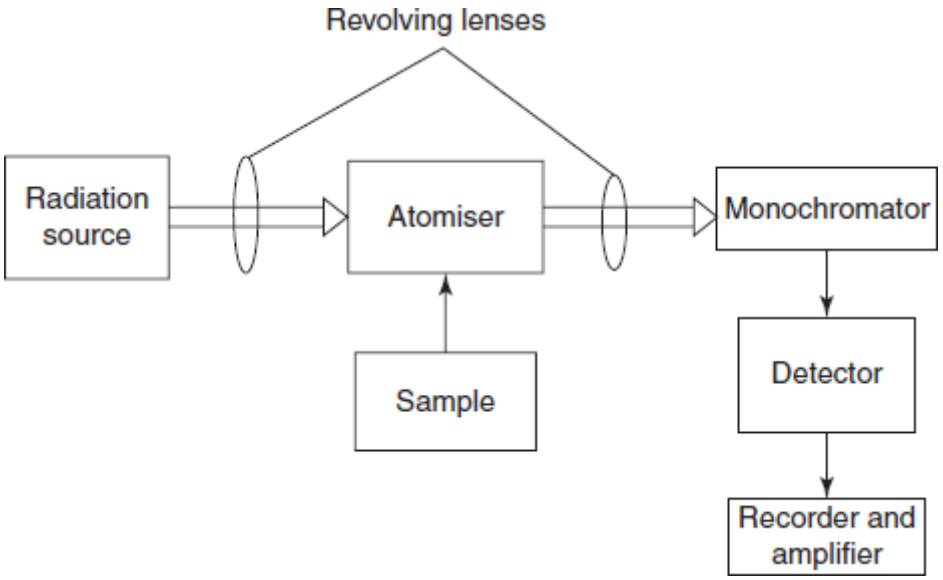

Fig (2-9): Atomic absorption spectrometer schematic.

To analyze a sample, it has first to be atomized and this is most commonly performed using flame and electro-thermal atomizers. The gaseous atoms are then irradiated by optical radiation, the radiation source being either an element-specific source of line radiation or a source giving continuum radiation. The light then passes through a monochromator to separate the element-specific radiation from other radiation emitted by the radiation source, and this is then finally measured by a detector.[126]

2.6 Scanning Electron Microscopy (SEM).

In scanning electron microscopy (SEM) images of a sample are produced by scanning the surface with a focused beam of electrons. The beam electrons interact with atoms of the sample producing signals that contain information about the surface composition and topography of the sample. The electron beam is scanned and the position of the beam is correlated with the detected signal which is processed to produce an image. SEM can give resolution better than 1 nm. Specimens are scanned in a high vacuum in conventional SEM, or in variable pressure or environmental SEM in a low vacuum or wet conditions. Observation can also take place in a wide range of cryogenic or elevated temperatures with specialized instruments.[131]

The most common SEM mechanism generates secondary electrons which are emitted by atoms excited by the electron beam and it is these which can be detected in this mode. The number of secondary electrons generated and therefore detected depends in part on specimen topography. Thus, by scanning the sample to generate secondary electrons, a special detector can display an image of the topography of the surface.

SEM samples must be prepared to withstand the vacuum conditions and irradiation by the high energy beam of electrons, and yet be small enough to fit the specimen stage. Samples are rigidly mounted on to a specimen stub using an electrically conductive adhesive. SEM is used extensively in industry to detect defects of semiconductor wafers, and such instruments can examine any point of a 300 mm semiconductor wafer. Many instruments also have stages that can tilt an object of such size to 45° and can undergo a 360° rotation.

Non-conductive specimens become charged when scanned and particularly when in secondary electron imaging mode, this can cause scanning faults giving image artefacts. For conventional SEM, specimens must be made electrically conductive, at least at the surface, and earthed to prevent the accumulation of static. Metal objects require little preparation except for cleaning and conductively mounted on to a specimen stub. Non-conducting materials are coated with an ultrathin electrically conducting material, such as gold, deposited in a low-vacuum by splutter coating or by high-vacuum evaporation. Coating with heavy metals may give rise to a high signal/noise ratio with samples of low atomic number. [131]

2.7 Ultraviolet Absorption Spectroscopy (UV/vis).

UV/vis uses wavelengths of ultraviolet and visible light in the range 10 - 400 nm and 400 - 780 nm respectively. This energy is absorbed by UV/vis active molecules and results in changes in the electronic distribution in the molecule i.e. promotion from the ground state to excited states within the system.[132]

Electrons in the ground state molecular orbitals are promoted to anti-bonding molecular orbitals. The electrons in a molecule are found in three situations: namely as sigma bonds (σ), pi (π) bonds, or non-bonding electrons including lone pairs. When irradiated with electromagnetic radiation of suitable wavelength electrons are excited and promoted from the highest occupied molecular orbital (HOMO) to the lowest unoccupied molecular orbital (LUMO) and result in an excited or anti-bonding state. The following should be noted:

1. Sigma bond electrons occur at the lowest energy level and are the most stable, hence require an input of energy to be elevated to a higher energy state. Therefore, these electrons generally absorb light of a shorter wavelength (higher frequency) in the ultraviolet spectrum and as such these transitions are rare.
2. Pi bond electrons are found at a much higher energy level when in the ground state. They are, therefore, relatively unstable and excited more easily and requiring less energy for excitation. Such electrons, therefore, absorb energy in the longer wavelength ultraviolet and visible regions.
3. Non-bonding (n-electron) electrons are, generally, electrons found as lone pairs, are of still higher energy levels than π-electrons and, therefore, excitation by both ultraviolet and visible light is possible.

Thus, most of the energy absorption is in the ultraviolet-visible region is due to π-electron or n-electron transitions. The electronic states for any given system are well defined, for instance, the double bond of 2-butene has a defined energy level for its π-electrons and can absorb a specific (i.e. quantized) amount of energy for excitation to the π* energy level.

The concentration of an absorbing species is obeys the Beer-Lambert law (Equation 10):

$$A = log_{10}\left(\frac{I_0}{I}\right) = \epsilon . c . L \qquad (10)$$

A is the absorbance in absorbance units (AU), I_0 is the intensity of incident light of given wavelength, I is the intensity of transmitted light of the same wavelength, *L* is the path-length, and *c* the concentration. For a given absorbing species and the particular wavelength used, ϵ is the constant called the molar extinction coefficient. This constant is specific for the species in a given solvent, for a particular temperature and pressure.[132]

2.8 Dialysis.

Dialysis is used for the purification and isolation of the products from a reaction mixture. Use is made of a semi-permeable membrane tubing made from cellulose. The reaction mixture is inserted into the tubing and the tubing is then immersed in the solvent of choice. For water based reaction mixtures water is used to immerse the tubing. The membrane permits the passage of small molecules from the high concentration within the mixture to the low concentration of the immersion medium as a result of diffusion. In water, the osmosis process enables water to pass through a semi-permeable layer to in an effort to reach equilibrium. The tubing will only allow sufficiently small molecules to pass through the semi-permeable membrane. Larger molecules are too large to pass though the pores in the tubing and are retained.[133]

The reaction mixture when placed into the dialysis tubing is sealed with plastic clips and then placed in a large volume of water with sufficient room to rotate freely. The water in the mixture will then cross the semi-permeable membrane from the hypertonic solution (higher solute concentration than the immersion solution) in an attempt to attain equilibrium, see **Fig (2-7)**.

The tubing specifically used was Spectra/Por® Regenerated cellulose membrane. It does not acquire an electric charge and does not absorb the solutes used. It is hydrophilic, spontaneously wettable with a very high wet strength. It has the advantage of being chemically resistant and is suitable for aqueous and organic media. Spectra/Por® grade 1 was used with its molecular weight cut off point of 3500 Daltons.

The general dialysis procedure was as follows. The tubing was cut allowing for extra tubing length (i.e. 10% of total volume of the sample) for a small head space. This enables the tube to float and avoid being caught up in the rotating stirrer bar. The tubing was then placed in a large beaker of de-ionised water.

Typically, dialysis was allowed to run for two or three days. The immersion medium was regularly changed i.e. after the first hour, then 4, 10 and 24 hours later.

Finally, the purified product was freeze-dried and fully characterised.[133]

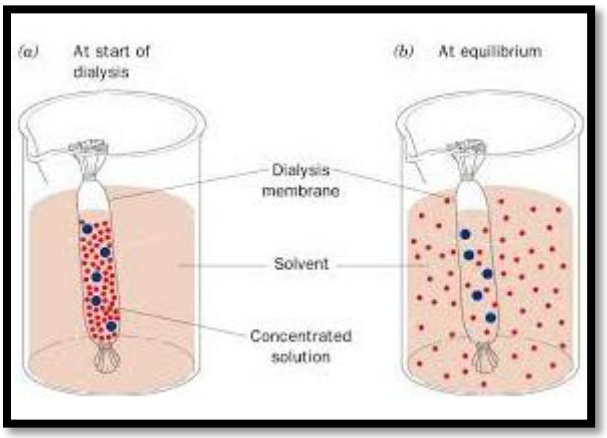

Fig (2-10): Illustration of the Principle of Dialysis. [134]

Chapter 3: Isolation and f alginate from Welsh and Irish brown seaweeds

3.1 Introduction.

Alginate is the major constituent of brown seaweeds and comprises up to 40% of the dry weight of the plant. It exists in the form of magnesium, calcium and sodium salts of alginic acid in the cell wall matrix providing both rigidity and flexibility to the algal tissues. The quality and quantity of the extracted alginates depends on the algae species and the season of harvest. There are between 1,500 and 2,000 species of brown algae known worldwide.[3, 135] As stated in **Chapter 1.2.1** the alginate content varied with the species. **Table (3-1)** details the composition of extracted alginate for various species.

Table (3-1): Percentages of mannuronic acid (M) and guluronic acid (G), M/G ratios and percentages of the three principal types of block structures in alginates extracted from various commercial species of brown seaweeds.

Entry	Species of seaweeds	M%	G%	M/G	MM	GG	MG	REF
1	*A. nodosum*	60.0	40.0	1.5	38.4	20.7	41.0	[24]
2	*L. digitata*	59.0	41.0	1.43	49.0	25.0	26.0	[24]
3	*L. japonica*	69.3	30.7	2.26	36.0	14.0	50.0	[24]
4	*M. pyrifera*	61.0	39.0	1.56	40.6	17.7	41.7	[24]
5	*L. hyperborea*, fronds	56.0	44.0	1.28	43.0	31.0	26.0	[24]
6	*L. hyperborea*, stems	30.0	70.0	0.43	15.0	60.0	25.0	[24]
7	*S. fluitans (Florida*)	54.0	46.0	1.18	36.0	28.0	36.0	[136]
8	*S. fluitans (Cuba*)	34.0	66.0	0.52	25.0	57.0	18.0	[137]
9	*S. vulgare (Brazil*)	56.0	44.0	1.27	55.0	43.0	2.0	[138]

Data for the M/G content of the different species of seaweeds as presented in the review paper of Qin (2008) and others is given in **Table (3-1**). The data compares alginate content extracted using the same alkaline method. Furthermore, the extracted alginates were characterized using

the same NMR methodology. It is thus possible to make valid comparisons using this data.

It can be seen from the data listed that the composition of extracted alginate depends on the species examined. Thus, the M/G ratio for instance, can vary widely, between 2.26 and 0.43, as seen in the table. This wide variation is also evident when comparing species within the same genus as seen in entries 2, 3, 5 and 6 for the genus *Laminaria.*
From entries 7 and 8, it can be seen that the alginate composition can even vary within the same species, in this instance *Sargassum fluitans*, and this illustrates that geographical location is also a determining factor. Entry 7 for *S. fluitans* from Florida gives an M/G ratio almost twice that for the same species found in Cuba (entry 8) of 1.28 and 0.47. Presumably this feature if found in other species. It is likely that the differing composition will give rise to different mechanical properties as required for the particular environmental conditions encountered by the species in question.

Table (3-1) also details the composition within the different parts of the same plant for a given species. Thus, entries 5 and 6 for *Laminaria hyperborea* fronds and stem respectively give an M/G ratio of 1.28 and 0.52 respectively. This variation in composition may reflect the different physical stresses that the different parts of the plant experience.
It is also found that the harvesting season for any given seaweed species affects the yield and chemical composition of alginate extracted. Thus, for brown seaweeds, for instance, although harvested at the same geographic location and using the same extraction conditions, the season will affect the composition of the alginate, particularly the M/G ratio and this in turn will give rise to various physical and chemical properties.

In a study of alginates from a Brazilian seaweed species *Sargassum filipendula* the effect of harvesting season was examined.[139] Harvesting was undertaken during different seasons of year i.e. the fall of 2009 (May), the spring of 2010 (November) and the summer of 2011 (February). **Table (3-2)** below presents the data gathered including the M/G ratio and the percentage yield.

Table (3-2): M/G ratio and the yield percentage of alginates extracted from Brazilian seaweed *Sargas-sum filipendula* during different seasons of the year.[139]

Harvested season	M/G ratio%	yield %
Fall 2009 (May)	0.75	17.0
Spring 2010 (November)	0.78	17.2
Summer 2011 (February)	0.60	15.1

The study found that the Brazilian seaweed *S. filipendula* consists of 15.1% to 17.2% by dry weight of alginate, with spring samples showing the highest yields for the biopolymer. A linear non-regular, block-wise order of d-mannuronic (M) and l-guluronic (G) acids was found as a consequence of the different seasons and stages of the life cycle. It was also observed that the M/G ratios for all algae studied was below 1.0.[139]

The alginate extraction conditions for *Sargassum vulgare* have been subject to study particularly with regard to temperature and time and their effects on yield. The alginate yield was found to increase with temperature. Thus, after 3 hours of heating, it was found that the yields obtained were similar at temperatures of 60 and 80^{o}C. The best yield was obtained after 5 hours of extraction at a temperature of 60 or 80 ^{o}C. This value of 16.9% is approx. 40% higher than for the sample extraction at 25^{o}C.[138] Davis *et al* [137] gives values of between 21.1–24.5% for *S. fluitans* and for *S. oligocystum* 16.3–20.5% depending on the extraction method used. In another study, Davis[140] obtained even higher yields of 45% and 37% respectively for the same species. It was also found that under these conditions, the extracted alginate in addition to the higher yield was of a more viscous nature.

Brown seaweeds are particularly plentiful in cold northern waters and a few species are also found in tropical regions. A variety of species of brown seaweed can be found along the coasts North Wales and Ireland.[141] This relative diversity may be attributable to location as this area is situated at the boundary of three oceanic climate zones and subject to a large tidal range.
Alginate of brown seaweed species have been widely studied, however, little work has been done on alginates from the *Fucus vesiculosus* species.[142] In particular, no studies have been reported on the composition of alginates from Welsh and Irish seaweeds.

The aim of this chapter is to report upon the extraction of alginates from Welsh and Irish seaweeds by different extraction methods and under various conditions, including Na_2CO_3 and enzymatic assisted methods, in order to assess their efficacy. Further, the study investigated the effect of location and season on the chemical composition and physical properties of the alginates extracted from the brown seaweed *F. vesiculosus.* The extracted alginates were characterized by different techniques including NMR and FT-IR, to determine their composition and the M/G ratio. GPC and viscosity measurements were also used to determine the M_W and the physical properties were investigated using DSC. A study was also undertaken to hydrolyze alginates obtained from a particular extraction and the reaction products were then characterised.

The locations where species were harvested in the Irish Sea geographical area are indicated in **Fig (3-1)** below and centre around the Dublin and Anglesey regions.

Fig (3-1): The geographical locations (Welsh and Irish coast) of the coast where the *F. vesiculosus* brown seaweeds were collected.

3.2 Experimental

3.2.1 Chemicals and materials.

Sodium alginate (low viscosity, 1% in water at 25^{o} C: 5-40 cps, labelled as (Alg-A) and alginate lyase (10,000 units per gram), deuterium oxide, cellulase and protease were purchased from Sigma Aldrich.

Sodium carbonate (Na_2CO_3), formaldehyde solution (HCOH), hydrochloric acid (HCl 37%), sodium hydroxide (NaOH), industrial methylated spirit (IMS i.e. as a substitute for ethanol), acetone (analytical reagent grade)

Bio-Rad Protein Assay Reagent Kit, sodium chloride and sodium bromide were all purchased from Fisher Chemical and used as supplied.

3.2.2 Collection of brown seaweeds.

The brown seaweed species, S. fluitans (bladderwrak), was collected from two different locations using a standard procedure i.e. from the Anglesey coast of North Wales and from Seapoint Beach in Dublin.

Initially, the material identity was confirmed with the generous assistance of the Bangor University dept. of Ocean sciences who provided the expertise of an algae taxonomist who also provided a suitable protocol for identification.

Collection was undertaken over a two year period in the two seasons of each year i.e. winter 2015 , summer 2016, winter 2016 and summer 2017 and was labelled respectively WW-1, WS-1, WW-2, WS-2, IW-1, IS-1, and IW-2. The time of collection was the same at each collection session (8 am) and was performed at the beginning of August (for summer) and the beginning of October (for winter).

The material was robust and large enough to be gathered by hand without compromising health and safety considerations. Collection took place at low tide and samples placed in clean plastic containers which were then sealed and labelled noting details' of location and time of collection.

The samples were then stored for a short time in a cool place out of direct sunlight. Subsequently, the seaweeds were washed with an abundance of water to remove extraneous matter

and air dried in ambient air for 5– 7 days. The dry material was then ground in a blender for ten minutes to produce material of the consistency of fine particles as preparation for extraction.

In order to understand the variation in alginate composition for the different plant parts, samples of *F. vesiculosus* seaweed collected in one season, i.e. summer 2016 (S-1) were used. The effect of morphology on composition required different parts of the plant to be taken, namely the lower and the upper parts of the seaweed. The top and the bottom parts of the Welsh and Irish seaweed plants were labelled as TWS-1, BWS-1, TIS-1 and BIS-1 respectively. **Table (3-3)** summarises collection details for the brown seaweeds samples used in this study. **Fig (3-2)** gives an illustration of brown seaweed in its natural habitat.

Table (3-3): Location and Time that seaweeds samples were collected.

Entry No.	Sample name	Collection location	Collection time
1	WW-1	North Wales	Winter 2015(October)
2	WW-2	North Wales	Winter 2016(October)
3	TWS-1	North Wales	Winter 2016 (October)
4	BWS-1	North Wales	Summer 2016 (August)
5	WS-2	North Wales	Sumer 2017 (August)
6	IW-1	Dublin	Winter 2015(October)
7	IW-2	Dublin	Winter 2016(October)
8	TIS-1	Dublin	Summer 2016 (August)
9	BIS-1	Dublin	Summer 2016 (August)

Fig (3-2): Seaweed of species *S. fluitans* collected from two locations of Irish Sea i.e. Anglesey (North Wales) and Seapoint (Dublin Ireland).

3.2.3. Extraction procedure.

Alginates were extracted according to a modified procedure of Calumpong *et.al.*[143] 25 g of dried algae were soaked in 500 mL of 2% formaldehyde solution in de-ionized water under continuous mechanical stirring for 4 hours at room temperature. The supernatant was discarded after filtration and the moist seaweed was washed twice with de-ionized water then soaked in 0.2M HCl at room temperature for 3 hours under continuous stirring. After filtration and washing with water, the solid residues were transferred into a 3-neck round-bottom flask and placed on a heating mantle with a mechanical stirrer. Extraction was performed by addition of 800 mL of 2% Na_2CO_3 at 100 ^oC for a period of 3 hours. Conditions for extraction were varied by employing other temperatures i.e. RT, 50 °C and 60 °C and also two different extraction periods were used i.e. 24 hours for RT and 5 hours for 50 °C and 60 °C. This allowed a comparison to be made for the different methods. The extract was then filtered through standard filter paper and the crude alginate was precipitated by the addition of IMS in the proportion of 3:1 by volume and the precipitate was finally obtained by centrifugation (5000 rpm for 10 minutes). The sodium alginate collected was washed twice with aliquots of 100 mL acetone and dried

at 65 °C in an oven. The sodium alginate sample was finally purified by dissolution in 2 % Na_2CO_3 and re-precipitated with EtOH, washed twice with IMS and acetone and finally dried at 65^{o}C. The yield of alginate was expressed as percentage dry weight. See **Fig (3-3)** for schematic.

In an alternative enzyme assisted isolation, the same extraction procedure as above was followed but after the addition of Na_2CO_3, 50 mg of cellulase enzyme was added to the extraction mixture.. This was expected to aid the release of more alginate by the degradation of any proteins in the alginate cell walls which may be bound to alginate. In a further modification to the enzyme assisted extraction, the enzyme protease was used instead of the cellulase and used in 30 and 50 mg portions of protease respectively. The period of extraction was 5 hours for all the enzyme extractions at a temperature of 50 ^{o}C. Separation of the product from such enzymic methods was performed using the procedure as given for Na_2CO_3 method and this was performed by a similar centrifugation method.

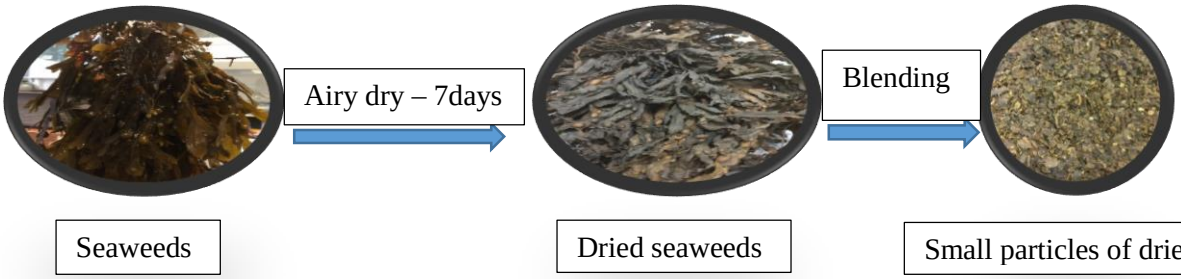

Seaweeds

Airy dry – 7days

Dried seaweeds

Blending

Small particles of dried seaweeds

1-Treatment with HCOH

2- Treatment with HCL

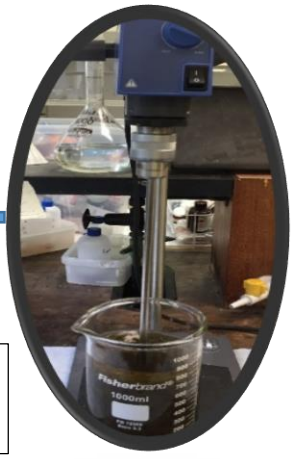

Extraction with 2% Na_2CO3 at different condition of temperature and time

Centrifugation
(10 mins, 5000 rpm)

Seaweeds residues

Supernatant

IMS

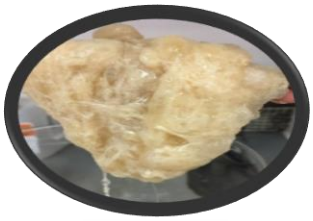

1- Wash with acetone
2- Dry at 65°C
3- Purification

Alginate

Dried purified alginates

Fig (3-3): Scheme of isolation of alginate from brown seaweed using Na_2CO_3

3.2.4 Characterisation of alginate.

3.2.4.1. Nuclear Magnetic Resonance Spectroscopy (^{1}H NMR).

5 mg of each alginate sample was dissolved in 1 mL D_2O and freeze- dried, then each sample was dissolved in 1 mL of D_2O and freeze- dried overnight to allow for the exchange of hydroxyl protons with deuterium. The lyophilized samples were then dissolved in 1 mL D_2O and transferred to NMR tubes. After employing various conditions on the NMR instrument (Bruker 500 MHz) it was found that optimal spectra were obtained at a temperature of 70^{o}C. Typically, 500 scans (i.e. irradiation using the entire radio wave spectrum) for the samples was required as the low concentration of analyte means that it is difficult to observe useful signals and the data from hundreds of scans must be averaged in order to bring the signal-to-noise ratio down to acceptable levels for the un-hydrolyzed samples. The resulting spectra were processed and the baseline corrected using the MestReNova™ software application. The ^{1}H NMR for hydrolyzed samples was prepared using 10 mg sample of alginate in 1 mL of D_2O and a 64 scans were used.

3.2.4.2 Fourier Transform Infra-red Spectroscopy (FTIR).

Fourier-transform infrared analysis (FT-IR) of the samples was carried out using a Fisher Scientific FT-IR spectrophotometer to identify the functional groups. The dry samples were prepared in KBr pellets of diameter 13 mm. A sample of approximately 0.1-1% dilution of the alginate was prepared by thorough mixing into 200 to 250 mg of fine halide powder which was then compressed into pellet form using a die. The external pressure was applied without the need for de-gassing as this was found adequate for our samples. A transparent pellet was obtained and a maximum scan number of 40 was used to obtain the spectra.

3.2.4.3 Gel Permeation Chromatography (GPC).

10-15 mg of alginate samples were dissolved in 3 mL of 0.2 M $NaNO_3$ and 0.01 M NaH_2PO_4 buffer solution of pH 6.8. The sample's solutions were filtered with a WHATMAN 0.2 μm PVDF w/GMF (Glass MicroFiber) syringe filter and then transferred into GPC glass vials to

be measured. All the chromatograms were performed using a PolarGel 7.5 mm x 300 mm column and eluted with NaH_2PO_4 buffer solution at a flow rate of 1.0 mL/min and the separation was carried out at 30°C. An on-line refractive index (RI) detector (Shimadzu RID-6A) was used to measure the relative concentration of polymers eluting from the column.

3.2.4.4. **Differential Scanning Calorimetry (DSC) and Thermo Gravimetric Analysis**.

The DSC thermographic analysis was performed on a universal V3.7A TA (SDC Q600) instrument at a heating rate 10 °C per minute for the temperature range 25-800 ^{o}C under an inert nitrogen gas atmosphere using sample mass of approximately 15 mg. One heating curve was obtained for the sample in question. Morphological and chemical changes were inferred from the changes of the evolution/absorption of heat.

3.2.5 Protein residue quantification.

The amount of protein residues present in alginate was measured using the commercial Bio-Rad™ Protein Assay Reagent Kit and followed the standard assay procedures provided. Briefly, the standard calibration curve was created using the Protein standard 1, bovine gamma globulin. The dye reagent was prepared by dilution with distilled water in the ratio 1:4 and filtered to remove particulates.

Five dilutions of a protein standard were prepared. Initially a stock standard was prepared by adding 20 mL of distilled water to the dry reagent and mixed until thoughly dissolved to get a stock of dilution 1.4 mg/mL. The stock standard solution was then diluted with de-ionised water to get the required dilutions.

Alginate solutions were prepared at concentrations of 15, 10 and 5 mg/mL and incubated for 5 minutes at room temperature with the BioRad reagent. Proteins were detected by the appearance of a blue colour that results from the formation of a peptide complex. Using a spectrophotometer the protein concentration was measured at the absorbance at 595 nm, which is specific for the blue colour of the protein complex. The absorbance maximum for an acidic solution of Coomassie® Brilliant Blue G-250 dye shifts from 465 nm to 595 nm when binding to protein occurs.

To quantify the results, light absorbance levels were compared with a standard curve that was produced using bovine albumin. For the presentation of the results, concentrations were converted to the equivalent milligram of proteins per gram of dry alginate.

3.2.6. Hydrolysis of alginates.

Hydrolysis was performed by two methods namely under acidic conditions and by an enzyme catalyzed procedure.

3.2.6.1 Acidic hydrolysis.

To 100 mL 1% aqueous solution of alginate, 5 mL of 3M HCl was added and heated for 30 min at 100 ^{o}C under nitrogen, the mixture was cooled and centrifuged. The soluble fraction, (F1) containing soluble products of hydrolysis, was neutralised with 1M NaOH to pH7. The alginate was obtained by precipitation in 100 mL of IMS. The precipitate was retrieved as a solid fraction via centrifugation and then suspended in 0.3 M HCl and heated for 2h at 100 ^{o}C under nitrogen. After centrifugation of this fraction the supernatant, Fraction 2 (F2), was neutralised with 1 M NaOH to pH7 and the obtained as a solid by precipitation in IMS. The solid fraction from the second centrifugation (F3) was neutralised to pH7 and obtained as a solid after precipitation in IMS and then freeze-dried.

3.2.6.2 Enzymatic hydrolysis.

5g of alginate was dissolved in 500 mL of 50 mmol tris-HCl buffer, pH 7.5, and Alginate 200™ unit lyase (2mg) was then added. The mixture was incubated at 30 ^{o}C overnight. Then the solution was heated to 100^{o}C and kept for 10 minutes at this temperature to stop the hydrolysis. The solution was filtered after cooling, 250 mL of methylated spirit was added and the precipitate, fraction 1, (F1) was collected by centrifugation, the supernatant alginate portion, fraction 2 (F2), was collected by evaporation.[144]

3.3 Results and discussions.

3.3.1 Yield of extracted alginate.

There are many factors influencing the yield of the extracted alginate. As shown in **Table (3-4)** and **Fig (3-4)** the effect of the location (Irish or Welsh) and the season of harvesting can be seen showing that the higher yields and, therefore, higher alginate content in the plant was obtained from the Irish seaweeds (about 32 ± 1.6-34 ± 1.5%) comparing to Welsh seaweeds (at about 20 ± 2.05-21±2.05 %). For both locations, seaweeds harvested in winter are slightly higher in alginate than those harvested in summer. This may be the result of the longer growing season, although the differences are small being only one percentage point for the Welsh seaweed.

This finding confirms the results for work by Bertagnolli [139] on the species *S. filipendula* collected during fall and spring seasons where yields of 17.0 ± 0.1% and 17.2 ± 0.3%, respectively, were found. While algae collected for the summer season showed a lower alginate yield of 15.1 ± 0.1%. In turn these percentages were consistent with the observations found in brown algae of 10 to 40% by Torres *et al*.(2007) who obtained a yield of 16.9 ± 0.7%.[138]
It should also be noted from our study that in the Irish seaweed that there a difference between one year and the next in the two year study.

From **Table (3-5)** and **Fig (3- 5)**, the percentage yield of alginate extracted from Welsh seaweed in winter 2015 under different extraction conditions involving temperature, time and enzyme can be seen. Enzyme extraction of alginate gives the highest yield (25 ±0.3%). Of the non-enzymic methods it appears that temperature is the overriding factor for higher yields e.g. 21 ± 0.5% for extraction at 100 ^{o} C. It should be noted that the stated extraction times were different it was at these time points that the reaction mixtures became viscous due to release of the polysaccharide from the plant and was, therefore, considered to be the point when full extraction occurred under the conditions of the experiment and thus, considered that each reaction had proceeded to an equivalent point. Thus, the comparison for extractions at 60 °C and 50 °C for a duration of 5 hours, confirms the effect of higher temperature on yield.

Table (3-4): The yield of alginate extracted from Irish and Welsh seaweeds for different seasons.

Entry	Sample name	Yield %
1	WW-1	21 ± 2.0
2	WW-2	21 ± 2.1
3	IW-1	34 ± 1.5
4	IW-2	33 ± 1.5
5	WS-1	20 ± 2.0
6	WS-2	20 ± 2.1
7	IS-1	32 ± 1.6

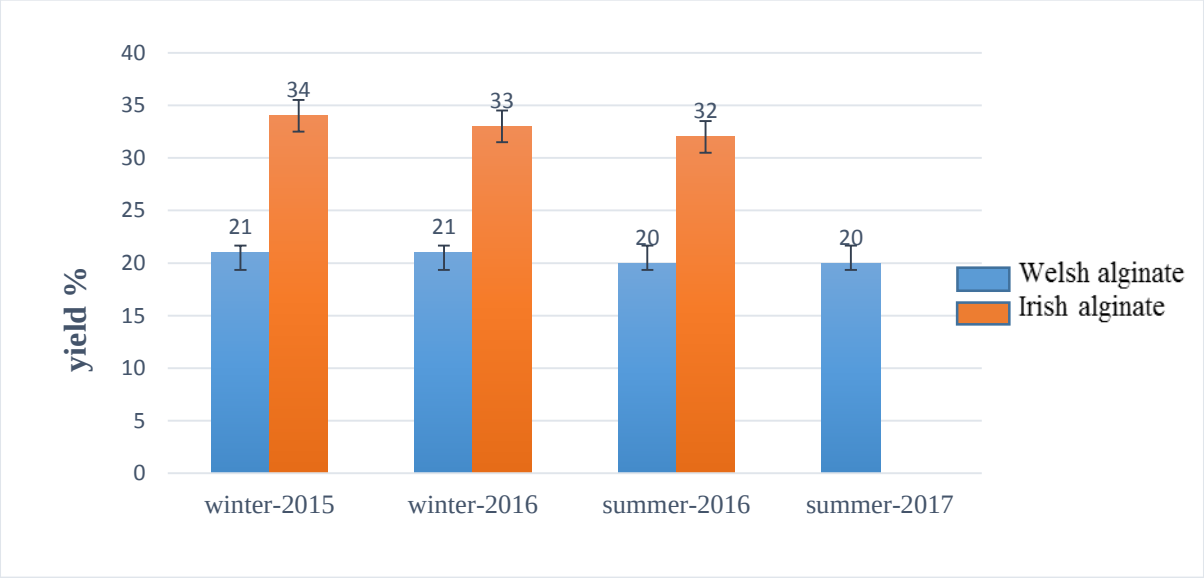

Fig (3-4): The percentage yield of alginate extracted from Irish and Welsh seaweeds at different season.

Table (3-5): Yield under different extraction conditions of alginate from Welsh seaweeds harvested during winter 2015 (WW-1).

Entry	Extraction temperature (°C)	Extraction time (hours)	Yield%
WW-1	100	3	21±0.5
WW-1	60	5	18.5±0.4
WW-1	25	24	16.2±0.3
WW-1	50	5	18±0.4
WW-1 (P)	50	5	25±0.3
WW-1 (C)	50	5	25±0.3

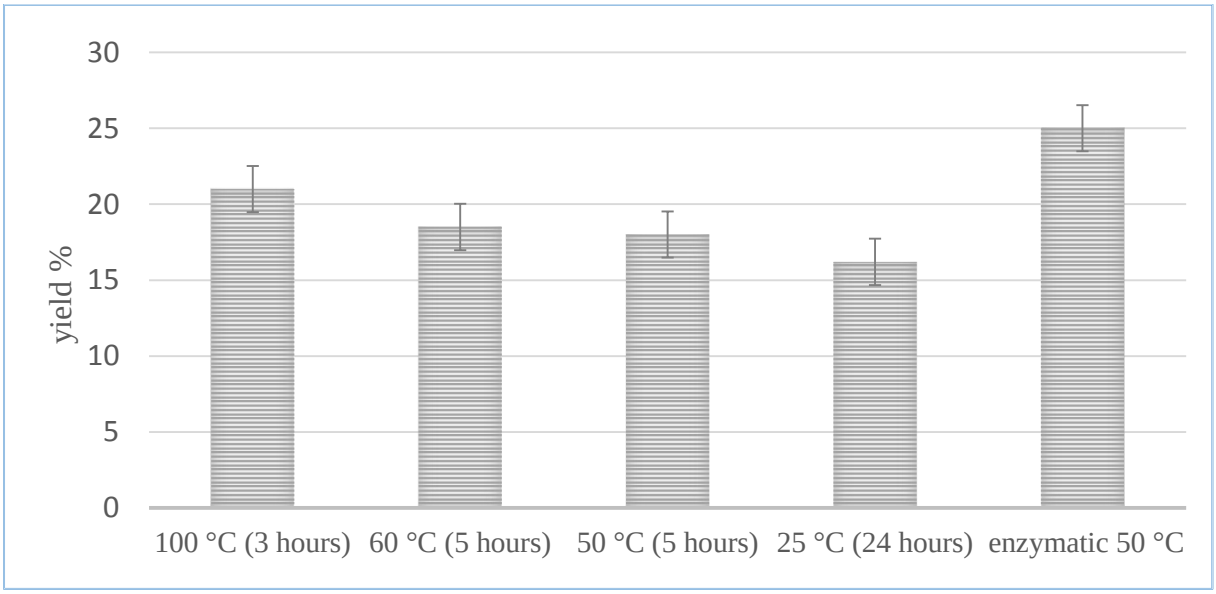

Fig (3-5): Percentage yield under different extraction conditions of alginate from Welsh seaweeds harvested during winter 2015 (WW-1).

As can be seen from **Fig (3-6)** it was found that higher yields were obtained from the bottom of the seaweed compared to the top of the plant for both Irish and for Welsh seaweeds which were collected during the summer of 2016 (32 and 40% for the Irish and 20 and 45% for the Welsh respectively). The total yield (combining both top and bottom) confirms that Irish seaweeds have a higher alginate content than the Welsh (72% and 65% respectively) but the Welsh

seaweed has a greater proportion of its alginate in the bottom of the plant (i.e. 69.23% compared to the Irish 55.55%). The reason for this is beyond the scope of this study but may be an adaptation for more flexibility required in this part of the plant. The anatomy of the species *S. fluitans* is shown in **Fig (3-7)**. The terminology `top` refers to the terminal and lateral branches of the plant, while bottom refers to the main stem or stipe of the plant.

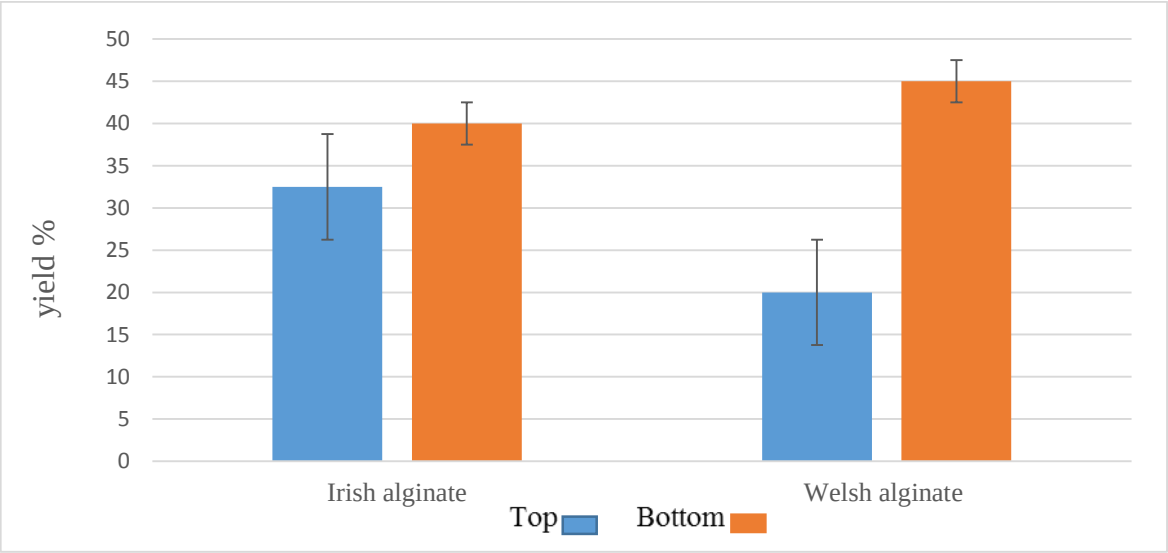

Fig (3-6): The yield percentage of alginate from top and bottom part of Irish and Welsh seaweeds harvested during summer 2016 (TIS-1, BIS-1, TWS-1 and BWS-1 respectively).

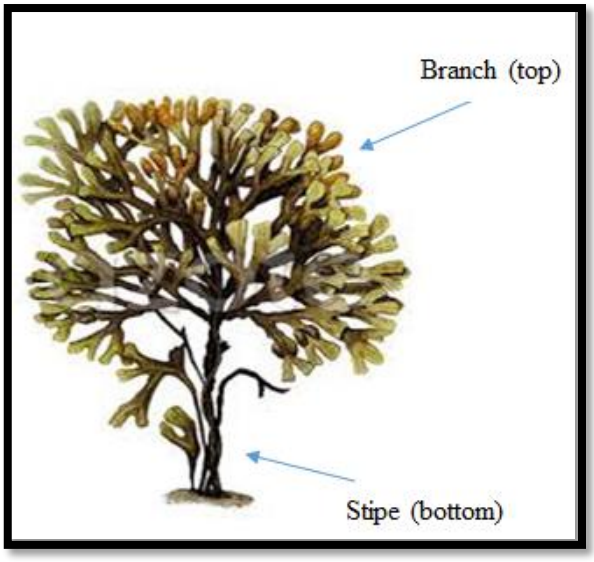

Fig (3-7): Anatomy of *S.fluitans.*

3.3.2 Determination of the M/G ratio and relative composition of alginate.

After the extraction and purification of alginates, characterisation was undertaken to determine the relative content of the two uronic acids which constitute the alginate and, therefore, account for the properties of the material. The ^{1}H NMR method is the main technique used for analysis and determination of the relative proportion of the M and G units.

To ascertain the best preparative conditions for the NMR procedure a standard commercial grade was initially used and these results were the applied for the analysis of our extracted material.

Initially, alginate samples for NMR analysis were prepared at a concentration of 10 mg/mL but were found to be too viscous. A higher temperature of 70°C failed to correct the problem and it was decided to hydrolyse the material but this also was ineffective. It was subsequently found that a lower concentration of non-hydrolysed material of 5 mg/mL at a temperature of 70 °C was the most effective.

The ^{1}H NMR spectra of commercial sodium alginate samples at different temperatures, 50, 60, 70 and 80 °C are shown in **Fig (3-8).** The spectra illustrate the importance of choosing the appropriate temperature for ^{1}H NMR analysis. For temperatures between 25 and 50°C the water signal fully or partially overlapped with the anomeric signals at 4.4 and 5.2 ppm used for M/G-ratio determination.[145] Although 60°C temperature was found to be satisfactory to shift the water peak outside that region, it was still too close, such that the intensity of H5 of the GG peak, which resonates at 4.4 ppm, appears to be affected by water suppression, therefore an even higher temperature was necessary. A temperature of 70°C was found to be sufficient for the recovery of all the anomeric peaks from the water suppression effect. **Fig (3-8)** clearly shows that the higher the temperature, the better the peak resolution, and that is due to the absence of hydrogen bonding within the molecule at high temperatures. It can be concluded that for analysis the higher temperature positively affects the viscosity thereby reducing the peak broadness and moves the DOH resonance far from the more diagnostic signals.

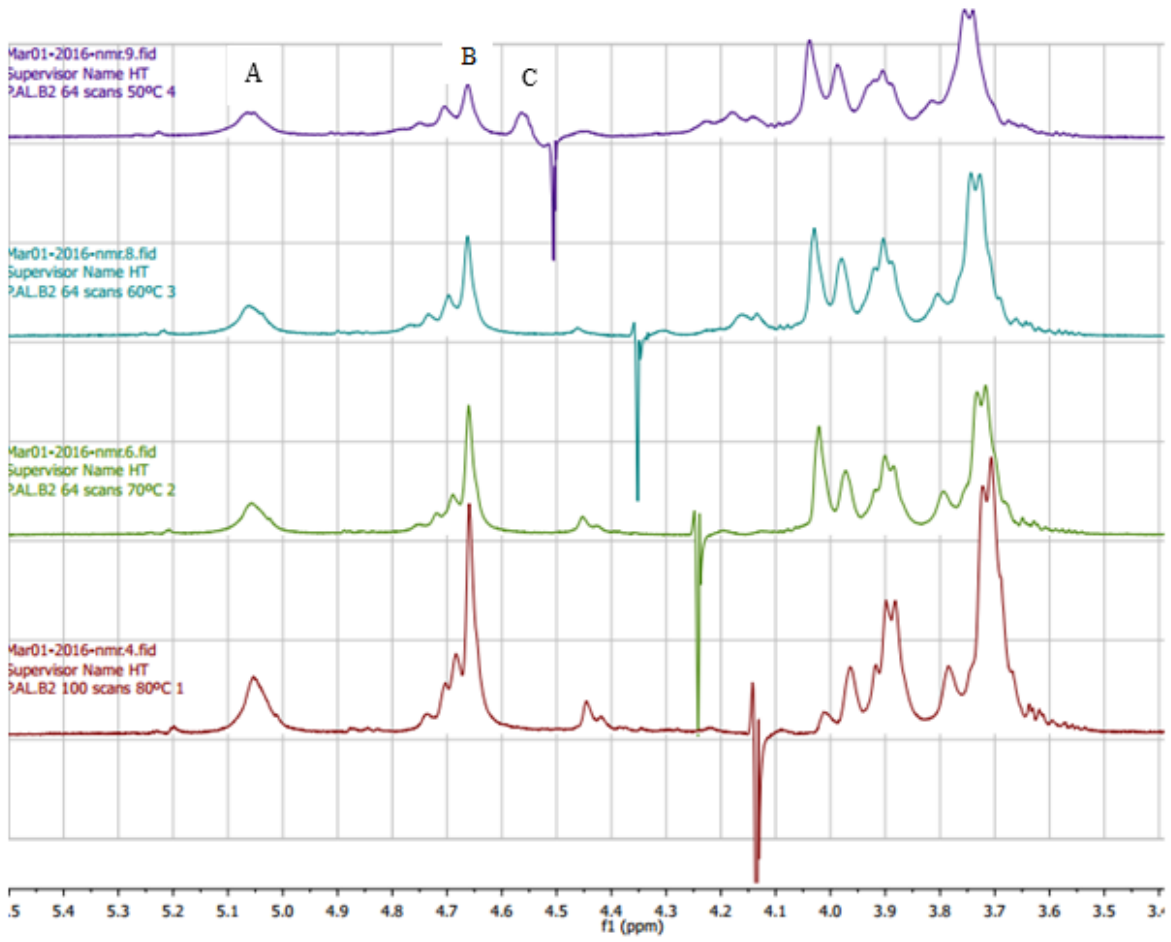

Fig (3-8): ^{1}H NMR of commercial alginate (AlG-A) showing the temperature effect on water signal displacement.

The anomeric regions of the ^{1}H NMR spectra of sodium alginate samples is shown in **Fig (3-9)** shows specific peaks assignments for guluronic acid anomeric proton (G-1) at 5.17 ppm (peak A); guluronic acid H-5 (G-5) at 4.56 ppm (peak C); and mannuronic acid anomeric proton (M-1) at 4.76 ppm (peak B) and also the C-5 of alternating blocks (GM-5) at 4.82 ppm imbricated with peak B. This anomeric region can also give information about the linkage between G-blocks and M-blocks as it was previously reported.[146, 147] M-1M and M-1G represent the anomeric proton of an M residue neighbouring another M residue or a G residue, respectively. MG-5M, GG-5M, and MG-5G refer to the H-5 proton of the central G residue in an MGM, GGM, or MGG triad, respectively. G-1 refers to the anomeric proton of G residues and GG-5G refers to the anomeric proton of G residues in G-blocks.

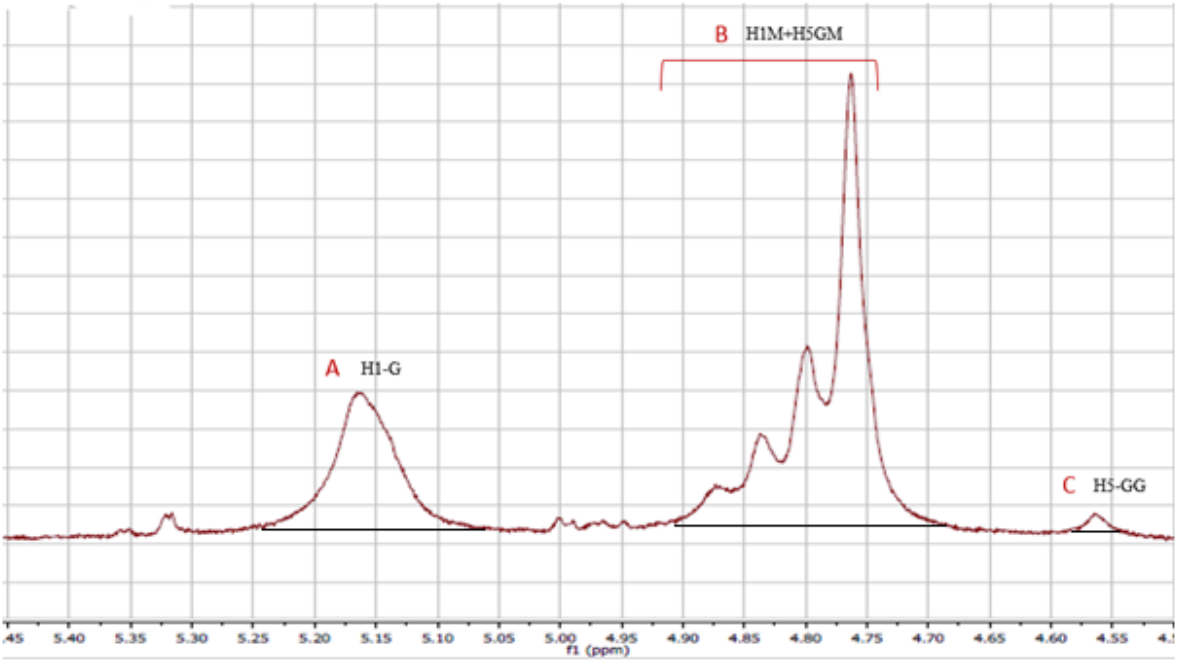

Fig (3-9): Assignment of the H1 and H5 signals for M and G residues in (AlG-A) with integration limits shown as horizontal lines.

Composition and also the block structures of alginate molecules are also often determined by ^{1}H NMR spectroscopy. [148,19] The method proposed by Grasdalen (1983) and Grasdalen *et al.* (1979) [26, 146] makes it possible to calculate the M/G ratio and to determine the block structure. The signals and the relative area of anomeric protons can be used for the quantitative analysis of the individual guluronic acid (F_G) and the doublet G–G (F_{GG}) fractions. Grasdalen in his 1983 paper uses a method which requires integration of the four individual peaks which together comprise the composite peak B and are evident from inspection of **Fig (3-9)**. The methodology for such a four peak integration is given in **Chapter 1.2.2**. However, a modification of this method is given in his earlier paper of 1979 and was adopted for this study. This was because it was not always possible to obtain high resolution spectra when using material of high viscosity despite conducting analysis at higher temperatures. Thus, to allow for valid comparisons to be made the composite peak approach was adopted for all spectra analysis. An earlier trial comparison was made using the individual peak integrations which permitted triad analysis but such a refinement was not necessary for diad quantification and the composite peak method was more practical. Therefore, no significant loss of accuracy resulted using this method.

The areas under the peaks A, B and C can be used to calculate F_G and F_{GG} using the following equations:

$F_G=I_A/ (I_B+I_C)$, (1)

$F_{GG}=I_C/ (I_B+I_C)$ (2)

The fraction M is deduced from:

$F_M=1-F_G$ (3)

The diad fractions F_{GG} and F_{MM} can be calculated from the following relationships.[149]

$F_G=F_{GG}+F_{GM}$ (4)

$F_M=F_{MM}+F_{MG}$ (5)

And the M/G ratio is calculated explicitly by

$M/G= (1-F_G)/F_G$ (6)

A complete description of the alginate monomer sequence is not possible using the method as presented which was used to determine the doublets only. However, it may be illustrative to use a parameter Ɛ, defined by the equation (7) to determine the heterogeneity of the alginate samples.[23]

$Ɛ=F_{MG} / F_M*F_G$ (7)

Table (3-6): M/G ratios and compositional data of commercial alginate and alginates extracted from Welsh and Irish seaweeds for winter and summer seasons for years 2015-2017.

Entry	Sample name	F_G	F_M	M/G	F_{GG}	F_{MM}	F_{MG} F_{GM}	Ɛ
1	WW-1	0.52	0.48	1±0.02	0.37	0.33	0.15	0.60
2	WW-2	0.40	0.60	1.5±0.03	0.18	0.38	0.22	0.91
3	IW-1	0.31	0.69	2.2±0.03	0.28	0.66	0.03	0.14
4	IW-2	0.34	0.66	1.9±0.01	0.26	0.58	0.08	0.35
5	WS-1	0.25	0.75	3.0±0.02	0.09	0.59	0.16	0.85
6	WS-2	0.33	0.67	2.03±0.03	0.21	0.55	0.12	0.54
7	IS-1	0.25	0.75	3.0±0.04	0.19	0.69	0.06	0.32
8	Alg-A	0.46	0.54	1.2±0.01	0.04	0.12	0.42	1.68

The M/G ratio is an indicator of the gelation behaviour of alginates. Divalent cations such as Ca^{2+} are known to strongly interact towards the G-block rather than the M-block, to form the well-known egg-box model. The homo-polymeric regions F_{MM} and F_{GG} and the hetero- polymeric region F_{MG} are also considered parameters that can predict the properties of alginate gels.

From **Table (3-6)** the alginate samples gave Ɛ in the range 0.14-0.91, which suggests in general terms that structures are of the homo-polymeric block type (Ɛ < 1).[146]

The results presented shows that all the extracted alginates are rich with mannuronic acid residues M since M/G value is greater than 1. Generally, the amount of M content is less in winter than in summer for both (Irish and Welsh) alginate. However, the M content is higher for the Irish than the Welsh in the winter season, although there is some variation year by year. This might reflect different local environments for the species concerned *F. vesiculosus*. The effect of higher temperatures can be seen from observing summer data. For both Welsh and Irish the M content is higher in summer. Warmer and perhaps more dynamic conditions may require the flexibility a high M content confers.

Of course, the relative M content is a very approximate indicator of mechanical properties. The Ɛ parameter is a measure of the heterogeneity for the same M/G content and the table confirms that the higher the M/G the higher the parameter. This also correlates with a lower homo-polymeric content as given by F_{GG} and F_{MM}. Thus, Irish seaweed has, for a relatively small increase in M content, the M residues are distributed over a greater homo-polymeric region with the effect of reducing the relative hetero-polymeric content.

In the summer season the alginate M content increases, as measured by the M/G ratio, for both Irish and Welsh seaweeds. This reflects a higher M content (F_M) and consequently a lower G content (F_G).The corresponding F_{GM} figures have reduced compared to the winter, indicating that the higher M content is distributed in the heterogeneous regions and would be expected to confer more flexibility to overall character. Again the heterogeneity is indicated by the higher Ɛ parameter. The Ɛ parameter can only be considered as a rough measure and gives rise to the anomalous figure of 0.85 for WS-1 although a relatively lower heterogeneity in the M content can be expected. This can be explained by the lower F_G value which has the effect of distorting the Ɛ parameter because the F_G figure is in the denominator in the definition of Ɛ. Overall, it can be concluded that there are real differences in the compositional fractions, such that the Irish samples appear to have high amount of Homo-polymeric blocks of both M and G; while Welsh samples contains more of hetero-polymeric block MG.

From **Table (3-7)** the alginate M and G content varies with the plant part taken. For both Welsh and Irish seaweeds, the alginate M content is relatively higher in the bottom of the plant in the given season of harvest. It is known that plant growth occurs in the bottom of the plant and as more M is made in the summer growing season this seems to be generated in the bottom of the plant and may indicate an anatomical need for greater flexibility in this part of the plant structure.

Table (3-7): M/G ratios and compositional data of alginates extracted from top and bottom part of Welsh and Irish seaweeds for summer 2016.

Entry	F_G	F_M	M/G	F_{GG}	F_{MM}	F_{MG}	Ɛ
TIS-1	0.30	0.70	2.3±0.02	0.14	0.54	0.16	0.76
BIS-1	0.25	0.75	3.0±0.04	0.19	0.69	0.06	0.32
TWS-1	0.45	0.55	1.2±0.01	0.23	0.33	0.22	0.88
BWS-1	0.25	0.75	3.0±0.02	0.09	0.59	0.16	0.85

It can be seen from **Table (3-8)** that the M/G ratio for the alginate extracted was the same value whatever method of extraction that was employed, at least for the conditions that were used in this study. Thus, for alginates obtained from the same seaweed samples the M/G ratio was the same irrespective of reaction conditions.

Table (3-8): M/G ratios for alginates extracted from Welsh seaweeds for summer 2016 showing the effect of extraction conditions.

Entry	Extraction temperature (°C)	M/G ratio
WW-1	100	1
WW-1	60	1
WW-1	25	1
WW-2	100	1.5
WW-2	50	1.5
WW-2 (P)	50	1.5
WW-2 (C)	50	1.5

To aid further understanding of the structure the FT-IR technique was employed. The FT-IR spectrum of our standard commercial alginate (AlG-A) is shown in **Fig (3-10)** as given by the IR instrument in use at Bangor University (model details given in chapter 2: Instrumentation and Methodologies). As this is a known pure sample it provided valuable reference data.

In the 3600-1400 cm^{-1} range, a broad band assigned to hydrogen bonded O-H stretching vibration at 3442.51 cm^{-1}, a weak signal at 2932.14 cm^{-1} was attributed to a C-H stretching vibration and the two bands attributed to the asymmetric and symmetric carboxylate group stretching vibrations at 1607.30 cm^{-1} and 1416.79 cm^{-1} respectively.[150, 151] The weak bands 1302 cm^{-1}, 1126.72 cm^{-1} and 1093.07 cm^{-1} were assigned to C–C–H and O–C–H deformation, C–O stretching of pyranose rings the band at 1031 cm^{-1} may be also due to C-O stretching vibration. The fingerprint region, for anomeric assignments, i.e. 950-750 cm^{-1} show bands at 947 cm^{-1} which was assigned to a –C-O stretching vibration of the uronic acid residues, another at 891 cm^{-1} was assigned to the C1-H deformation vibration of the β mannuronic acid residues. The signal at 818 cm^{-1} appears characteristic of Mannuronic acid residues.[152, 153]

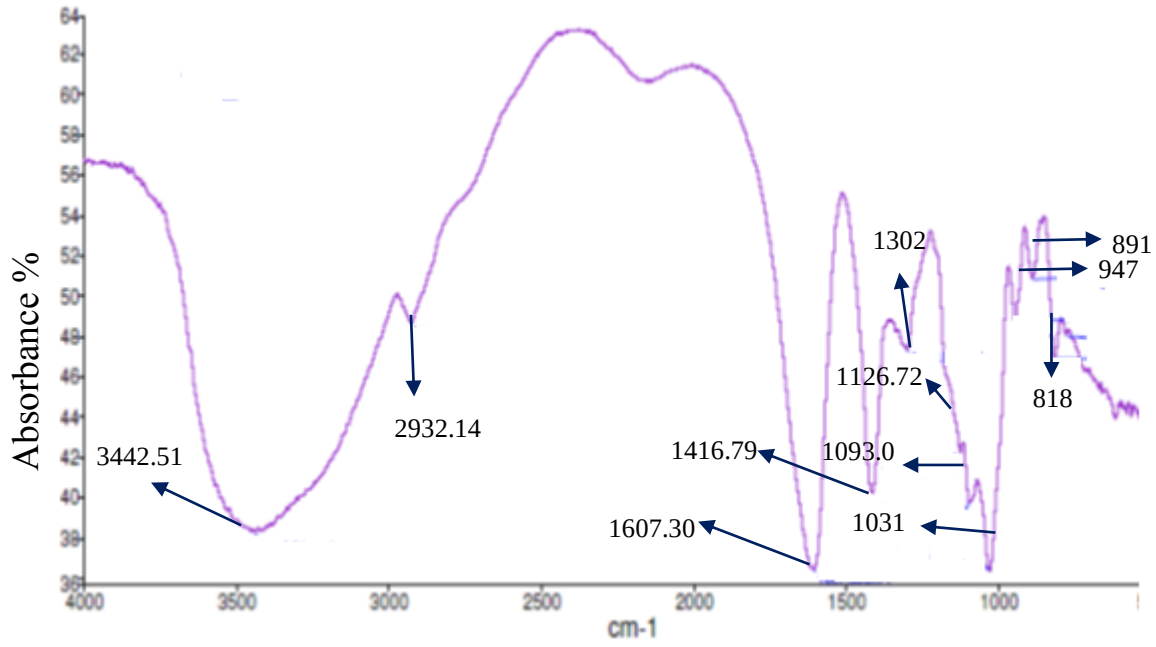

Fig (3-10): FT-IR spectrum of commercial alginate (ALG-A).

For the extracted alginates in this study, it can be expected that similar FT-IR absorption positions as the model commercial alginate are obtained and these are presented in **Table (3-9)** below with their specific values given.

Table (3-9): Main peak assignments for extracted Irish and Welsh alginates.

Sample	O–H Stretching (cm^{-1})	C–H stretching (cm^{-1})	COO^- asymmetric (cm^{-1})	COO^- symmetric (cm^{-1})
IW-1	3456.74	2929	1634.17	1453.89+shoulder1410
IW-2	3443.42	2926.09	1622	1417
WW-1	3464.35	2925.35	1626.71	1453.58
WW-2	3400.36	2988.8	1621.52	1453.94+shoulder1412
WW-2 (50 °C)	3435.36	2907	1633.93	1453.34
WW-2 P	3434.76	2964	1622.10	1415.78
WW-2 C	3454.45	2947.7	1626.81	1447.16+shoulder1406
TIS-1	3443.92	2924.87	1625.78	1412.45
BIS-1	3457.99	2923.98	1641.62	1412.10
TWS-1	3448.58	2944	1627.08	1417.24
BWS-1	3453.07	2924.39	1619.78	1420.78
WS-2	3452.70	2925.98	1618.55	1419

Note: WW-2 (50 ^oC) refers to extraction at 50^oC, WW-2 P is the protease extraction and WW-2 C is the cellulase extraction.

Generally, for extracted alginate, absorption peaks for the carbonyl group which should appear at 1607.30 cm^{-1} and 1416.79 cm^{-1} have been shifted to higher wavelengths and this may be due to protein impurity in the extracted alginate which would give rise to the stretching of the two bonds of the amide group in protein i.e. the amide (N-C=O) and (N-H) respectively. It should be noted that the FT-IR method used did not allow for a quantitative assessment of the protein content in our samples but confirmed that such protein contamination was present. The protein contamination was determined by another procedure (see 3.3.3 Protein residue quantification).

It can be observed that generally the amide signal shifts were present more in the samples taken in winter than in summer and indicate that protein contamination was lower perhaps reflecting a relatively higher alginate content in summer when in the growing season M synthesis is higher.

As stated previously, alginates vary, depending on species, parts of the plant season etc., and present different proportions and/or different alternating patterns of guluronic and mannuronic units. The presence of these acids can be identified from their characteristic bands: while the guluronic units originate a band at approximately (1025-1031 cm^{-1}) the mannuronic units originate a band at approximately (1095-1100 cm^{-1}). Thus, the guluronic/mannuronic concentration ratio, characterizing a certain alginate sample, can be inferred from the relative intensity ratio of these two bands.[154]

Table (3-10): **The M/G ratio of extracted alginate from Welsh and Irish seaweeds obtained by FT-IR.**

Sample	Peak assignment (M)	Peak assignment (G)	M/G ratio
IW-1	1095.19	1030.32	0.98
IW-2	1097.2	1032.68	1.01
WW-1	1092.50	1029.05	0.90
WW-2	1092.78	1030.20	1.00
TIS-1	1097	1031	1.03
BIS-1	1092.7	1037.10	1.10
TWS-1	1095.15	1030	0.96
BWS-1	1093.5	1035.6	1.09
WS-2	1095	1028.16	1.08

The M/G ratio was estimated by FTIR analysis, as shown in **Table (3-10)**, but the results obtained are not in good agreement with NMR results as in **Tables (3-6)** and **(3-7)**. This is expected as FT-IR is a less accurate quantitative analytical technique. Some authors have found that there is a greater agreement for alginates with a lower M/G ratio. [155] However, the M/G ratios from FT-IR analysis do show a high M value i.e. a ratio is about 1 or more, which was also confirmed by our NMR data.

3.3.3 Protein residue quantification.

The protein content in samples of extracted alginate was measured to assess the effect of certain factors such as, location and extraction condition on the purity. All measurements were in triplicate. A range of alginate concentrations were prepared i.e.15 mg/mL, 10 mg/mL and 5 mg/mL, but it found that optimum results were obtained from the lowest concentration. The standard calibration curve for the assay protein used in this measurement is shown in **Fig (3-11).** It is to be noted that are two data point (at approx. 0 and 5 µg/mL) that appear to be an outliers. These data points were retained and used to obtain the line of best fit and its derived equation of the regression line as the zero data point for the blank sample must by its nature have validity.

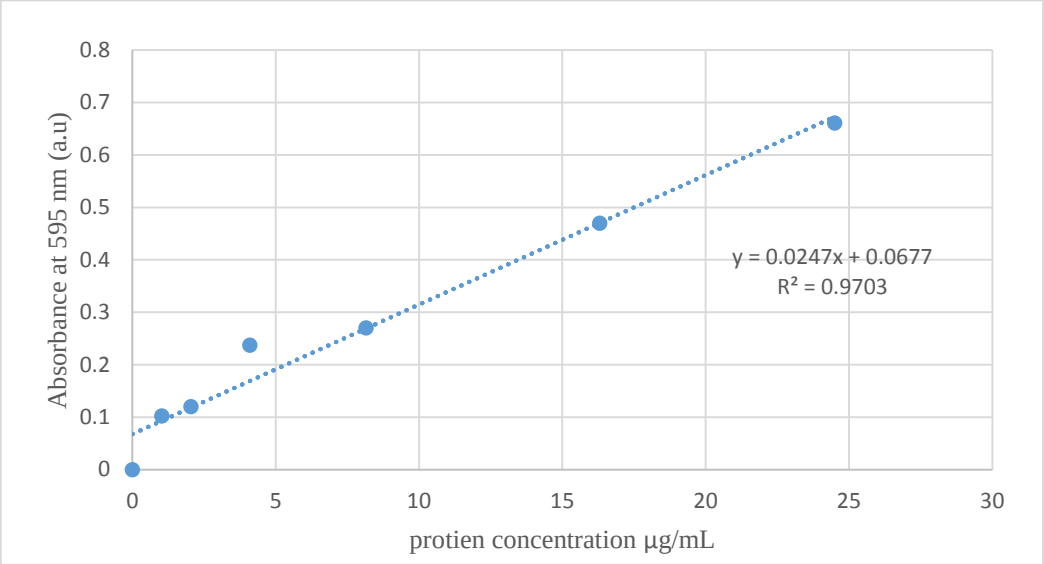

Fig (3-11): The BSA standard calibration curve.

Table (3-11) below shows the protein content in various samples and it confirms that using enzymes (protease or cellulase) gives extracted alginate higher in purity than the alginate extracted without enzymes. In addition for the alginate extracted using the same extraction method for different locations (Irish and Welsh) it is found that the alginate from Irish seaweeds contains a higher protein content.

Table (3-11): The protein residue in extracted alginates from Welsh and Irish seaweeds harvested during winter 2016 at different extraction conditions.

Entry	Sample Name	Extraction Temperature (°C)	Protein (µg/mL)
1	IW-2	100	36.8 ± 0.5
2	WW-2	100	18± 0.4
3	WW-2 (50 °C)	50	24.4 ± 0.5
4	WW-2 (50 mg P)	50	16.7 ± 0.3
5	WW-2 (30 mg P)	50	13.2 ± 0.3
6	WW-2 (50 mg C)	50	15 ± 0.2

Note: IW-2 and WW-2 extracted at 100 °C

Note: Protease (P) and cellulase (C)

From entries 4 and 5 it can be seen that the concentration of protein is decreased by using of 30 mg of the enzyme rather than 50 mg. As the enzyme itself is a protein it is possible that it becomes part of the impurity and therefore reducing its concentration will also reduce contamination. It should also be noted that enzymes being biological catalysts are suited to working at low concentrations. This also has the advantage of being more economical for possible commercial application.

Comparing entries 2 and 3 the effect of temperature can be seen. A higher temperature reduces the amount of impurity (lower protein content). This is probably due to decomposition of protein at the higher temperature.

3.3.4 Molecular weight of extracted alginate.

The molecular weight of extracted alginates have been determined using Gel permeation Chromatography (GPC) as the main technique.

It is known that the molecular weight has a significant effect on solution viscosity. With an increase in molecular weight viscosity of the polymer solution also increases at a critical value

of molecular weight, chain entanglement occurs, and the polymer solution tends to exhibit non-Newtonian behavior since the slope of the shear stress versus shear rate curve will not be constant as we change the shear rate. Thus, the molecular weight distribution has a large effect on rheology.[156]

The molecular weight of both alginates (Irish and Welsh) as determined by GPC at different seasons are shown in the table below. Extraction was performed by the enzymatic procedure as this gave a lower protein impurity in test samples. The samples chosen where from the top of the seaweed.

Table (3-12): The molecular weight of extracted alginates from Welsh and Irish seaweeds for winter and summer seasons for years 2015-2017.

Sample	WW-1	WW-2	WS-1	IW-1	IW-2	IS-1
Mw (g/mol x 10^5)	8.27±0.35	9.69±0.42	5.67±0.25	4.90±0.20	6.15±0.30	5.59±0.28
Mn (g/mol x 10^5)	5.67±0.26	2.39±0.17	1.43±0.09	1.04±0.05	2.08±0.12	1.07±0.07
PDI	1.54±0.04	4.05±0.05	3.50±0.04	4.71±0.06	2.96±0.05	3.8±0.04

Analysis of the data shown in **Table (3-12)** confirms that Welsh alginate is higher in molecular weight than the Irish for the same season, although the Irish alginate in solution was observed to be more viscous and this may reflect the different composition and molecular weight distribution. The data given represent averages and thus suggests significant real differences between Irish and Welsh seaweeds. It is also observed that for both the Welsh and Irish alginates that higher molecular weights were found in the second winter indicating climatic factors were at work (for the Welsh winter 9.69 x 10^5 g/mol compared to 8.72 x 10^5 g/mol and for the Irish 6.15 x 10^5 g/mol compared to 4.90 x 10^5 g/mol). **Table (3-12)** also shows that, generally, the PDIs were broad with a value greater than 2, and no particular trend was observed.
Table (3-13) presents data for Welsh alginate extracted under different extraction conditions.

Table (3-13): The molecular weight of extracted alginate from Welsh seaweeds under different extraction conditions (during winter 2015 and 2016).

Entry NO	Samples name	Mw (g/mol x 10^5)	Mn (g/mol x 10^5)	PDI
1	WW-1(100 ^oC)	8.27±0.35	5.67±0.26	1.54±0.04
2	WW-1 (60 ^oC)	7.23±0.32	4.07±0.17	1.77±0.06
3	WW-1(25 ^oC)	1.13±0.03	4.07±0.15	2.77±0.07
4	WW-2 (100 ^oC)	9.69±0.42	2.39±0.17	4.05±0.05
5	WW-2 (50 ^oC)	7.06±0.30	1.35±0.04	5.24±0.08
6	WW-2 (30 mg P)*	6.28±0.29	2.89±0.10	2.17±0.06
7	WW-2 (50 mg P)*	5.24±0.25	1.37±0.05	3.81±0.08
8	WW-2 (C) *	4.33±0.19	1.14±0.03	3.79±0.07

The enzymatic extraction take place at 50 ^oC. P stands for protease, C stands cellulase.

Alginates from experiments Entries 1, 2 and 3 were extracted at different temperatures and it shows that the molecular weight of extracted alginate is affected by the extraction temperature. A higher extraction temperature leads to a higher molecular weight. This may be the consequence of a higher temperature releasing larger molecular species from the cell wall matrix of the seaweed; the higher the temperature, the more efficient the release. This may also reflect a greater denaturation of binding proteins and also hydrolytic proteins within the cell wall matrix. The GPC curves for three alginate samples extracted at different temperature (**Fig (3-14))** gives a visual confirmation of these results. The shortest retention time was for WW-1 (100 ^oC).

Comparison of data, see **Table (3-14)** for different parts of the plant reveal that for both Irish and Welsh seaweeds the alginates in the lower plant were higher in molecular weight than the top. This correlates with the casual observation that the extract solution appears more viscous for extractions from the lower plant. Incidentally, the lower plant extract solutions were also seen to be darker in appearance but this requires further study as to the cause and may correlate to the higher M content which is known to give rise to a higher viscosity.

The molecular weights are very similar for both Welsh and Irish seaweeds in the summer season. This is evidently to be expected when comparing the same species in the same season.

This similarity does not hold for the winter season, the winter conditions may be different for the two locations. A more detailed study would be needed to clarify this point **Table (3-12)**.

Table (3-12): The GPC determined Mw of the top and bottom parts of extracted alginate from Welsh and Irish seaweeds for summer 2016.

	Bottom part		Top part	
Sample	**M_W (g/mol x 10^5)**	**PDI**	**M_W (g/mol x 10^5)**	**PDI**
IS-1	6.75	4.08	4.42	4.12
WS-1	6.33	4.19	5.00	3.50

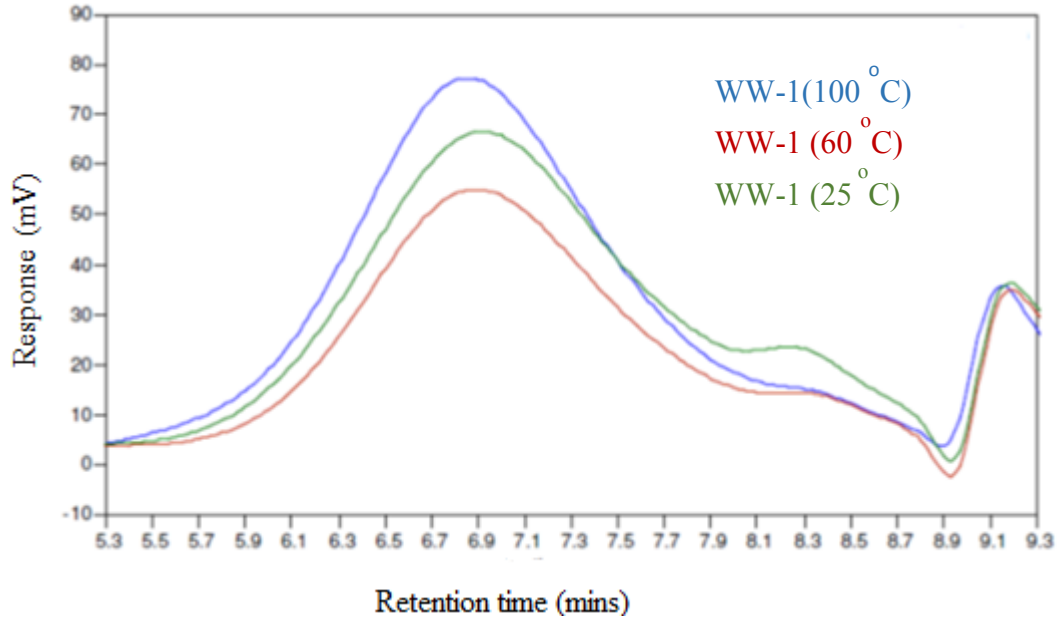

Fig (3-12): Chromatogram showing M_W distribution for extractions at different temperatures [25, 60 and 100 °C].

3.3.5. TGA/ DSC analysis.

A thermo-gravimetric analysis was undertaken to compare the moisture and ash content of the extracted alginate samples with the commercial brand. The TGA curve indicates the change in

mass of the sample during the heating cycle. The DSC curve is useful to identify the thermal transitions within the material.

Data is as given in **Table (3-15)**, which was obtained for the TGA and DSC measurements of alginate samples. Typically, under heating, sodium alginate loses its mass gradually, as observed by TGA, during four or five stages. The first stage is a dehydration, which takes place between 23 ºC and 100 ºC when an endothermic peak accompanies the moisture loss. All samples were found to have moisture present despite the fact that the drying process ensures that drying was carried out to constant mass. The presence of hydrophilic groups within the polymer's block structure inevitably results in the binding of water from, for instance, ambient atmospheric moisture that occurs during sample storage and handling. This would be considered a constant for materials of a similar composition and, therefore, a characteristic feature in the TGA curve for air-dried material. The mass loss in the range to 100ºC, therefore, represents the moisture content of the sample. The extracted samples from **Table (3-15)** have a moisture content between 10-15%. The Welsh (WS-1) sample on the other hand have ca. 3.1%. The presence of moisture in all samples, thus, should be a consideration were ascertaining the concentration of prepared alginate solutions as otherwise their concentrations will be overestimated.
Following dehydration, three or four-decomposition stages take place in the given temperature ranges and these result in a final decomposition to produce ash.

The Table allows a comparison to be made between the alginate from Irish and Welsh seaweeds (entries 2 and 3) during winter. It can be seen that the Irish seaweed has a higher ash content than the Welsh (35% and 23% respectively). Perhaps the most arresting point is seen when a comparison is made between the WW-1 with WS-2 (entries 2 and 4) when it is seen that the latter has a much lower moisture content (i.e. 3.1% and 15% respectively). The moisture content at 3.1% is, in fact, markedly the lowest for all the samples tabulated.

The other major point to note from the TGA/DSC curve is the rapid rate of decomposition for the first decomposition phase which probably results from loss of low molecular weight species from decomposition at a relatively low temperature. The decompositions 1 and 2 for the commercial alginate (entry 1) can be considered, for this analysis, as a single decomposition as the change is gradual with only a small mass loss during the first decomposition.

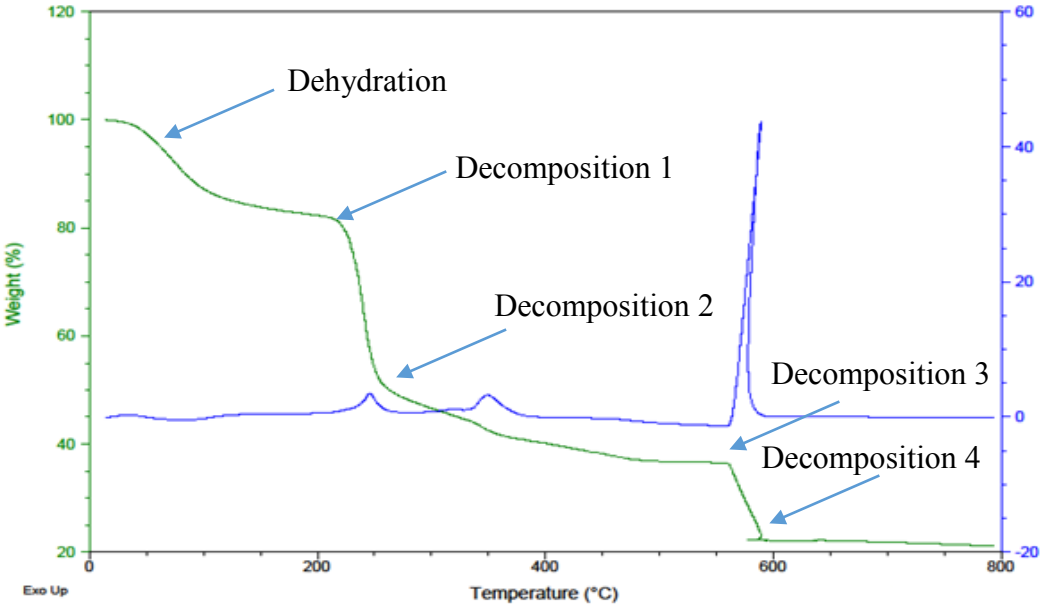

Fig (3-13): DSC/TGA curve of commercial alginate (ALG-A) obtained under nitrogen.

Table (3-15): Thermal decomposition data of commercial alginate, Irish alginate extracted in winter 2015 and Welsh alginate extracted in (winter 2015 and summer 2017).

Entry	Sample	Thermal Behaviour	ΔT ºC	Mass loss %	DSC
1	ALG-A	Dehydration	100	13	-
		Decomposition 1	100-230	7	endo
		Decomposition 2	230-250	28	endo
		Decomposition 3	250-580	14	endo
		Decomposition 4	580-600	16	endo
		Ash content		22	
2	WW-1	Dehydration	100	15	-
		Decomposition 1	100-250	30	endo
		Decomposition 2	250-600	12	endo
		Decomposition 3	600-670	20	endo
		Ash content		23	
3	IW-1	Dehydration	100	10	-
		Decomposition 1	100-250	35	endo
		Decomposition 2	250-580	10	endo
		Decomposition 3	580-600	10	endo
		Ash content		35	
4	WS-2	Dehydration	100	3.1	-
		Decomposition 1	100-250	33	endo
		Decomposition 2	250-550	26.8	endo
		Decomposition 3	550-680	18.5	endo
		Ash content		18.6	

3.3.6 Acidic and enzymatic hydrolysis.

The molecular weight and M/G ratio can be controlled by means of hydrolysis by acidic or enzymatic methods to yield different fractions varying in their Mw and M/G ratios and which can, therefore, be modified in their properties and applications. In this study, HCl and alginate lysis enzyme are used to break the glycoside bond in the alginate backbone. For this procedure

BIS-1 and BWS-1 were hydrolysed with acid and 3 fractions were obtained from each sample and TWS-1 has been hydrolysed using the lysis enzyme. The following tables show the different fractions obtained from each alginate as a result of hydrolysis.

Table (3-16): The Mw and M/G ratio of fractions obtained by acidic hydrolysis of alginate extracted from bottom part of Welsh and Irish seaweeds in summer 2016 (S-1) .

Sample	yield%	M/G	Mw(g/mol x 10^5))
BIS-1	-	3	365
F1(I)	20	1.32	205
F2(I)	41	1.7	0.42
F3(I)	38	2.12	305
BWS-1	-	3	347
F1 (W)	31	1.5	147
F2 (W)	44	1.7	0.5
F3(W)	22	2.8	290

High yields were obtained but material was heavily contaminated with NaCl and NaOH. It can be seen from **Table (3-16)** that the M content increases with the fraction number i.e. the first soluble fraction obtained from hydrolysis and, therefore, the most labile is the lowest in M content. Subsequent fractions are seen to be higher in M content and are increasingly less susceptible to hydrolysis. The third faction is seen to have the highest molecular weight, which is also consistent with its resistant to hydrolysis.

Alginate lyase was used to catalyse the degradation of alginate (**Table (3-17)**). The soluble fraction obtained was seen to be richer in G, as shown by a low M/G this would seem to indicate that the enzyme is specific for either M or G.[22] This may afford a method of obtaining a source material of higher G content for use in hydrogels for improved performance.

Table (3-17): The M/G ratio and Mw of fractions obtained by enzymatic hydrolysis of alginate extracted from top part of Welsh seaweeds in summer 2016 (S-1).

Sample	Yield %	M/G	Mw(g/mol x 10^5)
TWS-2		1.2	5.00
F1(TWS-2)	16	7.3	3.30
F2(TWS-2)	76	0.35	1.31

3.4 Conclusion.

In this chapter, alginate extracted from Irish and Welsh seaweeds of the species *F.vesiculosus* is described. In addition to location other influencing factors were studied such as the harvest season and the various methods of extraction on the properties of the extracted alginate. The extraction was performed using a traditional method with sodium carbonate and also enzymic assisted methods were employed. It was found that the yield was affected by location, season and method of extraction.

Irish seaweeds gave higher yields than the Welsh (32 ± 1.6-34 ± 1.5% and 20 ± 2.05%-21± 2.05% respectively) and for both the winter yields were higher comparing with summer (1% higher for the Welsh and 1.34% for the Irish for winter and summer respectively). For different extraction temperatures, it was found that the higher temperature is the overriding factor for higher yields. Thus, for the non-enzymic method for Welsh seaweed the yield was 21%. It was also found that using enzyme extraction of alginate gave the highest yield with highest alginate content and the least protein impurity, thus for the Welsh seaweed a yield of 25% was obtained for the enzymatic extraction method. .

The M/G ratio of extracted alginate varied from 1 to 3 and depended on the location, season and part of the plant. The Irish alginate was found to be higher in M content than the Welsh for the same season (0.4-1.2 % higher for Irish seaweed in winter) and the M content was higher in summer than in winter for both Irish and Welsh alginate being 0.06 % higher for the Irish and 0.27%- 0.07% higher for the Welsh. The bottom part of the plant is higher in M content than the top (0.7% higher for the Irish and 8% higher for the Welsh) probably resulting from a requirement for increased flexibility.

The M/G ratio was unaffected by the extraction conditions used, at least for the alginate extracted from the same seaweed for the same location at the same season. i.e. the M/G ratio for the alginate extracted from Welsh seaweeds for winter 2015 (WW-1) at temperatures 100, 60 and 25 ^{o}C was 1.0 and the M/G ratio for the alginate extracted from Welsh seaweeds for winter 2016 (WW-2) at 100 and 50^{o}C, either with or without enzymes was 1.5.

The molecular weight of extracted alginate ranged between 9.69 and 4.42x10^{5} g/mol depending on the location, season, extraction conditions and the part of the plant. Generally the Welsh

alginate was higher in molecular weight than the Irish (i.e. 7.80 and 5.15x$10^{5.}$ g/mol kD respectively, on average) and the alginate extracted for the winter season was higher in molecular weight for both Irish and Welsh than the alginate extracted at summer season (the Welsh winter average was 9.20 x10^5 g/mol compared to Welsh summer 5.52 x10^5 g/mol and Irish winter was 5.52 x10^5 g/mol compared to 4.42 x10^5 g/mol for summer). Additionally, the alginate extracted from the bottom of the plant is always higher in molecular weight than that from the top part (for Irish summer seaweed (bottom) 6.75 x10^5 g/mol compared to 4.42 x10^5 g/mol for the top and for Welsh 6.33 and 5.00 x10^5 g/mol respectively). For summer, yields both Irish and Welsh had very approximately a similar molecular weight. The molecular weight of extracted alginate is affected by the temperature. A higher extraction temperature leads to a higher molecular weight (for Welsh seaweed at 100^{o}C an M_w of 8.27 x10^5 g/mol compared to 1.13 x10^5 g/mol at 25 ^{o}C)

The heating profiles were similar for both types of alginate and the ash content for all alginates was approx. between 10 -20% depending on season and geographic location. DSC also showed the alginate extracted from Welsh seaweeds for summer 2017 (WS-2) gave a moisture content of 3.1%.

Acidic hydrolysis was found to progressively increase the yield of product with time for both Irish and Welsh alginates. However, the M content increased relative to the G content with increasing hydrolysis. Thus, for Irish summer alginate (bottom) with an original M/G of 3 upon hydrolysis subsequent fractions increased from 1.32 to 2.12 as the G content was lost as a soluble product.

Enzymic hydrolysis was found to be a rather more specific method yielding soluble products, which were higher in G content showing that the m content was more resistant to enzymic hydrolysis. Thus, for the top part of Welsh summer seaweed the M/G ratio was 0.35 compared to an original 1.2 for the non-hydrolysed material.

Chapter 4: Grafting Alginate with PCL and investigation of swelling properties of its bulk gel

4.1 Introduction.

Chemical modification of alginates can be used to enhance existing properties such as improvement of the strength by covalent crosslinking, to increase hydrophobicity of the alginate backbone, and to improve biodegradation. Chemical modification can also introduce completely new properties.[21]

Chemical grafting is an effective method for modifying the structure and properties of many biopolymers. Graft copolymerization of natural polysaccharides has become an increasingly important procedure for synthesising advanced materials as a way of realising their great potential.[157, 158] In particular, graft copolymers containing many side chains covalently attached to a linear backbone have interesting properties including worm-like conformations, and compact molecular dimension with useful chain end effects particularly in comparison with their corresponding linear counterparts of similar molecular weight.[159, 160]

To understand the correlation between the structure of polymers and their properties and appreciate any specific applications of polymers, graft copolymers with various branched topologies and compositions have been successfully synthesized, including copolymers with homopolymer and copolymer side chains. Also, star-like multi-arm graft copolymers and graft-on-graft copolymers have been synthesised.[159, 160] Synthesis has been achieved in general by three different strategies, including grafting through, grafting-from and grafting-onto. See **Fig (4-1).**

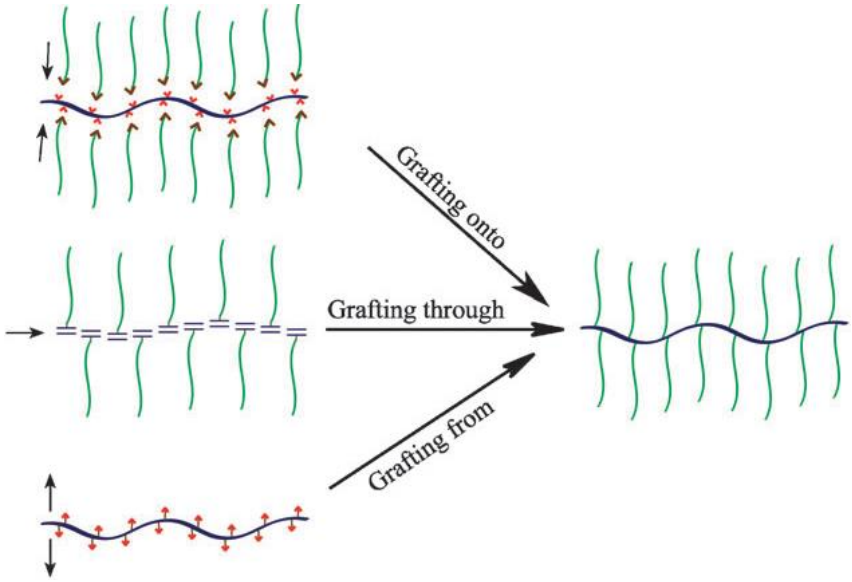

Fig (4-1): The different strategies of grafting.[161]

In the **grafting-onto** strategy**,** side chains are attached to a linear backbone by a coupling reaction **Fig (4-1)** in which the linear backbone and side chains are prepared independently. This strategy includes utilisation of non-covalent interactions where non-covalent bonding motifs are added as functional groups onto the polymer and via complementary recognition mechanism units in the backbone and side chains are linked through a specific binding interaction. Non-covalent interactions include hydrogen bonding, coordination metal–ligand complexes and electrostatic attraction. This non-covalent strategy can, therefore, introduce features such as reversibility and stimuli-responsibility and so allow more controllability.

In the **grafting through** strategy graft copolymers are prepared by polymerizing the macromonomers containing polymerizable end groups to create a linear backbone **Fig (4-1**). Here, the length of the side chains, the length of the backbone and the grafting density can be controlled to the required degree of polymerization by appropriate selection of constituents.

In the **grafting-from** strategy, the side chains are formed from the initiation- group contained within the macromolecule structure, i.e. macro-initiator, which can be added directly via an initiation-group-containing monomer or by functionalization of the main chain with the initiator.

Graft copolymers have been synthesised by the combination of different polymerization methods such as ROMP, ROP, living/controlled radical polymerization, and living anionic polymerization. [161]

In particular, alginate can form hydrogels by physical and chemical cross-linking methods to produce cross-linked three-dimensional networks, which by virtue of their hydrophilic character are capable of retaining their high water content. However, the hydrophilicity of pure alginate based materials limits potential applications as their mechanical strength decreases with increased water intake as crosslinking is easily destroyed in biological buffers, which contain chelators of calcium ions or monovalent electrolytes. Thus, such hydrogels will lose many of their initial swelling and mechanical properties within a few hours.[162] These limitations can be avoided when alginate is chemically modified with biodegradable hydrophobic polyesters to form amphiphilic alginate derivatives. As with many other amphiphilic polysaccharides hydrophobic clusters may form within their bulk which may offer potential for hydrophobic drug encapsulation.[163]

Biocompatibility can be compromised when amphiphilic polysaccharides are synthesized by grafting. [164] However, if aliphatic polyesters are used as hydrophobic modifications, creating polysaccharide grafted copolymers, both biocompatibility and biodegradability are retained. [165]

Dellacherie *et al*. [166, 167] have recently reported that micro-particles prepared from amphiphilic derivatives of sodium alginate grafted with long alkyl chains, are stable in aqueous NaCl solution and are even capable of encapsulating proteins for several days. In addition, hydrophobically modified alginate have been shown to produce strong hydrogels in aqueous solution and were used as protein carriers with characteristic controlled-release properties.

Hall [59] showed that calcium ion cross-linked hydrogels derived from amphiphilic alginate derivatives grafted with butyl chains could encapsulate both hydrophobic and hydrophilic molecules. This was achieved while retaining the gelling and non-toxic properties of non-derivativised alginate.

In this study, poly (ε-caprolactone) (PCL) with its long pendant hydrophobic group was used as the graft chain to alginate. PCL is a biodegradable aliphatic polyester easily synthesized by

the polymerization of ε-caprolactone (ε-CL) by various methods including cationic, anionic and coordination polymerization as well as by free-radical initiation.[168]

Due to its bio-compatibility, non-toxicity and excellent mechanical strength, PCL has been intensively investigated as a biomedical material.[169] It also has potential as a controlled-release matrix for active compounds such as drugs, pesticides etc. due to its property of high permeability to many small drug molecules.[168]

PCL-g-alginate can be synthesised by the catalytic ring-opening polymerization of the ε-CL utilising the –OH groups of the polysaccharide to function as the initiator.[170] Grafting onto polysaccharides has also been performed when the hydroxyl groups are protected, by silylation for example, permitting a reduction in the number of active sites required for partial grafting.[171] However, these methods are limited due to polydispersity in the length of the PCL chains and the use of non-aqueous solvents.

Alternatively, monodisperse PCL macro-monomers can be grafted to the hydroxyl groups of the polysaccharide backbone but this requires the functionalization of the terminal of the PCL polyester and/or the polysaccharide in which an organic solvent and high temperature are required to achieve high substitution rates of the hydrophobic structures. A further variation, involving an emulsion method, performed in aqueous media, to synthesise water soluble polysaccharides is available and this was the method used for this study.[163]

In this work the PCL chains were grafted on to alginate backbone using a "grafting-onto" technique to retain biodegradability and to increase the hydrophobicity of alginate. Hydrogels were made both from sodium alginate and also from PCL-g-alginate with various degrees of cross-linking using different Ca^{2+} concentrations. Their swelling properties were then studied in de-ionised water and saline solution. The graft PCL-g-alginate co-polymers were prepared with different molecular weights of PCL. The PCL in this study was prepared by ROP and the high M_W of PCL was prepared by supercritical CO_2 technology.

4.2 Experimental

4.2.1 Chemicals and materials.

Sodium alginate (AlG-A) (low viscosity, purchased from Sigma Aldrich) was used in this work and was characterised by means of Gel Permeation Chromatography (GPC) to have molecular weight of 237.2 kg/mol. Its M/G ratio was determined as 1.2 by ^{1}H NMR analysis and was labelled as "A". Welsh alginate, previously designated as WS-2 as per chapter 3, and with an M/G ratio 2.03, was also used for grafting with PCL and labelled as "W". Poly (ethylene glycol) (PEG) (Mw 400), ε-Caprolactone (97%), tin (II) 2-ethylhexanolate (95%), 1-ethyl-3-[3-(dimethylamino)-propyl] carbodiimide hydrochloride (EDCI), deuterium oxide and sodium dodecyl sulphate (SDS) were purchased from Sigma Aldrich and used as supplied unless stated otherwise. Potassium bromide, calcium chloride were obtained from Fisher chemicals. Poly (caprolactone) (PCL-10) was prepared in house according to the procedures described in 4.2.2. Five poly (caprolactone) samples with different Mw were kindly provided by Vornia Biomaterials (Dublin).

4.2.2 Preparation of PCL by ring opening polymerisation and characterisation.

PCL was prepared by ring opening polymerisation of caprolactone in the presence of PEG as an initiator and tin octoate Sn (Oct) $_2$ as a catalyst.

The catalyst/monomer ratio was set at 1 to 1000 and the initiator (PEG) to monomer ratio was 1 to 4 for a desired degree of polymerisation of 4 and 1 to 10 for a degree of 10.

The degree of polymerisation was to be 4 and 10. The polymerisations were carried out in bulk (without solvent) in a glass round bottom flask with a magnetic stirrer at 100 or 160 ^{o}C in an oil bath for 24, 42, 60 hours respectively under nitrogen gas. The typical procedure for the preparation of PCL with a degree of polymerisation of 4 was performed as follows; 5g (0.44 mol) of ε- Cl, 0.18 mg (0.044 mmol) of $Sn(Oct)_2$ and 4.4 gm (0.011 mol) of PEG were mixed in bulk for the required temperature and reaction time. The quantity of PEG was 1.75 g (0.0044 mol) was used to obtain a degree of polymerisation of 10. At the given time, the flask was

removed from the oil bath, cooled and the polymer analysed using ^{1}H NMR and FT-IR techniques. The measurement of ^{1}H NMR were performed at room temperature using $CDCl_3$ as solvent.

4.2.3 Determination of the tin content in poly (caprolactone) using AAS.

A standard calibration curve was prepared using the standard tin solution obtained from Sigma Aldrich. As supplied the Tin standard solution was 1000 mg/L, which was then diluted to appropriate concentrations using a prepared hydrochloric acid solution. The hydrochloric acid solution was prepared using 0.2 m HCL and de-ionised water in the ratio of 1: 9. Tin standards were then made, ranging from 0 (blank) to 100 mg/L, in order to construct a calibration curve

Samples of the poly (caprolactone**)** were prepared for analysis of their tin content by dissolving 1 g of the polymer in 10 mL of a mixture of concentrated sulphuric and nitric acids prepared in a ratio of 1:1. Samples were then left to thoroughly dissolve. The samples were then further diluted to a volume of 25mL using dilute HCl prepared in de-ionised water to a dilution of 1:9, as for the preparation of the standards. Analysis was performed in SpectrAA 220FS and samples were analysed at 235.5nm, with a lamp current of 7W, which is the appropriate wavelength for the concentrations used in this study.

The concentrations of tin in the samples was obtained by taking readings from the calibration curve and by applying a scaling up factor the amount of tin in the original 1 g sample was determined.

The atomiser fuel was acetylene and nitrous oxide to produce a reducing flame with a red cone 2 cm in length. The flame was emitted at wavelength 284.0 nm and light passed through a slit of width of 0.1cm. The nitrous oxide-acetylene flame is recommended for all tin determinations as per manufacturer's instruction manual.

4.2.4. Synthesis of poly (caprolactone)-g-alginate.

For the grafting of PCL on to alginate coupling was performed in heterogeneous media given the difference of solubility of both components, a two component mixture of water/dichloromethane was found suitable for both the hydrophobic PCL (dichloromethane soluble) and hydrophilic alginate (water soluble).

The hydroxyl groups of PCL cannot react easily with the carboxylate groups of alginate which were required to be ‘‘activated” by EDCI. Moreover, as the activator can only react with the carboxylic functions, the alginate was first partially converted to its acidic form by the addition of hydrochloric acid. However, alginate is liable to form gels at acidic pH [172], and to precipitate below pH 3.0.[173] As the viscosity of alginate solution markedly increases below pH 3.6, too high a difference in viscosity between the two phases (organic and aqueous) has to be avoided. Such a viscosity discrepancy could lead to a decrease of reactivity between the ‘‘activated” acid and the alcohol groups, thus, the pH was reduced to this value. As illustrated in **Scheme (4-2)**, polyester chains are thus grafted to the polysaccharide backbone via ester linkages.

A typical procedure is as follows [163]: an aqueous solution of alginate was prepared by solubilising 2 g of sodium alginate in 200 mL of water, HCl was then added until the pH reached 3.6 in order to partially protonate the alginate and the solution was then stirred for 24h at room temperature. Then an aqueous solution of EDCI was freshly prepared (0.13 g in 5 mL of deionised water) and then added, under vigorous stirring, to activate the carboxylic groups of alginate. The reaction between EDCI and –COOH functions of partially protonated alginate was carried out for 24 h at room temperature. Then, the surfactant sodium dodecyl sulfate aqueous solution (0.35% w/v) was added to the reaction mixture. PCL in the ratio of 5% wt of alginate was solubilized in 20 mL of dichloromethane and this organic phase was added drop by drop to the aqueous phase. The reaction was carried out for 24 hours at room temperature.

After the grafting was completed, the organic phase was evaporated and the reaction mixture purified by repeated dialysis in water removing unreacted EDCI and the surfactant SDS. Dialysis was continued for a week with regular changes of water. The material was then freeze-dried to before characterisation.

4.2.5 Characterisation of PCL-g-alginate.

4.2.5.1 Nuclear Magnetic resonance (^{1}H NMR) analysis.

NMR data was recorded using a Bruker 500 MHz machine at 70 ^{o} C. A scan number of 200 was used to reduce noise in the base line. The samples were prepared by dissolving approximately 10 mg in 1 mL of D_2O, which was then transferred to an NMR tube. The (HDO) peak of the solvent was eliminated using the NOESY app-1d suppression technique. The spectrum obtained was then processed using MestReNova application.

4.2.5.2 Fourier Transform Infra-Red (FTIR) spectroscopy analysis.

The FTIR spectra were obtained on a Bruker Tensor 27, using a scan range of 450 to 4000 cm^{-1}. For preparing samples of solids, KBr disks were prepared and have the advantage of no overlapping signals from the matrix (KBr). Samples were prepared by direct mixture where approx. 5 mg of sample was mixed with 50 mg of KBr powder, which is then compressed into a pellet.

4.2.5.3 Differential Scanning Calorimetry (DSC) and Thermo Gravimetric Analysis (TGA) analysis.

The DSC thermographic analysis was performed on a universal V3.7A TA (SDC Q600) instrument at a heating rate 10 ^{o}C per minute for the temperature range 25-800 ^{o}C under an inert nitrogen gas atmosphere. Morphological and chemical changes with the evolution/absorption of heat were measured.

4.2.6 Gelation method and swelling test.

Bulk hydrogels were prepared from the alginate and from the PCL–alginate graft by ionic

crosslinking with Ca^{+2} ions. Various volumes of 1% $CaCl_2$ solution in deionised water were added to alginate solution (i.e. 20, 50, 100, 200, 300, 400 and 500 µl aliquots of the Ca^{2+} solution added to 500 µl of alginate solutions and left to crosslink for 1 or 2 hours).

The hydrogels were typically fabricated according to the following procedures: 1% (w/v) alginate or 1% (w/v) PCL-g-alginate water solutions were prepared. Different volume of calcium chloride (1% w/v) (200 µl or 400 µl) was added to 500µl of polymer solutions (either 1% alginate or 1% PCL-g-alginate) respectively and then left for gelation to occur over a period of 1-2 hours. The gels were then allowed to air dry at room temperature for 3 days. See **Fig (4-2)**.

Swelling studies were then undertaken in which, to a known dry weight of the gel, (typically 0.5 g), water or aqueous sodium chloride solution (1% w/v NaCl), depending on which medium is under study, was added to allow for complete immersion of the gel. The increase in gel weight was measured daily in order to determine the swelling ratio. The above procedures were performed in triplicate for each sample.

The swelling ratio was defined as

$$\text{Swelling ratio (\%)} = (W_1 - W_0)/W_0 \times 100$$

Where W_1 is the weight of the swollen hydrogel and W_0 is the weight of dried hydrogel.

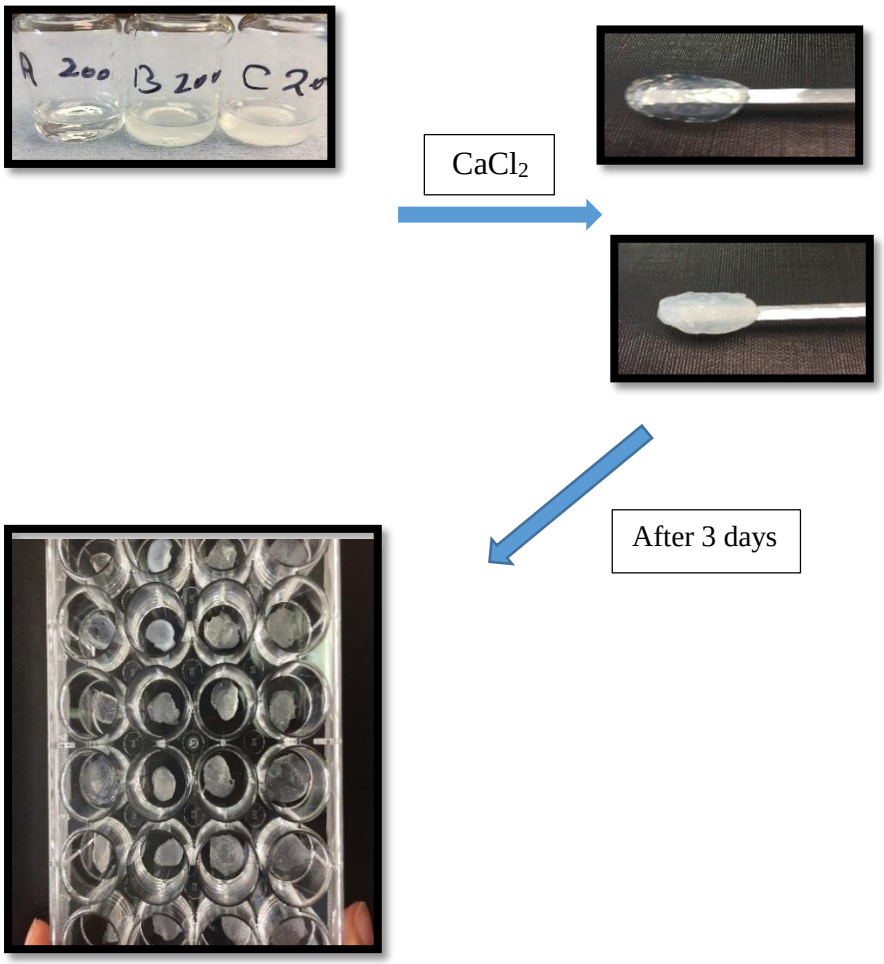

Fig (4-2): Preparation of bulk gels from alginate and PCL-g-alginate.

4.3 Results and Discussion.

PCL was prepared by the ring opening polymerisation of ε-Caprolactone in the presence of PEG as an initiator and tin octoate Sn $(Oct)_2$ as a catalyst. **Scheme (4-1)**

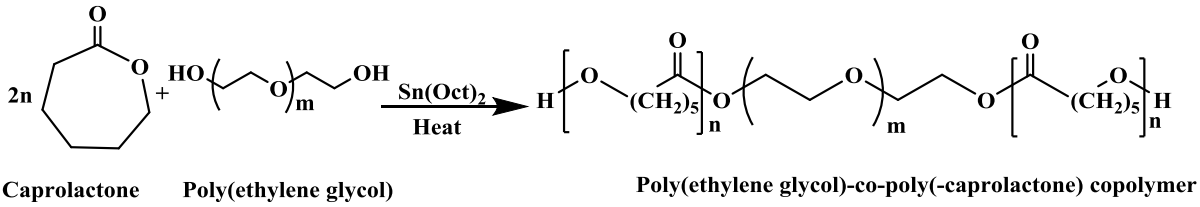

Scheme (4-1): Synthesis of poly (caprolactone) by ring opening polymerisation

The catalyst and monomer ratio was 1:1000 and the monomer and the PEG initiator molar ratio was [I]: [M] =1: 4 and 1:10 to obtain the two polymer samples with different chain length of the polymer.

The ring opening polymerisation (ROP) method was employed but the mechanism is still a matter of some debate.[174] The organometallic compound employed was tin octoate and this behaves as a initiator forming a complex with the carbonyl group of the PCL. Polymerisation is further initiated by the nucleophilic –OH group of the PEG. The tin octoate is approved as a safe additive by the Federal Food and Drugs Administration (FDA)[175] and this is a consideration in our aim to produce medically useful biomaterials.

The most likely mechanism for tin octoate involves its conversion to tin alkoxide, which is the actual initiator. Reaction then proceeds with the alcohol group of the PEG in accordance with the following equations: [174]

$$Sn(Oct)_2 + ROH \rightarrow Oct\text{-}Sn\text{-}OR + OctH \qquad (4\text{-}1)$$

$$Oct\text{-}Sn\text{-}OR + ROH \rightarrow Sn(OR)_2 + OctH \qquad (4\text{-}2)$$

To confirm the formation of the polymer ^1H NMR spectra are shown in **Fig (4-3), (4-4) and (4-5)** for PEG (400), ε-CL and PCL respectively.

Fig (4-3) illustrates the three peaks which were assigned to methylene protons i.e. the peak at

3.65ppm is due to the protons of the terminal carbon, the peak at 3.55ppm to the protons of the penultimate carbon and the remainder of the protons, within the central residues, were assigned to the peak 3.6ppm.

From **Fig (4-4)** assignments for peaks of caprolactone were taken as 1.7, 1.8, 2.58 and 4.2 ppm and were respectively attributed to the methylene protons of $–(CH_2)_3-$ and labelled "b and c", peak "e" is due to protons of $-OCCH_2-$, and peak "a" represents the protons of $–CH_2OOC-$. The methylene peak in the monomer CL at 4.2 ppm shifts to a new value of 4 ppm in the polymer as shown in **Fig (4-5)**.

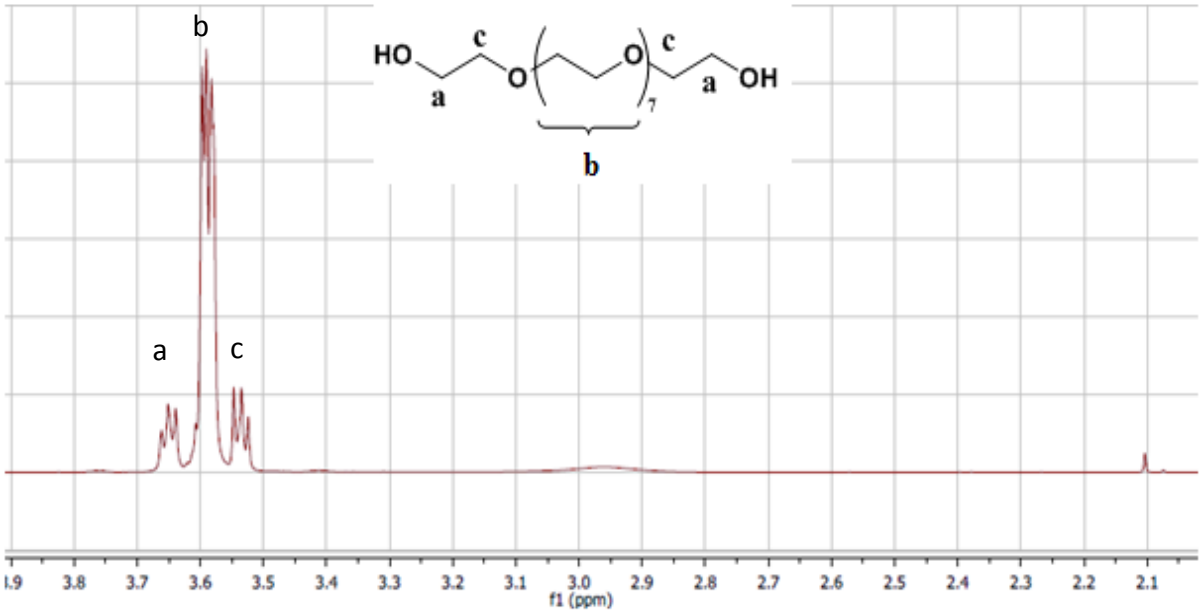

Fig (4-3): ^1H NMR spectrum of PEG 400 in $CDCl_3$ at room temperature.

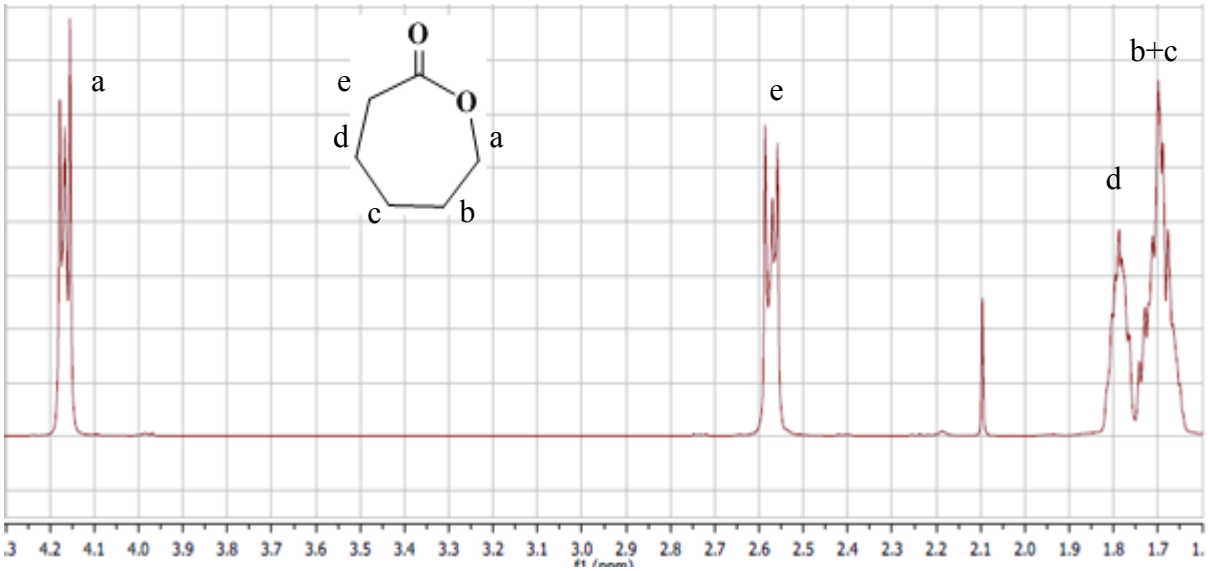

Fig (4-4): ^{1}H NMR spectrum of ε-CL in $CDCl_3$ at room temperature.

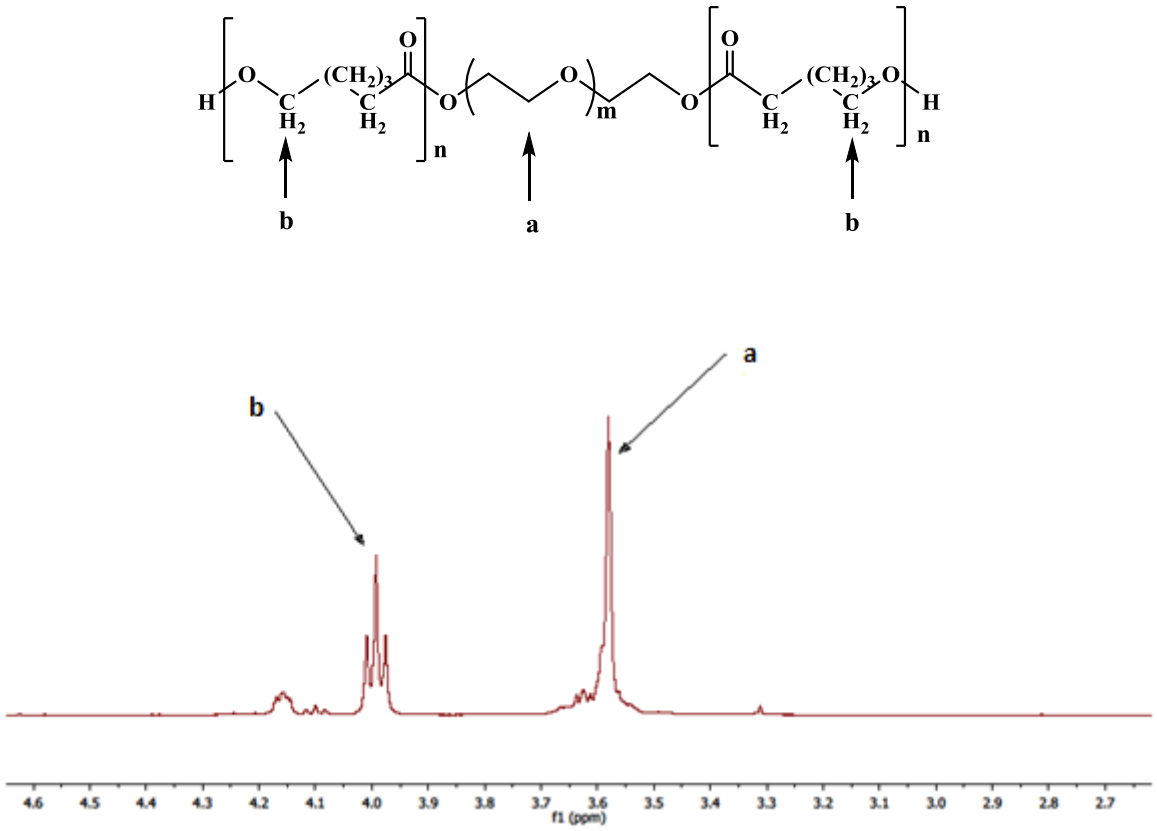

Fig (4-5): ^{1}H NMR spectrum of PCL in $CDCl_3$ at room temperature.

The conversion of ε-CL monomers was calculated by comparing the integration of ε-CL methylene peak at 4.2 ppm (which indicates ant unreacted monomer) with the peak at 4 ppm in the polymer. The degree of polymerization was calculated by comparing the integration of the PEG methylene signal and the signal at 4.2 ppm. **Table (4-1)** shows the results of polymerization of CL with different ratio of PEG at 100 and 160 ^{o}C for 24, 42 and 60 hours.

Table (4-1): **Effects of temperature, reaction time and monomer: initiator ratio on the polymerisation of ε -CL.**

Entry	**a**	**b**	**c**	**d**	**e**
1	1:4	100	24	-	-
2	1:10	100	24	2	22
3	1:4	160	24	2.34	62
4	1:10	160	24	9.4	82
5	1:4	160	42	2.5	61
6	1:10	160	42	9.18	81
7	1:4	160	60	3	70
8	1:10	160	60	9.7	82

a = molar ratio of monomer and initiator [M]: [I]

b = temperature of the reaction, T, (^{0}C)

c = Reaction time (Hours)

d = Degree of polymerisation (PCL chain length)

e = Percentage of conversion (%)

The degree of polymerisation (DP) of the graft co-polymer was then determined. Firstly the number of residual (-O-CH_2-CH_2-) in the PEG was calculated as follows:

Mw of repeat unit = 44

Average Mw of PEG (as given by manufacturer) =400

Therefore, number of repeat units in each molecule is (400-18)/44= 8.7

This value approximates to a whole number of 9 residues per PEG molecule which for the purpose of NMR integration is equivalent to 36 protons as there are 4 protons per PEG residue. The integration for the PCL peak at the chemical shift of 4 is equivalent to the number of residues of ε-CL added per PEG molecule multiplied by 2 as there are 2 protons per residue.

Typically, the degree of polymerisation (DP) was determined, as for example entry 8 in **Table (4-1)** and is given by DP= (36*0.54)/ (2*1) =9.72 residues of PCL/mole of PEG.

Where 0.54 is the integration value for chemical shift 4.00 and 1 is the integration value for the chemical shifts for the methylene groups of PEG.

It was seen that the resulting polymer was determined by the amount of the initiator, temperature and the reaction time. The highest degree of polymerization was obtained for molar ratio 1 monomer to 10 initiator at 160^{o}C for 60 hours.

FT-IR spectra were obtained and used to characterise the PCL. The spectrum shows the main absorption bands in PCL structure, one at 2935cm^{-1} attributed to the asymmetric stretch of –C-H bond hydroxyl group and 2865.5 cm^{-1} for the symmetric stretch -C-H hydroxyl group, a band at 1733 cm^{-1} which was attributed stretching of the carbonyl group. This compares to literature values of 2940 cm^{-1} , 2860 cm^{-1} and 1722 cm^{-1} respectively in the literature[176] see **Fig (4-6)**

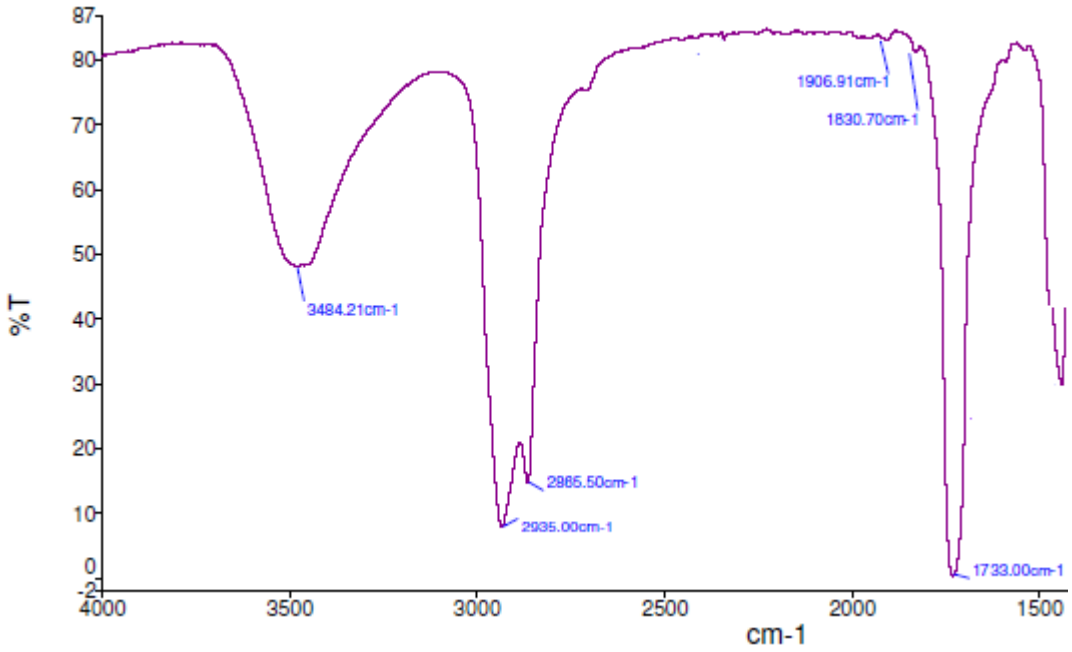

Fig (4-6): FT-IR spectrum of poly (caprolactone) PCL.

For this work, PCL prepared with degree of polymerisation 10 was chosen to be grafted onto alginate backbone and this PCL was designated low Mw. 5 further samples of PCL, prepared using the supercritical CO_2 technique, were also chosen and they were designated as high Mw. The tin content was determined in each sample and the sample with the lowest tin content was chosen for the next stage of the study, as in any biomedical application, purity is a necessary consideration. Tin is known to be toxic.

To quantify the tin content Atomic Absorption Spectroscopy was used .A calibration curve was constructed using calibration standards of $SnCl_2$ of known concentration to give corresponding absorbance readings **Fig (4-7**).

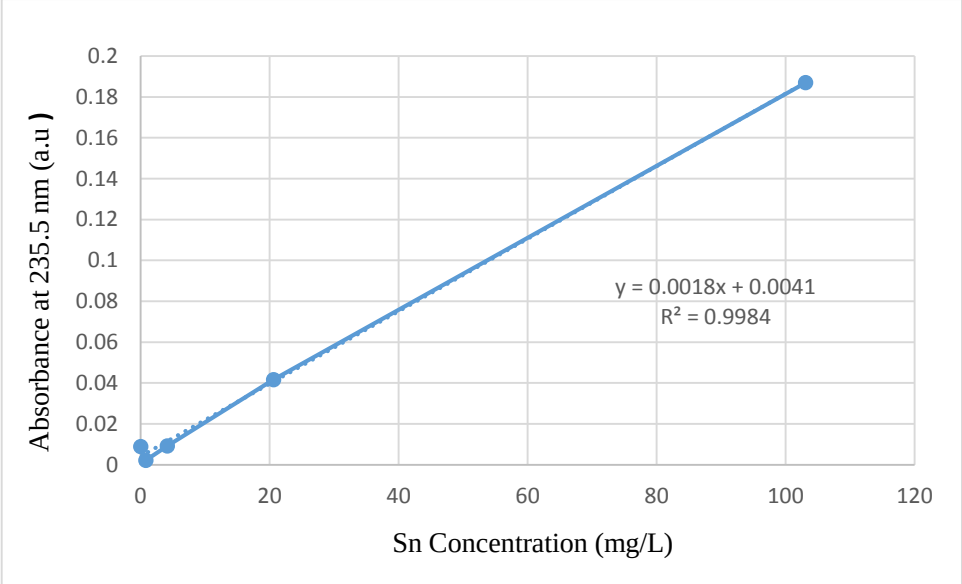

Fig (4-7): Calibration curve for tin (Sn) standard**.**

Before analysis, the sample was dissolved in HCl and sulphuric acid as given in the experimental procedure.

The tin content in mg/L of various samples of PCL was then determined after adjustment for any contaminant by deducting the value for tin found in a blank sample. These values were then converted to parts per million (ppm) as can be seen in **Table (4-2)**.

For subsequent experiments sample 4 was used as this high molecular weight PCL (12.6 kg/mol) was lowest in tin and, therefore, more appropriate considering its potential for medical use.

Table (4-2): Tin content of samples of Poly-caprolactone as determined by AAS analysis (values converted to mg/L from experimental value quoted in ppm).

Sample	Conc. of Sn (mg/L)	Sn content in ppm
1	20	500
2	15	386
3	16	415
4	5	133
5	12	311

Poly-caprolactone with lowest tin content was selected as the high molecular weight option for grafting on to alginate using the EDCI reaction given in **Chapter 4.2.4** the scheme for which is given in **Scheme (4-2).** Low molecular weight Poly-caprolactone was also used for grafting and this also was prepared by the same procedure. Two alginate samples have been used in this work to be grafted with PCL, the commercial alginate (ALG-A) and Welsh alginate (WS-2) which were labelled as "A" and "W" with M/G ratios 1.2 and 2.03 respectively.

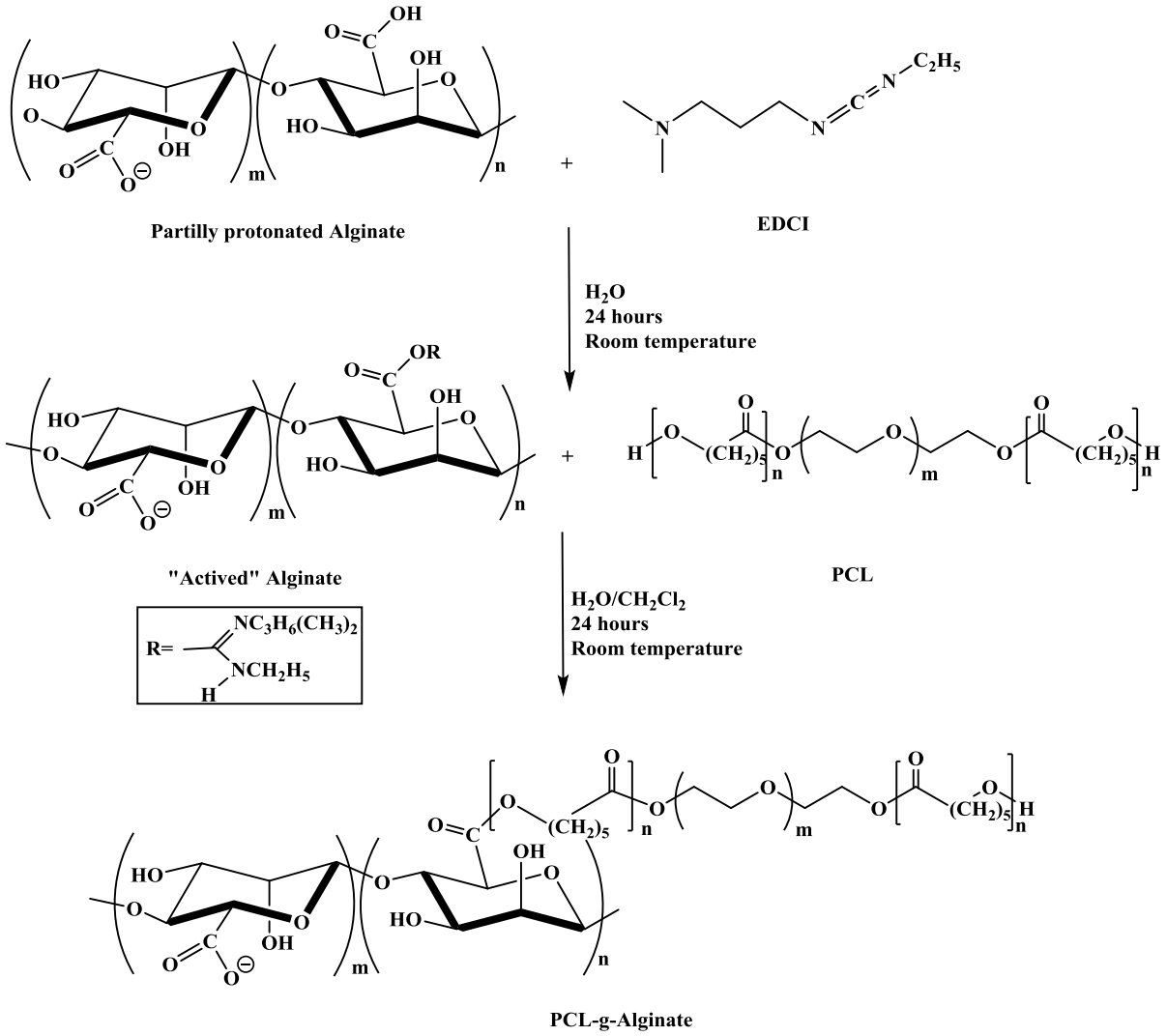

Scheme (4-2): Synthesis of PCL-g-alginate.

The material was firstly characterised by the FTIR technique. This was compared with the

spectrum for the pure alginate before grafting. The FTIR spectra of PCL-g-alginate showed the –C=O stretching vibration of the PCL chains characteristically at 1728 cm^{-1} that was not present in the alginate spectrum. This new peak is derived from the PCL as it is coincident with the PCL reactant but it is possible that it is wholly or partly due to unreacted PCL as it was not possible to be certain that purification was complete. From the underlying esterification procedure there are grounds for supposing the successful attachment of the PCL chains to the alginate backbone. See **Fig (4-8)** for the spectrum of PCL-g-(ALG-A). NMR and DSC/TGA were then undertaken as further evidence for grafting.

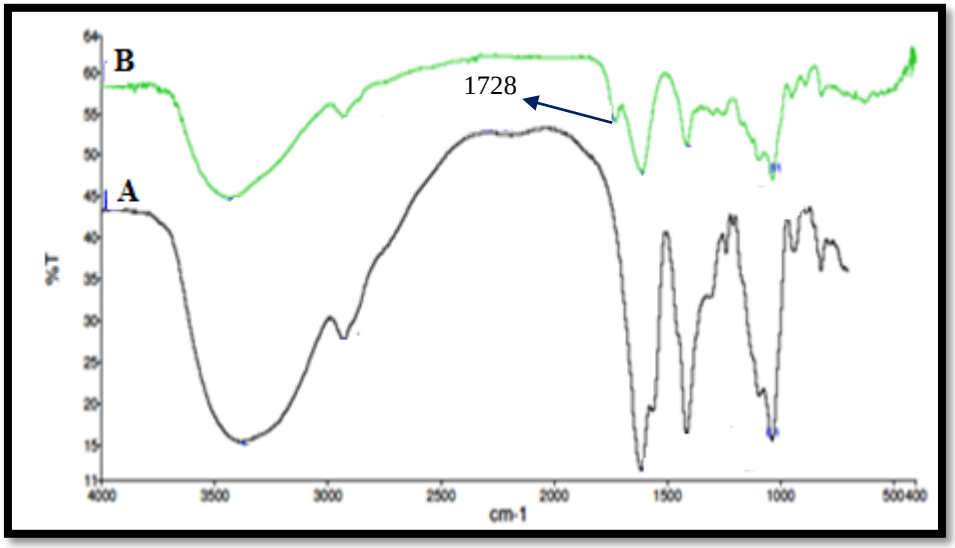

Fig (4-8): FTIR Spectra of **(A):** Alginate (ALG-A) before grafting and **(B):** its grafting derivative (PCL-g-(AlG-A)).

The table below shows the efficiency of the grafting rate (defined as the weight percentage of PCL with respect to alginate) of all the grafted alginate in this study, as calculated using NMR analysis.

Table (4-3): The efficiency: grafting weight percentage of PCL-g-alginate prepared in this study.

Sample	Sample code	Theoretical Grafting Weight percentage (%)	Efficiency: Grafting Weight percentage (%)
PCL–g-A (low M_W of PCL)	B	5	4.9±0.3
PCL-g-A (high M_W of PCL)	C	5	3.2±0.2
PCL-g-A (low M_W of PCL)	D	10	5.8±0.4
PCL-g-W (High M_W of PCL)	E	5	-

Note: (A)-Commercial alginate and (W) - Welsh alginate

For sample B the molecular weight for the alginate is 2.37 x 10^5 g/mol and as each residue G or M has a molecular weight of 1.76 x 10^5 g/mol, the number of residues is, therefore, given by 237,200/176 = 1348 approx.

The ratio of M/G is 1.2 therefore the number of G residues is 1/2.2 *1348 =613. Therefore, there are 613 anomeric protons for the C1 atom per mole of alginate.

The PEG has 9 residues represented as (b) in the spectrum with an integration value of 0.45 which is equivalent to 36 protons. The integration value for (a), the alginate G residue for C1 was 1.00 **Fig (4-9)**.The accuracy of integration depends on where the integration limits are drawn. The integration values used represent the average of the three best estimates.

Therefore, the number of moles (n) of PCL per Alginate molecule is given by

$$\frac{613\times0.45}{36} = 7.66$$

On a relative weight basis the PCL is calculated for a molar ratio of 1:7.66 alginate to PCL given the M_w of Alginate is 237200 and 7.66 moles of PCL Mw 1539.4.Thus,

$$\frac{7.66\text{x}1539.4}{237200} = 4.9\%$$

Thus, 4.9% of the graft co-polymer is PCL by weight. This figure is compares with 5% for the feed ratio and indicates a high yield value.

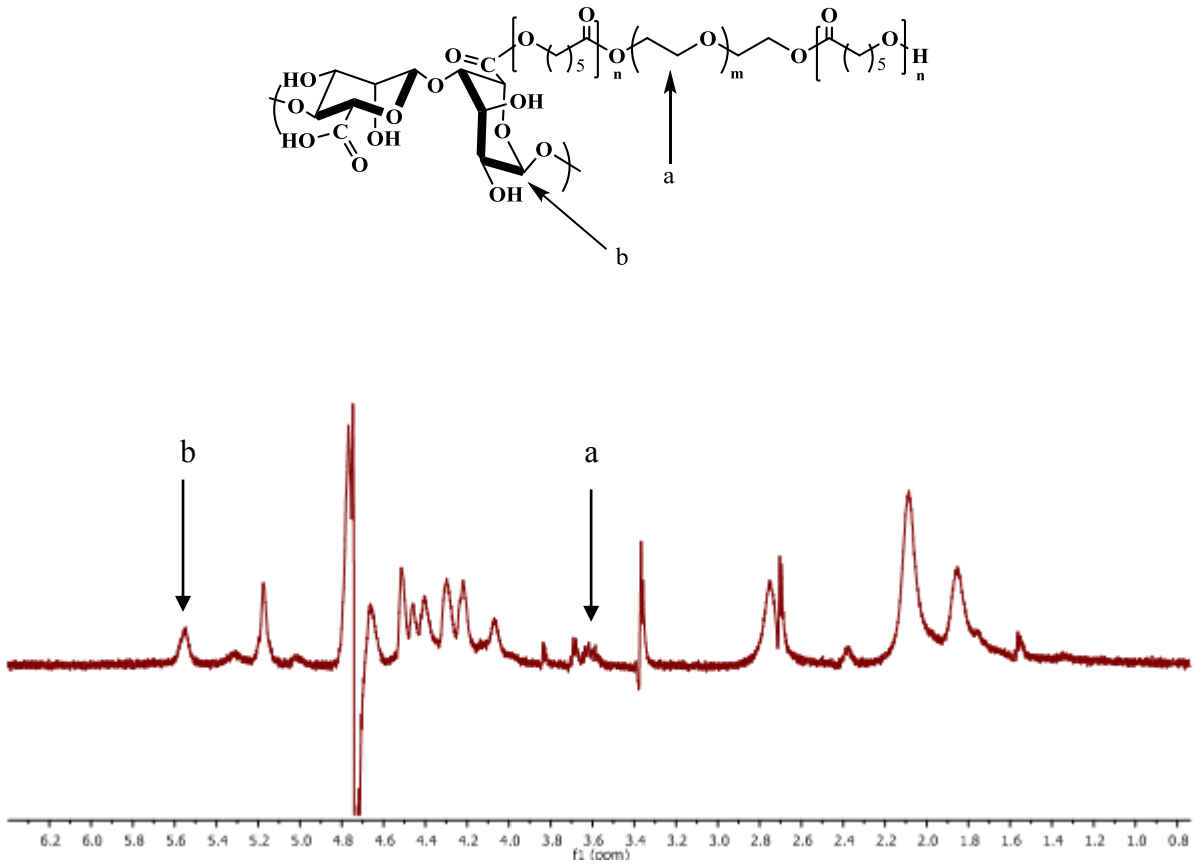

Fig (4-9): ^{1}H NMR spectrum of Poly (caprolactone) -grafted -alginate (ALG-A) [sample B in Table (4-3)] in D_2O at 70^{o}C.

The DSC/TGA technique was also used to determine the grafting rate and to provide a comparison with the NMR method. It is possible to determine the relative weights of the alginate and PCL domains and thereby to determine the molecular weight of the graft from comparisons of weight change in the graft material compared with Alginate and PCL for the same temperature range. However, the TGA curves for the graft co-polymer and for the pure Alginate showed that they were similar and both were thermally stable. See **Fig (4-10).** It is, therefore, evident that the PCL content does not have any noticeable effect on the thermal behaviour of

the alginate thus, making a determination of relative abundances very difficult to determine.

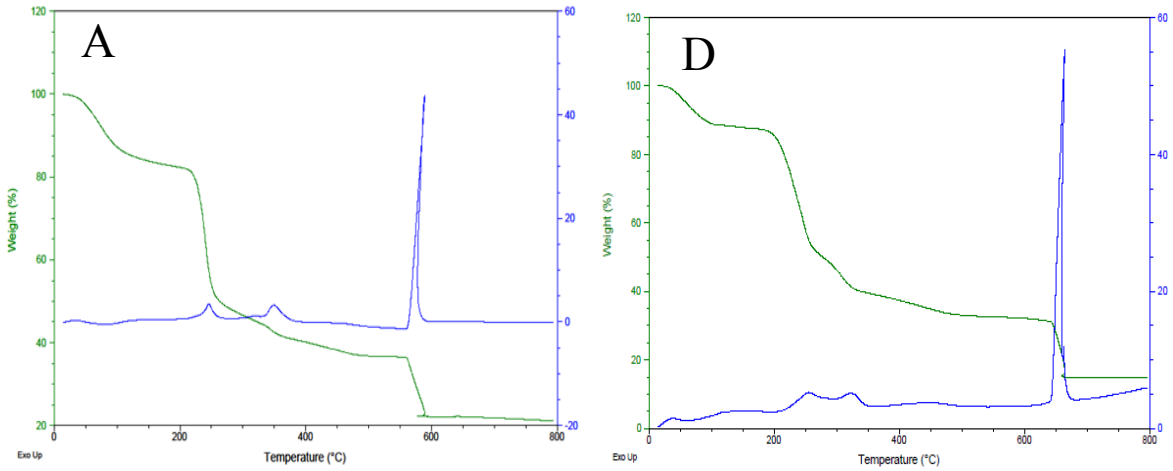

Fig (4-10): DSC/TGA of **(A)** commercial alginate (ALG-A) and its derivative (PCL-g-(ALG-A) sample (**D**) in Table (4-3).

Amounts less than 100 µl were found to give bulk gels, which were mechanically very weak and found to disintegrate on handling. The duration of the crosslinking period (one or two hours) was found to be irrelevant (at least under the experimental conditions pertaining). For the rest of the study bulk gels using 200 and 400 µl were used. The swelling properties were studied in two media, distilled water and NaCl.

Swelling study.

The swelling behaviour of the hydrogels was investigated by comparing the swelling in pure water and in saline media. It is known that, for dilute solutions of alginate-PCL, for short PCL chain lengths intramolecular interactions result in a decrease of the hydrodynamic radius of the copolymer coil (collapsed state) despite the electrostatic repulsions present in such an anionic polymer backbone.[164] For PCL longer chain lengths intermolecular hydrophobic aggregations result with consequent greatly increased viscosity. These intermolecular associations are favoured in a saline environment, when such systems, are screened from electrostatic charges by the electrolyte NaCl. Hydrogels are also expected to exhibit these effects and the PCL graft

length is anticipated to affect the swelling ratio of hydrogels as hydrophobic clusters are favoured in the aqueous NaCl medium.

The terminology used for the swelling conditions is given in **Table (4-4)** below:

Table (4-4): Conditions used for the preparation of alginates and PCL-g- alginates bulk hydrogels.

Experiment no.	Polymers	Volume of $CaCl_2$ (µl)	Swelling media		Sample name
			H_2O	NaCl solution	
1	A	200	✓		A200 in H_2O
2	A	200		✓	A200 in NaCl
3	A	400	✓		A400 in H_2O
4	A	400		✓	A400 in NaCl
5	B	200	✓		B200 in H_2O
6	B	200		✓	B200 in NaCl
7	B	400	✓		B400 in H_2O
8	B	400		✓	B400 in NaCl
9	C	200	✓		C200 in H_2O
10	C	200		✓	C200 in NaCl
11	C	400	✓		C400 in H_2O
12	C	400		✓	C400 in NaCl
13	D	200	✓		D200 in H2O
14	D	200		✓	D200 in NaCl
15	D	400	✓		D400 in H2O
16	D	400		✓	D400 in NaCl
17	W	200		✓	W200 in NaCl
18	E	200		✓	E200 in NaCl

Note (i) Sample code: A-commercial alginate, B-PCL-g-A (low M_w PCL) 5%, C-PCL-g-A (high M_w PCL) 5%, D-PCL-g-A (low M_w PCL) 10%, E-PCL-g-W (high M_w PCL) i.e. Welsh alginate at 10% PCL grafting efficiency.(ii) box tick denotes the swelling medium chosen (see **Table (4-3)**.

The results from the swelling study are presented as plots below. It is observed from **Fig (4-11) - Fig (4-15)** that for materials A, B, and C the greatest swelling occurs in the saline medium and that within each medium i.e. saline or water, greatest swelling occurs for samples with lowest calcium content. This is consistent with the `egg-box` structure for alginate hydrogels where alginate polymer chains are physically cross-linked with divalent ions such as Ca^{2+} which bind with $-COO^-$ groups mainly within the poly(guluronate) domains. Thus, on swelling, it is reasoned that a hydrogel with a less cross-linked structure (i.e. with lower calcium content) is able to allow aqueous solvent greater access to hydrophilic domains within its structure. In addition, in saline media the Na^+ ions are engaged in an ion exchange process with the Ca^{2+} ions resulting in greater electrostatic repulsions between COO^- groups causing a relaxation of polymer chains and, thus, enhancing the swelling.[177]

In **Fig (4-14)**, comparing A, B and C in saline medium, the lower cross-linked materials (i.e. lower Ca^{2+} content) have the greatest swelling. Also, for the lower cross-linked samples the greatest swelling is seen in A200 (in NaCl), then followed by B200 (in NaCl) and C200 (in NaCl) which contain increasing hydrophobic PCL content. From **Fig (4-14),** it can also be seen that for the high Ca^{2+} gels higher hydrophobic content is able to disrupt this cross-linking and, paradoxically, enables greater swelling within the hydrophilic soaking medium. Thus, the higher cross-linked material C400 (in NaCl) swells more than the less hydrophobic B400 (in NaCl) and its co-incident curve A400 (in NaCl).

From **Fig (4-15)**, for swelling in water, again the greatest swelling occurs for low Ca^{2+} content i.e. C200 (in H_2O) followed by B200 (in H_2O) and then A200 (in H_2O) i.e. swelling increases with higher hydrophobic content and this is the reverse of that seen for these materials in the saline solution.. It is seen that in hydrogels with higher Ca^{2+} content, i.e. materials with higher cross-linking, that B400 (in H_2O) has greater swelling than A400 (in H_2O) followed by C400 (in H_2O) revealing a complex situation giving no discernible pattern.

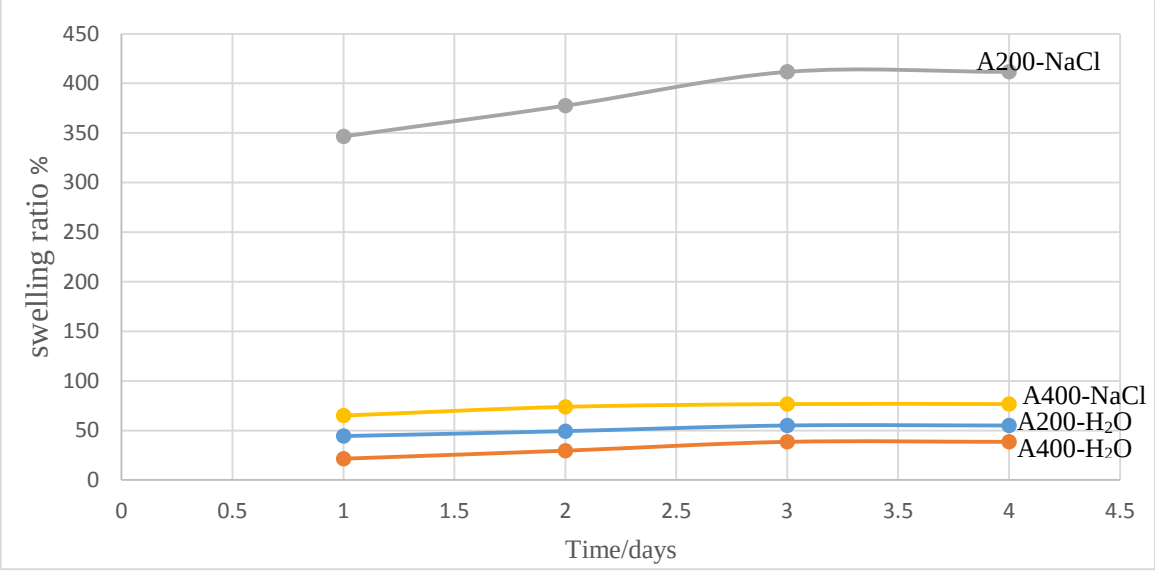

Fig (4-11): Plot of Swelling Ratio vs. Time for bulk gel of ungrafted alginate A in swelling media H_2O and 1% (w/v) NaCl. Samples used, defined in accordance with Table (4-4). Data points represent the average within an error range of ± 2%.

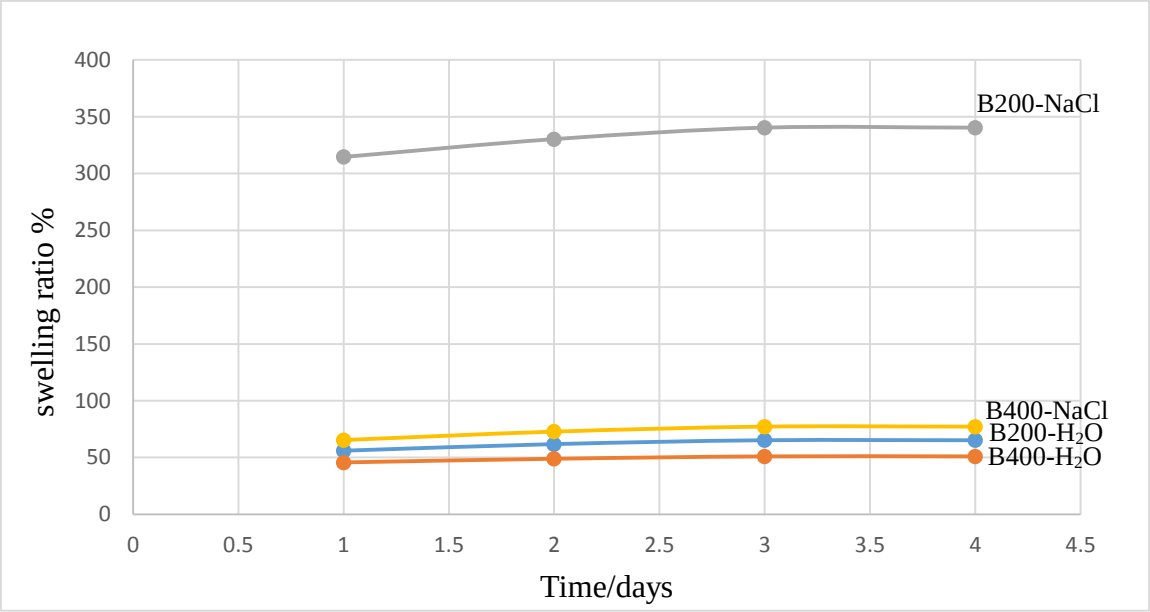

Fig (4-12): Plot of Swelling Ratio vs Time for the bulk gel of PCL-g-alginate A (co-polymer sample B as in Table 4-3) in swelling media H_2O and 1% (w/v) NaCl. Samples used, defined in accordance with Table (4-4. Data points represent the average within an error range of ± 2%.

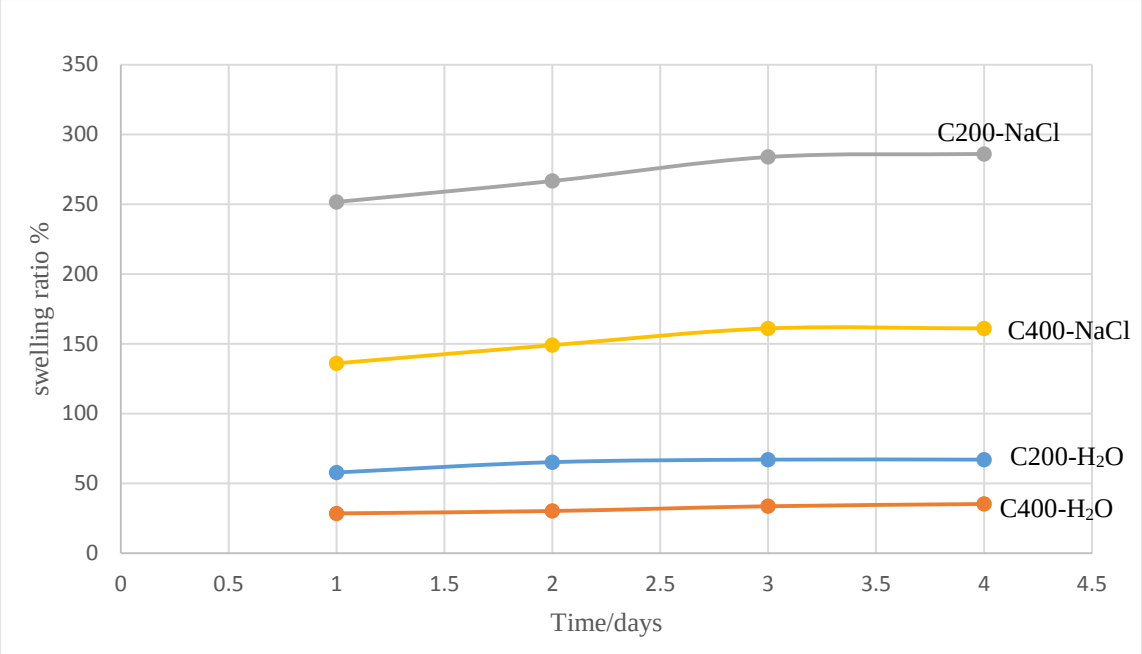

Fig (4-13): Plot of Swelling Ratio vs. Time for bulk gel of PCL-g-alginate A (co-polymer sample C as in Table 4-3) in swelling media H_2O and 1% (w/v) NaCl. Samples used, defined in accordance with Table (4-4). Data points represent the average within an error range of ± 1%.

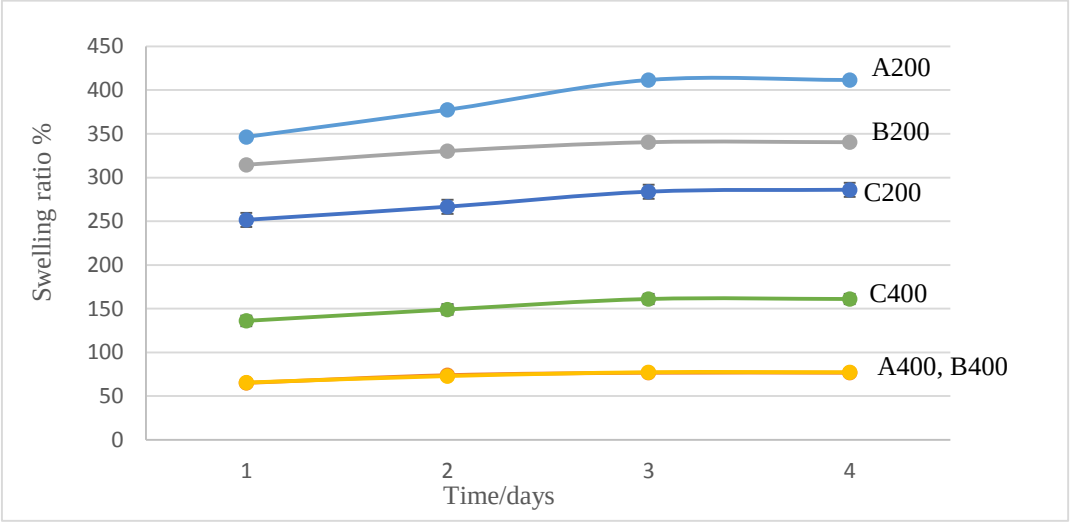

Fig (4-14): Plot of Swelling Ratio vs Time in 1% (w/v) NaCl solution for bulk gel of alginate A before grafting and after grafting with low and high Mw of PCL (samples A, B and C as in Table 4-3). Samples used, defined in accordance with Table (4-4), A400, B400 are overlapped. Data points represent the average within an error range of ± 1.5 %.

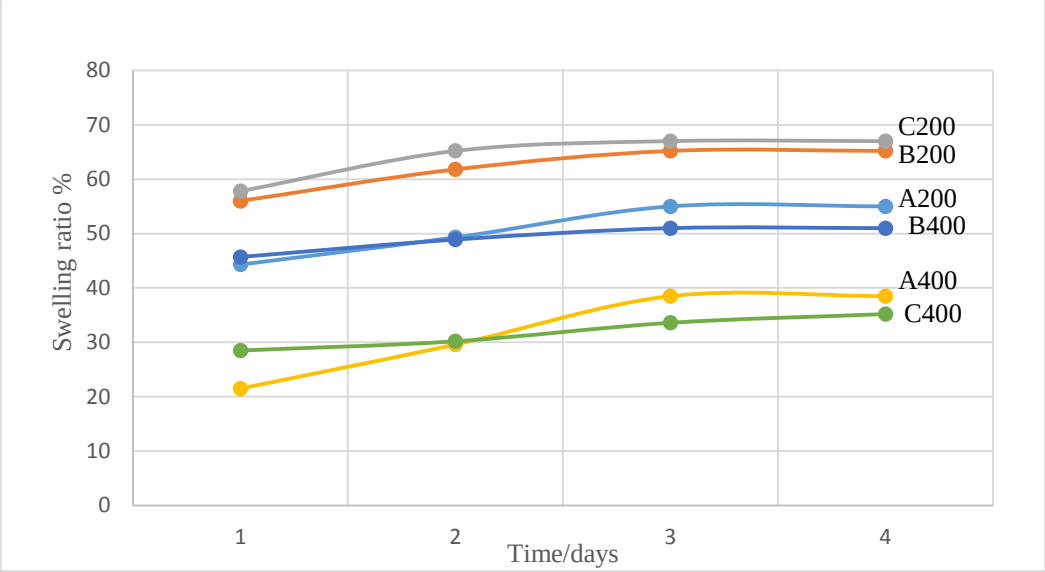

Fig (4-15): Plot of Swelling Ratio vs. Time in de-ionised water for bulk gel of alginate A before grafting and after grafting with low and high Mw of PCL [samples A, B and C as in Table 4-3]. Samples used, defined in accordance with Table (4-4). Data points represent the average within an error range of ± 2%.

Fig (4-16) shows the effect of grafting ratio on the swelling behaviour of sample D (commercial Alginate) which has higher grafting ratio (10%) than the previous sample (B 5%). This behaviour follows the same pattern seen with the other materials A, B, C, in both water and in saline solution.

Fig (4-17) and **(4-18)** provide a comparison for the three materials A, B, and D by comparing the swelling behaviour of the pure alginate before grafting (A) , and alginate grafted with 5% PCL (B) , and alginate grafted with 10% of PCL (D) both in water and in saline solution. For the lower cross-linked materials there appears to be an anomaly in that the more hydrophobic material, D 200, swells less than B 200. From previous discussion above, more hydrophobicity should mean more swelling but it appears that the higher cross-linking density of D gives rise to more or larger hydrophobic domains within D resulting in restricted access for the water swelling medium.

This pattern in the swelling order is repeated for the higher ionically cross-linked materials

although they are found to swell less but evidently the same reasoning applies to explain the relative order.

In saline solution for the lower cross linked materials greatest swelling occurs for the more cross-linked materials .This is presumably due to ion exchange that if more Ca^{2+} are present then more is lost through exchange and more swelling results.

Also from **Fig (4-18)** for the higher cross-linked materials in saline the curve for ungrafted and high grafted material is co-incident. Both curves indicate more swelling than for the lower density grafted material which evidently reflects the balance of the various factors discussed.

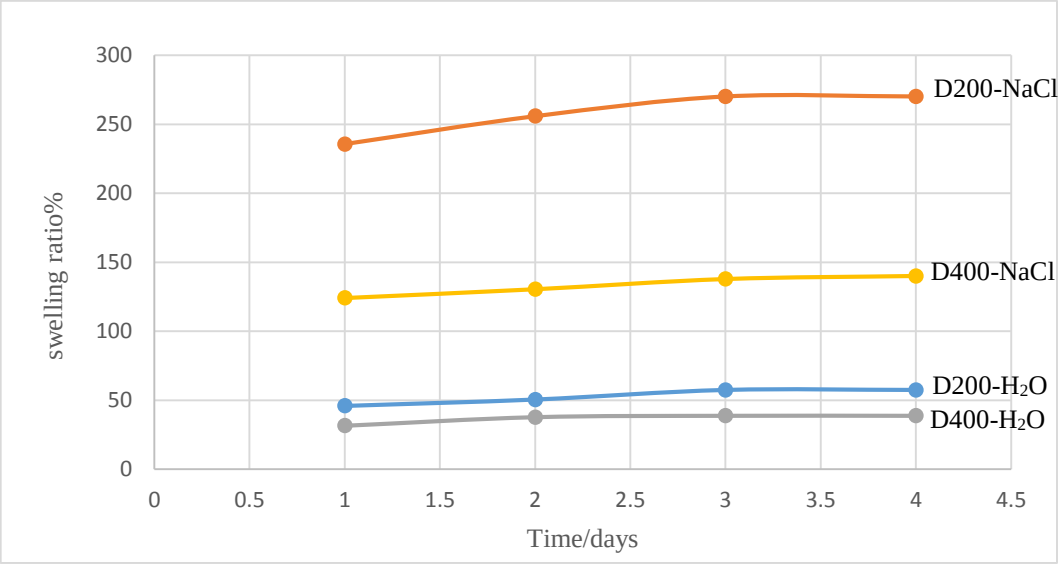

Fig (4-16): Plot of Swelling Ratio vs. Time for bulk gel of PCL-g-alginate A [sample D as in Table 4-3] in swelling media H_2O and 1% (w/v) NaCl. Samples used, defined in accordance with Table (4-4). Data points represent the average within an error range of ± 1%.

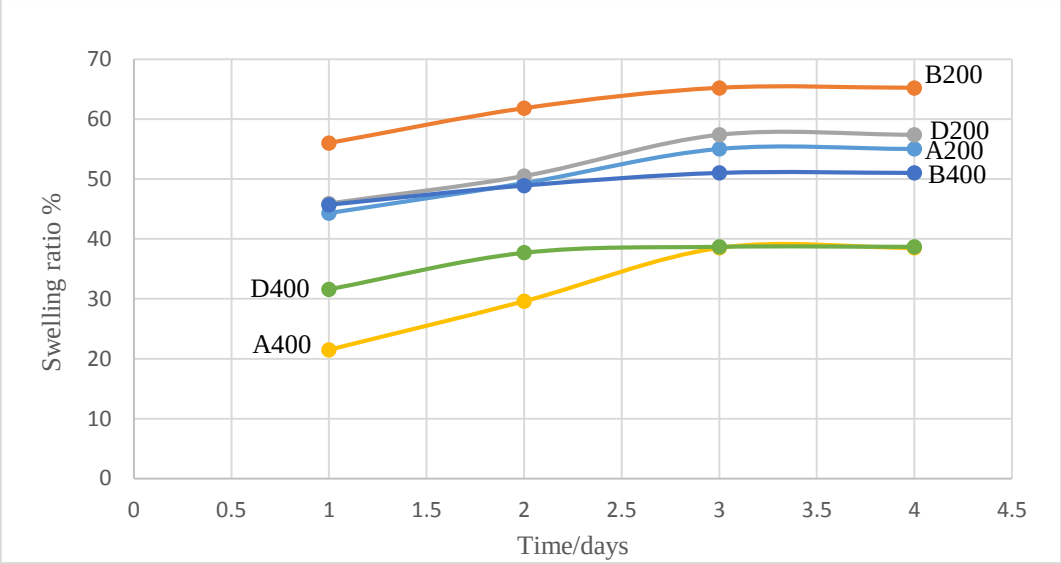

Fig (4-17): Plot of Swelling Ratio vs. Time in H_2O for bulk gel of alginate A before grafting and after grafting with low Mw of PCL [sample A, B and D as in Table 4-3]. Samples used, defined in accordance with Table (4-4). Data points represent the average within an error range of ± 1 %.

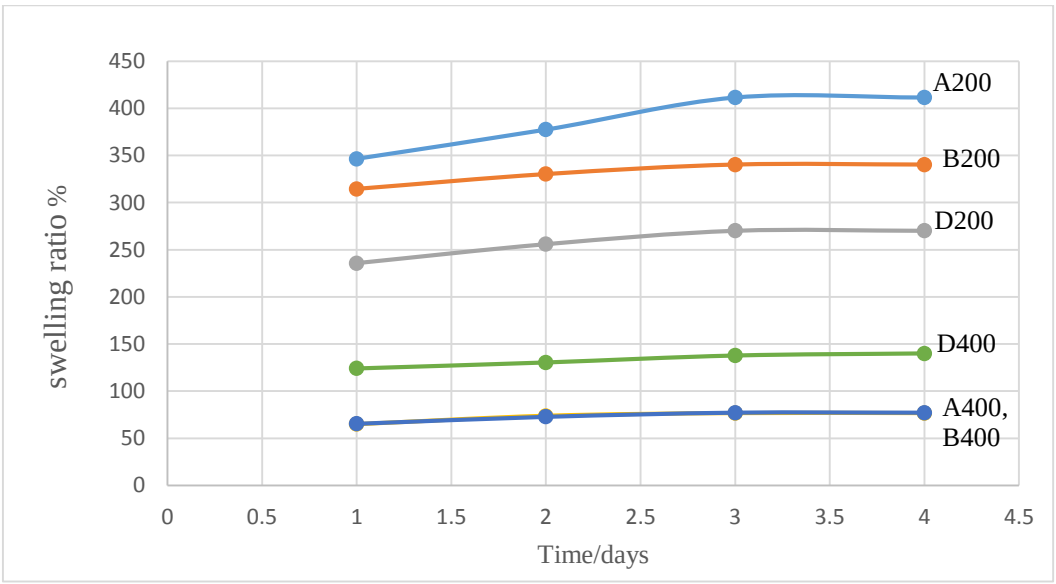

Fig (4-18): Plot of Swelling Ratio vs. Time in 1% (w/v) NaCl solution for bulk gel of alginate A before grafting and after grafting with low Mw of PCL [sample A, B and D in Table 4-3]. Samples used, defined in accordance with Table (4-4). A400 and B400) are overlapped. Data points represent the average within an error range of ± 2%.

The swelling behaviour in saline of Welsh alginate bulk gel (W) and its grafted derivative (E) is shown in **Fig (4-19)**. It can be seen that the more ionically cross-linked W-200 has the greater swelling than its more hydrophobic derivative. This reflects the fact that ion exchange loosens the material structure and allows for greater swelling.

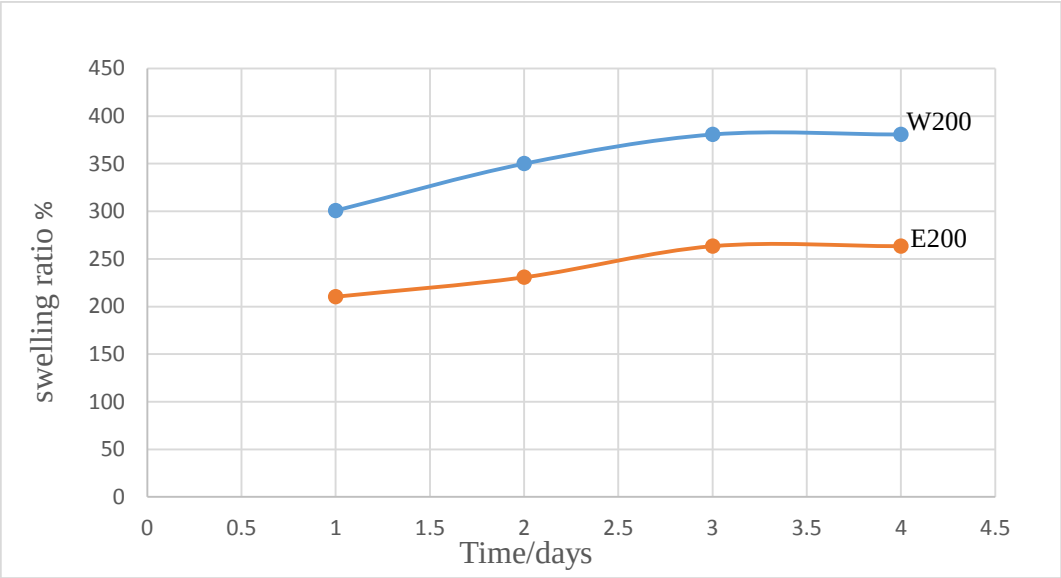

Fig (4-19): Plot of Swelling Ratio vs. Time in 1 %(w/v) NaCl solution for bulk gel of Welsh alginate before grafting (W) and after grafting with PCL [sample E in Table 4-3]. Samples used, defined in accordance with Table (4-4). Data points represent the average within an error range of ± 1.5 %.

The next figure, **Fig (4-20),** is a comparison between hydrogels derived from alginates of type A and W and their PCL grafted derivatives to understand the effect of M/G ratio. The W alginate which has a higher M/G value than A and it is known that that higher M content gives rise to less physically robust gels as the cross-linking is less effective between M residues. Thus, a weaker gel might be reasoned to give a greater swelling behaviour. However, in saline solution, where ion exchange occurs has a greater effect in the gel with higher G as this greatly opens up the material structure and therefore allows more swelling. Thus, the commercial alginate with more G swells more.

The derivatives are also found to swell less but the same order in swelling is followed and is explained by the same reasoning.

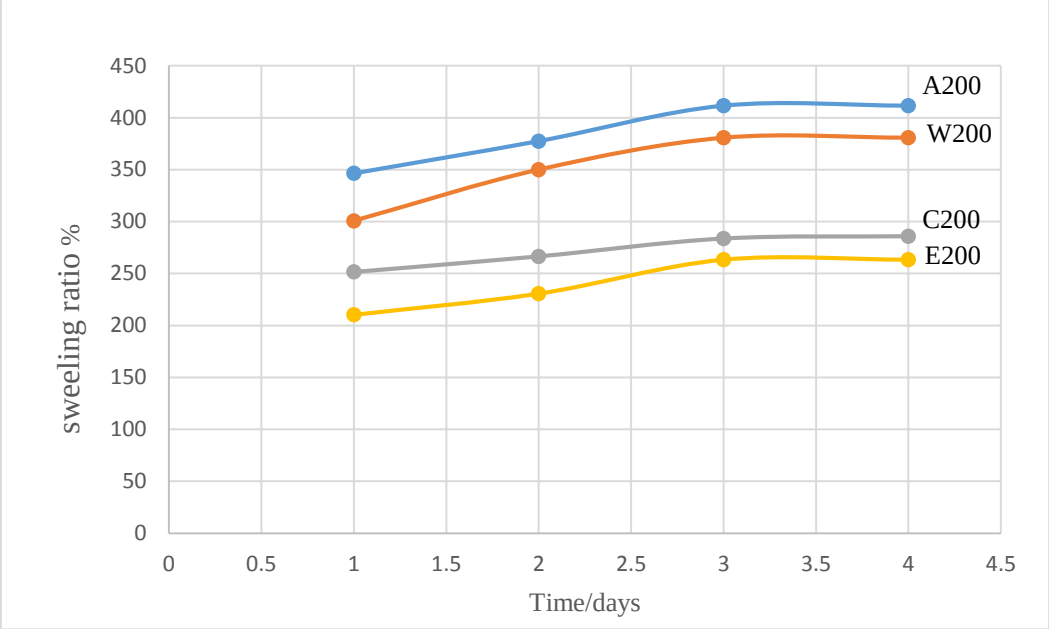

Fig (4-20): Plot of Swelling Ratio vs. Time in 1 % (w/v) NaCl solution for bulk gel of commercial alginate (A) and Welsh alginate (W) and their PCL grafted derivatives [sample C and E as in Table 4-3]. Samples used, defined in accordance with Table (4-4). Data points represent the average within an error range of ± 2%.

The hydrogels from the swelling study were further analysed by SEM after they had been thoroughly dried (**Fig (4-21)**) although the technique did not always give images clear enough and show the soft surface of all samples. Granular features are taken to be indicative that the material has undergone greater swelling. The images, thus, tend to support the trends observed in the swelling study for the low cross-linked materials in saline solution (see A200, B200 and C200).

For the higher cross-linked materials in saline it is found that the most granular image corresponds to the material with lowest swelling (see B400). This may be due to more localised swelling in the material structure which is presumed to occur when ion exchange occurs within the hydrophilic domains. As overall the material swells less, where media is absorbed this leads to greater disruption in the structure resulting in greater granulation being apparent, and this is particularly so in the visible outer regions.

In aqueous media overall the SEM images show less granularity and this reflects the lower swelling compared with saline media. The most granular image is seen for B400, which has

the greatest swelling for the higher cross-linked materials. This may further reinforce the conclusion that for swelling in saline that more localised swelling occurs and this has a more visually dramatic effect. Further the image for B400 is more granular than for B200 and thus although greater cross-linking may have occurred this resulted in fewer large hydrophobic domains and therefore less disruption on swelling. Also, in the C series C400 (in NaCl) appears particularly `bumpy` and this may reflect the effect of Na^+ ion exchange when the material was in a saline medium and which retains some Na^+ content on dehydration in the drying out procedure.

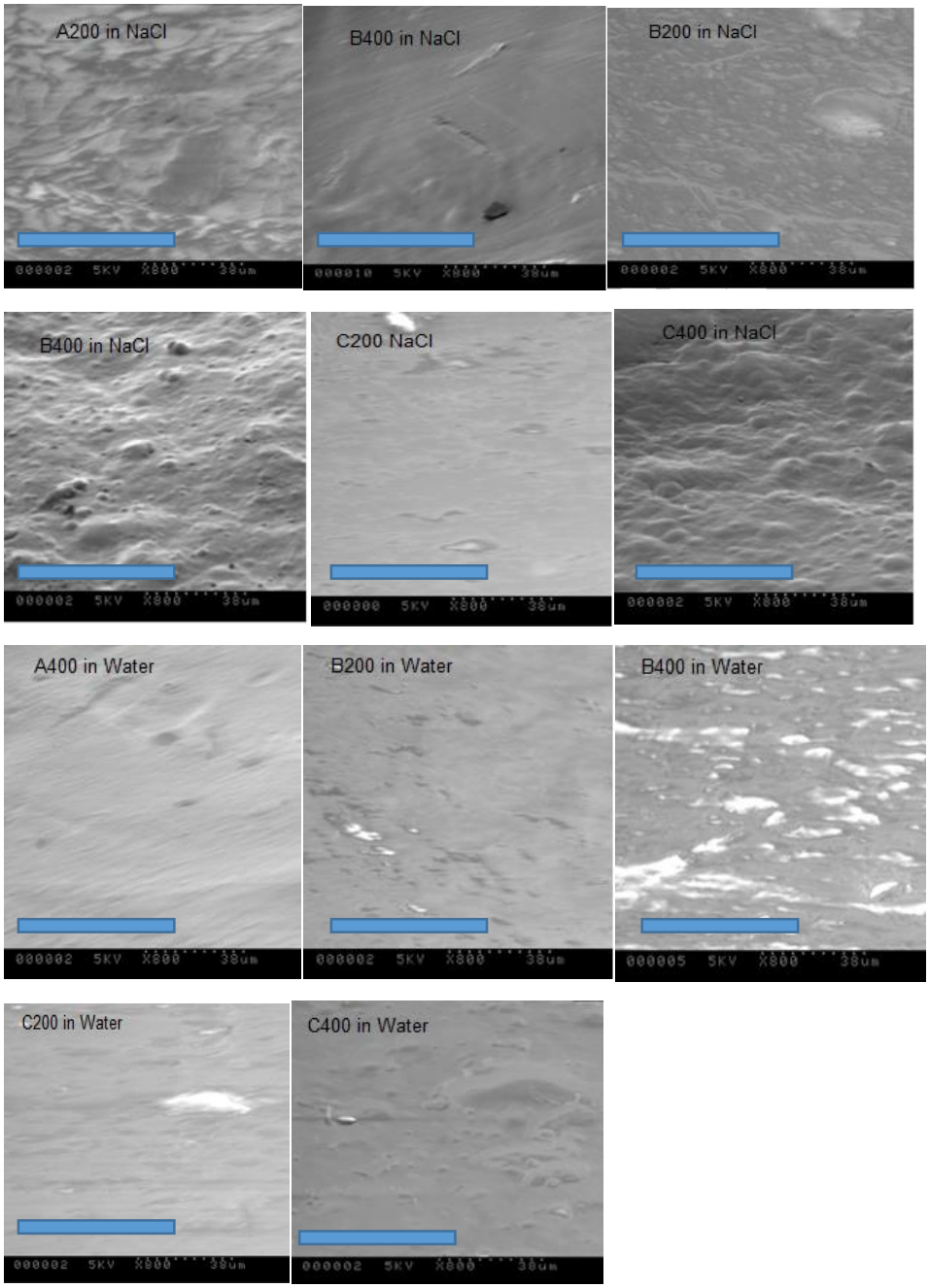

Fig (4-21): Scanning Electron Microscope (SEM) images of freeze-dried alginate hydrogels after swelling in the two swelling media H_2O and NaCl 1% (w/v): (A) alginate before grafting, (B) grafted with low M_W of PCL and (C) grafted with high Mw of PCL . Magnification is 800, (scale bar: 38 μm).

4.4 Conclusion.

In this work, water soluble PCL-grafted-alginates were prepared using two types of alginate with M/G ratio 1.2 and 2 i.e. r commercial alginate A and extracted Welsh alginate W respectively. Grafting was performed with PCL polymer of two molecular weights distributions by average i.e. 1.1 and 12.6 $kgmol^{-1}$ and grafting rates of 5 % and 10% by weight. An aqueous micellar grafting technique was used according to published procedures[163] and the grafted polymers obtained were characterised by NMR, FT-IR and DSC/TGA. Hydrogels were prepared using PCL-grafted-alginates and ungrafted alginate by ionic-crosslinking using Ca^{2+} at different concentrations.

Swelling studies were performed in DI water and saline for the cross-linked hydrogels. In water the results showed that the swelling ratio of the gels was affected by the crosslinking density and chain length of PCL in addition to the grafting ratio. This confirms very limited work in this area particularly for swelling in cross-linked unmodified alginates of varying degrees of cross-linking.[178] It was found for the lower cross-linked gels in water that the swelling ratio of the gels with a shorter PCL graft was higher than the alginate without grafting, and the one grafted with a longer PCL chain swelled most. Increasing the crosslinking density by increasing the amount of Ca^{2+} used lead to a decrease in the swelling ratio of the alginate gel and PCL-grafted-alginate gels. The greatest swelling occurring in the gel with low molecular weight grafting, while least swelling was found with the high molecular weight graft.

Swelling in saline solution found that low cross-linking gave highest swelling with the graft-free material giving the highest swelling. This was followed by the low molecular weight graft and finally the high molecular weight. Again the higher cross-linked material was more complex with highest swelling given by the low molecular weight graft followed by the graft free and then the high molecular weight graft.

For the material with higher grafting ratios (i.e. C with 5.8%) has the lowest swelling ratio as might be expected as a result of the presence of hydrophobic domains. In addition, bulk steric effects may lead to reduced ionic cross-linking and, therefore, limit the scope for further swelling in aqueous media. Further, with increased ionic cross-linking this further restricts the potential for swelling. Thus, the higher density grafting material with greatest cross-linking swelled the least having the lowest swelling ratio of all the materials studied. However, it

should be noted that high density cross linking with high molecular weight PCL was not studied.

A comparison of the commercial and Welsh alginates and their derivatives revealed that the commercial alginate swelled more than the Welsh. This is consistent with the findings that the commercial is higher in G residues and crosslinking would result in a stronger more compact gel. In saline solution, after ion exchange, the structure of the commercial was expected to undergo more swelling and the results confirmed this.

The study confirms that grafting PCL onto alginate can tailor its properties so that the hydrogels formed can be used in a variety of biomedical applications. Chapter 5 of this work details drug release studies using commercial and Welsh alginates and their derivatives.

Chapter 5. Alginate Micro-Beads prepared by a novel two-step ionotropic method as carriers for hydrophilic and hydrophobic drugs

5.1 Introduction.

The unique physical properties of hydrogels have sparked particular interest in drug delivery applications. Fine-tuning the density of cross-links in the gel matrix affords a means of controlling the porosity of the structure and thereby influences the swelling of the hydrogel in the swelling media. The porosity of the gel matrix also permits the loading of drugs and their subsequent release at a rate, which depends on the diffusion coefficient through the gel network. A major benefit of hydrogels for drug delivery may be largely pharmacokinetic as a depot formulation from which drugs slowly elute, to diffuse into the surrounding tissue or alternatively can be used for systemic delivery. Hydrogels are also generally highly biocompatible.[179]

Since their first use for drug encapsulation in the 1970s, alginate hydrogel particles of different sizes, structures, and morphologies have been made by many different methods.[180] Alginate have been used as an excipient in numerous types of dosage form ranging from tablets, suspensions, capsules and beads [110, 79], and used for encapsulation of various cargos such as protein drugs, living cells, enzymes, volatile compounds, food ingredients and catalysts [180] in addition to a wide variety of bio-active compounds have also been incorporated into alginate microparticles and larger diameter beads and these include various small molecules such as gastro-irritant , non-steroidal and anti-inflammatory drugs.[181]

All these examples exhibit variations in drug loading and release kinetics which depend upon the chemical characteristics of the cargo and its method of encapsulation as well as the composition of alginate polymer.[182, 33]

The choice of particle size and morphology depends on several factors including the requirements of the target application. The classic morphologies are beads, which are defined as spheres that have diameters larger than 1000μm where the immobilized cargo, either hydrophilic or lipophilic, is typically dispersed throughout the polymer matrix.[180]

For the controlled release of drugs, the bead design has been used to manipulate drug diffusion.[183] Spherical beads have been used for oral delivery of probiotics cells[184] also impregnated with sulphamethoxazole as a model drug[185], and also loaded with ranitidine hydrochloride.[178]

Alginate hydrogels used for the encapsulation of drugs are typically prepared by cross-linking with metal ions such as Ca^{2+} in a process known as ionotropic gelation.[186, 187] Two methods are employed, i.e. the external and internal gelation. They differ in how the cross-linking ions are introduced. External gelation is the established and most widely used technique of ionotropic gelation, and the only method to produce spherical beads. In this process, Ca^{2+}ions are introduced externally to the discrete alginate droplet, which is delivered drop-wise by pipette into a calcium chloride solution. Ca^{2+}ions diffuse inwardly to occupy the interstitial spaces between the alginate polymer chains to initiate cross-linking. Thus, typically, an alginate solution containing the drug cargo is extruded dropwise into a gelling bath containing Ca^{2+}ions (e.g. calcium chloride solution, see **Fig (5-1**). Upon contact, the Ca^{2+} ions diffuse from within the droplet to cross-link with the alginate polymer chains at the alginate-droplet periphery. This results in the initial formation of a semi-solid membrane encasing the liquid core of the droplet.[188] Prolonged immersion of the droplets in the media bath allows for further diffusion of Ca^{2+} across the membrane via a concentration gradient, leading to the solidification of the core. As a result, an alginate bead is formed in which the cargo is embedded randomly within the cross-linked matrix.

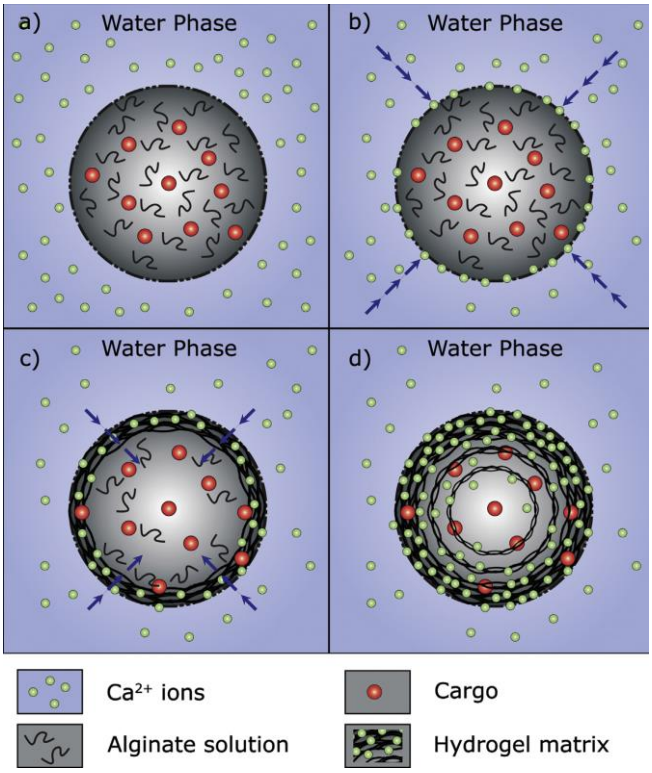

Fig (5-1): Mechanism for bead formation by external gelation: (a) alginate droplet in contact with calcium solution, (b) inward diffusion of calcium ions, (c) inward gelation of droplet, and (d) completed gelation.[184]

A drawback to the external gelation technique is that the beads prepared may not have a fully homogeneous structure if the Ca^{2+} ions are not diffused fully into the alginate matrix. However, it is supposed that beads with a uniform cross-linking density would allow the system to be fine-tuned to a more controlled drug-release rate. Thus, in contrast to particles formed via external gelation, an internal gelation technique is more likely to produce a homogenous structure.[189] In the internal gelation method an aqueous solution or liquid oil containing Ca^{2+} ions is delivered dropwise into a bath of alginate solution.[180] Upon contact, the Ca^{2+} ions diffuse and cross-link with the alginate polymer chains at the interface of droplet in the external medium. The gelation continues until all the free Ca^{2+} ions are exhausted from within its droplet. By the end of the process, the original liquid droplet is enclosed within a continuous semi-permeable membrane of Ca-alginate. This is in contrast to external gelation method in which the Ca^{2+} ions diffuse inward from the external medium into the interior of the alginate droplet.

Alginate particles prepared by external gelation tend to have a denser structure with smaller pore sizes at the surface of the particle compared to beads prepared through internal gelation which have a more even distribution of the Ca^{2+} cations throughout the particle.[69]

As an enhancement, a novel procedure was employed to further fine tune cross-linking density, by which beads prepared by internal gelation were then dropped by pipetting into a solution containing Ca^{2+} ions.

The aim of this study was the synthesis of spherical beads using Alginate and their PCL copolymer derivatives which were encapsulated with two different model drugs. Carmoisine was selected as the hydrophilic model and β-carotene as the hydrophobic model. Carmoisine dye (M_W = 502.43 g/mol) which is a water soluble small molecule possessing a negative charge in aqueous polar media **Fig (5-2)** , the β-carotene is a hydrophobic dye which is non-toxic and bio-compatible (for structure see **Fig (5-3)**).

The beads were to be prepared by a novel external ionotropic gelation method in a two-step procedure involving the internal and external approach. This method was compared with an established one-step external ionotropic method.

5.2 Experimental.

5.2.1 Chemicals and materials.

Carmoisine dye (M_W = 502.43 g/mol), β-carotene and surfactants Tween80 and Span were purchased from Sigma-Aldrich. Fused, granular calcium chloride ($CaCl_2$), dimethyl sulfoxide (DMSO), cyclohexane and sodium chloride (NaCl) were purchased from Fisher Scientific. All materials were used without further purification. Five different alginates were chosen in this study to form the spherical beads, i.e. commercial alginate and its PCl grafted derivative, also including alginate obtained from locally sourced Welsh and Irish seaweeds and a grafted derivative was synthesised from the Welsh alginate.

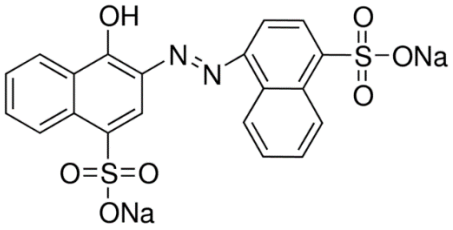

Fig (5-2): The chemical structure of carmoisine.

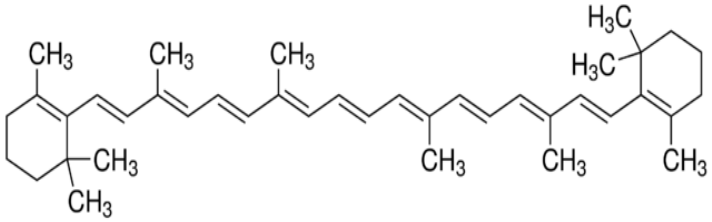

Fig (5-3): The chemical structure of β-carotene.

5.2.2 Preparation of carmoisine encapsulated alginates beads by the one-step and two-step method.

Beads formed by one-step ionotropic external gelation (Ca-ALG-1step). Carmoisine dye, 2 mg, was dissolved in 10 mL of 1% alginate solution and this was added dropwise via a syringe from a fixed height of 4 cm to a 5% (w/v) calcium chloride solution. Beads were formed almost immediately on contact. All the beads were the collected using a spatula and subsequently freeze-dried.

General method for the formation of beads by the two-step ionotropic external gelation method (Ca-ALG-2step).

Step 1: Ca-alginate particles were prepared by the internal method as per **Table (5-1)**. Sodium alginate was dissolved in deionised water under magnetic stirring at room temperature and 2 mg of carmoisine dye was then dissolved in 10 mL of the alginate solution. 1 mL of $CaCl_2$

solution was then dropped into the magnetically stirred (200 rpm) alginate solution over a period of 40-50 seconds using a micro-pipette from a standard height of 4 cm with continued magnetic stirring for two hours. This method of delivery was a standardised procedure that allowed for calcium addition to be judged comparatively. The resultant Ca-alginate particle formations were left to stabilise over-night at room temperature without further stirring.

Step 2: the Ca-alginate particles prepared in step one (Samples 5, 11 and 17) in **Table (5-1)**, were extruded dropwise, using a syringe, (10 mL) into a 100 mL aqueous $CaCl_2$ solution of 5% (w/v) concentration in deionised water. The resulting beads (Ca-ALG-2 step) were then left in the gelling medium for 5 mins before removal from the solution by filtration and subsequently freeze dried.

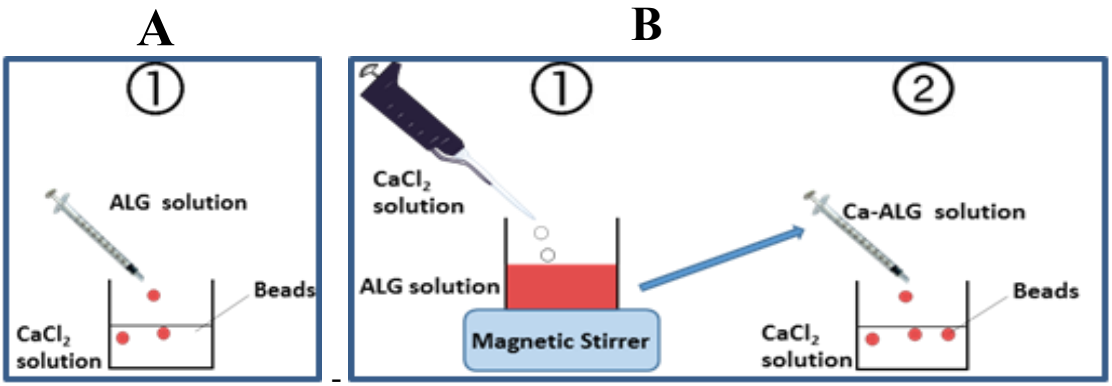

Fig (5-4): Preparation of beads by ionotropic external gelation method: (**A)** one step method approach (Ca-ALG-1step) and **(B)** two step method approach (Ca-ALG-2step).

Table (5- 1): **Ca-alginate particles prepared in step 1 of the 2-step method.**

Experiment No.	Alginate Conc. (% w/v)	$CaCl_2$ conc. (mg/mL)
1	0.1	0.01
2	0.1	0.06
3	0.1	0.4
4	0.1	2.0
5	0.1	4.0
6	0.1	10.0
7	0.5	0.01
8	0.5	0.06
9	0.5	0.4
10	0.5	2.0
11	0.5	4.0
12	0.5	10.0
13	1.0	0.01
14	1.0	0.06
15	1.0	0.4
16	1.0	2.0
17	1.0	4.0
18	1.0	10.0

5.2.3 Preparation of alginate beads encapsulated with β-carotene.

Two methods were used for the preparation of β-carotene encapsulated beads, the two-step method and an emulsion method.

5.2.3.1 Preparation of alginate beads encapsulated with β-carotene by two-step method.

The poor solubility in water of the hydrophobic β-carotene required the use of the solvent DMSO to enhance its solubility

First step: A mixture of β -carotene, alginate and 7 parts of water to 3 parts of DMSO was made and stirred until homogenous in appearance. Alginate solutions were made by dissolving sodium alginate (0.1 g) in water (5.5 mL) in glass vial 1. Whilst this was stirring, a new mixture was made in a separate glass vial. Beta-carotene (2 mg), DMSO (3 mL) and deionised water (1.5 mL) were added into glass vial 2 and stirred until no particulates remained. After full dissolution, the contents of vial 2 were added to vial 1 and stirred for 5 minutes. Ca-ALG hydrogel beads were made by dropping $CaCl_2$ solution (1 mL, 0.4 mg/mL) into the alginate solution with a 1mL syringe, over a time range of approximately 40-50 seconds. This solution was magnetically stirred at 200 rpm for 2 hours. The Ca-Alg mixture was subsequently taken off the stirrer and left to stabilise on the work-bench overnight at room temperature.

Second Step: This procedure was identical to the general procedure as given above using carmoisine red food dye

5.2.3.2 Preparation of alginate beads encapsulated with β-carotene using the Emulsion method.

Step1: An alginate solution was made by mixing 0.2 g of alginate, 19 mL of deionised water and 1 mL of Tween80 surfactant in a 100 mL beaker. The mixture was allowed to stir until the alginate was completely dissolved. In a glass vial, 4 mg of β-carotene was added to 2 mL of cyclohexane along with a small stirrer bar and left to mix. Once all the β-carotene had completely dissolved, this mixture was added to the alginate solution and left to stir for 1 hour at 1000 rpm. Afterwards, 2 mL of 0.4 mg/mL $CaCl_2$ solution was added dropwise.

Step 2: Following stabilisation of this mixture, it was then added dropwise to 200 mL of 5% $CaCl_2$ solution. The fully formed beads were removed using a spatula and dried using Kimtech absorbent wipes. Finally, the alginate spherical beads were collected and freeze-dried for future use and testing.

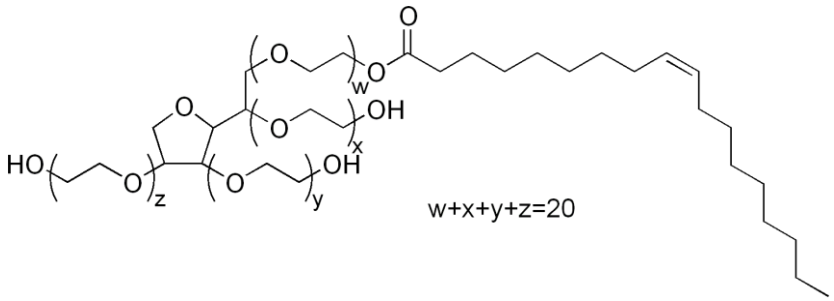

Fig (5-5): The chemical structure of tween80 (Polysorbate 80)

5.2.4 Morphology study.

The external surface morphology of the freeze-dried Ca-alginate particles, prepared as per step 1 in the two-step method, were studied using a 1984 Hitachi model S-520 scanning electron microscope (SEM), operating at 15 kV. Samples were prepared for SEM by mounting onto 0.5-inch aluminium specimen stubs using double-sided adhesive carbon pads. The freeze-dried particles (entries 5, 11 and 17 in **Table 5-1**) were then coated with a thin layer of gold (approx. 20 nm thickness) in a high vacuum thermal evaporator. Note: beads from step 2 were examined without gold coating.

5.2.5 Swelling study.

The pre-weighed freeze-dried beads were suspended in 1mL portions of either of two different aqueous media i.e. deionised water and NaCl 1% (w/v).At the set time intervals the beads were

extracted from the solution and immediately dried with tissue paper to remove surface liquid from the beads. The weight was then obtained (W_1) and the weight change with respect to time was calculated:

Weight change (%) = $(W_1 - W_0)/W_0 \times 100$

Where W_0 and W_1 represent the initial and swollen weight of the beads, respectively. All studies were performed in triplicate.

5.2.6 Release Study.

Encapsulation efficiency was determined by UV-vis spectroscopy. A calibration curve was prepared by measuring absorbance at 515nm using a solution of carmoisine at various concentrations in calcium chloride solution, see **Fig (5-15)**. The carmoisine concentration was measured in the supernatant liquid after the beads where extracted. The difference between carmoisine concentrations represent the amount taken up by the beads and, therefore, a measure of encapsulation efficiency.

The release of model drugs from freeze-dried beads was performed at room temperature in deionised water and NaCl (1% w/v). In a glass vial, approximately 15-20 beads (60 mg) were placed in 1 mL of the aqueous solution. At specific time intervals (i.e. 10, 20, 30, 60, 120 and 140 mins), a 750 μL aliquot was withdrawn and immediately replaced with the same volume of fresh solution. The calculated concentration of model drug in the sample aliquots was determined by measuring the absorbance at 515 nm in a quartz cuvette, recorded on a UV/Vis Spectrophotometer (UNICAM UV-4). All studies were performed in duplicate and the dye release at each interval with respect to time was determined:

Dye release (%) = [dye release] / [dye loaded] × 100

5.3 Results and discussion.

5.3.1 Preparation of alginate beads using one-step and two-step ionic crosslinking methods encapsulated with carmoisine.

The initial work involved an internal ionotropic gelation method using alginate and induced by the addition of $CaCl_2$ to prepare Ca-alginate, to be utilised in Step 2. This method has the advantage of being inexpensive and could be carried out under mild ambient conditions. Immediate gelation occurs by the interaction of the alginate polymer chains with Ca^{2+} divalent ions to give rise to a three-dimensional network structure within particles of small dimension. In particular, the solution-gel transition occurs as the Na^+ ions in Na-ALG are replaced with Ca^{2+} (cross-linker) ions from $CaCl_2$ to form the well-known "egg-box" structure, in which the cations pack and ionically cross-link the ALG chains.[42] The resulting ionic bridges between the chains occur at room temperature, independent of organic solvents or high shear pressure, ideal for the encapsulation of sensitive drugs that may lose their activity when exposed to harsh conditions.[177] Other metal crosslinking ions can be used (e.g. Cd^{2+}, Pb^{2+}, Co^{2+}), however, given the increased toxicity of these ions, with respect to drug delivery applications calcium is commonly employed as it is considered economical and clinically safe.[20]

To standardise conditions for the experiment the micropipette, dropping time, dropping height and magnetic stirrer speed factors were kept constant for all gelations. Therefore, the delivery of the calcium chloride solution was maintained over 40-50 seconds from a height of 4 cm and under a magnetic stirring rate of 200 rpm. Thus, calcium addition could be quantified on a comparative basis. The concentration of the polymer and cross-linking agent variables were altered according to the eighteen compositions presented in **Table (5- 1) in order** to investigate the effect on the formation of ALG hydrogel.

Observations with respect to the viscosity and opacity of the stabilised formations exhibit a trend based on an increase in viscosity with higher combined alginate and $CaCl_2$ concentration. The highest concentration of alginate (1% (w/v)) used in this study produced a macroscopic gel when cross-linked with a high concentration $CaCl_2$ solution, see **Table (5-1)** samples 17 and 18, as it increases the cross-linking of polymeric chains to interlink across a network. For the preparation with more dilute alginate solutions (**Table (5-1)**, samples 1-6), the Ca-alginate

stability was altered, as the decreasing number of polymer chains present can prevent the formation of a macroscopic gel, but potentially induce Ca-alginate of small dimension particles (as the alginate molecules become more compact).

Further, the eighteen samples of Ca-alginate particles were studied by Ultraviolet-Visible Spectroscopy (UV-Vis). UV-Vis spectra were recorded in the range of wavelengths from 280 to 700 nm. Ca-alginate particles and the pure alginate present the same characteristic peak at 285 nm (λ max) of different absorption intensities. Maximum absorption values with lower absorption intensity than the control, suggest that the Ca^{2+} cations induce a rearrangement of the alginate polymer chains; allowing the formation of high local concentrations of Ca-alginate particle micro-domains instead of an infinite polymer network. For absorption intensities higher than the control, the viscosity of the solution increased forming a macroscopic, homogeneous hydrogel.

Hydrogel morphology is an important factor in the performance of drug delivery systems. The morphology of a polymer network will affect the ability of a drug to diffuse through a hydrogel system, i.e. the pore size in relation to the drug molecule dimension. To enable morphological characterisation, selected freeze-dried Ca-alginate particles (**Table (5- 1)**: Sample no. 1, 3, 7, 9, 11, 13, 15 and 17) were gold-coated to render them electrically conductive for SEM analysis. Micrographs were obtained at various magnification (×35, ×100, ×300 and ×700). **Fig (5-6)** illustrates three Ca-alginate particle surfaces (**Table (5-1)**: Sample no. 5, 11 and 17) and indicates clearly that combined alginate /$CaCl_2$ conc. influences the surface morphology. At magnification (× 100), a range of porosity is apparent and results from the collapse of the gel network onto the space previously occupied by retained water. It is evident (as seen in **Fig (5-6)**) that porosity increases as a result of decreasing alginate concentration and cross-linking density, with more water retained in dilute alginate solutions. It is seen from the Ca-alginate particle micrograph (**Fig (5-6)**: sample 5) that some particle aggregation has occurred, in contrast to sample 17 that indicates micro-particles obtained from a higher alginate concentration have smooth surfaces from extensive cross-linking.

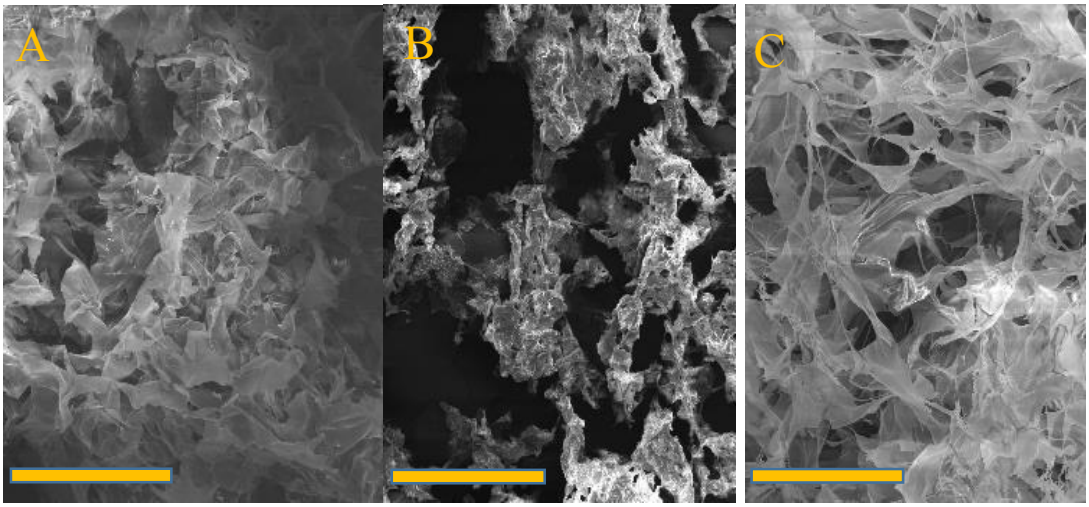

Fig (5-6):.SEM micrographs of freeze-dried Ca-alginate prepared in step 1 of 2-step method: **(A)** sample 17, **(B)** sample 11, **(C)** sample 5 (in Table (5-1**)**). Magnification is 100, (scale bar: 300 μm).

The second step in the preparation of (Ca-ALG-2step) micro-beads involved the use of the external ionotropic gelation technique. An aqueous suspension of Ca-alginate (e.g. samples 11, 17) previously prepared in Step 1, by the internal gelation method, was extruded dropwise into the $CaCl_2$ gelation media to form the spherical beads. These two particular samples were chosen as they are representative of a medium and a highly cross-linked sample (samples 11 and 17 respectively) and therefore, suitable for comparison being less likely to disintegrate on swelling. Gelation occurs from the outermost layer of ALG as the Ca^{2+} ions diffuse into the core of the material. By the addition of a cross-linked alginate (Ca-alginate) solution to a $CaCl_2$ solution, ionotropic gelation is performed twice, thereby, theoretically increasing the overall cross-linking density and resulting compaction of the beads with reduced porosity.

Bead morphology was investigated using SEM analysis. As depicted in **Fig (5-7)** the freeze-drying process leads to the reduction of bead dimensions and a modification to the surface. Thus, for sample 11, as seen in **Fig (5-7)**, the bead size ranges from 0.2-0.4 mm and this is reduced after freeze-drying by a factor of 0.5. SEM characterisation indicates that the freeze-dried beads have a rough surface, with an increase in surface roughness of the (Ca-ALG-2step) beads prepared by the two-step approach. This supports the view that an increase in cross-linking density should create smaller pores in the structure. Small pore size can have impact on

drug release profiles, as the drug should diffuse from the bead at a slower rate reducing the likelihood of burst release.

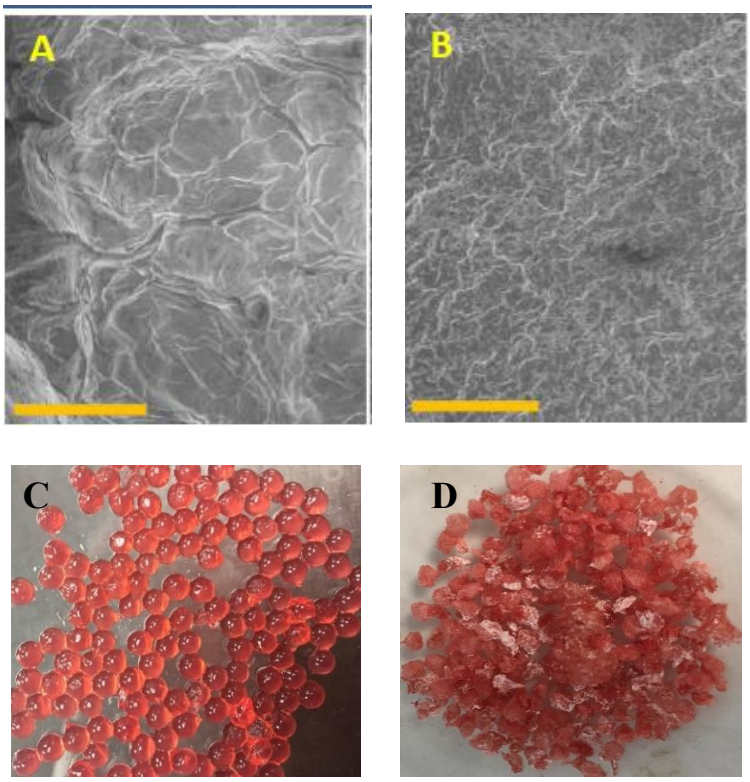

Fig (5-7): SEM surface micrographs of model drug-loaded freeze-dried beads: **(A)** (Ca-ALG -1step), from alginate 0.5% (w/v), **(B)** (Ca-ALG-2step) from sample 11 in Table (5-1). Magnification is 300, (scale bar: 100 μm). **(C)** and (D) are, respectively, wet and freeze-dried beads of (Ca-AlG-2step) from sample 11 in Table (5-1).

Given the results from a comparison of both gelation methods and the evident advantages of the two-step method, in all subsequent work this was the preferred method employed. Spherical beads were then prepared loaded with the hydrophilic model drug (carmoisine) using the various types of alginate at the concentration of alginate solution 1 % (w/v) and $CaCl_2$ of 4mg/mL in the first step of ionotropic gelation.

The effect of the M/G ratio on bead morphology can be seen from visual inspection as seen in **Fig (5-8)**. The commercial alginate (A) with M/G 1.2 gave a well-defined bead structure. This was again true for its PCL graft derivative (B). However, the Welsh alginate with M/G 2.03 appeared less robust and ill defined (C) and finally the Irish with M/G 3 (D) gave the least

defined structure. This behaviour is in accord with the well-observed fact that higher M content leads to more fragile gel. In view of the difficulty in using the fragile Irish hydrogel,further study of it was abandoned. Certainly, further work on this material would be very rewarding.

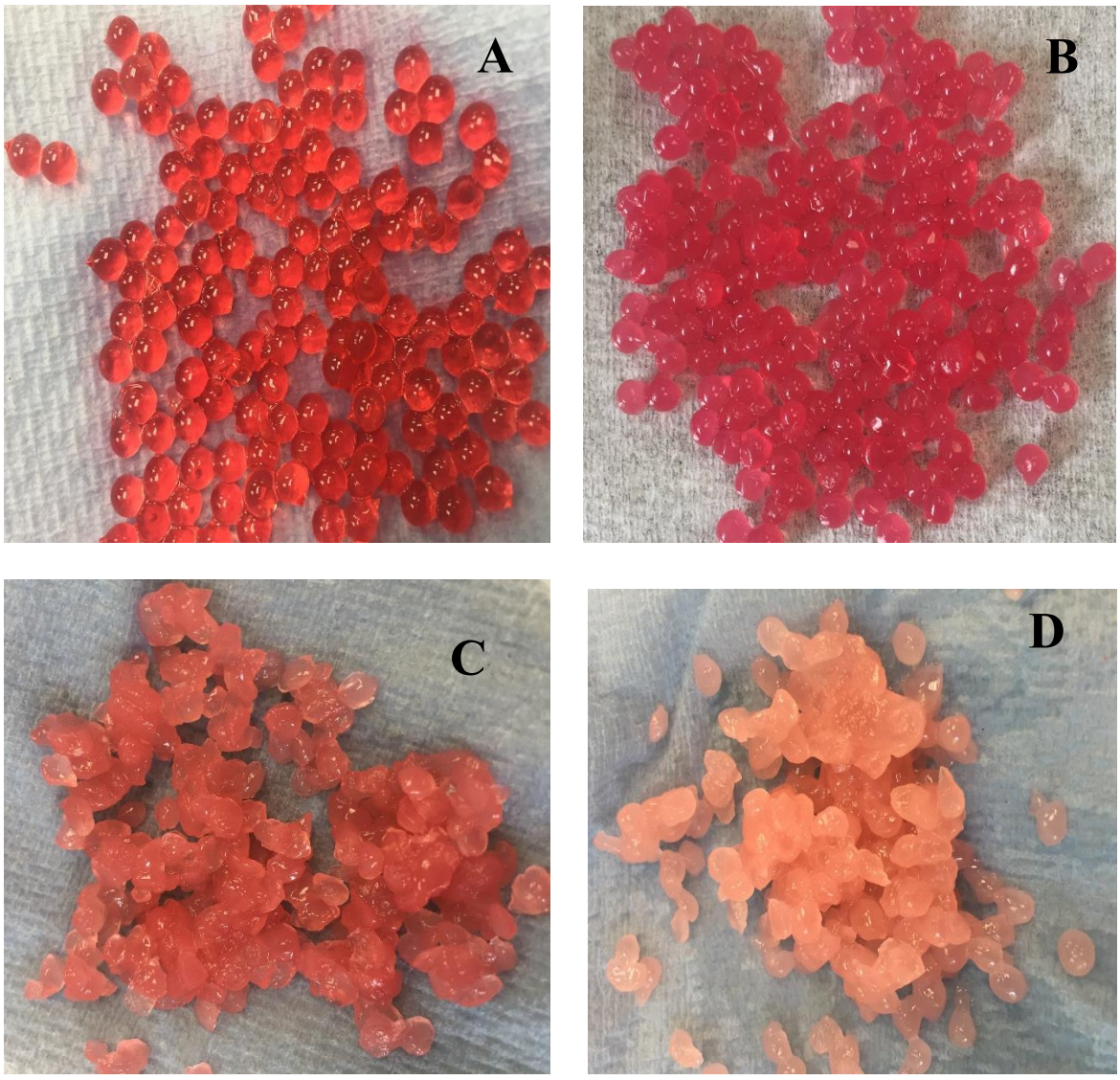

Fig (5-8): The effect of M/G ratio on formed spherical beads: **(A)** commercial alginate, **(B)** commercial alginate –graft **(C)** Welsh alginate and **(D)** Irish.

5.3.2 Preparation of alginate beads using the Emulsion method

Alginate beads incorporating the model drug β-carotene were made by the two-step method outlined above with a modification using an emulsion procedure.

The emulsion-based method is a procedure used for gelation to enable encapsulation of hydrophobic drugs. The water-in-oil (w/o) emulsion method was used for the emulsification of aqueous droplets of water-soluble biopolymers and is achieved by adding to a continuous oil phase using oil-soluble surfactants, the crosslinking of the biopolymer is facilitated with the water-soluble cross-linkers. By this procedure an alginate solution containing the cargo is emulsified by adding to the oil phase forming a w/o emulsion. Then a cross-linker, often $CaCl_2$ is added to the emulsion, resulting in the gelation of the alginate emulsion droplets followed by a phase separation of the emulsion.[190] In our attempt to encapsulate the hydrophobic model drug β-carotene the w/o emulsion method was followed using a modified procedure[191] in which β-carotene was dispersed in 10 mL of 1% aqueous solution of alginate. The aqueous phase was then emulsified in cyclohexane in the ratio of 1:10 cyclohexane/aqueous containing 2% (v/v) surfactant span 80 with stirring at 1000 rpm for 60 mins. Then, to induce gelation by the internal method, 5 mL of 0.2 m of $CaCl_2$ was added to the emulsion and stirred. Subsequently, to induce a further gelation by the external method, the mixture was then added dropwise into 5% $CaCl_2$ to form the final spherical beads. It was found that very fragile beads formed **Fig (5-9) B** .The procedure was further modified in which the aqueous phase incorporated the TWEEN 80 as the surfactant with the effect that when the solution of the β-carotene in cyclohexane was added to the alginate solution the surfactant was more able to ensure its homogeneous dissolution in the aqueous phase. Rapid stirring also facilitated the full dissolution of the drug.[191]

This modification proved more useful for our purpose in that the addition of a predominantly aqueous solution containing the microbeads was able to better disperse in the receiving calcium chloride solution. Thus, the second step of the gelation i.e. the external gelation is facilitated and the micro-particles formed by the first step can be further cross-linked at their particle peripheries. Thus, this modification has the advantage over the previous method, which introduced a hydrophobic hexane solution containing the microbeads in to a receiving aqueous calcium chloride with the phase difference inhibiting full dispersion despite the addition of surfactant.

It was thought likely that as the surfactant itself has affinity for the hydrophilic domains within alginate, the drug will also be transported into these domains.

The loaded beads appeared to have incorporated virtually all the β-carotene as no visible dye colouration remained in the supernatant after beads formed. The resultant beads were bright yellow in appearance in contrast to the red colour seen in the ionotropic two-step method.

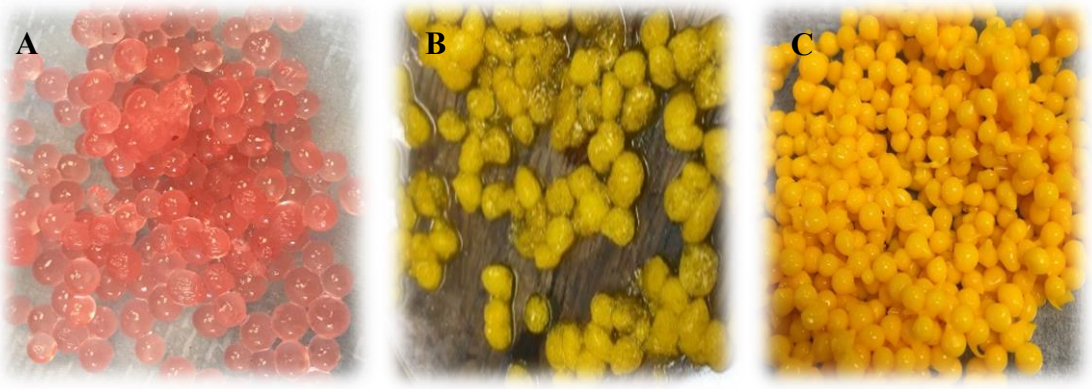

Fig (5-9): β-carotene loaded alginate beads formed by: **(A)** two step ionotropic gelation method according to the procedure 5.2.3.1, **(B)** water/oil emulsion method and **(C)** oil/water emulsion method.

5.3.3 Swelling study.

The release of the encapsulated model drugs and its dissolution in the swelling medium is influenced by the swelling behaviour of the polymer network. The swelling behaviour of beads was investigated in both NaCl solution at 1% (w/v) and in H_2O. The same trends in swelling were observed in both media but greater swelling occurred in the NaCl solution. Swelling was mainly associated with the hydration of the hydrophilic moieties in ALG, as the media solution penetrates the pores within the ALG framework and the consequent relaxation of the network.[192]

There is generally a weight increase for all beads in both media due to rapid swelling. Additionally, in saline media, there is also an ion exchange process in which the Na^+ ions replace the Ca^{2+} ions attached to the ALG G-block residues.[177] This causes the 'egg-box' structure to loosen, thereby, increasing the distance between polymer chains and thus favouring the fluid swelling process.

In NaCl solution, **Fig (5-10) A**, it can be seen that the beads display a weight increase before a decrease resulting from the dissolution of some polymer chains. Furthermore, this cross-linking factor was evident when comparing the behaviour of (Ca-ALG-2step) beads with their (Ca-ALG-1step) beads and suggests that beads prepared by the two-step method have a greater cross-linking density and more physical entanglements of the polymer chains which are likely to restrict the extent of swelling.

Effect of the concentration of alginate solution.

From **Fig (5-10),** it can be seen also that the cross-linking density affects the swelling with ALG 0.5% (w/v) swelling more than the ALG 1% (w/v) and this reflects the lower cross-linking for the lower concentration. This applies to 1step and 2 step preparations. It is also evident that the 1 step swells more than the 2 step again reflecting that the 1 step has a less homogeneous structure than the 2 step and therefore more likely to be disrupted with greater swelling. The same trends are seen for both saline and water media with greater swelling taking place in saline. This is likely due to ion exchange in saline.

Effect of grafting.

The effect of grafting can be seen from **Fig (5-11)** which shows that swelling is greater for the pure alginates both in water and in saline with greater swelling in saline. Here, the ion exchange is at work in saline. However, the grafted derivatives swell less than the pure. It could be caused by hydrophobic domains preventing swelling despite the supposed lower cross-linking in the grafts.

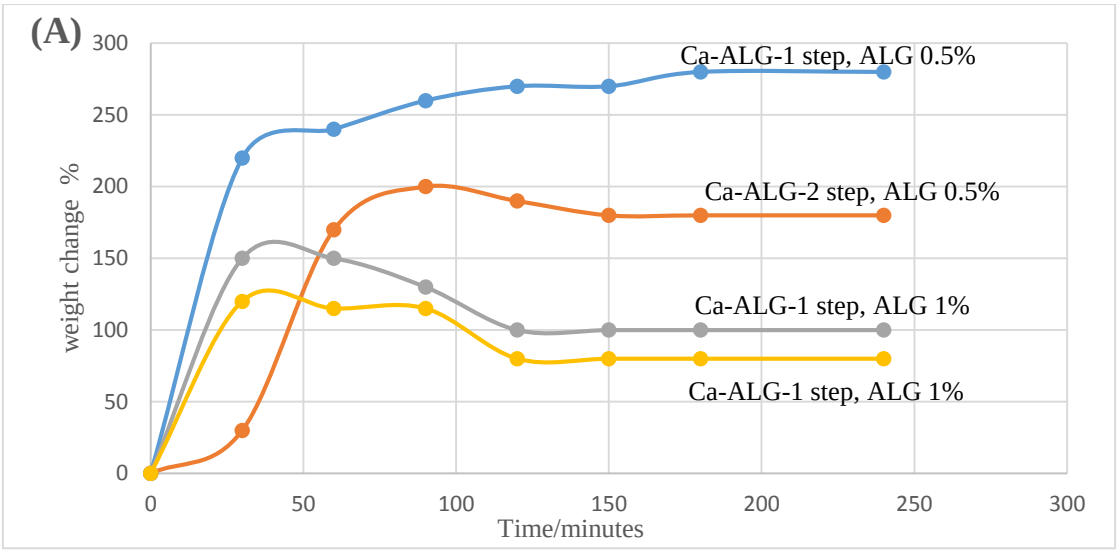

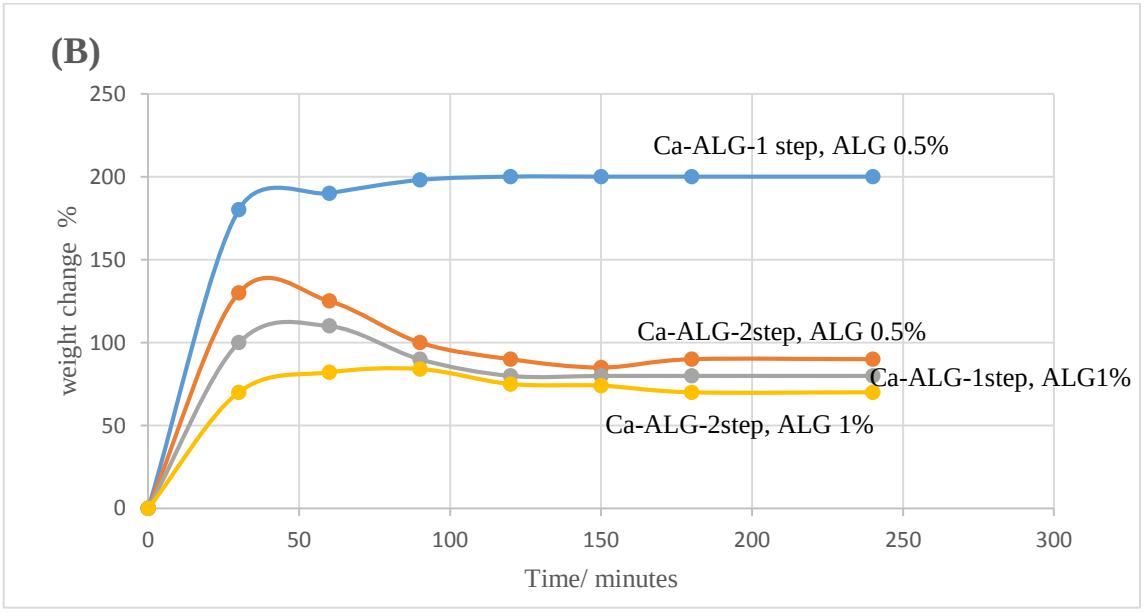

Fig (5-10): Swelling profile of freeze-dried beads showing the effect of cross-linking density on swelling, **(A)** in NaCl 1 %(w/v), **(B)** in distilled water. Data points represent the average within an error range of ± 2%.

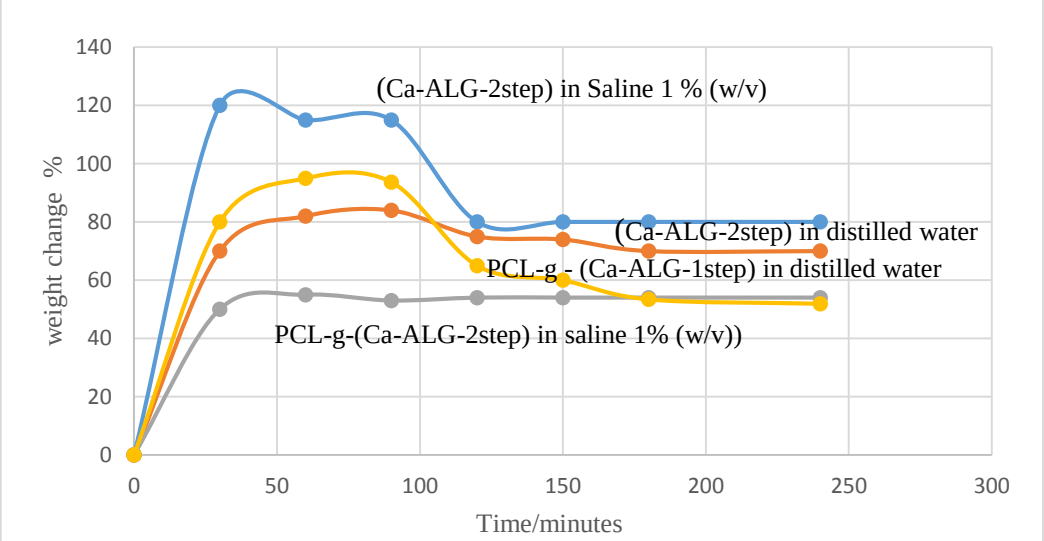

Fig (5-11): Swelling profile of freeze-dried beads showing comparison swelling of pure and grafted alginate. Data points represent the average within an error range of ± 1.5 %.

Effect of the loaded drugs.

Fig (5-12) compares swelling for both hydrophilic carmoisine and hydrophobic β-carotene in saline and in water as prepared by the two step ionotropic gelation and emulsion methods. The beads loaded with carmoisine had greater swelling than the β-carotene beads (120 and 70 % respectively) and this reflects the affinity for water due to the different cargoes. The β-carotene was also prepared with the addition of DMSO and this may interfere with swelling if there is any residual solvent in the structure. The emulsion material has the lowest swelling (50 %) but this is comparable to the other 2-step β-carotene loaded material. Thus, the reduced swelling compared to the carmoisine may be due the presence of the hydrophobic β-carotene cargo.

The slight difference in the swelling between the β-carotene loaded materials may also be due to the result of the residual presence of organic solvent i.e. the DMSO and cyclohexane in the emulsion material. The DMSO is a polar solvent and if any is present in the beads would enhance swelling in the aqueous media when compared to the hydrophilic cyclohexane. The presence of residual solvent may be inferred from the colour of the beads, which were red for 2 step ionotropic method but yellow for the emulsion method. It appears that the solvent affects the colour of the β-carotene dye and this was apparent when preparing solutions for bead syn-

thesis. The beads retained these colours during swelling which indicates that any residual solvents stayed in the beads during swelling. Any further study should consider NMR to detect solvent in the beads.

The same trends were seen in water as in saline solution but swelling was less in water as (82 , 70 ,60 %) for a, b and c beads respectively, see **Fig (5-12**) **B** particularly for the hydrophilic carmoisine.

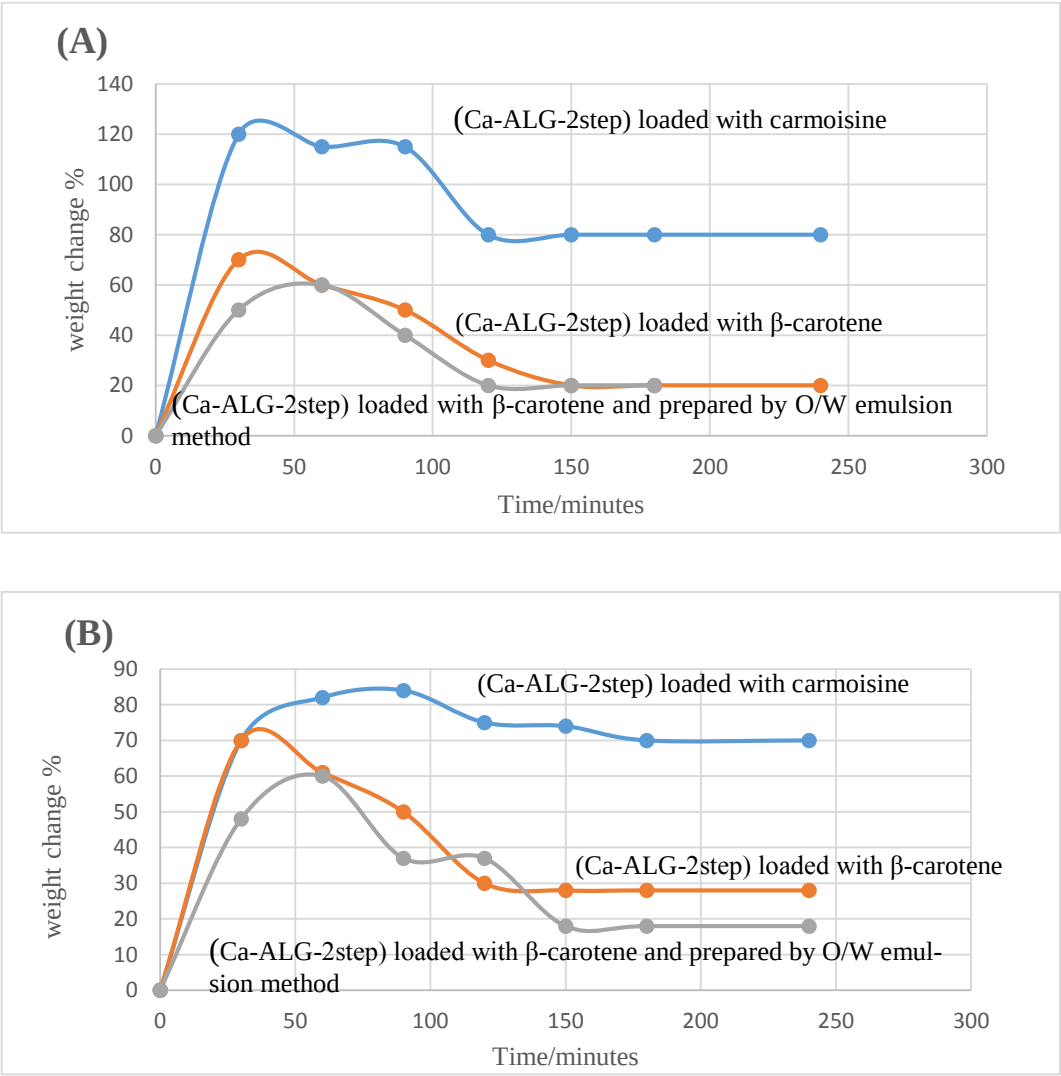

Fig (5-12): Swelling profile of freeze-dried beads in **(A)** Saline 1 % (w/v), **(B)** distilled water. Data points represent the average within an error range of ± 2%.

Swelling of Welsh alginate beads (loaded with carmoisine) and its grafted derivative.

Fig (5- 13) provides a comparison of the swelling profiles for Welsh alginate beads in pure and grafted form in both water and saline solution. Swelling is highest for the grafted derivative and was marginally highest in water media (55%). This is a consequence of the hydrophobic domains present which result in a lower ionic cross-linking. Hydrophobic domains may allow the material to expand even more. The same trend is observed for the Welsh materials in water but the lower swelling (18%) reflects greater cross-linking as the absence of grafting permits ionic cross-linking. It should be noted that Welsh alginate also has a relatively high M content which is less favoured for cross-linking that materials with more G content.

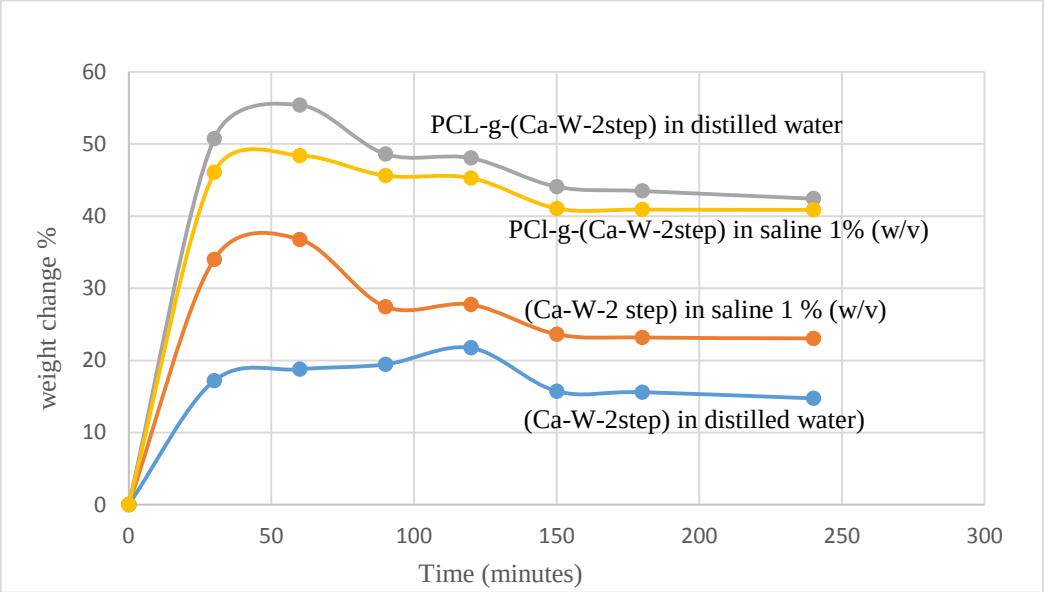

Fig (5-13): Swelling profiles of freeze-dried beads of Welsh alginate (W) and its grafted derivative loaded with Carmoisine. Data points represent the average within an error range of ± 1%.

5.3.4 Encapsulation efficiency and Release study.

For entries 1 and 2 for **Table (5-2)** for beads prepared by the two different methods, entry 1 indicates that 23% of the dye in the preparation solution (2 mg of dye per 10 mL of alginate

solution.) was encapsulated by the beads. This compares with 54.4 % of the dye that was taken up by the same weight of beads as seen in entry 2. Therefore, the encapsulation efficiency is a relative measure of the uptake of dye for the samples selected and allows us to compare the dye content in the samples.

In the case of model drug β-carotene no model drug was left in the $CaCl_2$ solution after removing the beads from the solution. This indicates that drug uptake was 100%, and therefore, is taken as a 100% encapsulation efficiency. The two methods used for loading beads with beta carotene required the use of organic solvents to dissolve the dye in alginate solution i.e. DMSO and Cyclohexane and it is seen that as all the dye was taken up evidently the alginate is very efficient at taking up the hydrophobic dye at least under these conditions and, further, was found to be very efficient at retaining the dye within its hydrophobic domains.

This is well illustrated in **Fig (5-14)** below. In (A) it is seen that no dye is left in the supernatant resulting in red loaded beads. In (B) the β-carotene has again been fully absorbed with none left in the supernatant while the beads are yellow. In (C) the supernatant retains some red colouration after dye loading showing that dye uptake less than 100%.

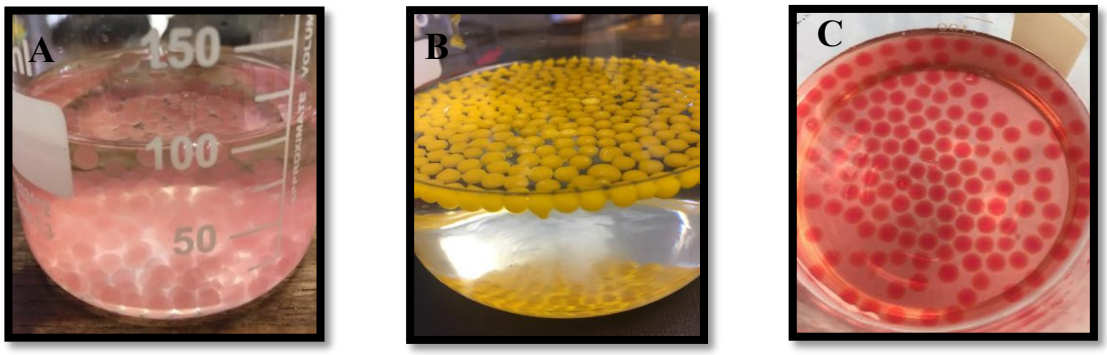

Fig (5-14): Dye loading during preparation into commercial alginate beads: (**A**) (Ca-ALG-2step) beads loaded with β-carotene and prepared by ionotropic gelation method, (**B**) (Ca-ALG-2step) beads loaded with β-carotene and prepared by hexane/ water emulsion method and (**C**) (Ca-ALG-2step) beads loaded with carmoisine in aqueous preparation.

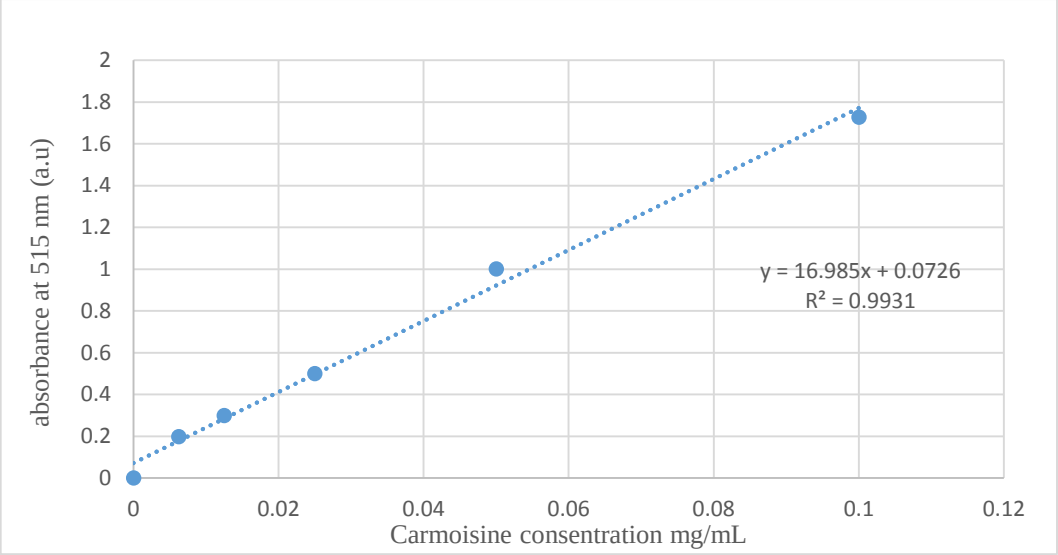

Fig (5-15): Calibration curve for carmoisine dye in $CaCl_2$ solution.

Table (5-2): Encapsulation efficiency of Ca-alginate spherical beads prepared from commercial (ALG) and Welsh (W) alginate using different method to encapsulate the model drugs.

Sample	Model Drug	Preparation Method	Encapsulation Efficiency (%)
(Ca-ALG -1step)	Carmoisine	Ionotropic gelation	23
(Ca-ALG- 2step)	Carmoisine	Ionotropic gelation	54.4
PCL-g –(Ca-ALG -2step)	Carmoisine	Ionotropic gelation	63
(Ca-ALG-2step)	β-carotene	Ionotropic gelation	100
(Ca-ALG-2step)	β-carotene	Oil in water Emulsion	100
(Ca-ALG-1step) *	Carmoisine	Ionotropic gelation	12.3
(Ca-ALG-2step) *	Carmoisine	Ionotropic gelation	20.6
(Ca-W-2step)	Carmoisine	Ionotropic gelation	18.8
PCL-g-(Ca-W-2step)	Carmoisine	Ionotropic gelation	31.1

*Concentration of alginate is ALG 0.5% (w/v)

The release of dye was studied in two different media namely water and saline, the calibration curves of the carmoisine in these different media were obtained **Fig (5-16) A** and **B**.

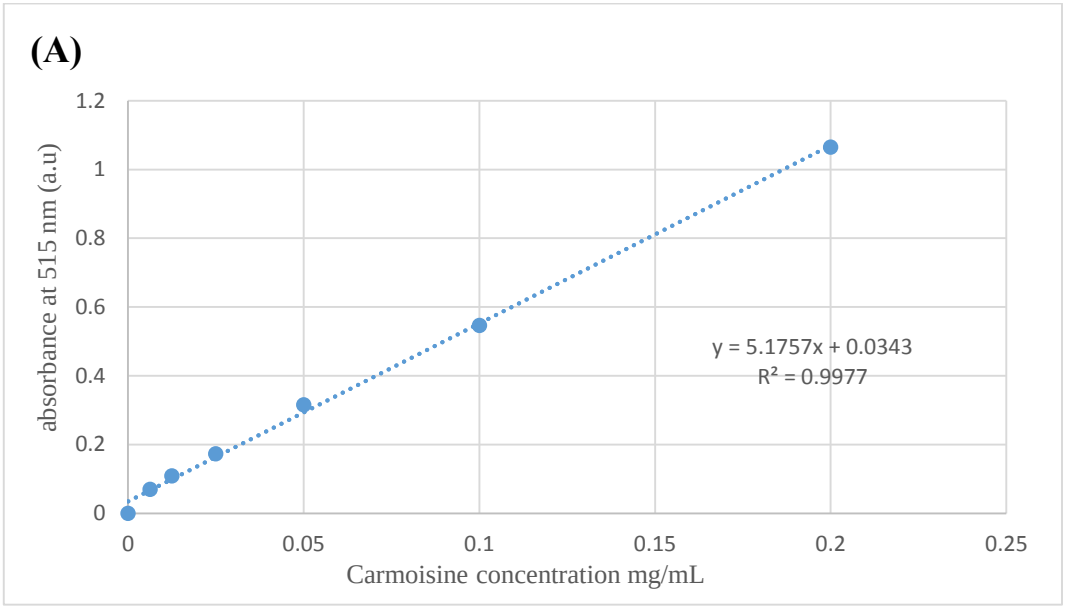

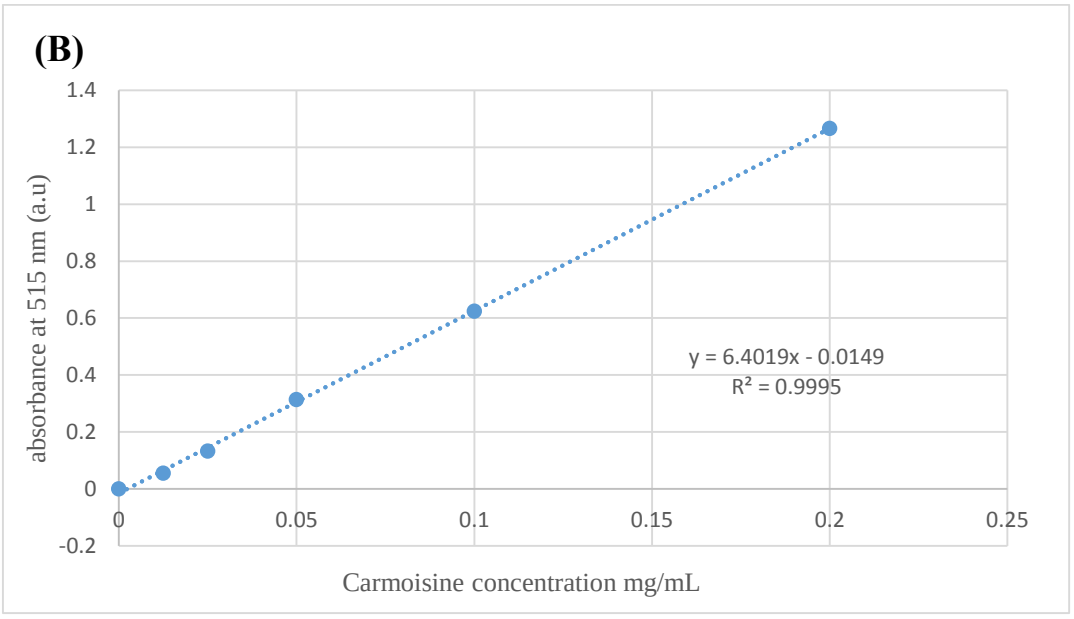

Fig (5-16): The calibration curve of carmoisine: **(A**) in NaCl 1% (w/v) and **(B)** in distilled water respectively.

The release profiles are given in **Fig (5-17) A** and **B**. It is observed that all the beads give a rapid release within 10 minutes i.e. (Ca-alg-1step), ALG 0.5 % (w/v) 89%, (Ca-AlG- 2step),

ALG 0.5% (w/v) 85.32% , (Ca-ALG-1step) ALG 1% (w/v) 80.31% and finally (Ca-ALG-2step),ALG 1%(w/v) was significantly less at 64.8%.It therefore appears that the low alginate concentration gives rise to a more rapid release as the ionically bound dye is released through diffusion. However, this is overridden by the more cross-linked material slowing down the release as seen in (Ca-AlG- 2step), ALG 1% this material is more likely to have a structure less accessible to the water medium and therefore prolonging the release.

Swelling in saline solution significantly increase the release profile for all the materials. Thus, (Ca-ALG-1step), ALG 0.5 % (w/v) 91.44%, (Ca-AlG- 2step), ALG 0.5% (w/v) 87.5, (Ca-ALG-1step) ALG 1% (w/v) 82.59 and finally (Ca-ALG- 2step), ALG 1 %(w/v) was significantly increased to 70.34%. The same ranking was seen as for water and the ion exchange process would appear to open up the hydrogel structure enabling a more rapid release.

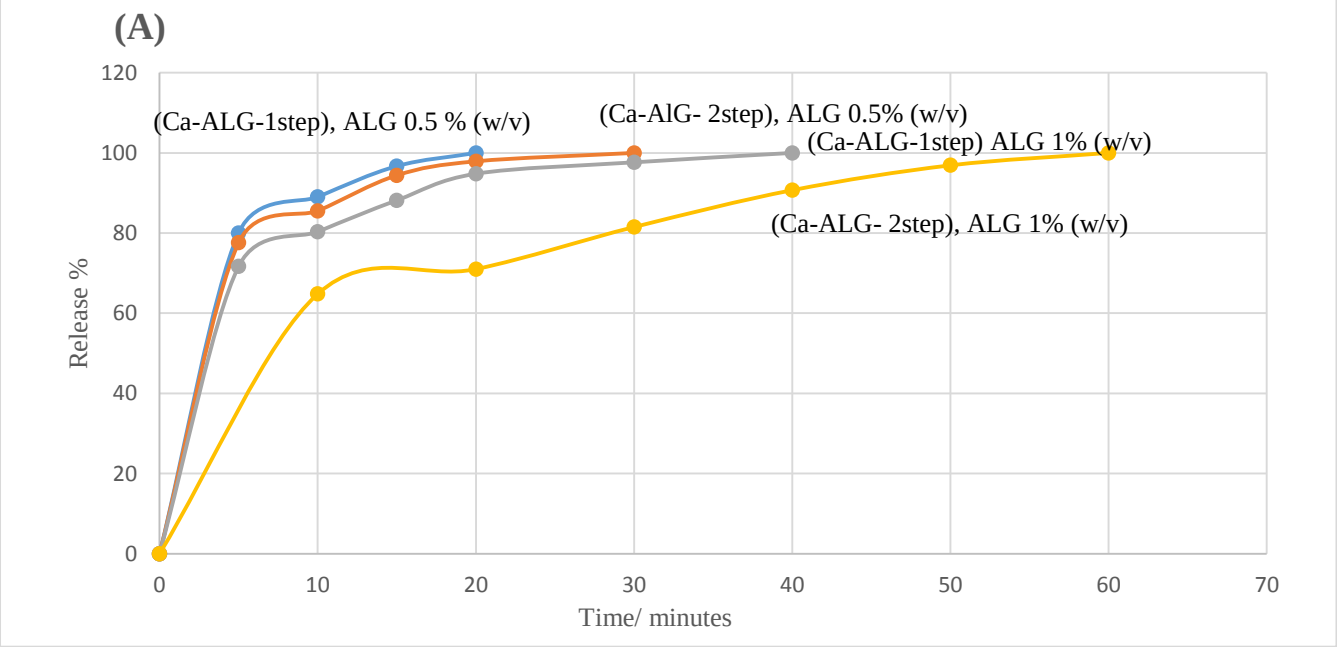

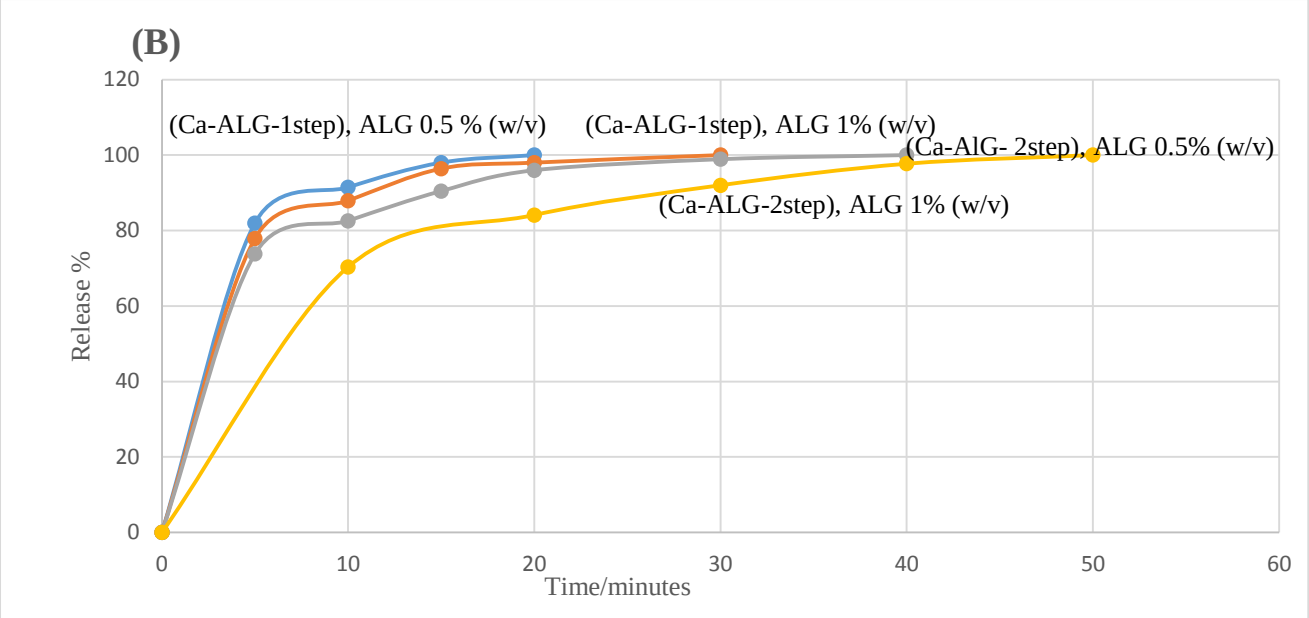

Fig (5-17): Release profile of carmoisine dye (model drug) from freeze-dried Ca-(ALG) beads in swelling media: (**A**) water and (**B**) NaCl 1 % (w/v). Data points represent the average within an error range of ± 1.5 %.

The effect of grafting on drug release can be seen from **Fig (5-18)** where comparison is made between the performance of commercial to Welsh alginates in both saline and water media.

The same general release profiles can be seen with an initial rapid drug release. The Welsh pure alginate beads release their cargo more rapidly than that commercial and the Welsh grafts again discharge their loads more rapidly than the commercial. This is the case in both water and in saline media but release is more rapid in saline. Thus, the release of all its cargo took 150 mins for the commercial graft in water but took 140 mins in the saline solution.

The Welsh alginate beads and the graft derivative are richer in M content and this would suggest a less cross-linked structure which is less likely to form the classic egg box structure with a Ca^{2+} ions. This looser structure being more accessible to the swelling medium would allow a more rapid drug release.

It is seen that the presence of hydrophobic PCL grafts slows down the drug release again the commercial is less rapid than the Welsh and may again be because it is more cross-linked.

Thus, the factors slowing the release of the drug might be of important consideration in any clinical application.

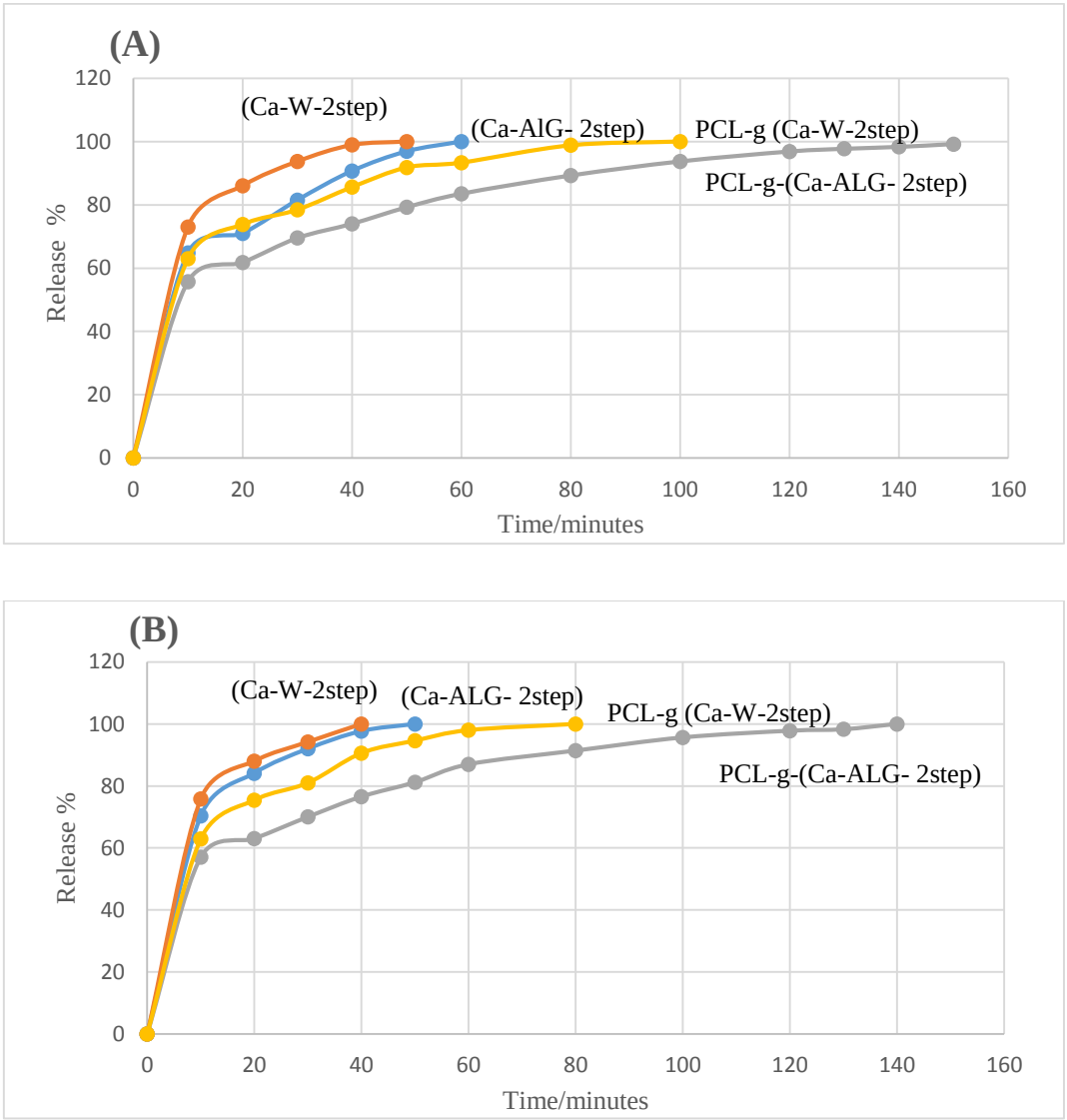

Fig (5-18): Release profile of carmoisine dye (model drug) from freeze-dried Ca- alginate (commercial and Welsh) beads and their grafted derivatives in swelling media: (**A**) water and (**B**) NaCl 1 % (w/v). Data points represent the average within an error range of ± 2%.

The release of carmoisine dye is well illustrated by inspection of **Fig (5-19)** below. The pure ungrafted commercial alginate beads (A) is seen to gradually lose it colour and is completely colourless after 50 minutes. The grafted commercial alginate (B) retains its colour for longer but eventually becomes colourless after 140 minutes.

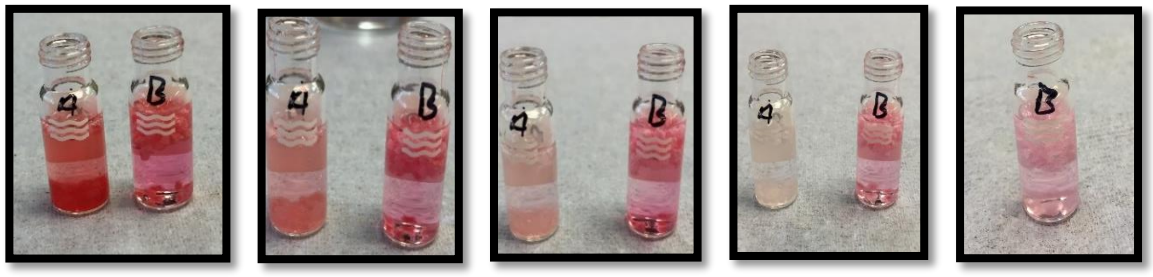

After 10 minutes 20 minutes 40 minutes 50 minutes 80 miutes

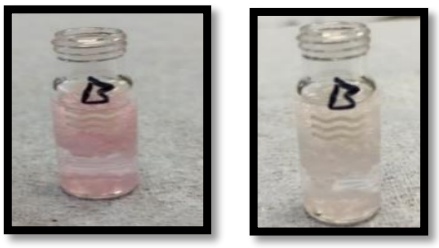

120 minutes 140 minutes

Fig (5-19): Comparison of release of loaded carmoisine from the freeze-dried beads over time: for beads of commercial alginate prepared by two step method (Ca-ALG-2step) **(A)** and **(B)** its grafted derivatives PCL-g-(Ca-ALG-2step) for 10, 20, 40, 50, 80, 120 and 140 mins respectively.

A release study for the β-carotene was performed in which beads of (Ca-ALG- 2 step) were made by ionotropic gelation and the emulsion method. Drug release was performed by immersion in aqueous media (water, NaCl). In both media there was no evidence for any release of the drug for a two week soaking period. Then the beads were soaked in PBS buffer (pH 7.45) for few days, there was no release but they started to lose their shape after 3 days which may be due to the ion exchange , this release profile (or lack of) in an aqueous medium is probably due to hydrophobic nature of the model drug .

5.4 Conclusion.

Spherical beads were prepared, such that, they were of a uniform cross-linked structure in the size range 0.2-0.4 cm, for both alginate and its grafted PCL derivatives. These were used as a matrix carrier for two model drugs. In addition to the traditional method of external ionotropic gelation, a novel two step procedure was employed using both internal and external gelation in an effort to increase the cross-linking density. This should result in an improvement in such properties as encapsulation efficiency and control of swelling and prolonging the release of the cargo drug.

Two model drugs were used, the hydrophilic negatively charged carmoisine and, as a contrast, the uncharged hydrophobic β-carotene. Four types of alginate were used as carriers i.e. a commercial alginate and its grafted PCL derivative and Welsh alginate and its grafted PCL derivative. Beads were prepared at two concentrations of 0.5% and 1%. It was found that greater swelling resulted for the 0.5% preparations and also resulted in a more rapid drug release. This applied for both the one-step and two-step methods.

The study showed that for the one-step method for the loading of carmoisine the encapsulation efficiency was generally low but this increased by employing the two-step procedure i.e. increased from 23% to 65%. The PCL grafted derivatives exhibited the longest release profiles with the two-step procedure being the longest. The incorporation of hydrophobic PCL as a grafted co-polymer also further modified the material by reducing the swelling.

β-carotene was found to have the highest encapsulated efficiency but for the test period of 15 days there was no release of is cargo. Further study of this behaviour would be very useful, particularly in view of possible clinical applications. Enzymatic controlled release can be further investigated.

Chapter 6: PLGA/alginate composite microspheres for hydrophilic protein delivery

6.1 introduction.

Proteins are increasingly being used as pharmaceuticals due to their high specificity and their property to be active at relatively low concentrations.[193] Recombinant DNA technology is allowing commercial exploitation of proteins in a rapidly growing pharmaceutical market. The major practical challenge is the physical and chemical instabilities of proteins and is one reason why protein pharmaceuticals are traditionally administered by injection rather than orally.[194] Biodegradable microspheres offer a possible attractive drug delivery system for proteins and peptides, due to their excellent biocompatibility and biodegradability.[195,196]

Microspheres or microbeads are spherical particles with diameters larger than 1000 μm with its immobilised cargo distributed throughout the matrix. Microcapsules are microspheres that contain a liquid core within a distinct membrane in which the cargo is contained. Efforts were directed towards microsphere synthesis. Poly (lactic-co-glycolic acid) (PLGA) has been extensively investigated in this regard. Biodegradable microspheres can be prepared by various methods, each with their own advantages and disadvantages and each giving rise to different properties for the microspheres synthesised. The encapsulation process ideally should allow optimal protein loading and result in a high yield of microspheres. The stability of the encapsulated protein should allow for uniformity and reproducibility between batches and the performance should allow for a low burst effect, adjustable release profiles and the microspheres should be free flowing. The encapsulation efficiency i.e. the ratio of the protein to the polymer matrix is a measure of the amount of protein encapsulated in the polymer matrix and should be as high as possible in order to deliver the maximum dosage in clinical usage.[197]

The most widely used methods for preparation of protein loaded microspheres include: (i) spray drying; (ii) phase separation–coacervation and (iii) double emulsion phase separation–coacervation.[197]

In spray–drying the protein is thoroughly dispersed in a polymer solution by high speed homogenization, and the homogenate is then is atomized in a stream of heated air. Solvent evaporates from the droplets formed and yielding microspheres instantaneously with typical sizes from 1 to 1000 μm depending upon conditions. This method requires high capital investment and the proteins require freeze-drying before they can be dispersed and homogenised in typically organic polymer solution. Such harsh conditions are likely to induce denaturation and aggregation to sensitive proteins and antigens and affect their stability during processing, storage and release and is thus of some concern. However, this method has been successfully used for recombinant human erythrospheres (Poietin)[198] and also for Parlodel depots (bromocriptine mesylate).[199]

In phase separation–coacervation the solid protein is dispersed into a solution containing polymer in dichloromethane but alternatives are normally used for pharmaceuticals. Silicon oil is then added at a suitable rate thus reducing the solubility of polymer. The polymer-rich liquid phase (coacervate) thus encapsulates the particles of the dispersed drug, the 'embryonic' microspheres are hardened and washed using heptane solvent. The major disadvantage of the method is possible residual solvents and relatively harsh preparation conditions. However, the method has been successful in producing diphtheria toxoid[200] and for Decapeptyl Depots.[201]

The third method, the double emulsion method, is a water-in-oil-in-water (w/o/w) technique. A protein in an aqueous solvent is emulsified with a non-miscible polymer solution contained in an organic solvent such as dichloromethane to form a w/o emulsion. The homogenization is performed using either a high speed homogenizer or sonicator. The primary emulsion is then quickly transferred to an excess of an aqueous medium which contains a stabilizer, usually polyvinyl alcohol. Further homogenization or rigorous stirring is required to form a double emulsion of w/o/w. Removal of organic solvent by vacuum and or heat, induces phase separation of polymer and a protein core to produce micro-spheres. The advantages of this method is that proteins can be encapsulated from an aqueous solution that can be performed on small scale giving high yields and encapsulation efficiencies. The disadvantage is that it is a complex process that can affect some polymer properties and can give rise to difficulties in modifying release profiles and may affect shelf life of antigens and stability of the microspheres. Proteins successfully encapsulated include influenza A vaccine[202], bovine serum albumin[203] , lysozyme[204], recombinant human epidermal growth factor[205] , LHRH agonist (Lupron Depot). [206]

This method is well suited to encapsulating water-soluble drugs such as peptides, proteins, and vaccines. The oil in water method is better suited to water-insoluble drugs like steroids. [207]

A major concern is possibly the structural or conformational integrity of the proteins during preparation, storage, and release from this type of drug-delivery system.[208, 209, 210] When two immiscible liquid phases (organic and aqueous) are mixed interfaces are created. The protein molecules in aqueous solution are usually dispersed into a polymer solution contained in an organic solvent by using a high-speed homogenizer or a sonicator (for a water-in oil emulsion).[209] with a resulting high interfacial area. Proteins, which may be surface active, tend to migrate to the aqueous/organic interface where they may unfold and change their conformation. [211] Protein structure or conformation may change due to the acidic conditions created inside the microspheres as a result of polymer degradation and possibly reaction of the protein with the polymer and/or its degradation products.[212] PLGA microspheres, in particular, those prepared by the double-emulsion method, present a situation in which a water-soluble drug is dispersed in the polymer matrix and is, therefore susceptible to exposure to these adverse factors. Therefore, protein stability during encapsulation and release is paramount for a successful controlled release system.

In an effort to improve protein stability, alginate microspheres are promising. An advantage is that the formulation can be made under relatively mild conditions with minimal denaturation. In addition, resulting gels can protect proteins from degradation during their release. Protein entrapped in alginate beads are typically prepared by injecting a solution of sodium alginate, containing the desired protein, as droplets, into a cross-linking solution such as the divalent Ca^{2+}. The biological activity of drugs is not impaired in the encapsulation process. The alginate bead is relatively inert to protein drugs and cells, however, a positively charged protein may, potentially, compete with Ca^{2+} ions for carboxylic acid sites in the alginate matrix. This has been shown with small drugs[213] resulting in protein inactivation such as with the protein transforming growth factor-beta (TGA-β1).[214] Additives may be required in such a case to protect the active agent. Thus, the addition of the anionic polymer poly(acrylic acid) protects the TGF-β1 from interacting with the alginate and thereby retaining its activity.[214] Alginate in the form of microcapsules, plain beads and coated beads has been used to entrap proteins e.g. melatonin [215], heparin [216], haemoglobin [217] and also vaccines [218,219] etc. Coated beads and microspheres were found to be better for oral delivery. Although, these Ca^{2+}-alginate beads can be prepared

by simple, mild procedures, it is found that there is significant loss of the drug during preparation of the beads, mainly, by leaching via the pores in the beads.[220, 221] This has prompted many attempts at modification of alginate for drug delivery purposes.

Low encapsulation and fast release from alginate gels of many proteins has led to various cross-linking or encapsulation methods, and/or employing protein-hydrogel interactions.[71] For example, insulin-loaded alginate microspheres prepared by mixing alginate with anionic polymers (e.g., cellulose acetate phthalate, dextran sulphate, polyphosphate), then coating with chitosan to protect the protein insulin at gastric pH, obtained its sustained release at intestinal pH.[222]

The purpose of this study is to develop a method to prepare microspheres with enhanced properties based on the double emulsion method. Such microspheres should be biocompatible and capable of loading with encapsulated hydrophilic proteins stabilised by association with alginate. Ideally, such a technique would allow control over cargo release. The standard method for preparing PLGA microspheres was modified by incorporating bovine serum albumin (BSA) and alginate inside PLGA microspheres through the double emulsion approach. Initially, the microspheres containing BSA and alginate were created by the solvent-evaporation method based on the formation of the multiple water in oil in water (w/o/w) emulsion procedure. The second emulsion step also introduced the Ca^{2+} cross-linking agent to gain access to the core of the micro particle and allowed the cross-linking of the alginate thus incorporating the protein in the matrix.
This method was used to further investigate the effect of using two different types of alginate i.e. commercial and extracted Welsh with their different M/G ratios. The micro-particles made were characterized using SEM analysis to determine their size and morphology, while the protein release behaviour was also studied.

6.2 Experimental.

6.2.1 Chemicals and materials.

Commercial alginate (ALG-A) with M/G ratio 2.3 and extracted Welsh alginate specifically WS-2 with M/G ratio 2.03

PLGA (lactide: glycolide 32 kDa); the chemical structure of PLGA is shown in **Fig (6-1)**.

Bovine serum albumin (BSA), Span 40, Bio rad protein assay kit and standard tin solution were purchase from Sigma-Aldrich.

Poly (vinyl alcohol) (PVA), molecular weight 8.9-9.8 x 10^3 g/mole , fused granular calcium chloride ($CaCl_2$), sodium chloride (NaCl), phosphate buffer solution (PBS) and dichloro-methane (CH_2Cl_2) were purchased from Fisher Scientific. All materials were used without further purification.

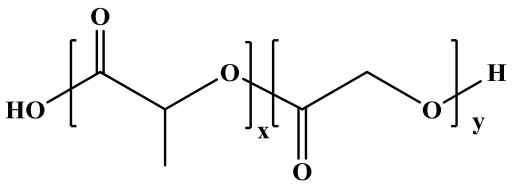

Fig (6-1): The chemical structure of PLGA.

6.2.2 Determination of tin content in Poly (lactic glycolic acid) PLGA.

The PLGA used in this study for the preparation of micro particles was prepared by ring-opening polymerisation using tin as a catalyst. Six samples were prepared and as these were to be considered from a clinical view, it was necessary to determine the tin content, as tin is toxic for clinical purposes. The tin content was determined by Atomic Absorption Spectroscopy (AAS)

A standard calibration curve was prepared in accordance with standard instructions as given in **Chapter 4.2.3** and is shown in **Fig (6-2).**

A PLGA sample was also prepared for analysis and subsequently run under the same instrument working conditions that pertained to the calibration.

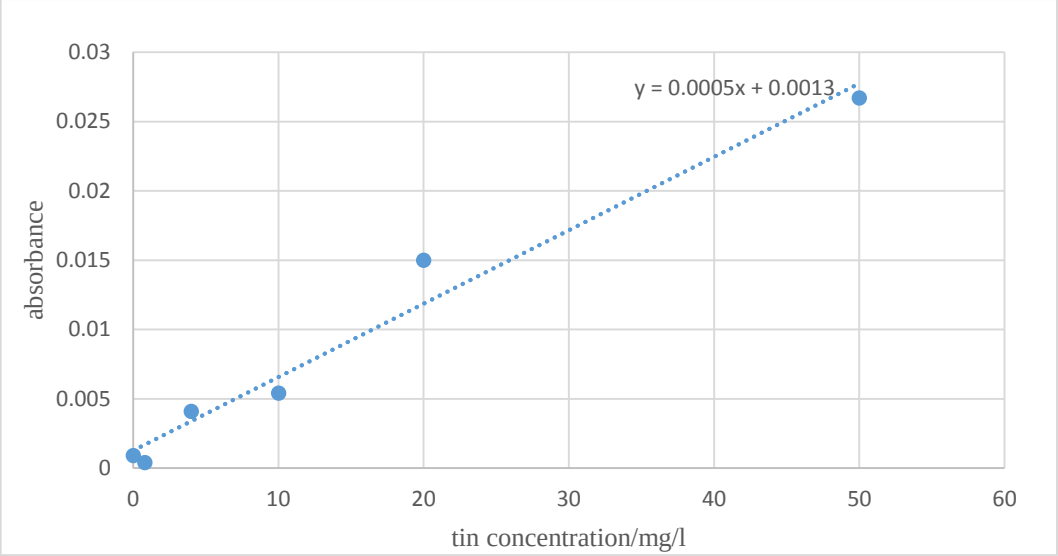

Fig (6-2): The calibration graph for tin standard.

6.2.3 Preparation method.

For the preparation of protein-loaded PLGA/alginate microspheres, a volume of 200 µL of 1% (w/v) alginate solution in water containing 10 µL of BSA in PBS buffer (i.e. 2 mg of BSA in 1mL of 1% PBS in de-ionised water) was added to a volume of 800 µL of 5% PLGA (w/v) dissolved in dichloromethane also containing 5 mg of the surfactant Span 40.The mixture was the vortexed for 30 seconds. The first emulsion was injected via a syringe needle into a volume of 100mL of 0.2% PVA solution while homogenising at 10,000 rpm, then homogenized for a further 10 seconds. 150 µL of 0.5 M $CaCl_2$ was injected into the double emulsion mixture to ionically crosslink the alginate polymer while homogenizing at 10,000 rpm.

The emulsion mixture was then stirred mechanically for 2 hours to evaporate off the dichloro-methane. The microspheres were collected and freeze-dried.

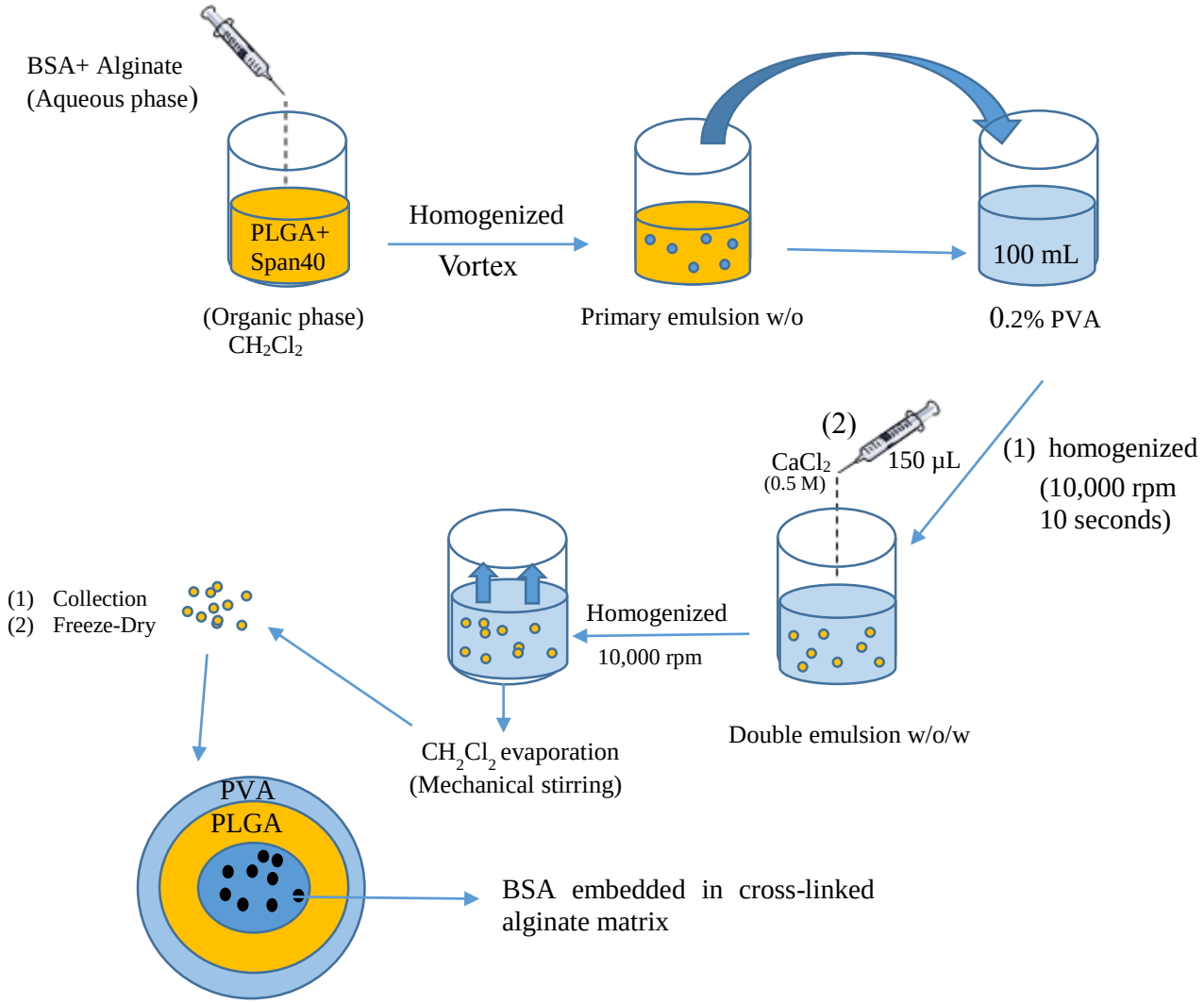

Fig (6-3): Preparation of PLGA/alginate microparticles encapsulating BSA protein.

6.2.4 Calculation of encapsulation efficiency.

After the double emulsion and the solidification of PLGA/ alginate microspheres were completed, the suspension was collected, and the concentration of BSA in the supernatants was determined by measuring the absorbance at 595 nm using UV-vis spectrophotometry.

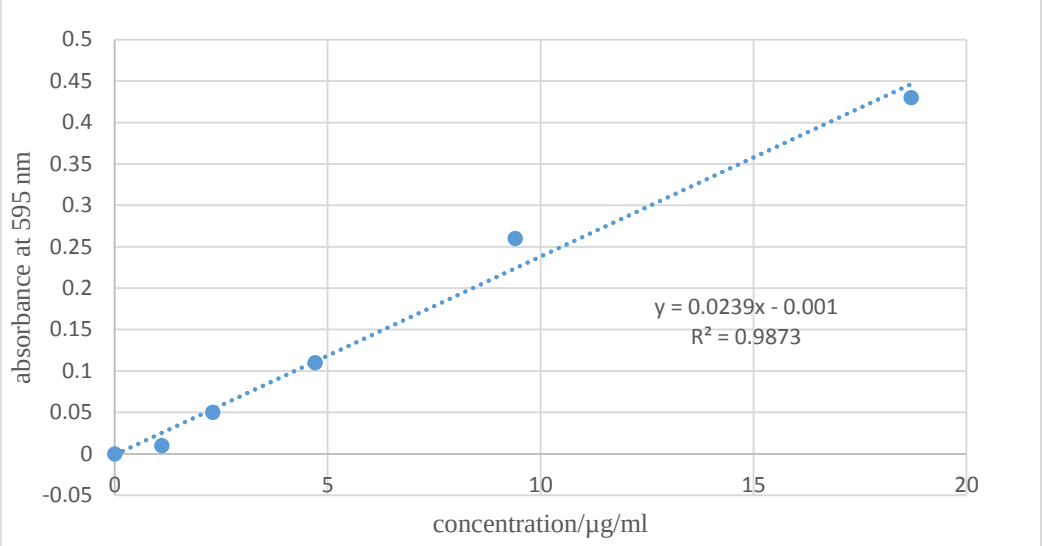

Fig (6-4): The calibration graph of protein (BSA) standard.

The calibration graph was prepared using a commercially available Bio-Rad Protein Assay Reagent Kit. (**See Chapter 3.2.4.1** Protein quantification)

6.2.5 Release study.

The release of the model protein BSA model was conducted at room temperature in different aqueous media: distilled water, 1% (w/v) NaCl and 1% (w/v) PBS. 1 mL of the aqueous medium was added to the freeze-dried microparticles (approx. 14 mg). At regular time intervals, 800 µl aliquot of solution was withdrawn and immediately replaced with the same volume of fresh solution. The *in vitro* release of proteins from the microspheres was determined by assessing the amount of BSA in each aliquot by measuring the absorbance at 595nm. Measurements were performed in duplicate. Thus,

Protein release (%) = [protein release] / [protein loaded] x100

6.3 Results and discussion.

The microspheres of PLGA/ alginate composite containing BSA were prepared by a double-emulsion w/o/w based on the solvent evaporation method. The sodium alginate was an additional component of the internal water phase as its purpose was to increase the loading efficiency of the hydrophilic peptide.[223] This incidentally leads to a considerable increase in the particle size which may also affect the release dynamics.[224] The tin content of the six samples of prepared PLGA was determined and the results are as given in **Table (6-1)**. Sample 3 was then chosen for use in the preparation of PLGA micro-particles as this is seen to have the lowest tin content. The two types of microspheres used in this study were prepared using the same materials and conditions and differed only in the type of alginate that was incorporated. The type of microsphere labelled MS1 was synthesised using commercial alginate (ALG-A) giving rise to PLGA/ALG-A microspheres and the second type, MS2, was by using Welsh alginate (WS-2) to form PLGA/WS-2 microspheres. The two alginates differed in their M/G ratio with commercial being 1.2 and the Welsh was 2.0. They also differed slightly in their molecular weights as indicated in their differing viscosities.

Table (6-1): Tin content of PLGA by AAS analysis.

Sample	Mw(KDa)	Tin conc. (mg/L)	Tin conc. (mg/g)
1	30	6	0.15
2	30	5.2	0.13
3	32	3.2	0.08
4	33	4.6	0.115
5	16	9.8	0.245
6	150	5.6	0.14

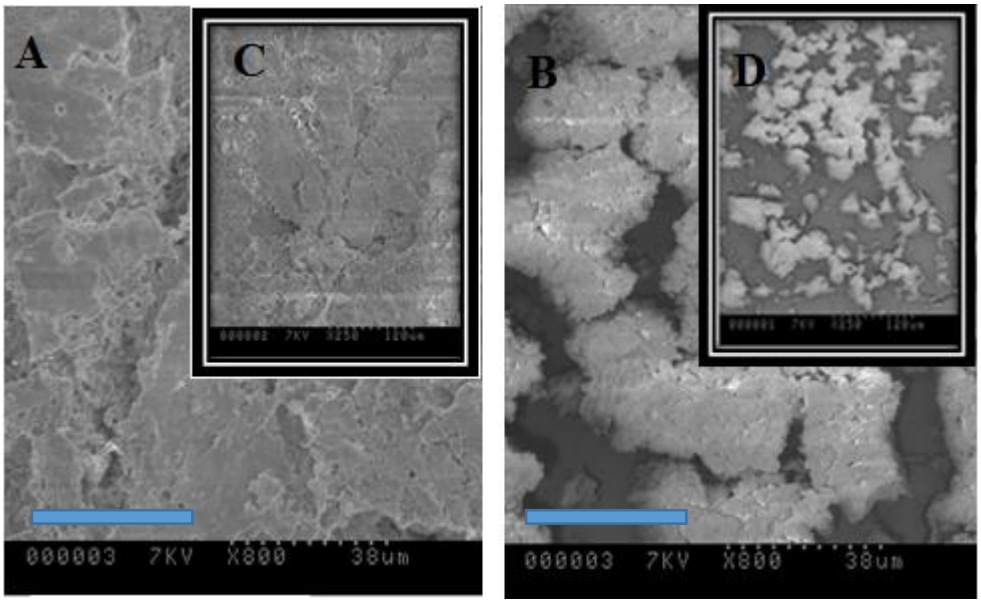

Fig (6-5): Scanning Electron Microscopy of PLGA/alginate microsphere: **(A)** MS1 formulated with PLGA/ALG-A (commercial alginate). Magnification is 800 X, (scale bar 38µm). **(B)** MS2 synthesised as PLGA/WS-2 (Welsh alginate). Magnification is 800 X, (scale bar 38 µm). **(C)** and **(D)** are MS1 and MS2 respectively. Magnification is 250 X, (scale bar 120 µm).

The size distribution of PLGA microspheres prepared by emulsification techniques has been shown to depend on the mixing speeds, the temperature, the PVA concentrations, and the volume ratio of oil and outer PVA phase. [203, 225, 197] The two types of microspheres prepared in this study were made using the same process parameters to produce microspheres of standard consistency, their only difference being the type of alginate incorporated. Electron micrographs of both types of microparticles i.e. incorporating commercial alginates and Welsh are shown in **Fig (6-5)**. In both images, no well-defined particles can be seen even at the highest magnification of 800X. It is possible that the particles may be of the order of between 7 and 3 µm which is the reported figure under similar conditions of preparation.[226] However, as particles in this study were prepared at higher homogenation rates (10,000 rpm rather than 3800rpm) the particles may thus be rather smaller.

From **(B)** image above the MS2 prepared using Welsh alginate appears more fragmented and this is consistent with their appearance in the bulk were they are fluffy in nature and this in turn may be related to less cross-linking as a consequence of their higher M content.

The encapsulation efficiency of both types of microspheres are shown in **Fig (6-6)** and was determined by measuring the concentration of the protein in the supernatant after micro-particle synthesis. Thus, the loading efficiency was calculated by subtracting the supernatant protein content from the initial protein content. **Fig (6-6)** shows that the MS1 microspheres were higher in encapsulation efficiency and this may be due to the different composition of the microspheres and particularly their different M and G content. It is possible the higher protein encapsulation is a consequence of the higher cross-linking that results from the higher G content. This is supported by the literature which asserts that high G content (in addition to relatively high molecular weight) of the alginate is the preferred matrix for protein entrapment.[227]

It may be envisioned that cross-linking causes the protein cargo to form higher local associations as a result of similar hydrophobicity and thus exhibit an overall higher encapsulation efficiency.

The higher G content of the MS1 microspheres also leads to a more cross-linked structure forming the better defined surface features as seen in the SEM of **(A)** in **Fig (6-5)**.

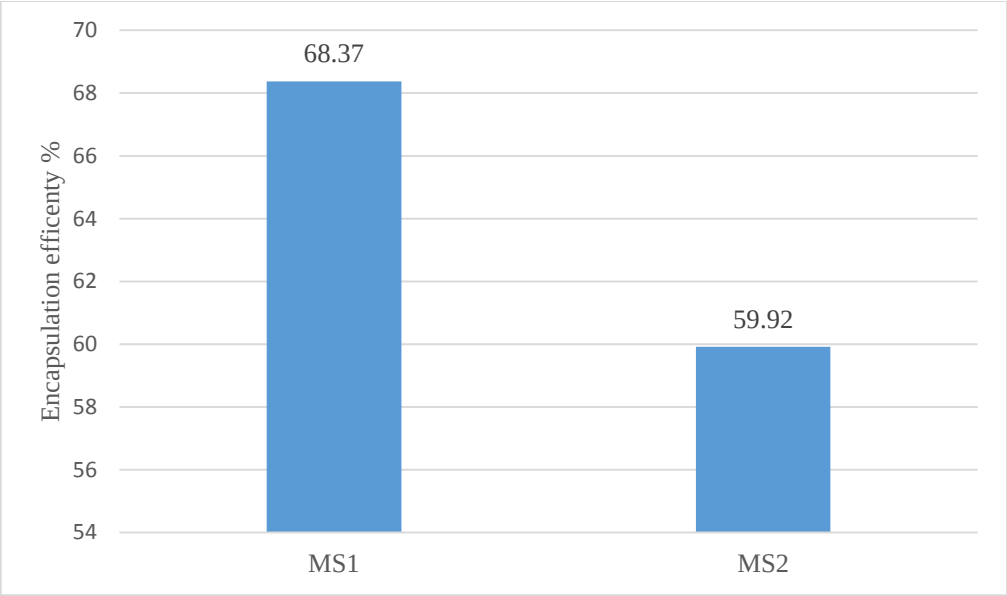

Fig (6-6): Encapsulation efficiency of PLGA/alginate microspheres: **MS1** formulated with PLGA/ALG-A (commercial Alginate) and **MS2** synthesised as PLGA/WS-2 (Welsh alginate).

The release of the protein drug from the both microspheres was compared over 10 days using three different aqueous media (see **Figs (6-7), (6-8), and (6-9)**.

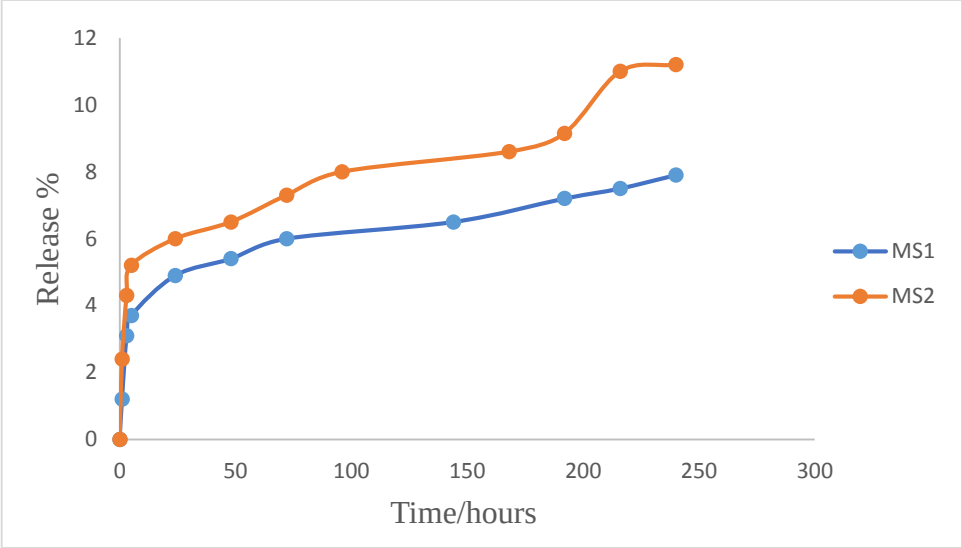

Fig(6-7): The release profile of BSA from MS1 formulated with PLGA/ALG-A (commercial alginate) and MS2 synthesised as PLGA/WS-2 (Welsh alginate) in H_2O.

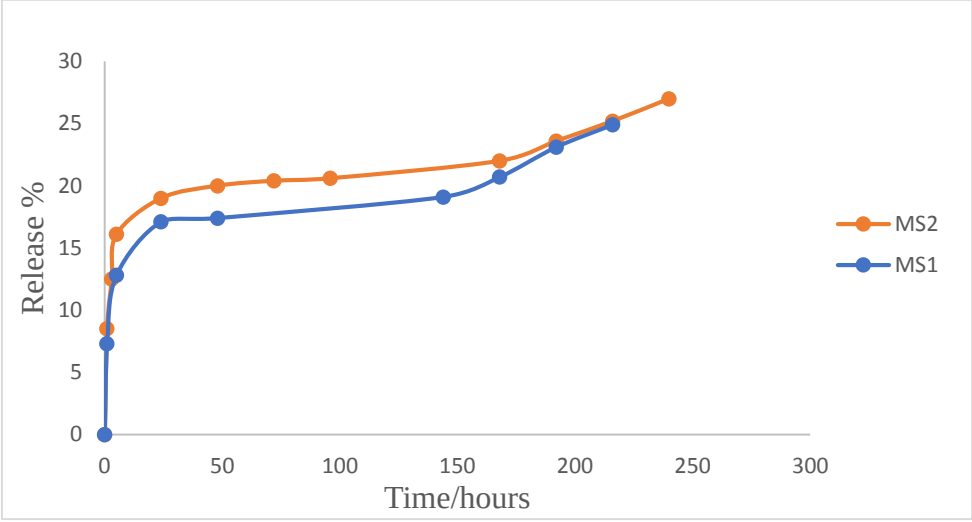

Fig(6-8): The release profile of BSA from MS1 formulated with PLGA/ALG-A (commercial alginate) and MS2 synthesised as PLGA/WS-2 (Welsh alginate) in 1% (w/v) NaCl.

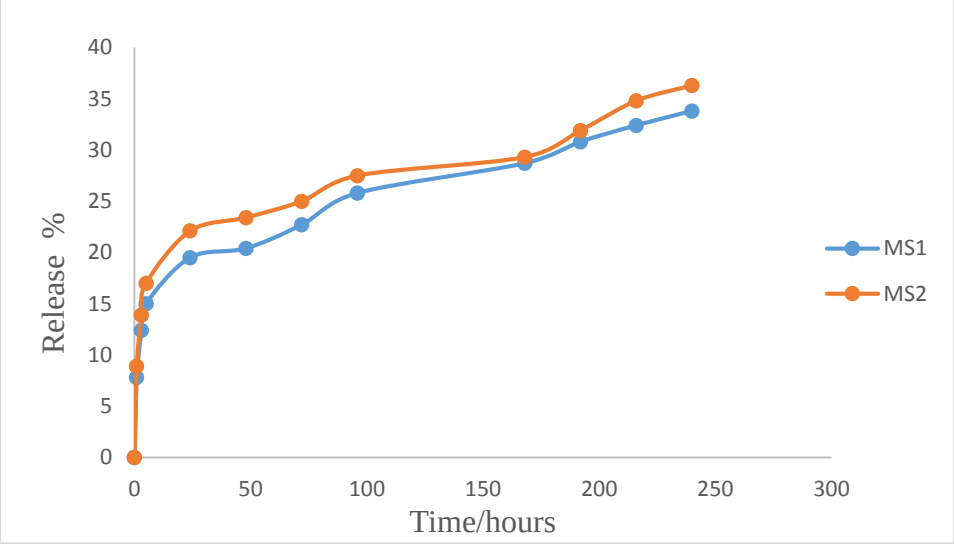

Fig (6-9): The release profile of BSA from MS1 formulated with PLGA/ALG-A (commercial alginate) and MS2 synthesised as PLGA/WS-2 (Welsh alginate) in PBS.

It can be seen from **Fig (6-7), (6-8) and (6-9)** that the greatest release was in PBS with MS2 containing Welsh alginate being 36% and MS1 containing commercial alginate was 34%. In water, the greatest release was observed with MS2 being 11% and MS1 8% and the saline was intermediate with MS2 25% and MS1 27%.

The release profiles followed a similar profile for both microspheres MS1 and MS2 and in all three media showed an initial phase of rapid release (burst release) followed by slowly increasing release of drug cargo.

The degradation of PLGA/alginate microspheres is thought to be influenced by various factors such as molecular weight, permeability to water, pore structure, additives, pH, and ionic strengths.[228] The hydrolysis of PLGA ester bonds in the backbone is the main mechanism for degradation of the PLGA polymer. The amorphous structure of PLGA matrix should permit fast water penetration into microspheres, with subsequent swelling and erosion.

The degradation is further complicated by the presence of the cross-linked alginate in which it is thought that cross links are cleaved by the loss of calcium ions which then diffuse out of the matrix. The calcium loss is more pronounced when the aqueous medium contains ions that can compete for binding sites as is evident from the saline and PBS results.
The release of the entrapped drug cargo involves two different mechanisms, that is, diffusion of the protein molecules and degradation of the polymer matrix.

The initial burst release is fast and large mainly due to the release of surface-bound BSA protein during the beginning of swelling phase, and diffusion through micro-pores.
Following the initial burst release, the BSA was released at a constant speed as microsphere hydration and degradation proceeded The burst release of protein is due to those protein molecules dispersing from close to the microsphere surface, which diffuse out in the initial incubation time. Thus, as the outer regions of the microsphere are more exposed to the media phase by virtue of a relatively larger surface area, diffusion will be more rapid than from the core.

It is thought that the presence of hydrophilic alginate might encourage the BSA protein to diffuse out into the aqueous medium. The releases of proteins from the microsphere matrix shows some similarity to the diffusion of macromolecules from hydrogel-like structures after immersion in water.[229]

Fig (6-10) and **(6-11)** show SEMs for microspheres having undergone 10 days incubation in aqueous media which were then freeze dried as a preparation for SEM. **Fig(6-10)** details the MS2 and generally shows a more fragmented structure than the MS1 and this may be a consequence of lower cross-linking as a result of higher M content in Welsh alginate. This is particularly evident from the water immersion and may go some way to explain the more rapid protein release. The MS1 (PLGA/commercial alginate microspheres) appear to exhibit a smooth surface and may be due to higher cross-linking as a result of higher G content. The effect of this is to reduce pore size and to slow down diffusion through the denser polymeric matrix. The SEM image for MS2 containing Welsh alginate in PBS is seen to very granular and may be thought to have resulted from the greatest extent of leaching of Ca^{+2} ions. The calcium ions after exchange at binding sites by sodium are then precipitated out of solution by forming insoluble calcium phosphate.

In PBS buffer the release rates are comparable for both MS1 and MS2 despite the lower G content of the Welsh alginate. This may confirm that once the calcium cross links are cleaved the two materials will perform equally. The slightly lower release from the MS1 (containing commercial alginate) may be a consequence of its higher molecular weight which gave rise to the higher viscosity observed during the preparation of the alginate solution. The release of the cargo in the saline medium was again seen to be comparable for both types of microbeads. However, the release in saline is somewhat slower than for PBS. This can therefore be reasoned to be due to the calcium ions released by ion exchange are still present for the structure in the

saline medium but are removed by precipitation from the PBS medium. In addition to its effects on PLGA degradation and dissolution, alginate might also act to slow protein release by providing a more favourable hydrophilic environment for the retention of protein. The G content influences the protein release rate. Low G content alginate and low molecular weight alginate are known to release encapsulated proteins at a much faster rate. Therefore, high G content and relatively high molecular weight alginate is a preferred matrix for protein entrapment.[227]

The SEM images also show the effects of degradation on the two types of microsphere with a comparison image taken before immersion. Thus, MS2 in **Fig (6-10)** MS2 (before immersion) shows the micro particle surface as more coherent compared with the later more granular appearance resulting from degradation. Similarly, for the MS1 images of **Fig (6-11)** where the surfaces are much smoother reflecting greater cross-linking.

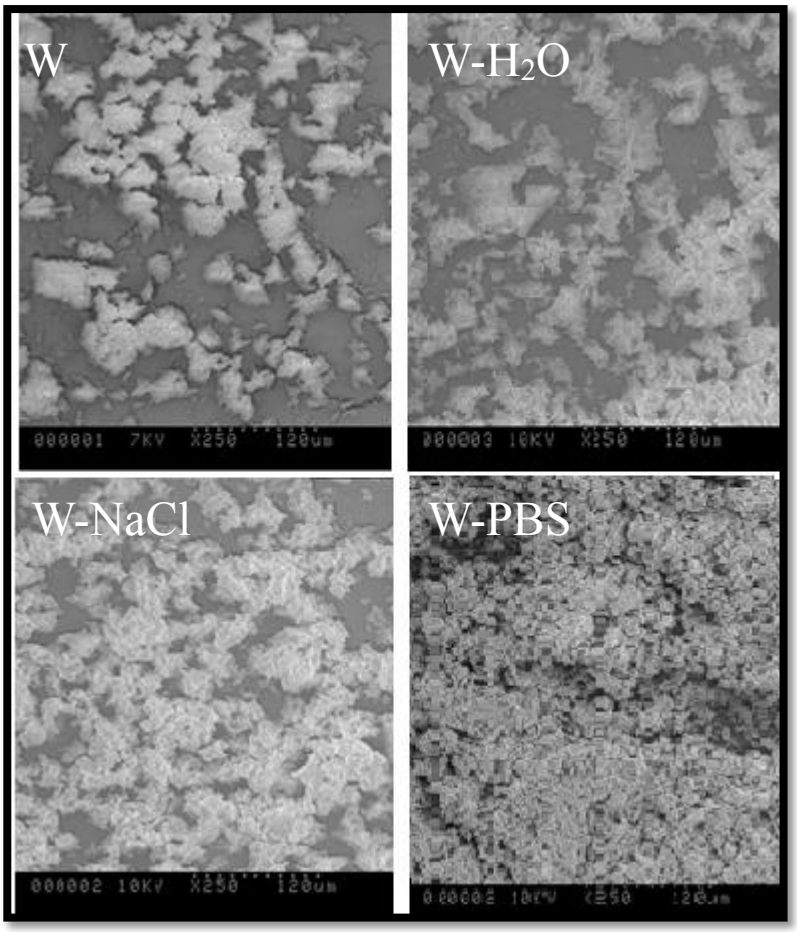

Fig (6-10): Scanning electron micrographs of BSA-loaded MS2 (PLGA/WS-2) composite microsphere prepared with Welsh alginate: **(W)** MS2 before incubation in aqueous media, **(W-H_2O)** after 10 days incubation in H_2O, **(W-NaCl)** after 10 days incubation 1% NaCl and **(W- PBS)** after 10 days incubation in BPS.

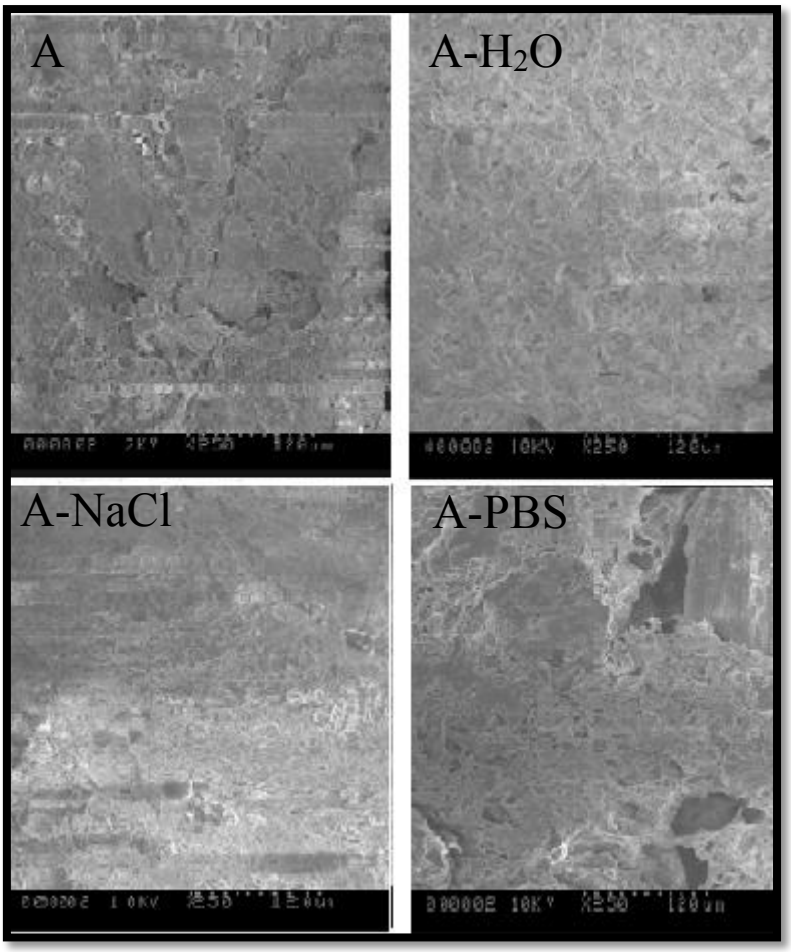

Fig (6-11): Scanning electron micrographs of BSA-loaded MS1 (PLGA/ ALG-A) composite microsphere prepared with commercial alginate: **(A)** MS1 before incubation in aqueous media, **(A-H_2O)** after 10 days incubation in H_2O, **(A-NaCl)** after 10 days incubation 1% NaCl and **(A-PBS)** after 10 days incubation in BPS.

6.4 Conclusion.

Previous studies have shown that PLGA only microspheres prepared using a double emulsion (w/o/w) technique result in low encapsulation efficiency for water-soluble macromolecules, and loss of bioactivity. Therefore, another hydrophilic biomaterial such as Alginate might improve performance.

In this study the performance of two types of microparticles was compared using Welsh and commercial alginates of concentration 1% w/v. The morphology of the microspheres studied by Scanning Electron Microscopy were found to be less than 4 μg. MS1 microspheres (commercial) were higher in encapsulation efficiently being 68.37±2% and Welsh alginate was 59.92±1.8%. The encapsulation efficiencies reflected the higher G content with consequent higher cross-linking.

The release of a model hydrophilic protein (BSA) was undertaken in three aqueous media where incubation was performed over 10 days. It was found that release was greatest in PBS buffer with Welsh alginate being 36% and commercial alginate being 34%. In water, the slowest release was observed with Welsh alginate being 11% and commercial alginate 8% whilst for the saline medium release was intermediate with Welsh 27% and commercial 27%. These results can be explained in terms of the diffusion of the medium with the polar media facilitation Ca^{+2} loss by an ion exchange process. Thus, it was found that the highest release rates correlated with lowest encapsulating efficiencies.

The release profiles followed a similar profile for both alginates and in all three media with an initial phase of rapid release (burst release) followed by slowly increasing release of drug cargo. SEMs for micro-particles before and after incubation showed more a fragmented porous structure after 10 days. The Welsh alginate showed more degradation than the commercial and this was correlated to the lower G content with a consequent lower cross-linking.

References

1 I. Wijesekara, R. Pangestuti and S. K. Kim, *Carbohydr. Polym.*, 2011, **84**, 14–21.
2 D. B. Stengel, S. Connan and Z. A. Popper, *Biotechnol. Adv.*, 2011, **29**, 483–501.
3 M. Rinaudo, *Polym. Int.*, 2008, **57**, 397–430.
4 V. Stiger-Pouvreau, N. Bourgougnon and E. Deslandes, in *Seaweed in Health and Disease Prevention*, eds. J. Fleurence and I. Levine, Academic Press, 2016, pp. 223–274.
5 S. L. Holdt and S. Kraan, *J. Appl. Phycol.*, 2011, **23**, 543–597.
6 L. O'Sullivan, B. Murphy, P. McLoughlin, P. Duggan, P. G. Lawlor, H. Hughes and G. E. Gardiner, *Mar. Drugs*, 2010, **8**, 2038–2064.
7 M. Lahaye and A. Robic, *Biomacromolecules*, 2007, **8**, 1765–1774.
8 Q. Li, J. Luo, C. Wang, W. Tai, H. Wang, X. Zhang, K. Liu, Y. Jia, X. Lyv, L. Wang and H. He, *J. Appl. Phycol.*, 2018, **30**, 2017–2027.
9 V. L. Campo, D. F. Kawano, D. B. da Silva and I. Carvalho, *Carbohydr. Polym.*, 2009, **77**, 167–180.
10 H. Chen, X. Yan, J. Lin, F. Wang and W. Xu, *J. Agric. Food Chem.*, 2007, **55**, 6910–6917.
11 N. Rhein-Knudsen, M. T. Ale and A. S. Meyer, *Mar. Drugs*, 2015, **13**, 3340–3359.
12 S. Ermakova, R. Men'shova, O. Vishchuk, S. M. Kim, B. H. Um, V. Isakov and T. Zvyagintseva, *Algal Res.*, 2013, **2**, 51–58.
13 M. B. LE Rioux, SL Turgeon, *Phytochemistry*, 2010, **71**, 1586–1595.
14 M. T. Ale and A. S. Meyer, *RSC Adv.*, 2013, **3**, 8131–8141.
15 S. Kraan, in *Carbohydrates Comprehensive Studies on Glycobiology and Glycotechnology*, ed. C.-F. Chang, www.intechopen.com, 2012, pp. 489–532.
16 M. Lahaye and C. Rochas, *Hydrobiologia*, 1991, **221**, 137–138.
17 Y.-T. Kim, E.-H. Kim, C. Cheong, D. L. Williams, C.-W. Kim and S.-T. Lim, *Carbohydr. Res.*, 2000, **328**, 331–341.
18 A. Usman, S. Khalid, A. Usman, Z. Hussain and Y. Wang, in *Algae Based Polymers, Blends, and Composites Chemistry, Biotechnology and Materials Science*, Elsevier Inc, 2017, pp. 115–153.
19 B. Larsen, D. M. S. A. Salem, M. A. E. Sallam, M. M. Mishrikey and A. I. Beltagy, *Carbohydr. Res.*, 2003, **338**, 2325–2336.
20 K. Y. Lee and D. J. Mooney, *Prog. Polym. Sci.*, 2012, **37**, 106–126.
21 S. N. Pawar and K. J. Edgar, *Biomaterials*, 2012, **33**, 3279–3305.
22 T. Y. Wong, L. A. Preston and N. L. Schiller, *Annu. Rev. Microbiol.*, 2000, **54**, 289–340.
23 T. A. Fenoradosoa, G. Ali, C. Delattre, C. Laroche, E. Petit, A. Wadouachi and P. Michaud, *J. Appl. Phycol.*, 2010, **22**, 131–137.
24 Y. Qin, *Polym. Int.*, 2008, **57**, 171–180.
25 O. A. Aarstad, Norwegian University of Science and Technology, 2013.
26 H. Grasdalen, *Carbohydr. Res.*, 1983, **118**, 255–260.
27 L. E. Rioux, S. L. Turgeon and M. Beaulieu, *Carbohydr. Polym.*, 2007, **69**, 530–537.
28 K. I. Draget, O. Smidsrød and G. Skjåk-Bræk, *wiley online Libr.*, 2005.
29 T. Andersen, B. L. Strand, K. Formo, E. Alsberg and B. E. Christensen, *Carbohydr. Chem.*, 2012, **37**, 227–258.
30 I. Donati and S. Paoletti, in *Alginates: Biology and Applications*, ed. B. H. A. Rehm, 2009, pp. 1–53.
31 A. Haug and B. Larsen, *Acta Chem. Scand.*, 1963, 17, 1653–1662.

32 S. N. Pawar and K. J. Edgar, *Biomacromolecules*, 2011, **12**, 4095–4103.
33 C. H. Goh, P. W. S. Heng and L. W. Chan, *Carbohydr. Polym.*, 2012, **88**, 1–12.
34 O. Smidsrød, R. M. Glover and S. G. Whittington, *Carbohydr. Res.*, 1973, **27**, 107–118.
35 O. Smidsrød, A. Haug, B. Larsen, B. von Hofsten, D. H. Williams, E. Bunnenberg, C. Djerassi and R. Records, *Acta Chem. Scand.*, 1966, 20, 1026–1034.
36 S. Holtan, Q. Zhang, W. I. Strand and G. Skjåk-Bræk, *Biomacromolecules*, 2006, **7**, 2108–2121.
37 P. Gacesa, *Fed. Eur. Biochem. Soc.*, 1987, **212**, 199–202.
38 A. Hauga, B. Larsen and O. Smidsrød, *Acta Chem. Scand.*, 1967, 21, 2859–2870.
39 O. Smidsrod and A. Haug, *Acta Chem. Scand.*, 1968, **22**, 1989–1997.
40 A. Haug and O. Smidsrød, *Acta Chem. Scand.*, 1965, **19**, 341–351.
41 O. Smidsrod and A. Haug, *Acta Chem. Scand.*, 1972, **26**, 2063–2074.
42 G. T. Grant, E. R. Morris, D. A. Rees, P. J. C. Smiti and D. Thom, *FEBS Lett.*, 1973, **32**, 195–198.
43 R. Kohn, B. Larsen, L. J. Sæthre, E. Sjöstrand and S. Svensson, *Acta Chem. Scand.*, 1972, 26, 2455–2468.
44 B. T. Stokke, O. Smidsrød, F. Zanetti, W. Strand and G. Skjåk-Bræk, *Carbohydr. Polym.*, 1993, **21**, 39–46.
45 I. Donati, S. Holtan, Y. A. Mørch, M. Borgogna, M. Dentini and G. Skjåk-Bræk, *Biomacromolecules*, 2005, **6**, 1031–1040.
46 H. J. Kong, D. Kaigler, K. Kim and D. J. Mooney, *Biomacromolecules*, 2004, **5**, 1720–1727.
47 C. G. Gomez, M. Rinaudo and M. A. Villar, *Carbohydr. Polym.*, 2007, **67**, 296–304.
48 Y. K.-D. HE Shu-Lan, ZHANG Min, GENG Zhan-Jie, YIN Yu-Ji~*, *Chinese J. Appl. Chem.*, 2005, **22**, 1007–1011.
49 K. H. Bouhadir, K. Y. Lee, E. Alsberg, K. L. Damm, K. W. Anderson and D. J. Mooney, *Biotechnol. Prog.*, 2001, **17**, 945–950.
50 G. Alban, S., Schauerte, A., & Franz, *Carbohydr. Polym.*, 2002, **47**, 267–276.
51 H. Ronghua, D. Yumin and Y. Jianhong, *Carbohydr. Polym.*, 2003, **52**, 19–24.
52 L. Fan, L. Jiang, Y. Xu, Y. Zhou, Y. Shen, W. Xie, Z. Long and J. Zhou, *Carbohydr. Polym.*, 2011, **83**, 1797–1803.
53 R. J. Coleman, G. Lawrie, L. K. Lambert, M. Whittaker, K. S. Jack and L. Grndahl, *Biomacromolecules*, 2011, **12**, 889–897.
54 C. Galant, A. L. Kjøniksen, G. T. M. Nguyen, K. D. Knudsen and B. Nyström, *J. Phys. Chem. B*, 2006, **110**, 190–195.
55 K. Abu-Rabeah, B. Polyak, R. E. Ionescu, S. Cosnier and R. S. Marks, *Biomacromolecules*, 2005, **6**, 3315–3318.
56 C. Müller, J. C. Cassel, A. Durand, E. Dellacherie, F. Vallée, S. Schimchowitsch, C. Kelche and M. Leonard, *Carbohydr. Res.*, 2009, **344**, 223–228.
57 J. S. Yang, Y. J. Xie and W. He, *Carbohydr. Polym.*, 2011, **84**, 33–39.
58 M. C. Carré, C. Delestre, P. Hubert and E. Dellacherie, *Carbohydr. Polym.*, 1991, **16**, 367–379.
59 H. Lyons, T. Pembroke, B. Murray, E. Broderick, H. Byrne and M. Hall, *J. Colloid Interface Sci.*, 2006, **298**, 154–161.
60 V. G. Babak, E. A. Skotnikova, I. G. Lukina, S. Pelletier, P. Hubert and E. Dellacherie, *J. Colloid Interface Sci.*, 2000, **225**, 505–510.
61 S. Pelletier, P. Hubert, F. Lapicque, E. Payan and E. Dellacherie, *Carbohydr. Polym.*, 2000, **43**, 343–349.
62 G. Sen, R. P. Singh and S. Pal, *J. Appl. Polym. Sci.*, 2010, **115**, 449–456.
63 L. X. Liu, M.Z., & Cao, *J. Appl. Chem.*, 2002, **19**, 455–458.

64 A. Sand, M. Yadav and K. Behari, *J. Appl. Polym. Sci.*, 2010, **118**, 3685–3694.
65 L. Yang, B. Zhang, L. Wen, Q. Liang and L. M. Zhang, *Carbohydr. Polym.*, 2007, **68**, 218–225.
66 S. Sakiyama-Elbert and J. Hubbell, *Ann Rev Mater Res*, 2001, **31**, 183–201.
67 E. M. Ahmed, *J. Adv. Res.*, 2015, **6**, 105–121.
68 H. Omidian and K. Park, eds. J. Siepmann, R. A. Siegel and M. J. Rathbone, Advances in Delivery Science and Technology. Springer, Boston, 2012, pp. 75–205.
69 J. P. Paques, E. Van Der Linden, C. J. M. Van Rijn and L. M. C. Sagis, *Adv. Colloid Interface Sci.*, 2014, **209**, 163–171.
70 R. Poojari and R. Srivastava, *Expert Opin. Drug Deliv.*, 2013, **10**, 1061–1076.
71 M. George and T. E. Abraham, *J. Control. Release*, 2006, **114**, 1–14.
72 M. Papageorgiou, S. Kasapis and M. G. Gothard, *Carbohydr. Polym.*, 1994, **24**, 199–207.
73 P. Eiselt, K. Y. Lee and D. J. Mooney, *Macromolecules*, 1999, **32**, 5561–5566.
74 K. Y. Lee, J. A.Rowley, P. Eiselt, E. M.Moy, K. H.Bouhadir and D. J.Mooney, *Macromolecules*, 2000, **33**, 4291–4294.
75 A. W. Chan, R. A. Whitney and R. J. Neufeld, *Biomacromolecules*, 2008, **9**, 2536–2545.
76 S. Varghese and J. H. Elisseeff, ed. C. Werner, Polymers for Regenerative Medicine. Advances in Polymer Science, vol 203. Springer, Berlin, Heidelberg, 2006, pp. 95–144.
77 K. Y. Lee and S. H. Yuk, *Prog. Polym. Sci.*, 2007, **32**, 669–697.
78 K. I. Drageta, O. GåserØd, I. Aunea, P. O. Andersen, B. Storbakken, B. T. Stokke and O. Smidsrød, *Food Hydrocoll.*, 2001, **15**, 485–490.
79 M. A, S. B. G and S. O, *Biotechnol. Bioeng.*, 1989, **33**, 79–89.
80 Y. A. Mørch, I. Donati, B. L. Strand and G. Skjåk-Braek, *Biomacromolecules*, 2007, **8**, 2809–2814.
81 S. Moe, K. I. Draget, G. Skjåk-Bræk and O. Smidsrød, *Food Sci. Technol.*, 1995, **67**, 245–286.
82 O. Smidsrød, *Faraday Discuss. Chem. Soc.*, 1974, **57**, 263–274.
83 G. Skják-Bræk, O. Smidsrød and B. Larsen, *Int. J. Biol. Macromol.*, 1986, **8**, 330–336.
84 O. Smidsrød, *Acta Chem. Scand.*, 1972, **26**, 79-.
85 L. H. Sperling, *Introduction to Physical Polymer Science*, John Wiley & Sons, 2005, The Fourth., 2005.
86 I. L. Andresen and O. Smidsørod, *Carbohydr. Res.*, 1977, **58**, 271–279.
87 S. T. Moe, K. I. Draget, G. Skjåk-Bræk and O. Simdsrød, *Carbohydr. Polym.*, 1992, **19**, 279–284.
88 J. Zhang, C. R. Daubert and E. Allen Foegeding, *J. Food Eng.*, 2007, **80**, 157–165.
89 I. Donati, Y. A. Mørch, B. L. Strand, G. Skjåk-Braek and S. Paoletti, *J. Phys. Chem. B*, 2009, **113**, 12916–12922.
90 A. Imeson, *Food stabilisers, thickeners and gelling agents*, Wiley-Blackwell, 2010, vol. 34.
91 E. Onsøyen, *Carbohydr. Eur*, 1996, **14**, 26–31.
92 I. A. Brownlee, A. Allen, J. P. Pearson, P. W. Dettmar, M. E. Havler, M. R. Atherton and E. Onsoyen, *Crit. Rev. Food Sci. Nutr.*, 2005, **45**, 497–510.
93 M. D. Ranken, *Handbook of Meat Product Technology*, Blackwell Science Ltd, 2000.
94 S. Devatkal and S. K. Mendiratta, *Meat Sci.*, 2001, **58**, 371–379.
95 K. Suklim, W. N. Eigel, C. G. Haugh, L. A. Granata, G. Flick and J. Marcy, *J. Texture Stud.*, 2004, **35**, 634–642.
96 D. K. Das Gupta, N. Roopa and R. K. Leela, *Am. J. Food Technol.*, 2007, **2**, 176–182.
97 S. S. Manjunatha and D. K. D. Gupta, *Int. J. Food Prop.*, 2006, **9**, 453–462.
98 F. Mancini, L. Montanari, D. Peressini and P. Fantozzi, *Leb. u.-Technol*, 2002, **35**, 517–

525.
99 D. Paraskevopoulou, D. Boskou and A. Paraskevopoulou, *Food Chem.*, 2006, **101**, 1197–1204.
100 A. Regand and H. D. Goff, *Food Hydrocoll.*, 2003, **17**, 95–102.
101 L. Z. Wang, L. Liu, J. Holmes, J. F. Kerry and J. P. Kerry, *Int. J. Food Sci. Technol.*, 2007, **42**, 1128–1138.
102 P. Gacesa, *Carbohydr. Polym.*, 1988, **8**, 161–182.
103 T. J. Ryan, *Dermatol. Clin.*, 1993, **11**, 207–213.
104 S. Thomas, *J. Wound Care*, 1992, **1**, 29–32.
105 W. Dettmar, G. Jolliffe, P. F. Field, D. Q. Mackenzie, B. Ie and A. Hanne, 2002, **1**.
106 S. K. Varma, H. P. Henderson and C. L. Hankins, *Br. J. Plast. Surg.*, 1991, **44**, 55–56.
107 B. Kneafsey, O`Shaughnessy, M. and K. C. Condon, *Science (80-.).*, 1990, **22**, 40–43.
108 I. R. Matthew, R. M. Browne, J. W. Frame and B. G. Millar, *Br. J. Oral Maxillofac. Surg.*, 1993, **31**, 165–169.
109 W. R. Gombotz and S. F. Wee, *Adv. Drug Deliv. Rev.*, 2012, **64**, 194–205.
110 A. Shilpa, S. S. Agrawal and A. R. Ray, *J. Macromol. Sci. - Polym. Rev.*, 2003, **43**, 187–221.
111 C.K. Kim and E.J. Lee, *Int. J. Pharm.*, 1992, **79**, 11–19.
112 Ý. A. Mørch, I. Sandvig, Ø. Olsen, I. Donati, M. Thuen, G. Skjåk-Bræk, O. Haraldseth and C. Brekken, *Contrast Media Mol. Imaging*, 2012, **7**, 265–275.
113 O. Smidsrød and G. Skja˚k-Brłk, *Trends Biotechnol.*, 1990, **8**, 71–78.
114 J. A. A. Fujii, D. T. Slade, K. Redenbaugh and K. A. Walker, *Trends Biotechnol.*, 1987, **5**, 335–339.
115 J. A. Rowley and D. J. Mooney, *J. Biomed. Mater. Res.*, 2002, **60**, 217–223.
116 J. Yang, M. Goto, H. Ise, C. S. Cho and T. Akaike, *Biomaterials*, 2002, **23**, 471–479.
117 P. J. . Hoor, *Nuclear Magnetic Resonance*, Oxford University Press, 2015, 2015.
118 Reusch and William, *'Infrared Spectroscopy'.*, Michigan State University. Retrieved 2006-10-27, 1999.
119 J. A. De Haseth and J. Wiley, 2007, 1–23.
120 J. M. G. Cowie, *Polymers : Chemistry and Physics of Modern Materials*, 3rd editio., 2007.
121 M. P. Stevens, *Polymer Chemistry, An Introduction*, Oxford University Press: New York, 3rd editio., 1999.
122 K. Matyjaszewsk and J. Xia, *Chem. Rev.*, 2001, **101**, 2922–2985.
123 John A Dean, *Handbook of Chemistry*, Mcgraw-Hill, Inc, Fifteenth., 1999.
124 E. Pungor and G. Horvai, *A Practical Guide to Instrumental Analysis*, CRC Press, 1994.
125 M. J. O'Neill, *Anal. Chem.*, 1964, **36**, 1238–1245.
126 D. A. Skoog, F. J. Holler and S. R. Crouch, *Principles of Instrumental Analysis*, Belmont, CA : Thomson Brooks, 6th editio., 2007.
127 A. W. Coats and J. P. Redfern, *Analyst*, 1963, **88**, 906–924.
128 X. Liu and W. Yu, *J. Appl. Polym. Sci.*, 2006, **99**, 937–944.
129 T. Zhang, J. Jin, S. Yang, D. Hu, G. Li and J. Jiang, *J. Macromol. Sci. Part B Phys.*, 2009, **48**, 1114–1124.
130 B. V. L`vov, *J. Anal. Chem.*, 2005, **60**, 382–392.
131 D. Mcmullan, *Scanning*, 1995, **17**, 175–185.
132 J. R. W, E. Skelly and G. M. F. II, *Undergraduate Instrumental Analysis*, CRC Press, 7th editio., 2014.
133 W. L. Henrich, *Principles and Practice of Dialysis*, Lippincott Williams & Wilkins, 4th editio., 2012.
134 Schoolworkhelper Editorial Team, *St. Rosemary Inst. © 2010-2019 | Creat. Commons*

4.0.https://schoolworkhelper.net/selective-permeability-of-dialysis-tubing-lab-explained/
135 C. Hoek, D. M. Hoeck Van den Hoeck, H. M. Jahns and M. Jahns, *Algae: an introduction to phycology*, Cambridge University Press, illustrate., 1995.
136 E. Fourest and B. Volesky, *Appl. Biochem. Biotechnol.*, 1997, **67**, 215–226.
137 T. A. Davis, M. Ramirez, A. Mucci and B. Larsen, *J. Appl. Phycol.*, 2004, **16**, 275–284.
138 M. R. Torres, A. P. A. Sousa, E. A. T. Silva Filho, D. F. Melo, J. P. A. Feitosa, R. C. M. de Paula and M. G. S. Lima, *Carbohydr. Res.*, 2007, **342**, 2067–2074.
139 C. Bertagnolli, A. P. D. M. Espindola, S. J. Kleinübing, L. Tasic and M. G. C. Da Silva, *Carbohydr. Polym.*, 2014, **111**, 619–623.
140 T. A. Davis, F. Llanes, B. Volesky and A. Mucci, *Environ. Sci. Technol.*, 2003, **37**, 261–267.
141 V. Venugopal, *Marine Polysaccharides; Food Applications*, CRC Press, Boca Raton, Florida, 2011.
142 K. Truus, M. Vaher and I. Taure, 2001, 1–9.
143 H. P. Calumpong, A. P. Maypa and M. Magbanua, *Hydrobiologia*, 1999, **398**, 211–215.
144 L. Li, X. Jiang, H. Guan and P. Wang, *Carbohydr. Res.*, 2011, **346**, 794–800.
145 M. Fertah, A. Belfkira, E. montassir Dahmane, M. Taourirte and F. Brouillette, *Arab. J. Chem.*, 2014.
146 H. Grasdalen, B. Larsen and O. Smidsrød, *Carbohydr. Res.*, 1979, **68**, 23–31.
147 Haug A., Smidsrod O. and Skjak-Braek G., *Carbohydr. Res.*, 1974, **32**, 217–225.
148 R. Panikkar and D. J. Brasch, *Carbohydr. Res.*, 1996, **293**, 119–132.
149 A. I. Larsen, B., Salem, D.M.S.A., Sallan, M.A.E., Mishrikey, M.M., Beltagy, *Carbohydr. Res.*, 2003, **338**, 2325–2336.
150 M. Mathlouthi and J. L. Koenig, *Adv. Carbohydr. Chem. Biochem.*, 1987, **44**, 7–89.
151 R. M. Silverstein and G. C. Bassler, *J. Chem. Educ.*, 1962, **39**, 546.
152 N. P. Chandia, B. Matsuhiro and A. E. Vasquez, *Carbohydr. Polym.*, 2001, **46**, 81–87.
153 N. P. Chandía, B. Matsuhiro, E. Mejías and A. Moenne, *J. Appl. Phycol.*, 2004, **16**, 127–133.
154 L. Pereira, A. Sousa, H. Coelho, A. M. Amado and P. J. A. Ribeiro-Claro, *Biomol. Eng.*, 2003, **20**, 223–228.
155 S. Sellimi, I. Younes, H. Ben Ayed, H. Maalej, V. Montero, M. Rinaudo, M. Dahia, T. Mechichi, M. Hajji and M. Nasri, *Int. J. Biol. Macromol.*, 2015, **72**, 1358–1367.
156 H. N. Cheng and T. G. Neiss, *Polym. Rev.*, 2012, **52**, 81–114.
157 D. A. da Silva, R. C. M. de Paula and J. P. A. Feitosa, *Eur. Polym. J.*, 2007, **43**, 2620–2629.
158 R. P. Singh, T. Tripathy, G. P. Karmakar, S. K. Rath, N. C. Karmakar, S. R. Pandey, K. Kannan, S. K. Jain and N. T. Lan, *Curr. Sci.*, 2000, **78**, 798–803.
159 M. Zhang and A. H. E. Müller, *J. Polym. Sci. Part A Polym. Chem.*, 2005, **43**, 3461–3481.
160 H. il Lee, J. Pietrasik, S. S. Sheiko and K. Matyjaszewski, *Prog. Polym. Sci.*, 2010, **35**, 24–44.
161 C. Feng, Y. Li, D. Yang, J. Hu, X. Zhang and X. Huang, *Chem. Soc. Rev.*, 2011, **40**, 1282–1295.
162 M. R. De Boisseson, M. Leonard, P. Hubert, P. Marchal, A. Stequert, C. Castel, E. Favre and E. Dellacherie, *J. Colloid Interface Sci.*, 2004, **273**, 131–139.
163 I. Colinet, V. Dulong, T. Hamaide, D. Le Cerf and L. Picton, *Carbohydr. Polym.*, 2009, **75**, 454–462.
164 E. Rotureau, E. Marie, E. Dellacherie and A. Durand, *Colloids Surfaces A Physicochem. Eng. Asp.*, 2007, **301**, 229–238.

165 C. Nouvel, C. Frochot, V. Sadtler, P. Dubois, E. Dellacherie and J.L. Six, *Macromolecules*, 2004, **37**, 4981–4988.
166 M. Leonard, M. Rastello De Boisseson, P. Hubert and E. Dellacherie, *J. Biomed. Mater. Res. Part A*, 2004, **68**, 335–342.
167 M. Leonard, M. R. De Boisseson, P. Hubert, F. Dalençon and E. Dellacherie, *J. Control. Release*, 2004, **98**, 395–405.
168 V. R. Sinha, K. Bansal, R. Kaushik, R. Kumria and A. Trehan, *Int. J. Pharm.*, 2004, **278**, 1–23.
169 N. T. Dai, M. R. Williamson, N. Khammo, E. F. Adams and A. G. A. Coombes, *Biomaterials*, 2004, **25**, 4263–4271.
170 R. Gref, J. Rodrigues and P. Couvreur, *Macromolecules*, 2002, **35**, 9861–9867.
171 L. Chen, Y. Ni, X. Bian, X. Qiu, X. Zhuang, X. Chen and X. Jing, *Carbohydr. Polym.*, 2005, **60**, 103–109.
172 K. I. Draget, G. Skjåk-Bræk, B. E. Christensen, O. Gåserød and O. Smidsrød, *Carbohydr. Polym.*, 1996, **29**, 209–215.
173 J. P. Ibáez and Y. Umetsu, *Hydrometallurgy*, 2002, **64**, 89–99.
174 C. Jérôme and P. Lecomte, *Adv. Drug Deliv. Rev.*, 2008, **60**, 1056–1076.
175 H. R. Kricheldorf, A. Stricker and D. Langanke, *Macromol. Chem. Phys.*, 2001, **202**, 2963–2970.
176 B. Abderrahim, E. Abderrahman, A. Mohamed, T. Fatima, T. Abdesselam and O. Krim, *World J. Environ. Eng. Vol. 3, 2015, Pages 95-110*, 2015, **3**, 95–110.
177 S. K. Bajpai and S. Sharma, *React. Funct. Polym.*, 2004, **59**, 129–140.
178 P. Rakesh, K. Vipin and K. Kanchan, *Res. J. Chem. Sci.*, 2015, **5**, 45–47.
179 T. R. Hoare and D. S. Kohane, *Polymer (Guildf).*, 2008, **49**, 1993–2007.
180 J.Y. Leong, W.H. Lam, K.W. Ho, W.P. Voo, M. F.X. Lee, H.P. Lim, S.L. Lim, B.T. Tey, D. Poncelet and E.S. Chan, *Particuology*, 2016, **24**, 44–60.
181 S. J. Hwang, G. J. Rhee, K. M. Lee, K. H. Oh and C. K. Kim, *Int. J. Pharm.*, 1995, **116**, 125–128.
182 J.O. You, S.B. Park, H.Y. Park, S. Haam, C.H. Chung and W.S. Kim, *J. Microencapsul.*, 2001, **18**, 521–532.
183 T. Østberg, E. M. Lund and C. Graffner, *Int. J. Pharm.*, 1994, **112**, 241–248.
184 Y. Li, C. Feng, J. Li, Y. Mu, Y. Liu, M. Kong, X. Cheng and X. Chen, *Int. J. Biol. Macromol.*, 2017, **105**, 924–930.
185 A.A.badwan, A.Abumalooh, E.Sallam, A.Abukalaf and O.Jawan, *Drug Dev. Ind. Pharm.*, 1985, **11**, 239–256.
186 S. Takka, Ö. H. Ocak and F. Acartürk, *Eur. J. Pharm. Sci.*, 1998, **6**, 241–246.
187 C. M. Silva, A. J. Ribeiro, I. V. Figueiredo, A. R. Gonçalves and F. Veiga, *Int. J. Pharm.*, 2006, **311**, 1–10.
188 H. Zhang, E. Tumarkin, R. Peerani, Z. Nie, R. M. A. Sullan, G. C. Walker and E. Kumacheva, *J. Am. Chem. Soc.*, 2006, **128**, 12205–12210.
189 D. Poncelet, *Ann. N. Y. Acad. Sci.*, 2010, **944**, 74–82.
190 J. K. Oh, R. Drumright, D. J. Siegwart and K. Matyjaszewski, *Prog. Polym. Sci.*, 2008, **33**, 448–477.
191 M. L. Soni, M. Kumar and K. P. Namdeo, *Int. J. Drug Deliv.*, 2010, **2**, 64–68.
192 E. Farahani-Vasheghani and F. Ganji, *Iran. Polym. J.*, 2009, **18**, 1–26.
193 H. J. C. Eriksson, W. L. J. Hinrichs, B. Van Veen, G. W. Somsen, G. J. De Jong and H. W. Frijlink, *Int. J. Pharm.*, 2002, **249**, 59–70.
194 W. Wang, *Int. J. Pharm.*, 1999, **185**, 129–188.
195 J. M. Anderson and M. S. Shive, *Adv. Drug Deliv. Rev.*, 2012, **64**, 72–82.
196 D. T. O'Hagan, M. Singh and R. K. Gupta, *Adv. Drug Deliv. Rev.*, 1998, **32**, 225–246.

197 V. R. Sinha and A. Trehan, *J. Control. Release*, 2003, **90**, 261–280.
198 B. Bittner, M. Morlock, H. Koll, G. Winter and T. Kissel, *Eur. J. Pharm. Biopharm.*, 1998, **45**, 295–305.
199 T.Kissel, Z.Brich, S.Bantle, I.Lancranjan, F.Nimmerfall and P.Vit, *J. Control. Release*, 1991, **16**, 27–41.
200 P. Johansen, L. Moon, H. Tamber, H. P. Merkle, B. Gander and D. Sesardic, *Vaccine*, 2000, **18**, 209–215.
201 T. W. Redding, A. V. Schally, T. R. Tice and W. E. Meyers, *Proc. Natl. Acad. Sci.*, 1984, **81**, 5845–5848.
202 A. K. Hilbert, U. Fritzsche and T. Kissel, *Vaccine*, 1999, **17**, 1065–1073.
203 Y. Y. Yang, T. S. Chung and N. Ping Ng, *Biomaterials*, 2001, **22**, 231–241.
204 Y. S. Nam, S. H. Song, J. Y. Choi and T. G. Park, *Biotechnol. Bioeng.*, 2000, **70**, 270–277.
205 K. Han, K. D. Lee, Z. G. Gao and J. S. Park, *J. Control. Release*, 2001, **75**, 259–269.
206 Y. Ogawa, M. Yamamoto, S. Takada, H. Okada and T. Shimamoto, *Chem. Pharm. Bull.*, 1988, **36**, 1502–1507.
207 Rajeev A. Jain, *Biomaterials*, 2000, **21**, 2475–2490.
208 Y. Tabata, Y. Takebayashi, T. Ueda and Y. Ikada, *J. Control. Release*, 1993, **23**, 55–63.
209 W. Lu and T. G. Park, *J Pharm Sci Tech*, 1995, **49**, 13–19.
210 T. Uchida, K. Yoshida, A. Ninomiya and S. Goto, *Chem. Pharm. Bull.*, 1995, **43**, 1569–1573.
211 L. Xiaohong, Y. Minglong, X. Chengdong and D. Xianmo, *Acta Polym. Sin.*, 1999, **2**, 156–161.
212 M. Tobío, S. P. Schwendeman, Y. Guo, J. McIver, R. Langer and M. J. Alonso, *Vaccine*, 2000, **18**, 618–622.
213 N. Segi, T. Yotsuyanagi and K. Ikeda, *Chem. Pharm. Bull.*, 1989, **37**, 3092–3095.
214 T. Espevik, M. Otterlei, G. Skjåk-Braek, L. Ryan, S. D. Wright and A. Sundan, *Eur. J. Immunol.*, **23**, 255–261.
215 B. J. Lee and G. H. Min, *Int. J. Pharm.*, 1996, **144**, 37–46.
216 E. R. Edelman, A. Nathan, M. Katada, J. Gates and M. J. Karnovsky, *Biomaterials*, 2000, **21**, 2279–2286.
217 M. R. Rasmussen, T. Snabe and L. H. Pedersen, *J. Control. Release*, 2003, **91**, 395–405.
218 B. Kim, T. Bowersock, P. Griebel, A. Kidane, L. A. Babiuk, M. Sanchez, S. Attah-Poku, R. S. Kaushik and G. K. Mutwiri, *J. Control. Release*, 2002, **85**, 191–202.
219 J. L. Romalde, A. Luzardo-Alvárez, C. Ravelo, A. E. Toranzo and J. Blanco-Méndez, *Aquaculture*, 2004, **236**, 119–129.
220 P. Liu and T. R. Krishnan, *J. Pharm. Pharmacol.*, 1999, **51**, 141–9.
221 M. L. Torre, P. Giunchedi, L. Maggi, R. Stefli, E. O. Machiste and U. Conte, *Pharm. Dev. Technol.*, 1998, **3**, 141–149.
222 C. M. Silva, A. J. Ribeiro, D. Ferreira and F. Veiga, *Eur. J. Pharm. Sci.*, 2006, **29**, 148–159.
223 Y. Ogawa, M. Yamamoto, H. Okada, T. Yashiki and T. Shimamoto, *Chem. Pharm. Bull.*, 1988, **36**, 1095–1103.
224 H. Jeffery and D. O'Hagan, *Pharm. Res.* 1993, **10** (3), 362–368.
225 S. Freiberg and X. X. Zhu, *Int. J. Pharm.*, 2004, **282**, 1–18.
226 P. Zhai, X. B. Chen and D. J. Schreyer, *Mater. Sci. Eng. C*, 2015, **56**, 251–259.
227 Y. Murata, K. Nakada, E. Miyamoto, S. Kawashima and S.-H. Seo, *J. Control. Release*, 1993, **23**, 21–26.
228 U. Bilati, E. Allémann and E. Doelker, *Eur. J. Pharm. Biopharm.*, 2005, **59**, 375–388.
229 X. Li, X. Deng, M. Yuan, C. Xiong, Z. Huang, Y. Zhang and W. Jia, *J. Appl. Polym.*

Sci., 2000, **78**, 140–148.